FLEXIBLE PAVEMENT SYSTEM - SECOND GENERATION, INCORPORATING FATIGUE AND STOCHASTIC CONCEPTS

by

Surendra Prakash Jain
B. Frank McCullough
W. Ronald Hudson

Research Report Number 123-10

A System Analysis of Pavement Design
and Research Implementation
Research Study Number 1-8-69-123

conducted

In Cooperation with the
U. S. Department of Transportation
Federal Highway Administration

by the

Highway Design Division Research Section
Texas Highway Department

Texas Transportation Institute
Texas A&M University

Center for Highway Research
The University of Texas at Austin

December 1971

The opinions, findings, and conclusions expressed in this publication are those of the authors and not necessarily those of the Federal Highway Administration.

PREFACE

This report presents the Flexible Pavement System Second Generation for the design of flexible pavements incorporating fatigue theory, linear elastic layered theory, and stochastic concepts. In terms of elastic and fatigue material properties and their stochastic variations with both space and time, loading, and environmental conditions, new models to predict pavement performance are developed for distress manifestations such as cracking, rut depth, and roughness. The proposed models can be directly used for the design of flexible pavements and can also be included in the Flexible Pavement Systems Computer Program already developed for the Texas Highway Department.

This report is also meant to be a background document for further work to be done to include the effects of temperature and other stresses in the flexible pavement systems model.

This is one of the reports in a series that describe the work done by the Center for Highway Research in the project entitled "The Development of a Feasible Approach to Systematic Pavement Design and Research." The project proposes a long-range comprehensive research program to develop pavement systems analysis and is unusual in that it is a joint effort by three separate research agencies. The project is supported by the Texas Highway Department in cooperation with the Federal Highway Administration Department of Transportation.

The AASHO Road Test data were a very good source of information and were used extensively throughout the analysis in this report for verification of the proposed models. The computer programs were written for the CDC 6600 computer in FORTRAN language.

This report is a product of the continued assistance of many people. The entire staff of the Center for Highway Research at The University of Texas at Austin must be thanked for their cooperation and contributions. Thanks are due to Nancy Braun for her very valuable assistance in the computer programming.

Finally, the support of the Federal Highway Administration and the Texas Highway Department is gratefully acknowledged.

Surendra Prakash Jain
B. Frank McCullough
W. Ronald Hudson

December 1971

LIST OF REPORTS

Report No. 123-1, "A Systems Approach Applied to Pavement Design and Research," by W. Ronald Hudson, B. Frank McCullough, F. H. Scrivner, and James L. Brown, describes a long-range comprehensive research program to develop a pavement systems analysis and presents a working systems model for the design of flexible pavements.

Report No. 123-2, "A Recommended Texas Highway Department Pavement Design System Users Manual," by James L. Brown, Larry J. Buttler, and Hugo E. Orellana, is a manual of instructions to Texas Highway Department personnel for obtaining and processing data for flexible pavement design system.

Report No. 123-3, "Characterization of the Swelling Clay Parameter Used in the Pavement Design System," by Arthur W. Witt, III, and B. Frank McCullough, describes the results of a study of the swelling clay parameter used in pavement design system.

Report No. 123-4, "Developing A Pavement Feedback Data System," by R. C. G. Haas, describes the initial planning and development of a pavement feedback data system.

Report No. 123-5, "A Systems Analysis of Rigid Pavement Design," by Ramesh K. Kher, W. R. Hudson, and B. F. McCullough, describes the development of a working systems model for the design of rigid pavements.

Report No. 123-6, "Calculation of the Elastic Moduli of a Two Layer Pavement System from Measured Surface Deflections," by F. H. Scrivner, C. H. Michalak, and W. M. Moore, describes a computer program which will serve as a subsystem of a future Flexible Pavement System founded on linear elastic theory.

Report No. 123-7, "Annual Report on Important 1970-71 Pavement Research Needs," by B. Frank McCullough, James L. Brown, W. Ronald Hudson, and F. H. Scrivner, describes a list of priority research items based on findings from use of the pavement design system.

Report No. 123-8, "A Sensitivity Analysis of Flexible Pavement System FPS2," by Ramesh K. Kher, B. Frank McCullough, and W. Ronald Hudson, describes the overall importance of this system, the relative importance of the variables of the system and recommendations for efficient use of the computer program.

Report No. 123-9, "Skid Resistance Considerations in the Flexible Pavement Design System," by David C. Steitle and B. Frank McCullough, describes skid resistance consideration in the Flexible Pavement System based on the testing of aggregates in the laboratory to predict field performance and presents a nomograph for the field engineer to use to eliminate aggregates which would not provide adequate skid resistance performance.

Report No. 123-10, "Flexible Pavement System - Second Generation, Incorporating Fatigue and Stochastic Concepts," by Surendra Prakash Jain, B. Frank McCullough, and W. Ronald Hudson, describes the development of new structural design models for the design of flexible pavement which will replace the empirical relationship used at present in flexible pavement systems to simulate the transformation between the input variables and performance of a pavement.

ABSTRACT

Design of flexible pavement is a complex procedure involving numerous variables. The systems approach can be considered as the best method for solving design problems. An important part of any pavement design system involves upgrading it in order to include the best possible technology. One of the distress mechanisms included in the conceptual flexible pavement design system, as a part of the fracture failure mode, is fatigue of the pavement materials. Its consideration on some rational basis and stochastic variations of the material properties in space and time need particular attention in the development of a working systems model.

New structural design models, for the second generation of the flexible pavement system, based on linear elastic layered theory, fatigue theory, and probability theory, are presented. Probability theory is used for variation in material properties and fatigue life and for calculation of the cracking index, based on probability of damage. The new design models are proposed to replace the empirical relationship used at present to simulate the transformation between the input variables and performance of a pavement. The serviceability and performance concepts from the AASHO Road Test have also been utilized. The fatigue phenomenon is considered and the inputs of the system are correlated in terms of elastic and fatigue material properties and their stochastic variations, loading, environmental conditions, and compaction characteristics under repeated loading to the distress manifestations, such as cracking and rut depth. Based on AASHO Road Test data, a correlation between cracking and slope variance was developed. Thus, models are developed for the cracking index, rut depth index, and roughness index to predict the pavement performance and present serviceability index. Computer programs have been developed for these models to aid in the various stages of the design.

The models have been verified by comparing predicted performance with that observed at the AASHO Road Test for 28 sections. The models compare very well and predict the observed data within the acceptable accuracy. Results of the sensitivity analysis for the cracking index model are included. It is

seen that the fatigue parameter B is the most significant and very sensitive variable and should be estimated very accurately.

Example problems are shown to compare the proposed models with the existing FPS models. The proposed design method shows various improvements and gives more realistic flexible pavement designs. A new rational procedure for an overlay design using damage theory is explained and is based on sound theoretical fundamentals. This is followed by a chapter on implementation of the proposed models for the flexible pavement system second generation. It is noted that the stress and strain calculations in the present analysis, by the direct use of the layered program, should be improved and replaced by a more efficient approach.

Conclusions have been based on the overall experience gained while working on this project. It is noted that only a few bonafide design procedures for flexible pavements exist at present and those in practice need improvements. The use of the proposed design procedure based on the theories discussed earlier give a new dimension to the flexible pavement design field. The characterization of material properties is a very important part of the whole design process and requires proper attention.

Recommendations have been made to aid planning of future work. The proposed design models are based on sound fundamentals, using the best state-of-the-art information, and are recommended for the design of flexible pavements and to be included in the pavement systems design computer programs already developed for the Texas Highway Department.

SUMMARY

New structural design models for the design of flexible pavement have been developed which will replace the empirical relationship used at present in flexible pavement systems to simulate the transformation between the input variables and performance of a pavement. Computer programs have been developed to quantify the distress manifestations, cracking, roughness, and rut depth in a pavement which are used to predict its performance. The models have been verified by comparing predicted performance with that observed at the AASHO Road Test. The overlay design procedure is improved and takes account of the damage to the existing pavement system.

The proposed method can be directly used for the design of flexible pavements and can also be included in the pavement system design computer program already developed for the Texas Highway Department for updating the system.

The development has the advantage of an immediate direct application and gives the background for further improvements in the existing design system.

IMPLEMENTATION STATEMENT

A separate chapter is included in this report discussing the details of implementation. The proposed structural design models can be used directly for the design of flexible pavements and can also be included in the existing FPS computer program.

The proposed method eliminates the present practice of expensive field measurements of material properties. The use of elastic constants, which are measured in the laboratory, can be more economical, convenient, and accurate. The laboratory measurements of elastic constants, tensile characteristics, and fatigue properties of pavement materials, are already in progress under a project at the Center for Highway Research at The University of Texas. Moreover, a computer program to calculate the elastic moduli of a two-layer system from measured surface deflection is already available and further work to complete the in-situ values of elastic moduli is in progress at Texas Transportation Institute, Texas A&M University. The proposed method has the new capability of predicting the nature of distress, i.e., cracking, roughness, and rutting, which cannot be done by any existing methods.

The proposed models can evaluate the effects of compaction, fatigue, and stochastic variations in material properties. The proposed models could also be used to give better evaluation of some of current black bases being proposed for pavements by the Texas Highway Department. The Flexible Pavement System FPS is already in use by several districts of the Texas Highway Department; hence, only a revised version of FPS, incorporating the proposed models, needs to be formulated. Thus, there is an excellent scope of the implementation of the proposed models in the near future without much efforts and organizational changes.

TABLE OF CONTENTS

APPENDICES

PART I

BACKGROUND

CHAPTER 1. INTRODUCTION

BACKGROUND

The design of flexible pavements requires knowledge of complex structural systems. Many variables are involved, including the behavior of soils and paving materials, combinations of static and dynamic loading, and different environmental and climatic conditions. Early design procedures for flexible pavements were primarily rule-of-thumb. In time, many empirical and semi-empirical methods of design were developed. The empirical nature of the methods is due in part to limited knowledge of the behavior of materials and of actual failure mechanisms and in part to the limitations of analytical techniques in handling the complex mathematical functions required.

The inability to predict pavement performance under certain conditions with any existing design method has been due to the manner in which design procedures were developed; a particular development was applicable only within certain limited geographic boundaries and suitable only for the characteristics of available materials, environmental conditions, and traffic loads within these boundaries.

Therefore, a more rational method of pavement design was needed, one which could predict the performance of a pavement under various sets of conditions. Such a method may be organized within the framework of the "systems approach" and must consider various variables, including physical, social, and economic. A project which proposed a long-range comprehensive research program to develop a pavement system analysis, "The Development of a Feasible Approach to Systematic Pavement Design and Research," was initiated in December 1968 by the Texas Highway Department, the Center for Highway Research at The University of Texas at Austin, and the Texas Transportation Institute at Texas A&M University, under the Cooperative Highway Research Program. Under this project, now entitled "Systematic Pavement Design," a computer program based on the systems approach and known as the Flexible Pavement Systems or FPS was developed for the design of flexible pavements (Ref 81). A general description of FPS and its development is given in Chapter 2. The basic models used

in FPS were obtained from Research Report 32-11 (Ref 162), which was the outgrowth of an attempt to apply the AASHO Road Test results to Texas conditions. More than 50 physical inputs and constraints are used in the FPS models and the output is a set of recommended pavement design strategies based on the present net worth of the lowest total cost. Total cost consists of initial construction, maintenance, overlays, users, seal coat, and salvage costs. The approach gives the designer considerably expanded scope and flexibility in exploring design options.

The performance subsystem, which is only a part of the whole flexible pavement systems model, uses the empirical relationship between the input variables and the pavement performance. A performance history is obtained from the prediction of present serviceability index (Ref 158), and failure of the system is evaluated in terms of minimum serviceability level and the total cost of the system. However, the present serviceability index is not obtained from the actual distress manifestations, i.e., magnitude of cracking, patching, roughness, and rut depth, but simply from some function of their combined values. This function, which was statistically derived from the AASHO Road Test data, is assumed to represent the present serviceability index at any time. The use of these empirical relationships, for materials not used at the AASHO Road Test, different environmental conditions, locations outside the limited boundaries, and with passage of time resulting in revision of the standards of safety and comfort, is questionable. In spite of all the technological developments and the theoretical background available in the present state-of-the-art for the design of flexible pavements, no existing design procedure, including FPS, can predict quantitatively the distress manifestations, such as cracking, rut depth, and roughness, which will appear in a pavement during its performance period. The distress mechanisms which are considered in the systems design approach for flexible pavements include, as a part of the fracture failure mode, fatigue of pavement materials. Fatigue plays an important role in the design of a pavement structure and its complete consideration on some rational basis is particularly important in the development of a working system model. Stochastic variations of material properties with space and time also need to be taken into account in a realistic design approach. Proper application and use of elastic layered theories need investigation. The problem of computation of permanent deformation should be analyzed. No rational overlay design procedure which is operational considers

the actual damaged and consolidated condition of the pavement at the time of an overlay.

OBJECTIVE

The general objective of this study is to upgrade the existing flexible pavement systems by attacking the problems of computing fatigue cracking, permanent deformation, and roughness and developing new structural design models. As discussed in the previous section, no existing pavement design method can predict, or attempts to, the condition of failure in a pavement at the end of the design period. In simple terms the main objective of the proposed developments is to quantify the distress manifestations in a pavement system in order to predict its performance and failure conditions. Inclusion of these new models in the performance subsystem of the existing flexible pavement systems, with necessary revision in the physical models (structural design models), will assist in the development of a second generation flexible pavement systems design model.

SCOPE

The approach described herein utilizes a theory of linearly elastic layers which is commonly termed "layered theory." It takes into account the fatigue behavior of the materials and their stochastic variations with space and time. The probability concept in the output of the system is considered in the analysis. The serviceability-performance concept of the AASHO Road Test has also been used. With the fatigue phenomenon considered, the inputs of the system are correlated to its distress manifestations, such as cracking and rut depth. Based on AASHO Road Test data, a correlation between cracking and the roughness index of the pavement is developed. Thus models for the cracking index, roughness index, and rut depth index are developed to predict the pavement performance and present serviceability index. The models are verified with AASHO Road Test data and example problems which predict the performance within the acceptable accuracy. These new models can be used directly for the design of flexible pavement and can also be included in the design computer programs for flexible pavement systems already developed for the Texas Highway Department.

This report is divided into five parts, each consisting of several chapters. Part I, the first three chapters, covers background material. Chapter 2 reviews existing theories and methods of flexible pavement design along with their limitations and contains a description of the flexible pavement system. Chapter 3 briefly gives background data on development of the proposed design procedure.

Part II, Chapters 4 through 6, reviews techniques used in development of the models proposed for the design of flexible pavements. Chapter 4 summarizes the concept of fatigue and its application to the design of flexible pavements. Chapter 5 contains a discussion on the characterization of materials and stochastic variations; the procedure for characterizing material properties, including the AASHO Road Test materials, is explained in detail. Chapter 6 explains the use of elastic theory and layered analysis in the design of flexible pavements.

Part III consists of Chapters 7 through 10, which describe the development of distress models for quantification of total distress index, cracking index, rut depth index, and roughness index, respectively.

Part IV, Chapters 11 through 14, is devoted to verifying the developed models with the AASHO Road Test data and describes the use of the proposed procedure. Chapter 11 contains the verification of the distress models developed in Chapters 7 through 10. Chapter 12 summarizes the results of a small sensitivity analysis of the parameters in the cracking index model and establishes a format for a proposed detailed sensitivity study. Chapter 13 summarizes the proposed fatigue models, contains example problems, and compares the present FPS with the proposed fatigue procedure. This chapter also describes the revision of the present FPS model. Chapter 14 is devoted to implementation.

Part V, Chapter 15, is the summary, conclusions, and recommendations.

CHAPTER 2. REVIEW OF EXISTING THEORIES AND FLEXIBLE PAVEMENT DESIGN PROCEDURES

EXISTING THEORIES AND PAVEMENT DESIGN PROCEDURES

Flexible pavement design procedures in the beginning were primarily "rules-of-thumb," i.e., procedures based on past experience. During the period between the first and second World Wars, engineers made concerted efforts to evaluate pavement performance and plate theory, and some rational methods for the design of rigid pavements were developed. Efforts to evaluate the structural properties of subgrade soil and to classify soils for use in correlating pavement performance with subgrade type also continued. The limitations to obtaining successful and satisfactory results were partly due to the limited knowledge of the behavior of materials and appropriate failure mechanisms and in part to the limited analytical solution techniques available for the complex functions required. Application of Boussinesq's theory of stresses in ideal masses was developed in 1883, but it was not until 1943 that Burmister first put forward his layered theory for two layers and conceptually presented the solution for three-layered system, giving some rational basis for the design of flexible pavements (Ref 14).

With the advent of World War II, the U. S. Army Corps of Engineers initiated a study of design methods that eventually led to the CBR design method. Following World War II, many state highway departments also started studies to develop pavement design procedures. Many independent design procedures were developed, based on various soil tests that were correlated with pavement performance, environmental considerations, experience, and theories, and at the present time numerous design procedures are in use.

Over the years, several road tests (Table 2.1) have provided a wealth of experimental data and observations. The AASHO Road Test, which cost about $30 million, was one of the most successful. One of the major objectives of the AASHO Road Test was to provide information which would be used in developing pavement design criteria and design procedures.

TABLE 2.1. IMPORTANT ROAD TESTS

Road Test Name	Year	Agency	Pavement Type
Arlington Test (Virginia)	1919	BPR	flexible and rigid
Bates Road Test (Illinois)	1920-23	BPR	flexible and rigid
Pittsburgh Road Test (California)	1930-40	Columbia Steel Co.	rigid
Stockton Road Track (California)	1930-40	Corps of Engineers	flexible
Hybla Valley (Alexandria, Virginia)	1944-54	HRB, AI, BPR	flexible
Maryland Road Test (Maryland)	1950-51	AASHO	rigid
WASHO Road Test (Idaho)	1952-53	WASHO	flexible
AASHO Road Test (Illinois)	1958-61	AASHO	flexible and rigid

BPR - Bureau of Public Roads

HRB - Highway Research Board

AI - Asphalt Institute

AASHO - American Association of State Highway Officials

WASHO - Western Association of State Highway Officials

The Committee on Theory of Pavement Design of the Highway Research Board recently prepared a review of existing theories and methods of pavement design (Ref 183). In their report, the design procedures are grouped under the following headings:

(1) elasticity methods,
(2) ultimate strength methods,
(3) semi-empirical and statistical methods, and
(4) empirical and environmental methods.

The elasticity methods are based on the criterion of limited stresses or strains as determined by calculations based on the theory of elasticity for certain values established empirically as safe. The ultimate strength method assumes that a pavement possesses an adequate safety factor against an assumed shear failure of the pavement system. The semi-empirical and statistical methods are based on studies of observed field behavior, followed by statistical analysis of data to correlate performance and other design factors involved. In the empirical and environmental methods, the pavement is designed based on soil classifications and environmental conditions. It can be seen that the bases for these four methods are quite limited in scope, and none of the methods can predict the actual distress manifestations during and at the end of the design life.

Methods based on systems approach, which can be considered the latest and best available, are discussed separately in more detail for the following reasons:

(1) to give background information for development of the new models developed in this dissertation;
(2) to show the lack of a rational basis and the improvements needed; and
(3) because the new design models developed in this dissertation, when included in the existing flexible pavement systems (FPS), will lead to the flexible pavement system - second generation.

EXISTING FLEXIBLE PAVEMENT SYSTEMS MODELS

It is practically impossible to describe completely pavement behavior with a single equation or model. To define this behavior and solve the problem of pavement design, a systems approach is required. It is a framework within which the multitude of physical and socio-economic variables involved can be sorted out and related in a meaningful way. For this study, systems approach is

defined as a systematic way of approaching, modeling, and solving a problem, utilizing available manpower, money, material, and time in the best possible way.

A 1967 NCHRP project led to the first work applying systems engineering to pavement design (Ref 78). In a similar but independent effort, Hutchinson and Haas (Ref 82) applied the systems approach to structuring the overall problem and several of the subsystems design problems. A phase development and description of the pavement systems is fully presented in Ref 81. The systems approach was recognized as the most logical by a large number of pavement design engineers at the Highway Research Board Workshop on Structural Design of Asphaltic Concrete Pavements at Austin, Texas, December 1970.

Development of Existing Flexible Pavement System

Two systems models for the design of flexible pavements, one based on deflection and the other on structural number, have recently been developed for the Texas Highway Department under the Cooperative Research Program (Ref 81). The primary purpose of the existing flexible pavement systems method was to provide the designer with a means for investigating a large variety of pavement design options in a systematic and efficient manner. It was not intended to replace a designer's decision-making prerogative, but rather to give him increased scope and flexibility (Ref 81).

The mathematical models developed for FPS are based on the established objective of providing from available materials a pavement capable of being maintained above a specific level of serviceability over a specified period of time, at a minimum overall cost. The computer program was written to provide an output of feasible pavement designs sorted by increasing total cost, to help the designer or decision-maker to make his choice as quickly and easily as possible (Ref 81).

Inputs and General Description of FPS (Ref 81)

Each of the two FPS models consists of a set of mathematical models that may be broken down into four types: (1) physical, (2) economic, (3) optimization, and (4) interaction.

A large number of input variables are considered in FPS to simulate the total pavement design approach as closely as possible.

Physical Models. These are simulations of the real-world performance of a pavement during the analysis period. Traffic models predict the traffic during the analysis and performance periods; environmental models take into account environmental conditions, considering temperature, regional factor, and swelling clay parameters; performance models predict the behavior of the pavement, based on the present serviceability index (PSI) concept developed at the AASHO Road Test, and include a pavement strength model based on either (1) surface curvature index (SCI) or deflection model (Ref 162), or (2) structural number and soil support models from the AASHO Road Test.

In the deflection model, the material in each layer is characterized by a stiffness coefficient which is entirely different from the structural number coefficients in the AASHO Interim Guides. The stiffness coefficient values for different materials are based on field measurements of pavement deflection.

The structural number model is based on the structural number and soil support parameters developed at the AASHO Road Test. Using the information from the AASHO Road Test, the AASHO Committee on Pavement Design developed a design method that was issued in the form of Interim Design Guides (Refs 64 and 65) in 1962. It was emphasized that the design guides were interim in nature and subject to adjustment based on experience and additional research. It was noted that careful consideration was required to assign strength coefficient values to materials not used at the Road Test. The design equations were derived for

(1) a specific set of paving materials,

(2) a single environment,

(3) an accelerated traffic period (two years compared to a normal design period of 20 years), and

(4) identical traffic (mixed traffic was not applied).

Though the Interim Guides approach is sound in that it recognizes the importance of soil support, traffic load applications, and climatic conditions, however, the problem is to quantify the effects of all these factors on some rational basis. In spite of large variability, certain weighted average values have been considered as constants and are used as the coefficients of relative strength in the pavement design procedure of the Interim Guide. The term "coefficients of relative strength" is misleading as these are essentially the regression coefficients in the structural number of thickness index equations

and supposedly represent some material characteristics. The values of 0.44, 0.14, and 0.11 represent weighted averages of coefficients of relative strength a_1, a_2, and a_3 determined from an analysis of performance and design (Ref 70). Actually these coefficients in the analysis varied from 0.83 to 0.33, 0.25 to 0.11, and 0.11 to 0.09, respectively. It is difficult, therefore, to consider the design performance relationships of AASHO as exact. To establish coefficients of relative strength for any other material as constants is also very difficult. Though it was appreciated and pointed out that these coefficients were related to the physical properties of the materials, no definite formulation was offered for the correct properties. Different agencies have made efforts to predict the correct values of these coefficients through correlations with CBR, cohesiometer values, and Marshal stability, but these correlations are also empirical.

In NCHRP Project 1-11 (Ref 117), a method was developed for selecting the structural coefficients based on layered elastic theory. Vertical compressive strain on the subgrade, surface deflection, and tensile strain of the asphaltic concrete were selected as the criteria to establish structural layer equivalency. It was shown that the equivalencies can vary according to various geometric environment and loading conditions and that several assumptions were required to account for these conditions. Charts were developed in terms of selected material properties, but these are also only approximate.

Even such a major effort as the AASHO Road Test could produce only an interim design guide, subject to adjustment based on experience and additional research.

NCHRP Project 1-11 (Ref 117) was conceived to evaluate the various techniques used and the results obtained by the individual states after applying the guides to pavement structure design. This information was collected from the various states and the results were summarized (Table 1 of Ref 117). The importance of the AASHO Interim Guides is apparent from its use by about 32 states. They are being widely used, partly because of the unavailability of any other, better, and more rational design procedure.

Economic Models. Economic models are used to determine the total cost of a design as well as a breakdown of the cost. All costs are converted to present value at appropriate interest rates which are supplied by the user. The present value represents the amount of money which would, if invested at the

present time, generate funds to accomplish the design scheme as specified. There are seven types of economic models used in FPS.

(1) initial construction cost model, which determines the cost of the initial construction based on the cost per compacted cubic yard of each material used;

(2) seal coat cost model, which calculates the present cost of the seal coats required during the performance period;

(3) overlay construction cost model, which together with a physical model determines when and how much to overlay as well as the cost;

(4) routine maintenance model, which predicts the cost of routine maintenance based on the optimum overlay and seal coat schedules;

(5) user's cost model, which determines the cost to the user due to traffic delays during overlay construction;

(6) salvage value model, which determines the value of the pavement remaining at the end of the analysis period; and

(7) total overall cost model, which relates all costs during the analysis period to their present value at the beginning of the period.

Optimization Models. The two optimization models used in FPS to determine a set of optimal designs, based on overall cost, are

(1) modified branch and bound technique, which systematically determines which initial construction designs will lead to a set of optimal designs.

(2) determination of the optimal overlay policy for each initial design, considering all possible policies.

Interaction Models. An interaction model is an algorithm which defines the interactions between two or more other models. For example, in finding the life of initial and overlay construction designs, a time must be determined which will satisfy both performance and traffic models. Because of the complexity of these models, it is necessary to use an iterative technique.

Design Flow Chart of FPS. A design flow chart for the deflection version, FPS2, is shown in Fig 2.1. The flow chart for the structural number version of FPS is similar except for a few changes in the list of parameters. This chart shows all parameters involved in the various models of FPS2. The design strategies consist of schedules giving optimal cost, pavement life, overlays, material arrangement and thickness, and seal coat. Each schedule is calculated by consideration of the various parameters, shown in boxes. From the flow

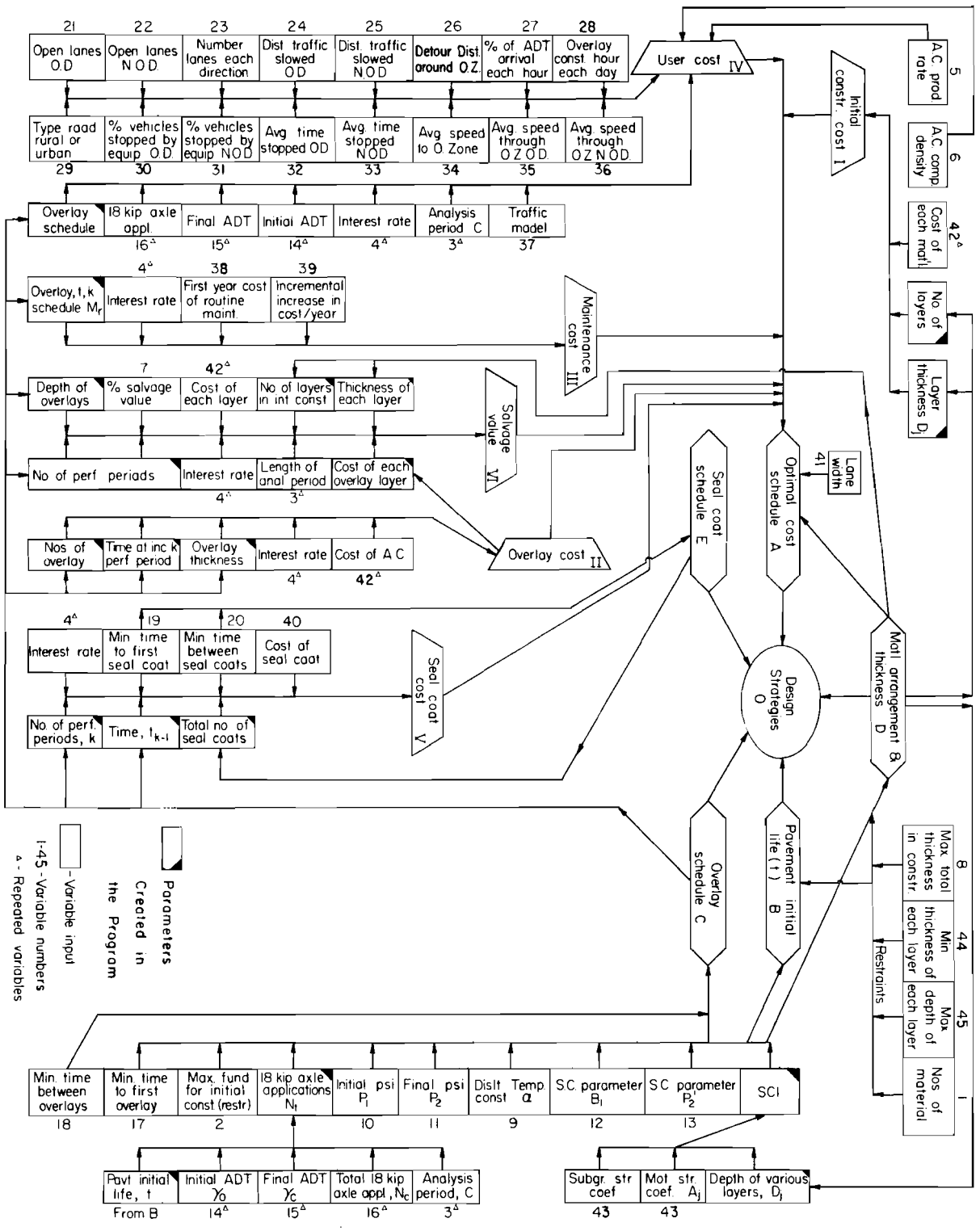

FIG. 2 1 FPS-2 DESIGN FLOW CHART

chart, it can be seen that the program involves a large number of variables (the number of inputs into the program is $\overline{6n + 44}$, where n is the number of materials considered for use above the foundation) which are intercorrelated in a complex optimization technique.

CHAPTER 3. DEVELOPMENT OF SECOND GENERATION FLEXIBLE PAVEMENT SYSTEMS

INTRODUCTION

The review of existing theories and various design procedures for flexible pavements in Chapter 2 showed the diversity and lack of rational basis for some present design procedures and the need for development of an improved design procedure.

The two existing flexible pavement systems models were also discussed in Chapter 2. A detailed evaluation of the FPS models in this chapter will show the need for updating and improving these models. Improved and updated structural design models, based on proper fatigue and stochastic considerations, are developed later in this report. These structural design models technically would fit into both existing FPS computer programs.

A basic work plan outlined in this chapter for the fatigue subsystem establishes the format of work plans for other areas, such as temperature stresses and stochastic variations in input design variables, which will be included in the existing FPS models at the appropriate stages.

EVALUATION OF THE EXISTING MODELS

Performance of a pavement is a measure of the accumulated service it provides and a function of the present serviceability history of the pavement, according to the AASHO concept of present serviceability index (PSI). The distress mechanism is the response which can lead to some form of distress when carried to a limit. Figure 3.1 shows the categories and examples of distress mechanisms in the pavement system.

Literature review shows that the best means presently available to account for all the distress modes in a pavement in the three categories shown in Fig 3.1 is the present serviceability index dquation developed at the AASHO Road Test (Ref 70). The roughness in the AASHO Road Test (Eq A7.1) is a function of distortion and disintegration modes. The cracking and patching terms are related to all three distress modes, and rut depth is a function of distortion mode only (Ref 78).

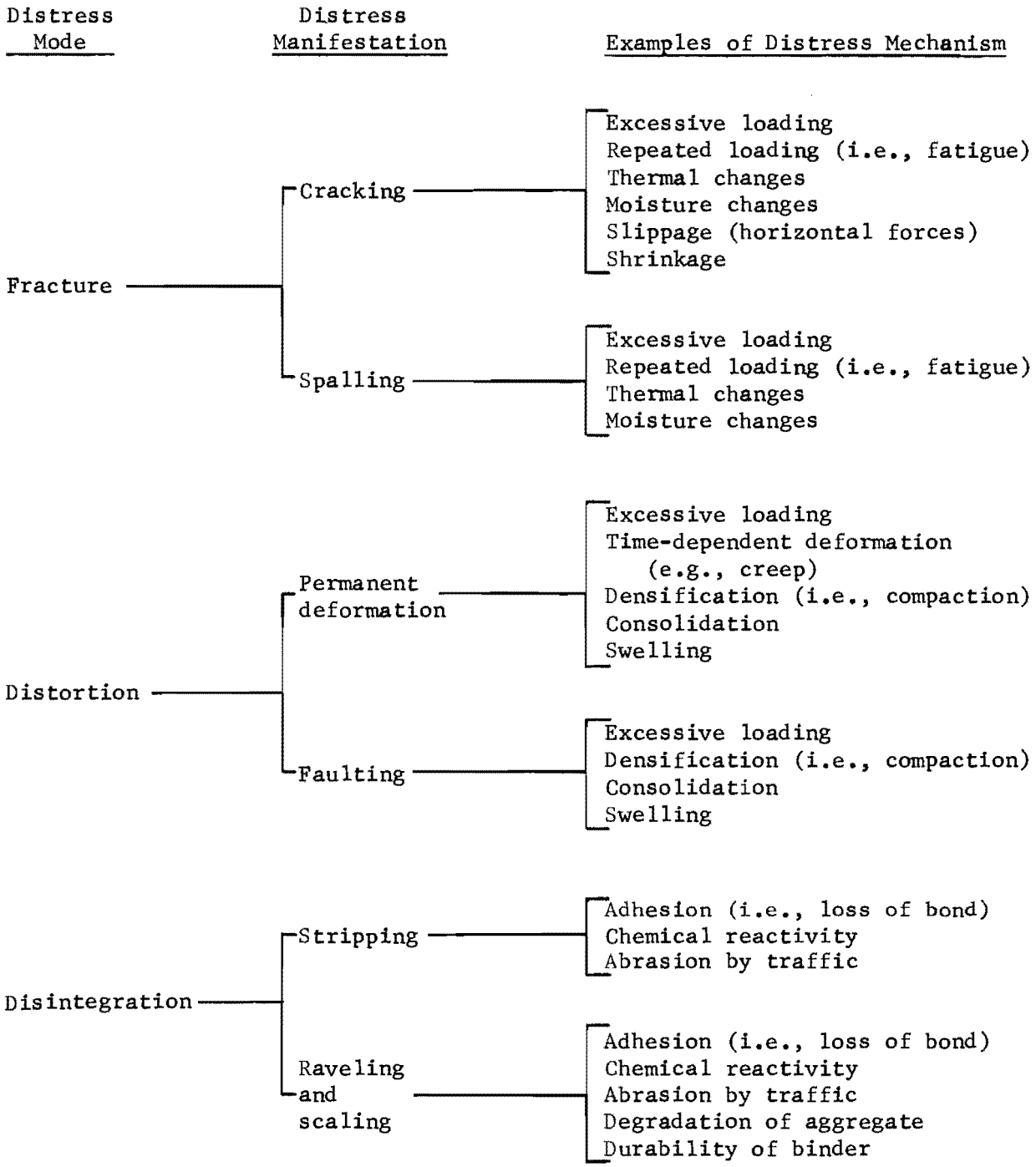

Fig 3.1. Categories of pavement distress (After Ref 78).

The FPS models (Ref 81) utilize the AASHO concept of pavement performance and are based on field results from AASHO Road Test and Texas Transportation Institute (Ref 158) test sections. The FPS also incorporated many variables to select a best and most economical design. Therefore, the FPS models represented the latest and best available design procedures. Though an effort was made to include as many factors from Fig 3.2 as the present state-of-the-art would permit, many factors still required improvements and considerations, as discussed below.

One of the distress mechanisms included in the systems approach for pavement design as a part of the failure mode is the fatigue of pavement materials (Fig 3.2). Fatigue plays a very important role in the design of a pavement structure and it should receive particular attention in the development of a working systems design model. This important mode of failure has not been given complete consideration in FPS, although the number of repetitions of axle load in FPS considers some kind of fatigue mode. The number of repetitions N, however, are related to PSI only empirically without any theoretical basis and without consideration of actual fatigue behavior of materials under repeated stress and strain. Fatigue theory, as it applies to the new design procedure, is discussed in detail in Chapter 4.

In the deflection model of the FPS, the materials in each layer are characterized by a stiffness coefficient, but no way has been found for defining or predicting the values of these coefficients from laboratory tests with suitable accuracy. These must be estimated from deflection measurements made on the same type of material on an existing pavement located in the same general area as the planned facility. The accuracy of the prediction of these coefficients by this method for the other materials is doubtful. In the AASHO model, the values of strength coefficients are empirical and, as discussed in Chapter 2, cannot be determined accurately by any available test method.

In the present FPS, the history of change in material properties during the lifetime of the pavement is not taken into account. At the time of an overlay, the material thicknesses and their original strength coefficients are assumed.

Structural number SN or surface curvature index SCI (Ref 81) are directly related to present serviceability index PSI without consideration of the stresses and distress in individual layers. Sections with the same SN or

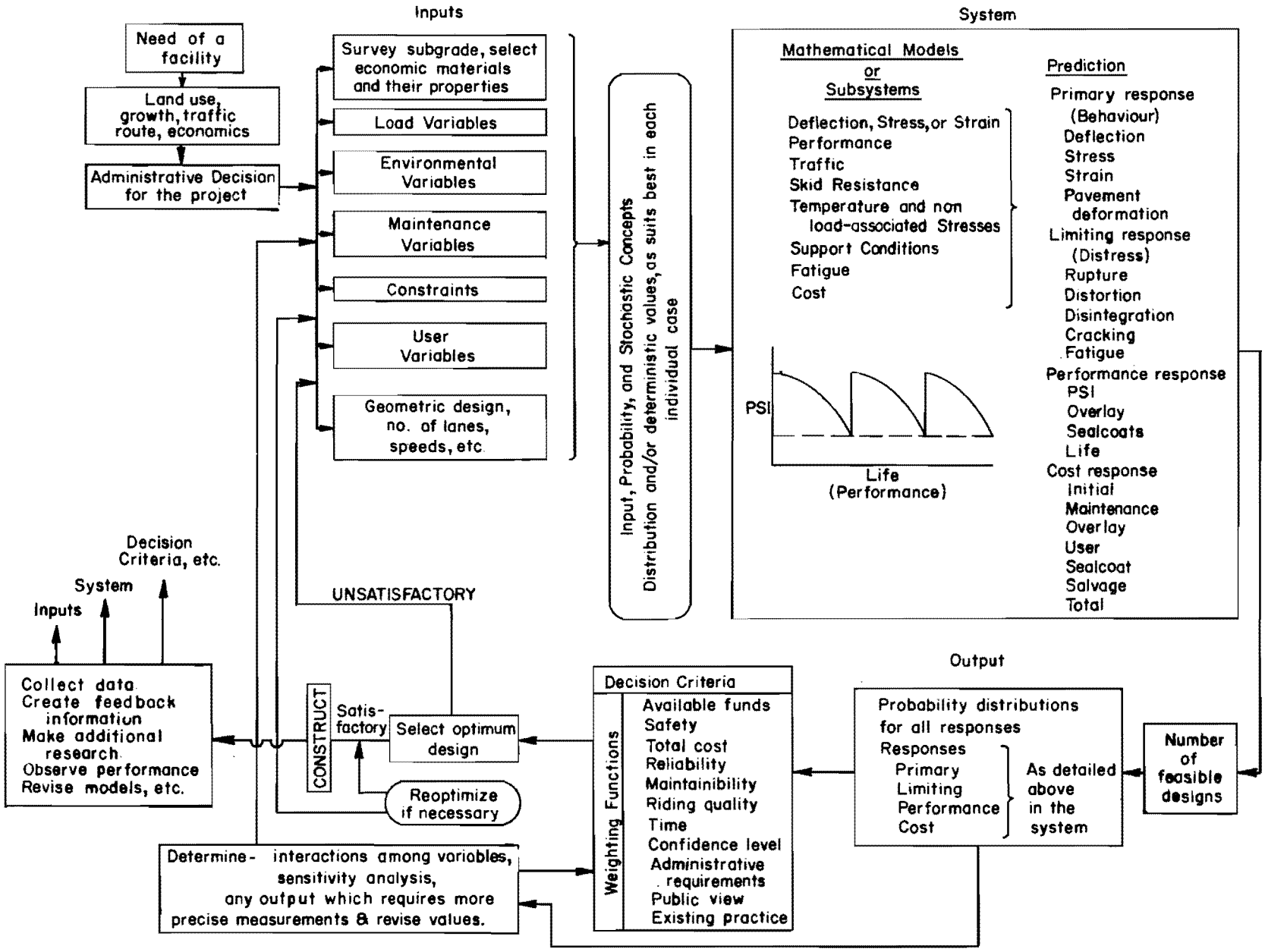

Fig 3.2. Conceptual pavement design system.

SCI are assumed to behave in the same way, irrespective of different combinations of thicknesses.

These methods use either strength coefficients or structural numbers; but neither strength coefficients nor structural numbers can be correctly defined nor assigned units, nor can their values be accurately predicted from laboratory tests.

Engineers working with materials recognize that the properties of materials in a specimen vary considerably from point to point and from time to time. These variations are certain to occur in a pavement structure also. Although these variations are recognized from a practical standpoint, the FPS or any other current design procedures do not take this variation into account directly.

In the present FPS model, as shown in Fig 3.3, the material properties, loading conditions, axle applications, and environmental conditions as input are related to the output, i.e., PSI, only empirically. Some rational and theoretical basis is needed for correlating the above factors. Different distress manifestations are not quantified separately.

The swelling clay parameters in the present FPS are very empirical in nature and need to be quantified on some theoretical basis.

PROPOSED REVISION OF FPS

Based on some noted discrepancies of FPS design methods and other factors discussed herein, a revision to the existing FPS is presented.

Factors to be Considered in the Design of Flexible Pavements

The design of flexible pavement requires consideration of several complex and interrelated factors. The conceptual pavement design system shown in Fig 3.2 details the inputs to the system, the different models needed, the predictions they provide, and the output from the system. It also includes the decision criteria and gives steps in selection of a best design. In the revision of the FPS, consideration of this conceptual pavement system is very important to assure that as many factors are included as the state-of-the-art permits.

Based on the work of Barksdale and Leonards (Ref 6) and other available literature, it appears that the following factors are those most important for the design of flexible pavements.

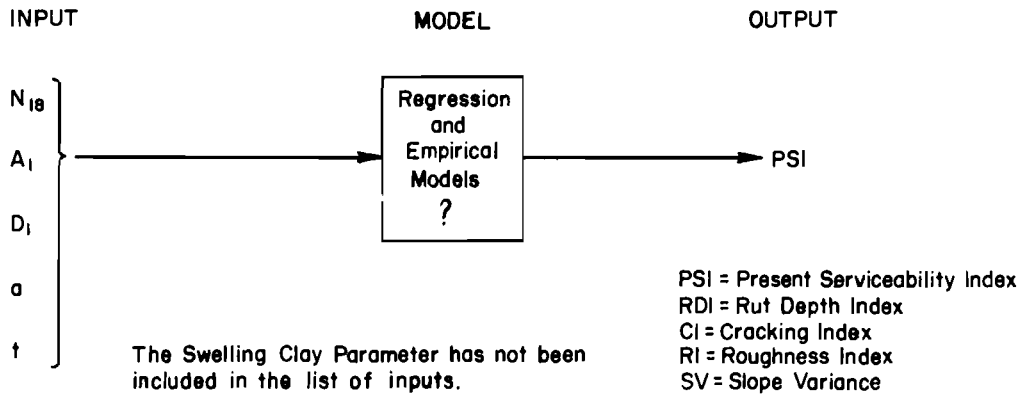

(a) Present FPS Model

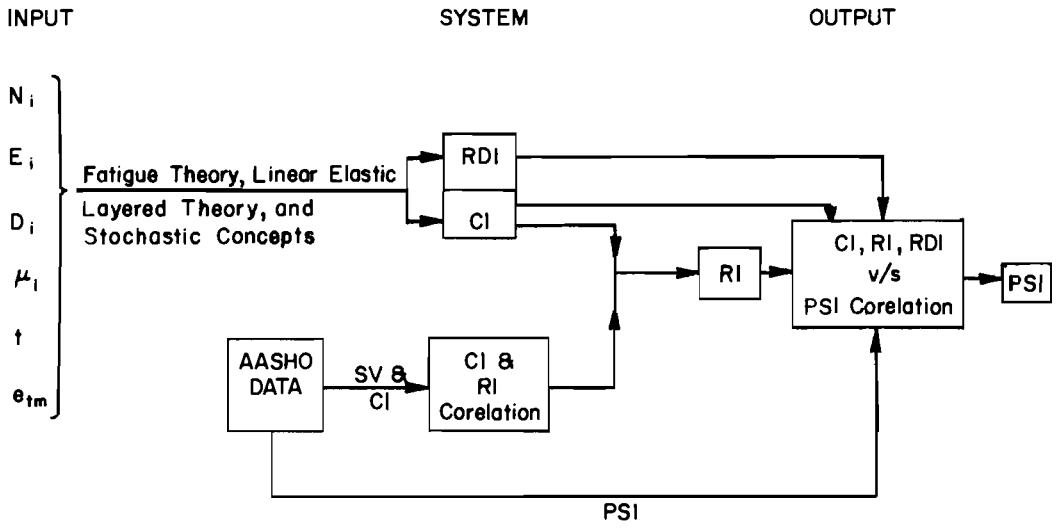

(b) Proposed FPS Model-Second Generation

N_i = Number of Single axle applications of i^{th} load group
N_{18} = Number of Equivalent 18 kip axle Applications
A_i = Structural Number or Strength Coefficent in AASHO & Deflection Model
D_i = Thickness of the Pavement Layers
E_i = Modulus Values of the Pavement Materials
μ_i = Poisson's Ratio
a = Daily Temperature Constant
t = Time since Initial Construction
e_{tm} = Environmental Effect of Temperature & Moisture Content

Fig 3.3. Present FPS model and proposed FPS second generation.

(1) Cracking and/or rutting due to stress and strain from wheel loads (Ref 6).

(2) Fatigue failure in the surface materials due to repeated flexing induced by elastic deformations in the underlying components of the pavement. Cracking of the surface materials can lead to deterioration of the entire pavement due to the resulting increase in transmitted stresses (Ref 6).

(3) Cracking and rutting of the surface material due to shear displacement and/or compaction of the base and subbase. Compaction of base materials generally leads to increased stability. Patching and resurfacing will restore the pavement, and further deterioration due to this cause is likely to be relatively minor. In any case, improved methods of compacting granular materials in the field and use of stabilized bases have reduced the occurrence of this defect (Ref 6).

(4) A general (punching) shear failure due to inadequate shear strength of the subgrade. Such failures occur rapidly under the action of a few heavy wheel loads and damage the pavement severely. A large increase in water content, due to frost action, for example, may lower the strength of the subgrade excessively. Proper subgrade sample analysis may help to avoid this type of failure (Ref 6).

(5) Cracking and rutting due to cumulative permanent deformation of the subgrade, base, and subbase layers which increases with increased stresses, traffic volume, and time (Ref 6).

(6) Aftereffects of cracking and rutting in the form of surface roughness or slope variance.

(7) Surface cracking due to extreme temperature variations.

(8) Other environmental effects, including the effects of foundations movements, swelling clays, asphalt oxidation, and change in support conditions.

(9) Effects due to stochastic variations in the material properties with space and time.

Extent to Which the Above Factors Are Considered at Present

On the basis of current theories, the ultimate strength methods discussed in Chapter 2 consider failure mechanisms (1) and (4) above. Layered theory can be utilized to calculate the stress and strain in the pavement layers to avoid failure mechanisms (1) through (5). However, none of the present procedures considered all the failure mechanisms (1) through (5). No theoretical approach is available to quantify the roughness of the pavement stated in item (6) above, other than the actual measurement of this distress on the pavements under consideration. Quantification of this distress by any theoretical means is open for future research. In this report, the surface roughness has been quantified by statistical analysis based on field data. Though a great deal of work has

been done for items (7), (8), and (9) and there are several ways to get qualitative information as to their effect on pavement, no quantitative and rational procedure is available which considers them in pavement performance.

SCOPE OF THE PRESENT REPORT

The proposed models for the design of flexible pavements developed in this dissertation utilize linear elastic layered theory, fatigue theory, and probability theory. Based on these theories and concepts as shown in Fig 3.3, factors (1) through (6) have been quantified on a more rational and theoretical basis. Factor (9) has been considered. The strength and stiffness coefficients of FPS are replaced by more realistic measurable properties, i.e., moduli of materials.

Considering the fatigue phenomenon, the systems input are correlated, in terms of measurable material properties, loading, and environmental conditions, to its distress manifestations, such as cracking and rut depth. Based on AASHO Road Test data, the correlation between cracking and roughness index is developed. The serviceability and performance concept of the AASHO Road Test has also been utilized. Thus, models are developed for distress manifestations to predict pavement performance and present serviceability index. The models have been verified with the AASHO Road Test data. In the present report, theoretical and empirical approaches have been combined to give the best design procedure possible within the present state-of-the-art.

In the revision of the FPS models, the new design models will replace the empirical relationship used at present to simulate the transformation between the input variables and performance of a pavement as shown in Fig 3.3. This revision will lead to the second-generation FPS. To develop second-generation FPS, the existing structural models for traffic load applications are replaced by the proposed design models, and existing economic and other models are used to study the various design strategies and obtain the best alternative design. The replacement of the existing FPS structural models for fatigue is explained in the following paragraphs.

The present serviceability index (PSI) of a pavement can be conceptually represented as

$$PSI = f[\text{fatigue (traffic load applications)}, \text{swelling clay}, \text{temperature stresses}] \quad (3.1)$$

For the second-generation FPS, the first term on the right of Eq 3.1 is quantified in this dissertation by improved performance and distress index models to replace the existing FPS structural performance model for traffic applications. The FPS swelling clay performance equation remains unchanged, but further improvements (Ref 187) in the models need to be investigated.

The last term of Eq 3.1, representing the deterioration in PSI due to major temperature stresses, is not presently considered in the FPS. Research on this item is in progress at the Center for Highway Research. The models developed for temperature stresses are planned for the second-generation FPS.

The existing FPS performance equation includes traffic and swelling clay parameters as given in Eq 3.2 (Ref 113).

$$P = 5 - \left[\sqrt{5 - P_{k-1}} + \frac{\beta S_k^2}{\bar{\alpha}} (N - N_{k-1})\right]^2 - 0.335 C_1 C_2 \left[e^{-\theta t_{k-1}} - e^{-\theta t}\right] \quad (3.2)$$

where

P = the present serviceability index at time t,

P_{K-1} = the present serviceability index at time t_{k-1},

β = a constant = 53.6,

S_K = the surface curvature index for K^{th} performance period,

N = the number of 18-kip equivalent load applications adjusted by the risk factors to give an acceptable confidence limit at time t,

N_{K-1} = the number of 18-kip equivalent load applications at the confidence level which occurred at the end of the $(K - 1)^{th}$ performance period,

$\bar{\alpha}$ = a temperature constant which varies geographically,

C_1 = the fraction of a roadway length that has expansive clay in locations that are likely to promote volume change,

C_2 = the maximum amount of differential heave that is likely to be noted along a roadway,

θ = a constant which determines the rate of heaving of the expansive clay.

$$N = \frac{N_c}{C_L(\gamma_c + \gamma_o)}\left[2\gamma_o t + \frac{\gamma_c - \gamma_o}{C_L} t^2\right] \quad (3.3)$$

where

N_c = the number of accumulated 18-kip equivalent load applications during the analysis period adjusted by the risk factor to give an acceptable confidence limit,

C_L = analysis period in years,

γ_o = average daily traffic at the beginning of the analysis period,

γ_c = average daily traffic at the end of the analysis period.

The underlined portion of Eq 3.2 represents the terminal PSI due to traffic load applications, and the other portion represents loss in the PSI due to swelling clay.

In the proposed models, the underlined portion of the existing FPS is replaced by the performance model developed in Chapter 7 (Eq 7.5) and distress index models developed in Chapters 8 to 10 (Eqs 8.7, 9.1, and 10.15). Based on values of distress indices computed from distress index models, the present serviceability index is obtained from the performance model (Eq 7.5). The PSI thus obtained is substituted for the underlined portion of Eq 3.2 and the final PSI is computed by subtracting the loss in PSI due to swelling clay. The distress index models and therefore the proposed performance model, as detailed in Chapters 7 to 10, is a function of several parameters, such as traffic load, actual number of traffic applications each month, the month in which the facility is opened for traffic, total time, several material properties and their stochastic variations, confidence level, deformation characteristics of materials, and environmental conditions, as compared to the factors in the existing FPS shown in the underlined portion of Eq 3.2.

The proposed procedure utilizes the actual load repetitions each month for each load group, instead of only one 18-kip equivalent load group. The traffic load repetitions N_{jt} for t^{th} month for j^{th} load group separately can be computed from Eq 3.4 if the traffic growth rate γ_j and initial traffic repetitions N_j of a load of level j are known:

$$N_{jt} = N_j(1 + \gamma_j)^t \tag{3.4}$$

However, if desired, with modification in the proposed procedure, Eq 3.3 can also be utilized for traffic computations.

Work on Items Not Covered in the Present Report

This report covers only a part of the whole work required to idealize the FPS models and continued research efforts are being made by various agencies and individuals (Ref 81) in this direction. Even for the second generation of FPS, further efforts are required and M. Y. Shahin and M. I. Darter, both of the Center for Highway Research, The University of Texas at Austin, are working to quantify the effects of surface cracking due to extreme temperature variations and stochastics for other variables not considered in this report, which will also be included in the second generation of FPS.

At present, the effects of foundation movements, asphalt oxidation, change in support conditions, etc., still need to be taken into account on some rational and theoretical bases and are fields open for further research.

BASIC WORK PLAN

The structural design procedure based primarily on fatigue and stochastic concepts and developed in this report can be considered as a subsystem of the whole "systems of pavement analysis, design, and management" or the "ideal pavement systems design" model. A flow diagram representing the work plan for developing this subsystem is shown in Fig 3.4. This figure represents a basic work plan for the subsystem developed in this report and it also establishes a format for other areas, such as the effect of extreme temperature variations, to be included in the pavement system in subsequent studies by others.

This report covers the steps that lead to development of a satisfactory design process; after that stage, the remaining process involves putting the concept into practice.

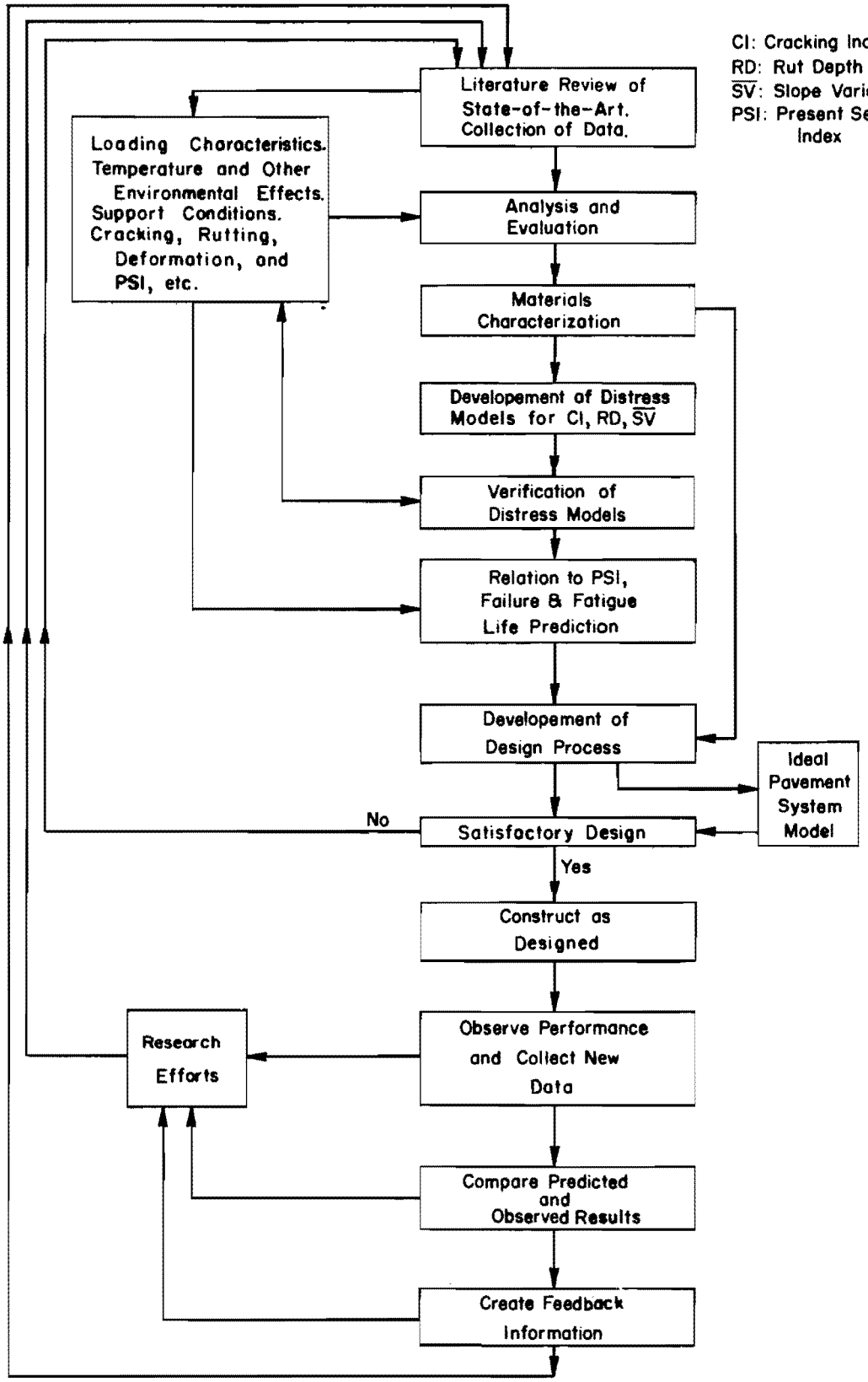

Fig 3.4. Basic work plan for a pavement design subsystem.

PART II

REVIEW OF AVAILABLE TECHNIQUES TO BE USED IN THE MODELS

CHAPTER 4. FATIGUE OF PAVEMENT MATERIALS

The importance of the proper consideration of fatigue* in pavement systems design and the proposed revision of the existing FPS models was discussed in Chapter 3. The object of this chapter is to provide an up-to-date review of fatigue theory as it applies to the design of flexible pavements in the design procedure proposed in this report.

INTRODUCTION TO FATIGUE

Fatigue type failure in the surface layer of a pavement, indicated by cracking on the surface, is caused by repeated tensile flexural strains from moving loads. As a wheel load passes over a pavement, it is subjected to a rapid build-up and decrease in stress, and the extreme fibers of the surface layer are subjected to repeated flexural strains. To simulate and study the effects of dynamic wheel loads, repeated load tests of surface, base, subbase, and subgrade materials are required. The material samples must be prepared and tested according to a procedure which closely simulates the field conditions.

Generally, the use of nomenclature in available literature for flexural fatigue tests on asphalt concrete and repeated load deformation tests on base, subbase, and subgrade materials has not been consistent and clear. The nomenclature used in this report is given in Appendix 6.

ASPHALTIC CONCRETE

Only in recent years has the fatigue behavior of bituminous materials been closely scrutinized; thus, the knowledge of asphaltic concrete fatigue behavior is not as well developed as it is for metals. In recent years

---

* The fatigue has been defined (Ref 42) as "Phenomenon of a fracture under repeated or fluctuating stress having a maximum value less than the tensile strength of the material."

considerable evidence has been accumulated to attest to the fact that flexible pavements exhibit distress due to flexural fatigue caused by the repetitive application of vehicular loads (Ref 100). Descriptions of fatigue studies development are given by Deacon (Ref 24) and Finn (Ref 42).

In 1953, Nijboer and van der Poel (Ref 24) suggested that fatigue may be a significant cause of cracking in asphalt pavements. Hveem (Ref 84) has presented evidence that distress due to fatigue cracking can and does occur in flexible pavements, especially when highly resilient subgrades are encountered. Extensive laboratory studies of asphaltic concrete mixture fatigue behavior have been carried out by Monismith et al at the University of California (Refs 124, 126, 127, 128, 129, and 130). Other investigators who contributed knowledge of fatigue in asphaltic concrete include Heukelom and Klomp (Ref 60), Saal and Pell (Ref 156), Papazian and Baker (Ref 141), Jiminez and Gallaway (Ref 95), Kirk (Ref 105), Vallerga (Ref 180), Garrison (Ref 48), Bazin and Saunier (Ref 5), and Finn and Hicks (Ref 181).

Finally, the WASHO and AASHO Road Tests proved that fatigue distress and failure are due to fatigue cracking in flexible pavements. Distress due to fatigue in pavements is influenced by heavy loads, a large number of repetitions, and the type of foundation materials.

Classes of Fatigue Cracking

Fatigue cracking in flexible pavements is generally characterized by map patterns (Ref 24). Four types of cracking were defined at the WASHO Road Test (Ref 74). In the AASHO Road Test (Ref 70), cracking was divided into three categories. Class 1 cracking was the earliest type observed and consisted of fine disconnected hairline cracks. As distress increased, Class 1 cracks lengthened and widened until cells were formed, causing alligator cracking, known as Class 2. When the segments of Class 2 cracks spalled more severely at the edges and loosened until the cells rocked under traffic, the situation was called Class 3 cracking.

Fatigue Failure Hypothesis

Pavement experiencing fatigue starts developing cracks which leads to other forms of distress. The combined effect of these distress manifestations is the measure of pavement performance. The process of fatigue deterioration may be described as

(1) existing flaws in the pavement, random distribution;

(2) nonvisible cracking: load repetition increases the number of flaws and widens existing flaws; this widening is not enough to be visible, but enough to cause distress and deformation. This stage is just prior to Class 1 cracks as defined earlier.

(3) visible cracking: Class 1 to Class 6 cracking as defined at the WASHO Road Test and Class 1 to Class 3 as in the AASHO Road Test. The increase in this form of cracking results in further increase of deformation in the form of roughness and rutting. Water percolation through these cracks may initiate the distress manifestations.

Cracking itself may be of a little significance in the PSI equation, but from the above discussion it seems that cracking is a good overall indicator of pavement performance and other forms of distress in the pavement. A hypothesis that cracking is preliminary to other forms of distress in a pavement, and the correlation of other distresses with the cracking index seems reasonable. Further development of design principles based on this type of hypothesis is dealt with in Chapter 10 of this report.

It is further hypothesized that as the fatigue cracking in asphaltic concrete starts from the existing flaws and the initial distribution of flaws in a structure is stochastic, the whole process of distress development and pavement performance prediction should be based on stochastic principles.

Laboratory Fatigue Tests

In fatigue testing the variation in the number of cycles to failure is usually quite large. The ratio of cycles to failure for identical specimens subjected to a given stress level has been reported to be as high as 100 to 1 (Ref 42). This fatigue is recognized as a stochastic process, and a sufficient number of specimens must be tested to predict a probability distribution (Ref 42).

Fatigue behavior in the asphaltic concrete is generally determined in repeated flexural tests in the laboratory in two ways:

(1) controlled constant load, or stress; and

(2) controlled constant deflection, or strain.

The controlled stress mode of loading results when the magnitude of the repetitive load applied to the test specimen is maintained constant. In such a test, the deflection of the specimen under each successive load application will gradually increase as damage occurs. In the controlled strain test, the

deflection or strain within the test piece is maintained constant by controlled reduction of each load applied to the specimen as damage is accumulated. Figure 4.1 illustrates each of these test modes (Ref 100).

Hicks (Ref 62) has attempted to evaluate the applicability of the controlled stress and strain tests on the basis of computations of elasticity applied to a three-layer pavement. Computations were based on a uniform surface load of 70 psi over a 5-inch radius. Figures 4.2 and 4.3 summarize the results of computations for tensile strain in the under side of the surface layer. In Ref 42 it was shown that a 1-inch thickness of asphaltic concrete surfacing would, for a given loading, be subjected to constant strain regardless of the total thickness of the pavement and the stiffness modulus of the asphaltic layer. Therefore, a constant-strain fatigue test was suggested for thin surface layers. Computations for stress are shown in Figs 4.4 and 4.5. These indicate that the thicker sections are subjected to a relatively constant stress, which suggests the constant stress mode of testing for thicker pavement surfaces (Ref 42).

In a fatigue life study of asphalt and cement-treated bases Gallaway (Ref 46) has made some plots based on linear elastic layered theory and verifies that thicker sections are subjected to a relatively constant stress condition.

Monismith in a paper presented at the University of Nevada in 1966 has suggested that for surface layers less than 2 inches thick the controlled strain mode of testing is applicable, while for asphaltic concrete layers 6 inches thick or greater, the controlled stress mode of loading is appropriate. Between these two thicknesses some intermediate mode of loading should be applied (Ref 100).

In NCHRP Report 39 (Ref 42), Finn explained that in addition to other reasons the in-situ pavement will generally be subjected to constant load conditions, and the loads during the lifetime will not be reduced to maintain a constant strain in the asphaltic layer. From this he concluded the constant stress test to be a more logical mode of laboratory testing for pavement designs.

Based on the following considerations, Kaisianchuk (Ref 100) suggested the controlled stress mode of loading to determine the fatigue response of the asphalt concrete:

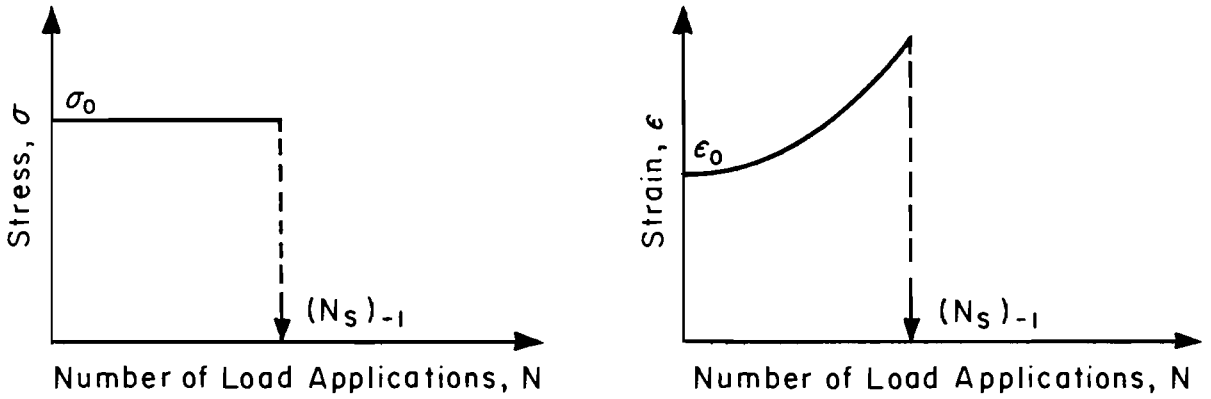

(a) Controlled - stress loading.

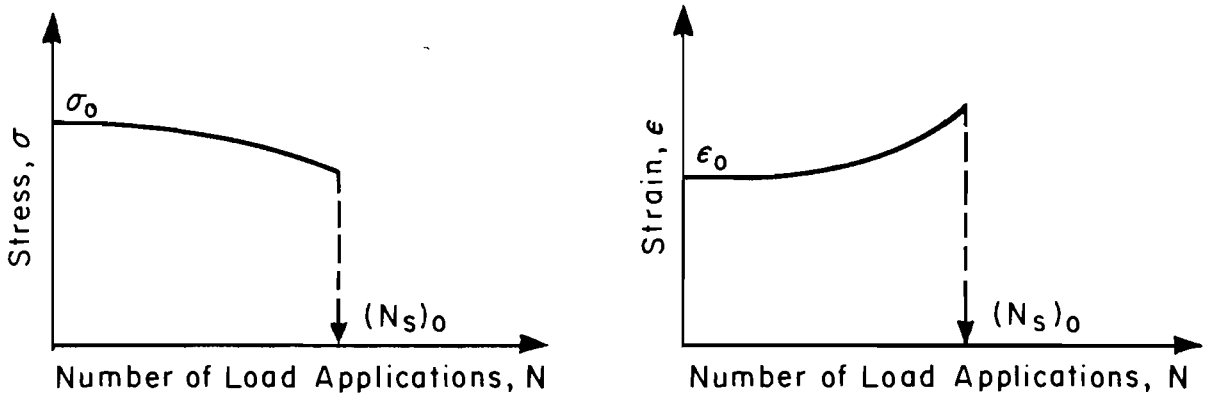

(b) Intermediate mode of loading.

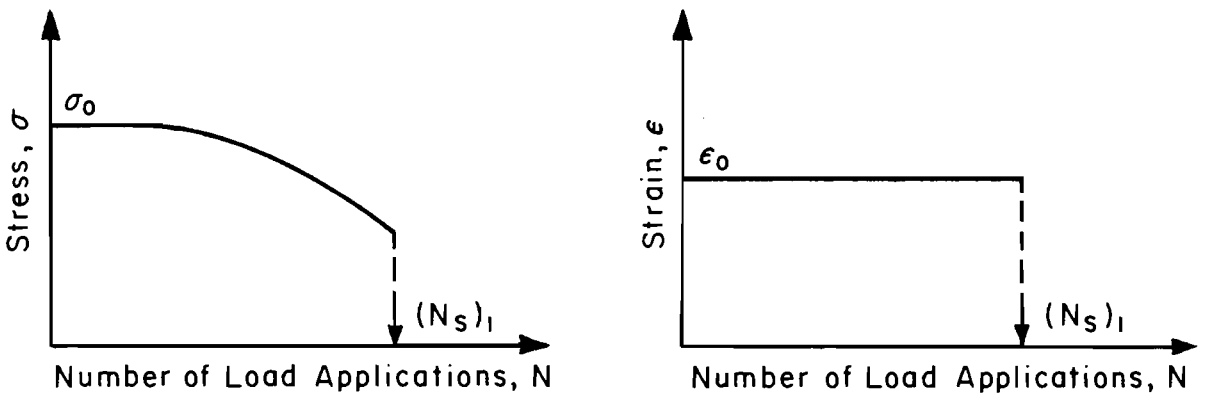

(c) Controlled - strain loading.

Fig 4.1. Schematic representation of fatigue behavior of asphalt paving materials for various modes of loading (after Monismith and Deacon).

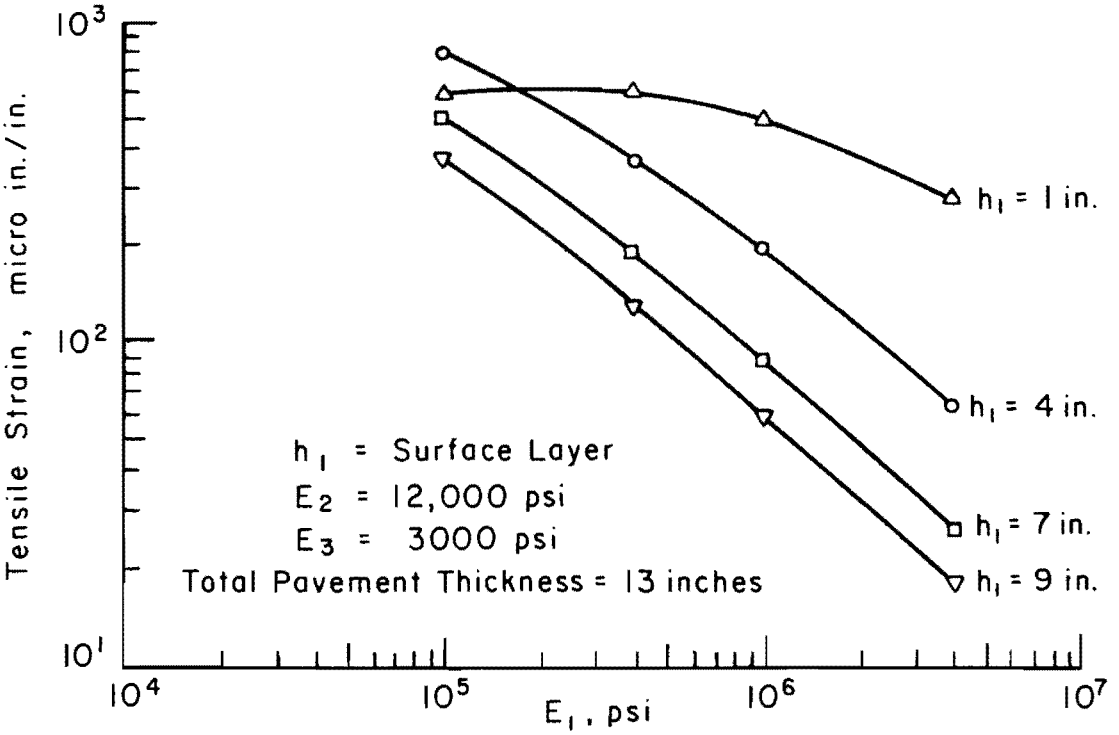

Fig 4.2. Induced tensile strain as a function of surface modulus, thin section (after Hicks).

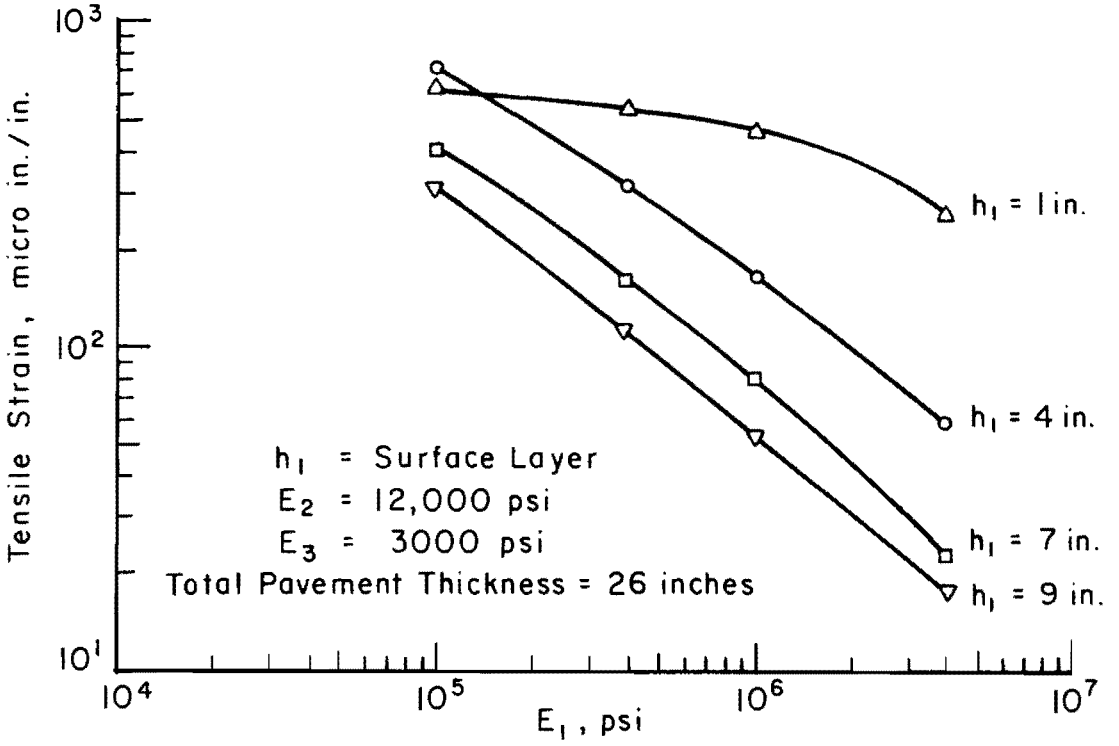

Fig 4.3. Induced tensile strain as a function of surface modulus, thick section (after Hicks).

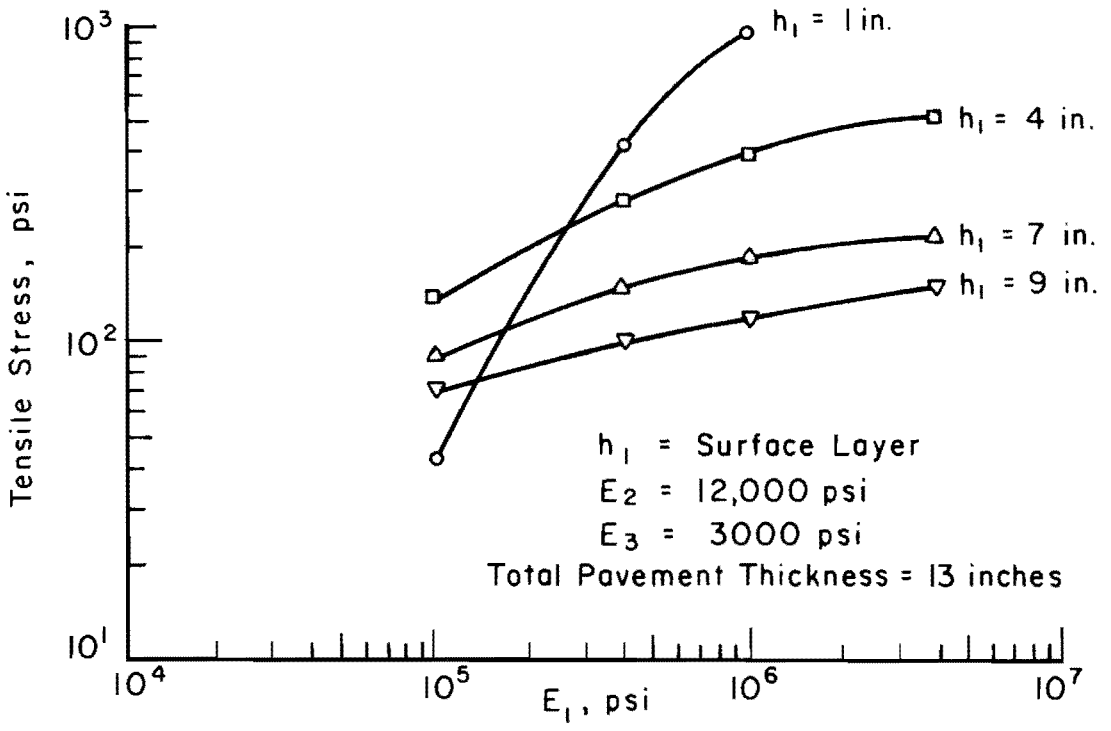

Fig 4.4. Induced tensile stress as a function of surface modulus, thin section (after Hicks).

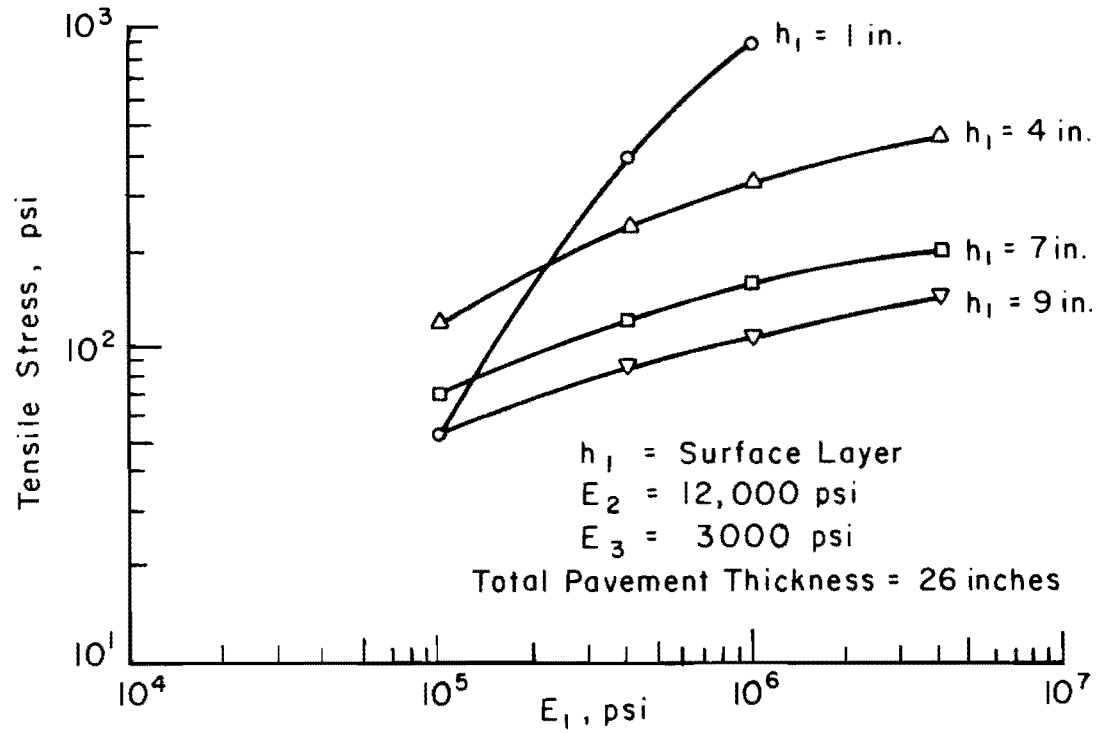

Fig 4.5. Induced tensile stress as a function of surface modulus, thick section (after Hicks).

(1) The majority of pavements in which fatigue in asphaltic concrete need be considered will be those in which high traffic volumes and weights will require relatively thick asphaltic concrete layers. In these cases, the controlled stress mode of loading is applicable.

(2) In the relatively small number of cases in which the controlled strain mode of test is applicable, the controlled stress mode will lead to shorter predicted lives and is, consequently, conservative.

(3) The controlled stress mode of loading fatigue test results in complete fracture of the test specimen so that no difficulties arise regarding the definition of service life. The test can also be more easily performed in that no regulation of loads is required.

In view of these discussions, fatigue test results based on the controlled stress mode of loading will be adopted in this report, as given in the following paragraph.

Fatigue Test Results

Laboratory fatigue test results are typically plotted as fatigue life against some measure of the load magnitude repeatedly applied to the test specimen. For the case of the fatigue testing of asphaltic concretes there is evidence (Ref 42) that this relationship may be adequately represented by a straight line on a plot of the logarithm of the fatigue life against the logarithm of the tensile strain level. For the controlled stress mode of testing, in which the strain level varies throughout the test, this linear relationship holds when the initial level of strain is employed. The logarithmic linear relationship can be expressed, as has been done by Pell (Ref 146) and Deacon (Ref 24), by an equation of the form:

$$N_j = A \left(\frac{1}{\epsilon_j}\right)^B \tag{4.1}$$

where

N_j = cycles to failure at a particular stress level,

ϵ_j = bending strain,

A and B = constants depending on mixture characteristics.

NCHRP Report 39 (Ref 42) contains a discussion of asphaltic concrete fatigue behavior under repeated loading. The following is a summary of the significant results of pertinent field and laboratory studies given in the report:

(1) Fatigue behavior of asphaltic concrete is similar to that of metal, wood, portland cement concrete, etc., and it appears in laboratory tests as well as in the field.

(2) A linear relationship exists between the log of stress or strain level and the log of repetitive loads to failure.

(3) Generally constant stress-type tests will respond with an increasing fatigue life to any mix property which increases the stiffness of the asphaltic concrete. For constant strain tests, the effect of stiffness modulus is reversed. However, at a very low temperature (approximately 32° F), the fatigue life is unaffected by the mode of testing. Table 4.1 exhibits some basic parameters to be considered in the discussion of the laboratory fatigue life test results applicable to the design of pavements. The table exhibits the effect of these parameters on the stiffness and fatigue behavior of asphalt concrete mixtures.

(4) Longer durations of load application are associated with reduced fatigue life.

(5) The change in stiffness modulus, deflection, or modulus of rupture during repetitive loading tests may be used to measure fatigue damage. A higher rate of damage appears to occur with the first 10 percent of the repetitive loadings, with a relatively constant and somewhat reduced rate for the next 80 percent of the loadings, followed by an abrupt change to failure.

(6) Tensile strain is the prime determinant of fatigue life. The test results when converted from stress to strain are essentially independent of the rate of loading (at least for less than 30 applications per minute) and temperature and closely follow the straight line realtionship given in Eq 4.1. Any difference in the test results was explained as due to the difference in the rate of crack proportion.

(7) Stress reversal appears to have little effect on the rate of the asphalt concrete cumulative damage.

(8) As long as the temperature and rate of loading do not vary markedly, a mixture of asphaltic concrete will act elastically up to approximately 0.1 percent strain. Thus, it is possible to analyze asphaltic mixtures according to the theory of elasticity for a given situation as represented by a modulus of elasticity or stiffness modulus value.

(9) Test procedures described in the report can be combined with the multilayered theory for computing stress and strain in the asphaltic surfacing and used, at least qualitatively, to predict expected performance.

TABLE 4.1. FACTORS AFFECTING THE STIFFNESS AND FATIGUE BEHAVIOR OF ASPHALT CONCRETE MIXTURES (After Kasianchuk)

Factor	Change	Result of Change		
		Stiffness	Fatigue Life in Controlled Stress Mode of Test	Fatigue Life in Controlled Strain Mode of Test
Asphalt penetration	Decrease	Increases	Increases	Decreases
Asphalt content	Increase	Increases(1)	Increases(1)	Decreases(2)
Aggregate type	Increase roughness and angularity	Increases	Increases	Decreases
Aggregate gradation	Open to dense gradation	Increases	Increases	Decreases(2)
Air void content	Decrease	Increases	Increases	Increases(2)
Temperature	Decrease	Increases(3)	Increases	Decreases

(1) Reaches optimum at level above that required by stability considerations.
(2) Not based on significant amount of data but seems reasonable on basis of other information.
(3) Approaches upper limit at temperature below freezing.

The use of constant stress test results in pavement design reduces the efforts required for laboratory fatigue investigations and provides the basis for development of a rational pavement design procedure based on fatigue, by use of Eq 4.1 and fatigue damage hypothesis.

Further simplification of laboratory investigations would make the design method even more practical. As observed by Kaisianchuk (Ref 100), attempts are being made to provide more simplifications.

Damage Hypothesis

Deacon (Ref 24) performed an analysis of the applicability of various compound loading hypotheses to the prediction of asphaltic concrete fatigue life from simple loading test results. The best available hypothesis seems to be the simple linear summation Miner's hypothesis (Chapter 8), and it will be used in this report.

Application of Fatigue Equation and Miner's Hypothesis

The application of the fatigue equation (4.1) and Miner's hypothesis is explained by the flow diagram shown in Fig 4.6.

The strain induced by the applied load is calculated by layered analysis. Substitution of the strain value in Eq 4.1 gives the value of N_j, the number of load applications of level j which will cause failure in simple loading. This value of N_j when substituted in Miner's hypothesis along with the known value of actual number of load applications of level j, n_j will give the "used life" of the pavement. The use of this life prediction in the actual design procedure as developed in this report is explained in Chapter 8, under development of the cracking index model.

UNTREATED GRANULAR AND FINE GRAINED MATERIALS

Untreated granular and fine grained materials have different fatigue problems than asphaltic concrete. Repeated applications of loads may result in sufficient cumulative permanent deformations in pavement layers consisting of these materials to cause failures, although a single application of the load would not. These materials in a pavement are normally subjected to a triaxial state of stress. Therefore, the fatigue behavior of these materials under an imposed traffic loading sequence must be analyzed for induced deformations under triaxial states of stress. Although it is unlikely that a method

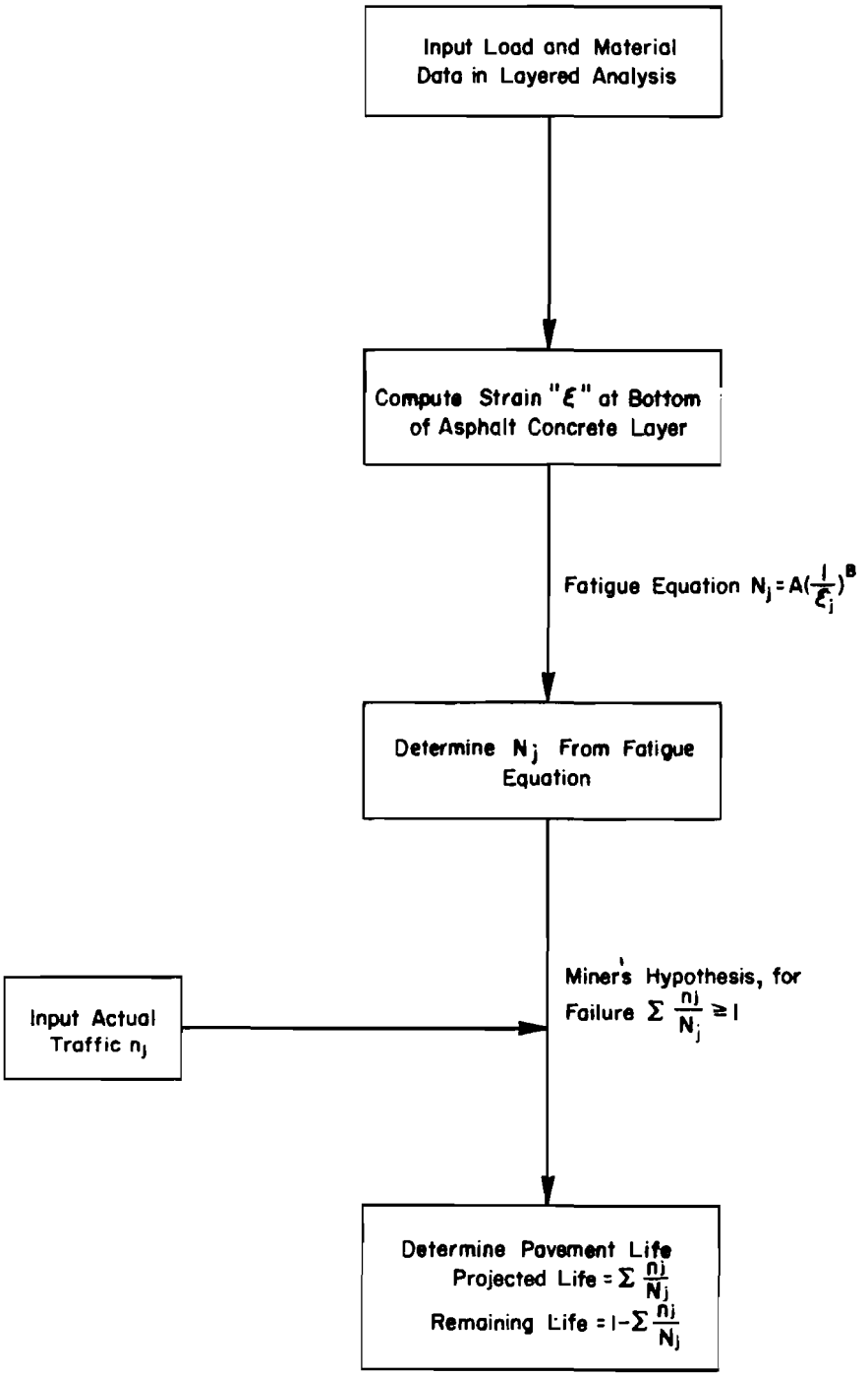

Fig 4.6. Life prediction from fatigue and Miner's hypothesis.

of pavement design will ever be developed to account for the true behavior of the complex polyphase materials used in flexible pavement, the following steps may prove to be a reliable practical approach for taking into account the proper fatigue behavior of these materials:

(1) establishment of deformation characteristics under repeated triaxial loading;

(2) analysis of stress, strain, and deformation; and

(3) analysis of distress and performance.

Though study of the relationship of stress repetition and deformation in roadway materials is not new, information on the deformation characteristics of materials under repeated loading with different combinations of axial and confining pressures which can actually be used directly in the development of a rational design method is very limited. The available information which can be used in these developments is discussed in Chapter 5.

Resilient Modulus

To characterize materials for the elastic layered analysis, the modulus of elasticity can be represented by the resilient modulus. NCHRP Report 35 (Ref 164) gives laboratory data for the repeated load test on granular and fine grained materials. By measuring the resilient (or elastic) strain in a repeated-load triaxial compression test, a resilient modulus can be determined at any number of load repetitions from

$$M_r(t) = \frac{\sigma d}{e_r(t)} \qquad (4.2)$$

where

$M_r(t)$ = modulus of resilient-deformation, psi (analogous to an elastic modulus) corresponding to a particular number of stress repetitions;

σd = repeated deviator stress, psi;

$e_r(t)$ = resilient axial strain corresponding to a particular number of stress repetitions, inches per inch.

Plate load tests at the subgrade surface indicate that the resilient modulus of clay soils varies with applied pressure and water content. The

resilient modulus decreases rapidly in the stress range of 1 to 10 psi (a range to be expected in the subgrades of well-designed pavements) and tends to have a constant value at higher stress levels. At equal ratios of applied stress to failure stress, values of resilient moduli of the subgrade soil determined from laboratory repeated load and plate load tests are essentially the same. The factors influencing the resilience of clays under repeated loads can be summarized as follows (Ref 164):

(1) Resilient deformations generally decrease with an increase in the number of load repetitions.

(2) Samples compacted to a high degree of saturation increase in strength with time.

(3) The resilient modulus generally increases with a decrease in the intensity of stress.

(4) A method of compaction which produces a dispersed structure tends to produce a lower resilient modulus.

(5) An increase in the degree of saturation at compaction decreases the resilient modulus (AASHO subgrade soil).

(6) In general, as the water content of the soil increases due to water absorption after placement, the resilience increases.

So long as there is no shear failure, repeated load triaxial compression tests on dry granular materials indicate the following relationship:

$$M_R = k\sigma_3^{\,n} \tag{4.3}$$

where

M_R = resilient modulus,

σ_3 = confining pressure,

k, n = constants.

The factors influencing the resilience of granular materials can be summarized as follows (Ref 164):

(1) Higher frequency of load repetitions increases the value of the modulus.

(2) The type of aggregate and percentage of material passing the No. 200 sieve have a definite effect on the resilient modulus.

(3) The difference between the moduli of loose and dense sand can be as much as 50 percent.

(4) An increase in saturation leads to a decrease in the resilient modulus.

(5) The resilient modulus is independent of the stress level so long as the stress is below a level that causes excessive plastic deformation.

The determination of an appropriate resilient modulus value for subgrades is not a simple problem since the selected subgrade modulus should take the previously noted factors into account. However, using an appropriate laboratory method it is now possible to simulate closely any desired field condition of a soil. For example, kneading compaction produces laboratory specimens with resilience characteristics similar to those observed in field specimens (Ref 164) for the same conditions of test. Thixotropy influence becomes insignificant after about 50,000 repetitions, which is only a fraction of the number of stress repetitions applied to a pavement (Ref 164). The influence of time which is much shorter in the laboratory, needs consideration though the deformation obtained in the laboratory will give conservative estimates of the performance in the field.

For granular materials, also, the laboratory evaluation of resilient modulus imposes several problems. In laboratory testing, estimates must be made for the void ratio, the expected degree of saturation, a reasonable rate of loading consistent with moving traffic, frequency of load applications, a representative number of repetitions consistent with the field conditions, and a representative stress condition based on best judgment and experience.

Applications of Repeated Load Test Results

The modulus of resilience of granular and fine grained materials is utilized in the layered elastic analyses to determine the stress and strain in the pavement layers. Then based on stress and strain values and cumulative deformation characteristics of these layers under repeated triaxial loading, the permanent deformation of layers in the form of rut depth is calculated. The computed values of rut depth are finally utilized for pavement performance computations. Development of a rut depth model, in which the above information and procedure are used, is further discussed in Chapter 10.

SUMMARY

In this chapter the proper fatigue theory and results of repeated triaxial loading tests as applicable to the flexible pavement design were discussed. To design the pavement on these principles, proper characterization of materials is needed to determine the characteristics which are used in the proposed design procedure. The material characterization is discussed next in Chapter 5.

CHAPTER 5. CHARACTERIZATION OF FLEXIBLE PAVEMENT MATERIALS

INTRODUCTION

A system transforms its input into output according to certain definite relationships which can be simulated by mathematical models using certain material properties. The basic properties of materials are complex physical functions. However, output responses for engineering analysis can be obtained by characterizing the materials for certain significant engineering properties such as stiffness, strength, etc. The literature shows that a great deal of effort has been devoted to measuring such material properties. However, uniformity in the test procedures and analysis of test results seems to be lacking. Many variables involved in material characterization which affect the material response in a system are given in Appendix 2, Table A2.13. Table A2.14 in Appendix 2 shows the details of the test configurations and Table A2.15 gives the various shapes of test specimens. Various variables shown in these tables affect the material response and point out the importance of having a uniformity in test procedures involved in determination of the basic material properties.

Hudson et al (Ref 78) through the systems approach to pavement design have demonstrated the need for characterizing material properties by means of constitutive equations which in turn can be used in mathematical models of pavement systems. The present analysis is based on linear elastic layered theory using fatigue properties of the materials and their stochastic variation in space and time. Therefore, the following material properties and their variations are required:

(1) elastic constants resilient or elastic modulus E and Poisson's ratio μ ;

(2) stochastic variations of elastic constants; and

(3) stress-strain relationships of materials as affected by time, temperature, and fatigue characteristics.

Table 5.1 is a summary of the tests required for material characterization for the design procedure discussed in this report. In the present analysis

TABLE 5.1. SUMMARY OF SAMPLING AND TESTING REQUIREMENTS (Ref 116)

	Elastic Constants		Strength and Deformation Tests	
Material Type	Sampling	Testing	Sampling	Testing
Asphaltic concrete	Intact or fragmented	Heukelom and Klomp 1. Asphalt penetration at 77° F 2. Ring and Ball softening point ° F 3. Aggregate volume concentration 4. Air voids 5. Time of loading 6. Temperature at which stiffness is required Nijboer Method 1. Marshall stability 2. Flow value 3. Time of loading 4. Temperature at which stiffness is required	Previously established or reproduced laboratory specimens	Fatigue
Granular Base and subbase	1. Density and moisture 2. Remolded specimens	Resilient modulus M_R	1. Density and moisture 2. Remolded specimens	Rupture envelope from triaxial shear. Repeated load triaxial tests varying axial and confining pressures for permanent and resilient strains. Fatigue.
Fine grained subgrade	1. Undisturbed push barrel 2. Density and moisture 3. Remolded specimens	Resilient modulus M_R	1. Undisturbed push barrel 2. Density and moisture 3. Remolded specimens	

distress and performance models developed in this report will be verified by the AASHO Road Test performance data. It is necessary, therefore, to characterize the materials used at the AASHO Road Test. Though the details which follow deal specifically with the characterization of the AASHO Road Test materials, the procedure, in general, is applicable for characterizing the materials which will be used with this design procedure.

ASPHALTIC CONCRETE

Stiffness

The response of asphaltic concrete to stress and strain is influenced by time and temperature to a pronounced degree. Asphaltic concrete under stress exhibits instant and time dependent strain, both of which may be partly recoverable and partly permanent. The time dependent part may be viscous or non-viscous. Instantaneous strain under moving traffic forms a large proportion of the total strain. Stress history is also important. The material's true response is nonlinear. Table 4.1 outlines the general effects of some variables on the stiffness of asphaltic concrete. However, the elastic properties of asphaltic concrete mixtures have been shown to be represented by its stiffness at a particular time of loading and temperature. A quasi-elastic modulus termed stiffness can be obtained by (1) the Heukelom and Klomp method (Ref 42) as modified by Van Draat and Somnner (Ref 38) for greater air voids and (2) the Nijboer method (Ref 173). The parameters required to define the stiffness by these methods are given in Table 5.1.

Appendix 2 details the calculation of the stiffness values of the asphalt concrete used at the AASHO Road Test. Table 5.2 gives the stiffness values adopted for the present analysis.

Poisson's Ratio

The Poisson's ratio or asphaltic concrete is not a very sensitive parameter in the layered analysis. Any standard test can be adopted to compute the value of this variable. According to NCHRP Report 39 (Ref 42) Poisson's ratio in general varies from 0.3 to 0.5 for a small deformation. A value of 0.3 is appropriate at cold temperatures (less than 40^{o} F) and at a loading time of 0.1 second. At higher temperatures and slower rates of loading the value may increase to 0.5. A value of 0.3 is reported by Deacon (Ref 26). For the present analysis, a value of 0.3 is adopted.

TABLE 5.2. STIFFNESS VALUES FOR ASPHALTIC CONCRETE (AASHO ROAD TEST MATERIAL)

Month	Temperature, ^{o}F	Stiffness Modulus, psi x 10^5
January	21^{o}	16.0
February	25^{o}	14.2
March	27^{o}	13.7
April	41^{o}	9.0
May	54^{o}	6.0
June	66^{o}	4.0
July	70^{o}	3.5
August	75^{o}	3.0
September	65^{o}	4.2
October	51^{o}	6.5
November	43^{o}	8.3
December	28^{o}	13.1

Stochastic Variation in Elastic Properties

The stochastic variation in stiffness values of asphaltic concrete in space have been considered in terms of the coefficient of variation, as detailed in Appendix 2. The values of standard deviations have been obtained from the available field and laboratory test results. An average value for the coefficient of variation is computed to be about 25 percent of the mean value. Variation of the stiffness value in time has been determined by monthly variation in temperature. Due to the relative insensitivity of Poisson's ratio in the layered analysis the stochastic variation in this parameter has not been taken into account.

Fatigue Test Data

Repetitive applications of tensile stresses smaller than the tensile strength ultimately cause fatigue cracking in asphaltic concrete. For controlled-stress loading, the mean fatigue life N is related to the initial tensile strain ϵ by Eq 4.1. The values of A and B depend upon the type of mixture, the condition of testing, and the failure definition. The values for B reported for the controlled stress mode of loading (Ref 26) vary from 2.5 to 5.9. The values of A for asphaltic concrete have been shown to vary from 10^{-6} to 10^{-10} (Ref 38). For asphaltic concrete used at the AASHO Road Test, no direct fatigue test results are available. A value of $B = 3.1$ and $A = 6.5 \times 10^{-7}$ was adopted for this analysis. These values correspond to the test results obtained at the University of California (Refs 24, 38, and 100) for similar asphaltic concrete mixtures.

Fatigue test data exhibit extreme variability. However, the fatigue life of specimens tested in simple, controlled stress loading with identical testing conditions can be approximated by a logarithmic normal distribution (Ref 24). The log of the standard deviation of fracture life varies from about 0.2 to 0.4 (Ref 24). However, Kaisianchuk (Ref 100) in his study of asphalt concrete has shown that the logarithm of the standard deviation of fracture life depends on the stress level, but could be assumed to be about 0.25 for a wide range of asphalt mixes. In view of the above and the fact that no fatigue test data for asphaltic concrete at the AASHO Road Test are available, the value of 0.25 was adopted for the purpose of analysis.

BASE AND SUBBASE GRANULAR MATERIALS

Resilient Modulus

A review of the limited data on the modulus of deformation for the materials used at the AASHO Road Test reveals a wide range of values. No direct test results applicable to the present analysis are available for the modulus values of AASHO Road Test materials. Various approaches through which modulus M_R values for AASHO materials for each month were selected are given in Appendix 2. Table 5.3 gives the M_R values adopted for this analysis.

Poisson's Ratio

Poisson's ratio is relatively insensitive in the elastic layered analyses, and typical values of 0.4 for the base and 0.45 for the subbase were adopted.

Stochastic Variation

Information on stochastic variations of elastic properties is not available for base and subbase granular materials used at the AASHO Road Test. Therefore, the standard deviation of modulus value was based on observed variations in the test results of other significant properties having direct relationship to the modulus value. An approximate value of coefficient of variation of about 25 percent was computed. The details of these computations are shown in Appendix 2. No stochastic variation in Poisson's ratio was considered.

Deformation Properties Under Repeated Loading

The behavior of granular materials under repeated loading is highly dependent on the degree of confinement. Haynes and Yoder (Ref 57) presented the results of undrained repeated-load triaxial compression tests on gravel and crushed stone used as base course at the AASHO Road Test. In these tests, a lateral pressure of 15 psi and a deviator stress of 55 psi were used. For the present analysis, curves representing the actual developed stresses in the pavement sections were required. A literature review revealed that the results of a study performed at Texas A&M University (Ref 35) on nine types of granular materials could be used to obtain this information. To ascertain the possibility of using this information to characterize the properties of the granular materials used at the AASHO Road Test, a comparison of various properties of the two materials was made. This comparison (Table 5.4) shows that the angular medium aggregate used for the A&M University test is similar to the AASHO base material and the rounded fine aggregate is similar to the AASHO subbase material.

TABLE 5.3. MONTHLY VALUES OF MODULUS OF RESILIENCE OF BASE AND SUBBASE OF AASHO MATERIAL

	M_R , psi	
Month	Base	Subbase
January	24,000	13,200
February	24,000	13,200
March	24,000	13,200
April	15,600	7,200
May	18,000	8,600
June	19,600	9,800
July	21,600	10,800
August	23,200	11,600
September	24,000	12,200
October	24,000	12,400
November	24,000	12,800
December	24,000	13,200

TABLE 5.4. COMPARISON OF ASSHO BASE AND SUBBASE MATERIAL WITH A&M TYPICAL AGGREGATE

Properties	Base Material		Subbase Material	
	AASHO	A&M	AASHO	A&M
Gradation	See Figures 5.1 and 5.2			
Optimum moisture content, %	7.6	7.0	7.7	7.3
Maximum unit weight	137.9	136.0	133.1	134.0
Texas triaxial class	1	1	3.7	3.0
Plasticity				
a) liquid limit	-	17.8	-	21.3
b) plasticity index	N.P. - 4.3	2.3	N.P. - 3.4	7.4
c) linear shrinkage	-	2.4	-	5.6
Los Angeles abrasion (500 revolutions)	23.9 - 28.3	25.3	25 - 35.4	27.3
Specific gravity	2.78	2.63	2.69	2.64
Permeability (ft/day)	.006 - 140	0.003	.0003 - 20×10^7	0.006
Brief description	Crushed limestone	Angular medium crushed limestone	Natural sand and gravel	Rounded fine limestone mixed with sand and other calcium carbonate

Table 5.5 compares the repeated load test results given by Haynes and Yoder (Ref 57) for the AASHO Road Test base material (curve s-1-c of Fig A2.1) with those given in the A&M University study for angular medium aggregate. The comparison is made for the total strain at an axial pressure of 70 psi and a confining pressure of 15 psi. The values of total strain in the two cases are approximately the same at 10,000 repetitions. A relatively large difference exists at 100,000 repetitions, which is not likely to influence the average results since the samples were near the failure point at these levels of strains and number of applications. There are many reasons for the difference between the total strain values. A part of the difference can be assigned to the difference in frequency and time of loading during the test in the two cases, as shown in Figs A2.2 and A2.3. Higher strain values would not have been obtained for the AASHO Road Test material if the time and frequency of loading were the same as those for the A&M test materials. For the reasons outlined above and since better data were not available, it is considered appropriate to characterize the fatigue characteristics of the AASHO Road Test base and subbase materials respectively by the angular medium and rounded fine aggregates used at the A&M University test.

Models to Characterize the "Repeated Load-Deformation" Characteristics

The values of permanent strain and corresponding load repetitions are tabulated in Tables 5.6 and 5.7 for various combinations of vertical and confining pressures. The range of values for stresses is selected to be comparable with the expected values in the pavement structures under normal traffic loads.

So that the data given in Tables 5.6 and 5.7 could be conveniently used for the present analyses a regression analysis was performed to predict the total strain value as a function of the number of load repetitions, vertical stress, and confining stress. The regression equations are given below.

Base Material:

Correlation coefficient $R^2 = 0.9938$

Standard error of residuals $\sigma = 0.0745$

$$\varepsilon = 0.57852 - 0.20640\ \sigma_3 + 0.07854\ \sigma_1 - 0.01464\ \sigma_3 \log N$$

$$- 0.00121\ \sigma_1 \log N - 0.00408\ \sigma_1\sigma_3 + 0.03846\ (\log N)^2$$

TABLE 5.5. COMPARISON OF TOTAL STRAIN FOR AASHO ROAD TEST AND TEXAS A&M UNIVERSITY TEST MATERIALS

Number of Applications	Total strain for AASHO Road Test material, %	Total strain for angular medium aggregate at A&M University test, %
100	0.21	0.15
1,000	0.41	0.6
10,000	1.08	1.0
100,000	4.4	1.3

TABLE 5.6. LOAD REPETITIONS AND DEFORMATION DATA FOR BASE MATERIAL IN % STRAIN E (FIG A2.8)

$\log N$ / σ_1 psi / σ_3 psi	2.0					3.0					4.0					5.0				
	10.0	20.0	30.0	40.0	50.0	10.0	20.0	30.0	40.0	50.0	10.0	20.0	30.0	40.0	50.0	10.0	20.0	30.0	40.0	50.0
1.0	1.2	1.7	2.1	2.5	3.1	1.3	1.8	2.2	2.6	3.2	1.4	2.0	2.3	2.7	3.3	1.5	2.2	2.4	2.8	3.5
3.0	0.5	1.0	1.6	2.0	2.5	0.6	1.1	1.7	2.1	2.6	0.7	1.2	1.8	2.2	2.7	0.8	1.33	1.9	2.3	2.8
5.0	0.2	0.5	0.9	1.4	1.8	0.3	0.6	1.0	1.5	1.9	0.4	0.7	1.1	1.6	2.0	0.5	0.8	1.2	1.7	2.1
7.0	0.05	0.2	0.5	0.8	1.2	0.1	0.3	0.6	0.9	1.3	0.15	0.4	0.7	1.0	1.5	0.2	0.5	0.8	1.1	1.7
9.0	0.01	0.05	0.2	0.5	0.9	0.04	0.1	0.3	0.6	1.0	0.07	0.15	0.4	0.7	1.1	0.1	0.2	0.5	0.8	1.2

TABLE 5.7. LOAD REPETITIONS AND DEFORMATION DATA FOR SUBBASE MATERIAL IN % STRAIN E (FIG A2.9)

log N / σ_1 psi / σ_3 psi	2.0					3.0					4.0					5.0				
	5.0	10.0	15.0	20.0	25.0	5.0	10.0	15.0	20.0	25.0	5.0	10.0	15.0	20.0	25.0	5.0	10.0	15.0	20.0	25.0
1.0	0.3	0.8	1.0	1.5	2.0	0.5	1.0	1.5	2.0	3.0	0.7	1.2	2.0	2.5	4.0	0.9	1.4	2.5	3.0	5.0
2.0	0.2	0.7	1.0	1.2	1.5	0.3	0.8	1.1	1.6	2.0	0.4	0.9	1.3	1.8	3.0	0.5	1.0	1.5	2.0	4.0
3.0	0.1	0.2	0.8	1.0	1.4	0.2	0.4	0.8	1.2	1.6	0.3	0.6	1.0	1.4	1.8	0.4	0.8	1.2	1.6	2.0
4.0	0.01	0.5	0.75	0.9	1.25	0.1	0.6	0.8	1.0	1.4	0.2	0.65	0.85	1.1	1.5	0.3	0.7	0.9	1.2	1.6
5.0	0.08	0.2	0.3	0.5	0.9	0.09	0.3	0.4	0.6	1.0	0.2	0.4	0.5	0.7	1.2	0.3	0.5	0.6	0.8	1.3

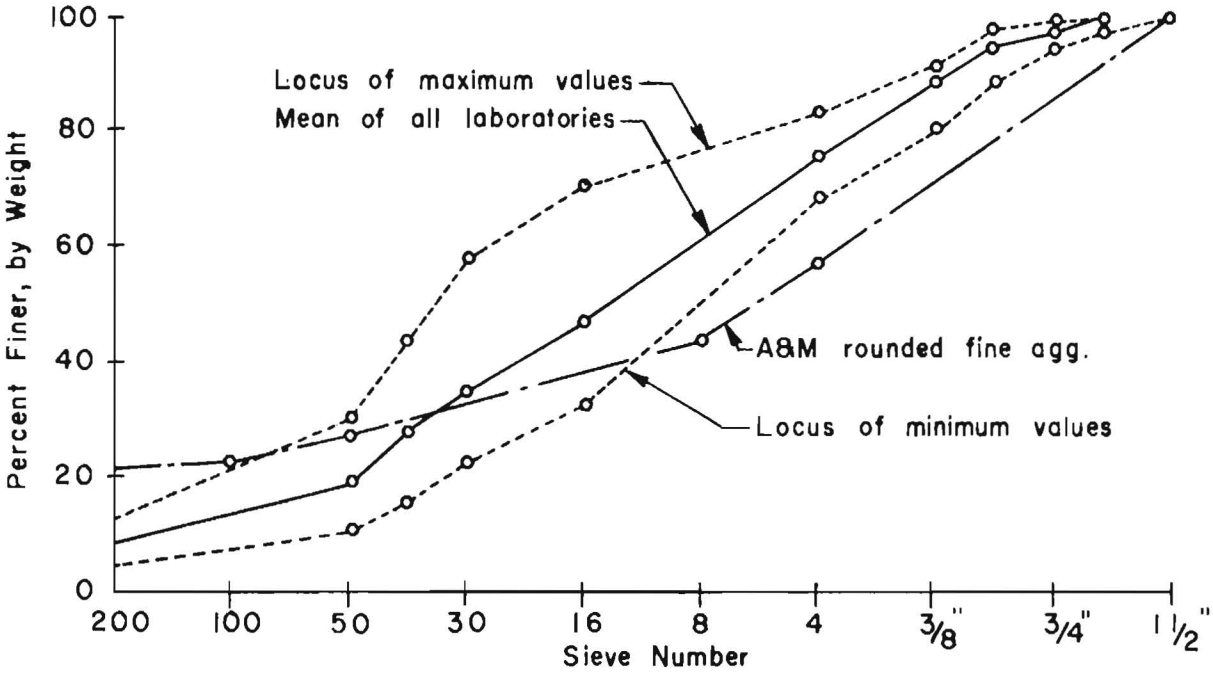

Fig 5.1. Grading curve for subbase.

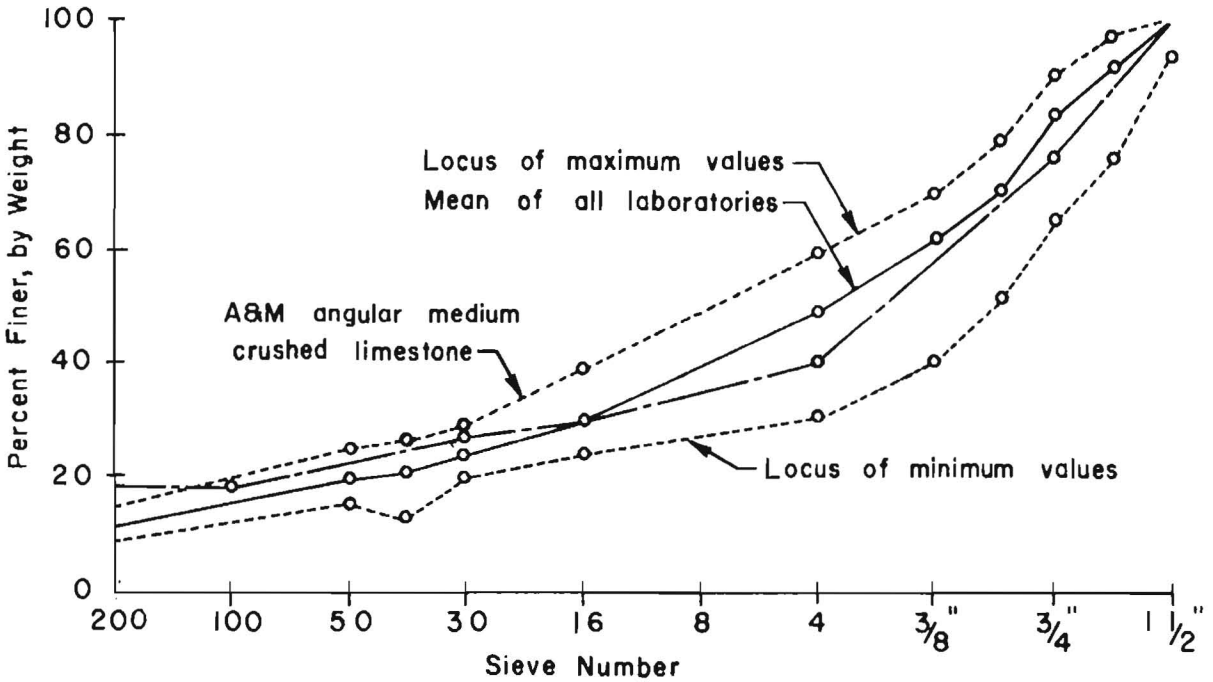

Fig 5.2. Grading curve for base.

Notes: (1) Dotted and firm lines show the result of AASHO Road Test materials (Ref 66).
(2) Chain line shows the result of A&M materials (Ref 35, Figs 3.5 and 3.6).

$$- 0.00093\ \sigma_1^2 - 0.00062\ \log N\ \sigma_3^2 - 0.00292\ (\log N)^3$$

$$+ 0.00204\ \sigma_3^3 + 0.0001\ \sigma_1^3 - 0.004\ \sigma_3^2\sigma_1 + 0.00006\ \sigma_1^2\sigma_3$$

$$+ 0.00046\ \sigma_1\sigma_3\ \log N \qquad (5.1)$$

Subbase Material:

Correlation coefficient $R^2 = 0.9772$

Standard error of residuals $\sigma = 0.1442$

$$\epsilon = -0.75465 + 0.25605\ \log N + 0.17009\ \sigma_1 - 0.14433\ \log N\ \sigma_3$$

$$+ 0.01187\ \log N\ \sigma_1 + 0.01139\ \sigma_1\sigma_3 + 0.04947\ \sigma_3^2 - 0.01132\ \sigma_1^2$$

$$+ 0.03340\ \log N\ \sigma_3^2 + 0.00115\ \log N\ \sigma_1^2 - 0.01885\ \sigma_3^3$$

$$+ 0.00025\ \sigma_1^3 + 0.00367\ \sigma_3^2\sigma_1 - 0.00072\ \sigma_1^2\sigma_3$$

$$- 0.01018\ \sigma_1\sigma_3\ \log N \qquad (5.2)$$

where

σ_3 = radial or confining stress, psi;

ϵ = percent permanent strain;

N = number of stress applications;

σ_1 = vertical stress, psi.

Each of the above equations is based on 100 observations. For an actual design problem, the designer will replace these equations with the actual properties obtained for the materials to be used.

CHARACTERIZATION OF SUBGRADE "FINE GRAINED COHESIVE SOILS"

Elastic Constants

A resilient modulus M_R of the subgrade soil can be determined by measuring the resilient strain in a repeated load triaxial compression test. Since the M_R value is sensitivie to many factors, as outlined in Chapter 4, the choice of a correct value is difficult. However, as detailed in Appendix 2, various approaches led to the selection of suitable values based on available information. Resilient modulus values at different moisture contents were studied and the monthly values adopted are shown in Table 5.8. Because Poisson's ratio is relatively insensitive in the layered analysis, a mean typical value of 0.5 for subgrade soils was adopted.

Stochastic Variation

No direct information was available for the stochastic variation of the M_R value. However, based on the general variations in other properties having a direct relationship with the M_R value, as outlined in Appendix 2, a standard deviation of about 25 percent of the mean value was adopted.

Deformation Properties Under Repeated Loading

The procedure developed in this dissertation requires stress-strain plots for various axial and confining pressure combinations. The AASHO Road Test subgrade soil was tested in the repeated load test (Ref 165) at a confining pressure of 3.5 psi for various axial stresses (Fig A2.10). The test was made at a moisture content of 15.3 percent. A variation in permanent deformation characteristic is observed due to variation in moisture content, but at the low stress levels encountered in the pavements this variation will be very small. For practical application of the method, repetitive load tests at various moisture contents expected in the field can be obtained for increased accuracy.

For AASHO Road Test subgrade soil, the repetitive load test curves are available only for 3.5 psi confining pressure. For the analysis, similar data are required for various confining pressures in the range expected in the analysis. To make use of the available information, it has been assumed that the total axial deformation is the same for the same deviator stress. Knowing the deviator stress $(\sigma_1'' - \sigma_3'')$ in the actual pavement, total strain corresponding

TABLE 5.8. MONTHLY VALUES OF MODULUS OF RESILIENCE OF AASHO SUBGRADE MATERIAL

Month	M_R , psi
January	6600
February	6600
March	6600
April	3600
May	4300
June	4900
July	5400
August	5800
September	6100
October	6200
November	6400
December	6400

to $\sigma_1' - 3.5$ can be obtained from the curves developed for a confining pressure of 3.5 psi. Equivalent vertical stress σ_1' will be computed as follows:

$$\sigma_1' - 3.5 = \sigma_1'' - \sigma_3'' \tag{5.3}$$

where

$\sigma_1'' - \sigma_3''$ = deviator stress in actual pavement,

σ_1' = equivalent vertical stress.

Table 5.9 shows the values of the permanent strains vs stress applications for various axial stresses at a constant confining pressure of 3.5 psi.

Regression Model to Characterize Deformation-Repeated Load Characteristics

To utilize the available information a regression analysis was performed on the data shown in Table 5.9, and the following regression model was obtained.

For $\sigma_3 = 3.5$, psi in compression

The correlation coefficient $R^2 = 0.99$, and the standard error of residuals = 0.16 = 0.0016 in/in.

$$\varepsilon = 0.35461\ \sigma_1 - 0.04064\ \sigma_1 \log N - 0.06511\ \sigma_1^2 + 0.00283\ \sigma_1^3 + 0.00744\ \sigma_1^2 \log N \tag{5.4}$$

where symbols are as previously defined.

In the case of actual design problems, the user may replace this regression equation by the data obtained from the tests on actual subgrade material.

SUMMARY

In this chapter the characterization of the materials applicable to the proposed models is described with special reference to the AASHO Road Test materials. Summary of sampling and testing requirements are shown in Table 5.1. The elastic moduli of the AASHO Road Test materials are shown in Tables 5.2, 5.3, and 5.8, while the repeated load-deformation characteristics are described by Eqs 5.1, 5.2, and 5.4. For actual problems, the user may characterize the

TABLE 5.9. REPETITIVE LOAD AND DEFORMATION DATA OF AASHO ROAD TEST SUBGRADE MATERIAL (FIG A2.10)

Confining preesure σ_3 = 3.5 psi

Moisture content = 15.3%

Axial stress σ_1	Number of stress repetitions N	Total strain % ϵ
0.0	1	0.0
0.0	10	0.0
0.0	100	0.0
0.0	1,000	0.0
0.0	10,000	0.0
0.0	100,000	0.0
0.0	1,000,000	0.0
6.6	1	0.1
6.6	10	0.2
6.6	100	0.3
6.6	1,000	0.4
6.6	10,000	0.6
6.6	100,000	0.8
6.6	1,000,000	1.0
9.7	1	0.2
9.7	10	0.4
9.7	100	0.6
9.7	1,000	0.8
9.7	10,000	1.0
9.7	100,000	1.2
9.7	1,000,000	1.5
16.0	1	0.6
16.0	10	1.8
16.0	100	3.0
16.0	1,000	4.3
16.0	10,000	5.7
16.0	100,000	7.0

materials as described in this chapter and may replace the regression models (Eqs 5.1, 5.2, and 5.4) by the data obtained from the tests on actual materials.

CHAPTER 6. USE OF ELASTIC THEORY AND LAYERED ANALYSIS IN THE DESIGN OF FLEXIBLE PAVEMENTS

The concept of linear elastic layered theory has been utilized in the design approach developed in this report. Thus, this chapter discusses the use of this theory in the proposed procedure for the design of flexible pavements.

INTRODUCTION

The use of linear elastic theory and layered analysis in the design of flexible pavements is becoming more feasible because of the relative ease of solution with the present generation of computers. In the past, direct application of the results to pavement design was generally unsuccessful for the following factors (Ref 131):

(1) complexity of solutions,

(2) difficulty in isolating the particular cause of distresses affecting the pavement performance, and

(3) lack of agreement between measured and predicted stress and strains.

The first factor has been partially eliminated as a problem by the development of computers. As far as the second factor, it is generally recognized that tensile strain in an asphaltic material is a major factor in determining the fatigue life, although any single theory based on elastic behavior of materials cannot account for all complexities and factors involved. Many discrepancies in the predicted and observed stresses and strains caused by the third factor are eliminated by a better understanding of material characterization and by more general methods of calculation. Thus, a rational design procedure is established in this report using linear elastic layered theory to calculate the tensile strains in the asphaltic concrete layers. The stresses and strains in the other layers are used to determine rut depth in a pavement system.

BEHAVIOR OF IDEAL MATERIALS

In the previous two chapters, the behavior of real materials was described. In the remaining portion of this chapter, the behavior of ideal materials, required by the theory, is described.

The strain of an ideal elastic body and the strain rate of a viscous fluid are both proportional to stress and independent of time. The strain of an ideal elastic body is recoverable upon unloading, but this is not the case for an ideal viscous body (Ref 183).

A deformation is said to be anelastic (to have delayed elasticity) if it is time-dependent and completely recoverable. An ideal elastic body may be represented by a spring, and an ideal viscous fluid by a dash-pot. Any combination of spring and dash-pot is said to represent viscoelastic behavior. Certain combinations of springs and dash-pots give rise to anelastic behavior (Ref 183).

Plastic deformations may or may not be time-dependent. Aspects of linearity or nonlinearity aside, the main difference between viscous deformation and time-dependent plastic deformation is the irreversibility of the latter. If the direction of the load is reversed, a viscous deformation will be completely reversible, but a plastic deformation will not be reversible (Ref 183).

For low stresses, asphaltic concrete and other pavement materials may behave in a linearly elastic fashion, while at higher loads, the stress-strain curve is nonlinear. Ideally, the pavement material may exhibit one or all of the following major types of deformation behavior (Ref 183).

Type of Deformation	Behavior for Instantaneous Deformation	Behavior for Time-Dependent Deformation
Recoverable	Elasticity	Anelasticity
Irrecoverable	Plasticity	Viscosity

In addition to the above factors, ideal materials are considered homogeneous and isotropic. For homogeneous materials, the elastic properties are identical throughout the material and in isotropic materials, the elastic properties are identical in all directions at any point within the material.

Elastic Materials

Elastic theories have been used for pavement within granular and fine grained materials, not because they are ideal elastic bodies but due to the availability of solutions. However, properly used, the theories give solutions which are accurate. The first and most widely known theory is that of Boussinesq (Ref 8), which deals with stresses in a homogeneous, isotropic, linearly elastic solid of semi-infinite extent subjected to a load applied normally to the surface. This theory is not fully utilized, since pavements with their layered structure do not satisfy the requirements of homogeneity. More realistic are the two and three-layered solutions developed by Burmister (Ref 14). With the advent of computers, solutions for up to 15 layers have been developed (Ref 116). Many solutions have been published for a layered homogeneous elastic solid loaded by a uniform vertical load over a circular area. These solutions are tabulated by Seed et al (Ref 164) and Morgan and Scala (Ref 131).

In an isotropic medium, only Young's modulus E and Poisson's ratio μ are required. In the Boussinesq solution, all stress components are independent of E and only the radial and tangential stresses are affected by the value of μ. In layered elastic systems, the stresses are influenced principally by modular ratios and not by absolute values. Displacements are influenced by the magnitude of E in a single layer and by the modulus ratios, as well as magnitudes of E in the multilayer system. Poisson's ratio also influences displacements but in a nonproportional fashion. The influence of μ is quite insignificant and has been largely ignored.

The difficulty in the use of the anisotropic solution lies in the difficulty in determining some of the parameters of real materials. This determination may not be needed for the accuracy required from a practical standpoint. The effect of nonhomogeneity at various depths of granular materials, where stiffness changes with confining pressure, has been considered by various authors and was discussed in Chapter 4.

Viscoelastic Materials

The stiffness of asphaltic concrete varies with temperature and rate of loading. To account for this, the viscoelasticity theory should be applied to solve for stress and strain. However, because of the additional complexity involved in assuming viscoelastic behavior, much asphalt pavement analysis has

been carried out using elastic theory. Complications of viscoelasticity in asphaltic concrete can be avoided by accounting for the influence of loading rate and temperature on asphalt stiffness by testing samples at the same rate of loading and temperature as observed in the field. Various methods of computing the stiffness have been developed, as explained in Chapter 5.

Although pavement and subgrade materials ideally exhibit viscoelastic behavior, the extent is considerably less than for asphalt concrete. Therefore, for these materials the complications of viscoelastic behavior can be avoided by the proper choice of testing technique.

COMPARISON OF PREDICTED AND OBSERVED BEHAVIOR

Ultimate decisions about the applicability of elastic theory to pavements can be based on the comparison of the following measured and predicted characteristics:

(1) stress in single and multilayered systems,
(2) vertical strains and deflections, and
(3) horizontal strains in asphalt layer.

Stress in Single and Multilayered System

The stress estimation from strain measurement has been reported to be one of the most straightforward ways to evaluate the usefulness of elastic theory (Ref 131). These measurements have been reported for both uniformaly prepared sand masses and fine grained soils (Ref 131). Considering the results of measurement in both single and multilayered systems, the following conclusions were derived (Ref 131).

(1) Vertical stress distributions for the appropriate boundary conditions are given with reasonable accuracy by both the Boussinesq single layer and the Burmister multilayered theories. For two-layered systems, the modular ratio used for unbound bases is probably only two to three, and the difference between the stresses predicted by the two theories is small. Variations from the assumed conditions of isotropy and homogeneity are unlikely to influence the vertical stress significantly.

(2) Radial stresses, except close to the surface in single-layered systems, are underestimated by both the single and multilayered theories. It has been suggested that better agreement would be obtained if the consideration of proper anisotropy of the material in the horizontal and vertical directions is taken.

Vertical Strains and Deflections

Direct application of elastic theory may not give very accurate results. However, approximate approaches based on the elastic theory have been developed and are discussed in Chapter 10.

Horizontal Tensile Strain in Asphaltic Material

The horizontal tensile strain at the base of an asphaltic layer has been widely accepted as the criterion for fatigue failure of these materials. The comparison between observed and predicted values from layered theory shows reasonable agreement. The strain values at the base of the layer are given most accurately and these are the ones which are used in fatigue design.

SUMMARY

The discussion in this chapter indicates that for all practical purposes, the use of linear elastic theory in pavement design gives solutions which are accurate enough from a practical standpoint. Complexity of solutions has been partially eliminated by the development of computers, making the use of the theory more feasible. A rational design procedure can be established by the use of stress and strain, which are calculated by this theory.

PART III

DEVELOPMENT OF MODELS

CHAPTER 7. DEVELOPMENT OF DISTRESS MODELS

The term failure as applied in the design of many engineering structures cannot be used for pavement systems. For example, a pavement could be considered to have failed according to structural design standards, such as appearance of cracks, but may still be capable of performing at a reduced level. A pavement should be designed and evaluated in terms of the level of service or performance it can provide. The categories of distress manifestations affecting the performance of a pavement system were introduced in Chapter 3. In this chapter, the distress index model for computing the pavement performance is developed.

There is a complex interrelationship between pavement component materials, pavement behavior, and performance of the pavement. As defined in NCHRP 1-10 (Ref 78), behavior is the reaction or response of a pavement to load, environment, and other inputs. Performance is a measure of the accumulated service provided by a facility and is a direct function of the history of the present serviceability index of the pavement according to the AASHO concept of PSI, as discussed in Appendix 7 of this report.

Distress mechanisms have been defined (Ref 78) as responses which lead to some form of distress when carried to an extreme limit. Figure 3.1 gives the three categories of pavement distress model which are limiting responses. In general, the distress index (quantification of the limiting responses) is expressed as some function of the measure of the limiting responses in space and time, the limiting responses being the function of distress mechanism, shown in Fig 3.1. When the distress index exceeds some acceptable level, the pavement system is considered to have failed.

IDEAL DISTRESS INDEX MODEL

A conceptual distress index can be expressed as follows (Ref 78):

$$\underline{DI}(\underline{x},t) = \underset{s=o}{\overset{s=t}{\underline{F}}} [\underline{C}(\underline{x},s), \underline{S}(\underline{x},s), \underline{D}(\underline{x},s)\underline{x},t] \qquad (7.1)$$

where

t = time;

$\underline{x}$ = position vector of a point referred to a coordinate system;

$\underline{DI}(\underline{x},t)$ = distress index, a matrix function of space and time;

$\underline{C}(\underline{x},t)$ = measure of fracture, a matrix function of space and time;

$\underline{S}(\underline{x},t)$ = measure of distrotion, a matrix function of space and time;

$\underline{D}(\underline{x},t)$ = measure of disintegration, a matrix function of space and time.

The distress index is a function of the history of the variable shown from time zero to current time t. In a systems framework, the parameters in Eq 7.1 must be quantified from the input parameters. The three modes of distress may be expressed as a function of load, environment, construction, maintenance, and structural variables in space and time.

For fracture:

$\underline{C}(\underline{x},t)$ is a function of load, environment, construction, maintenance, and structural variables, space and time; (7.2)

For distortion:

$\underline{S}(\underline{x},t)$ is a function of load, environment, construction, maintenance, and structural variables, space and time; (7.3)

For disintegration:

$\underline{D}(\underline{x},t)$ is a function of load, environment, construction, maintenance, and structural variables, space and time. (7.4)

The substitution of Eqs 7.2, 7.3, and 7.4 for fracture, distortion, and disintegration into Eq 7.1 gives a measure of a distress index. Based on the riding quality, economics, and safety as required in particular circumstances, acceptable limits to the distress index can be assigned. These limits define the failure of the pavement, thus giving a criterion for pavement design.

DEVELOPMENT OF DISTRESS INDEX MODEL

Development of an ideal distress index model is a complex problem; however, the AASHO Road Test concept of present serviceability index is recognized as the best to-date effort in this direction. The present serviceability index equation developed in the AASHO Road Test (Ref 70) is a widely accepted statistically derived regression equation which relates the distress manifestations to the present level of service. It has been found that in the view of highway users, the distress index can be very well explained and correlated in terms of

(1) slope variance $\overline{SV}$ (Appendix 7), which can be related to disintegration and distortion;

(2) rut depth $\overline{RD}$, which can be related to distortion;

(3) area of cracking C per thousand square feet, which is related to fracture; and

(4) area of patching P per thousand square feet, which is related to fracture, disintegration, and distortion.

At the AASHO Road Test, these four factors were measured and the distress index or PSI of the sections was calculated and defined according to the following equation for flexible pavements (Ref 70, Appendix F):

$$PSI = 5.0 - 1.9 \log (1 + \overline{SV}) - 1.375\overline{RD}^2 - 0.01\sqrt{C + P} \qquad (7.5)$$

The pavement design models were developed statistically, correlating PSI with axle load, repetitions of load, and the design variables (depths of various layers).

A distress index curve is shown in Fig 7.1. An increase in load repetitions will increase the distress in the pavement. The form of distress development is shown by curves for distress indices for cracking (DI_{CI}), rut depth (DI_{RD}), and roughness or slope variance (DI_{SV}). The cracking index curve shows that although there is cracking at the beginning of Stage III, theoretically actual distress in the pavement due to cracking starts at the beginning of Stage II. Once the visible cracking starts at Stage III, this effect tends to progress rapidly. The pavement has some roughness due to imperfect construction even in the beginning, and the roughness increases further with the number of load repetitions, as shown. The rut depth distress due to permanent

DI_{CI} = Distress Index due to Cracking

DI_{RD} = Distress Index due to Rut Depth

DI_{SV} = Distress Index due to Roughness or Slope Variance

DI_{TOTAL} = Total Distress Index

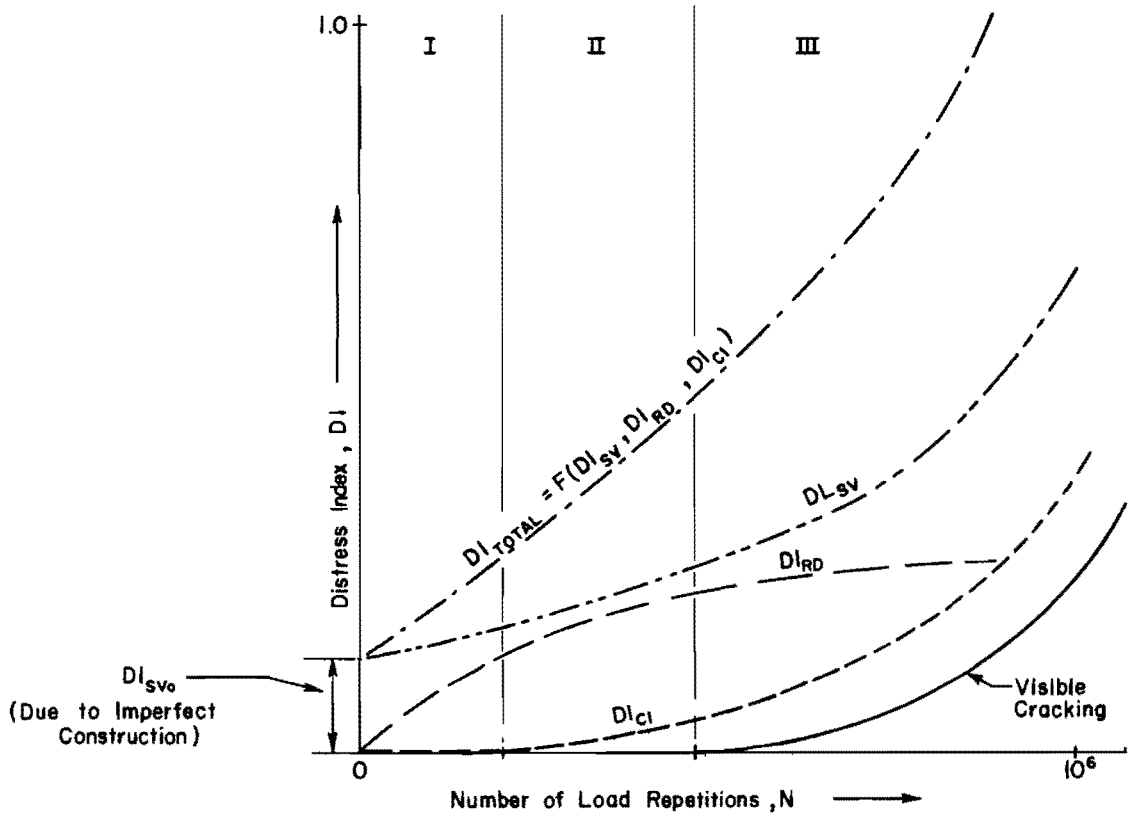

Note: For three stages I, II, & III shown above see Chapter H.

Fig 7.1. Distress index curves for flexible pavements.

deformation in pavement layers will progress at a decreasing rate. The total distress index curve, as shown, is the total effect of all three distress indices.

$$DI_{TOTAL} = f(DI_{SV}, DI_{RD}, DI_{CI}) \tag{7.6}$$

QUANTIFICATION OF DISTRESS INDEX MODEL

Examples of various distress mechanisms responsible for distress in pavement are shown in Fig 3.1. For an ideal pavement system design model, all possible distress mechanisms should be taken into consideration. However, for a real-world situation, this is not always possible and a compromise, based on the state-of-the-art, resources, and time, is necessary. Due to the limited scope of the present analysis, a direct consideration of shrinkage and slippage has not been possible. Because the AASHO Road Test was basically a fatigue test of short duration with no apparent effects of swelling clays and major temperature effects, these factors were not considered. The rupture distress mechanism has been computed in terms of the cracking index CI , and distortion in terms of slope variance $\overline{SV}$ is correlated to CI . Disintegration is one other factor which is not being considered directly in the present analysis.

In the AASHO Road Test, cracking and patching were the measured limiting responses. The measure of this response has been obtained theoretically in this report, based on fatigue and stochastic principles. This has been defined as the cracking index CI . Development of this model is explained in Chapter 8. The distress due to rut depth is represented as the rut depth index RDI , and the model is developed in Chapter 9. The distress due to slope variance, which is the measure of variation of a roadway surface from a desirable profile, is represented in the form of roughness index RI . The roughness index model is detailed in Chapter 10. The verification of the models has been performed with the AASHO Road Test data and is included in Chapter 11.

Based on the above discussion and the performance concept of the AASHO Road Test, the present serviceability index of a flexible pavement can be represented mainly as a function of the cracking index, roughness index, and rut depth index at any time during the pavement performance. If the above

three factors are known, an estimate of the pavement performance in terms of PSI can be made.

Mathematically,

$$PSI = f(DI) = f(CI, RI, RDI) \tag{7.7}$$

where

PSI = present serviceability index,

CI = cracking index,

RI = roughness index, and

RDI = rut depth index.

The steps involved in the development of an actual distress index model from Eq 7.7 are shown in a flow chart in Fig 7.2. This procedure requires the availability of some performance data. Since the procedure developed in this report utilizes the AASHO Road Test concept of performance, the present serviceability index equation, Eq 7.5, is adopted for the distress index model for the present analysis.

VERIFICATION OF DISTRESS INDEX MODELS

Because the distress manifestations CI , RI , and RDI are considered a very good measure of overall distress, the need to express each as a function of some measurable and well-established material behavior properties, pavement components, load factors, and environment factors in a working model is apparent. If such models are developed, then pavements can be designed rationally and their performance predicted in any arbitrary set of conditions. In the following chapters, such an effort is outlined and the development of the models explained.

The AASHO Road Test is an excellent source of performance data to verify the models developed in Chapters 8, 9, and 10, the measurements for which were obtained under different conditions. Therefore, the AASHO data have been fully utilized to verify the predicted performance curves of the developed models. Because of the extent of the AASHO Road Test, verification and good reproduction of the AASHO data will give confidence in the use of the developed models.

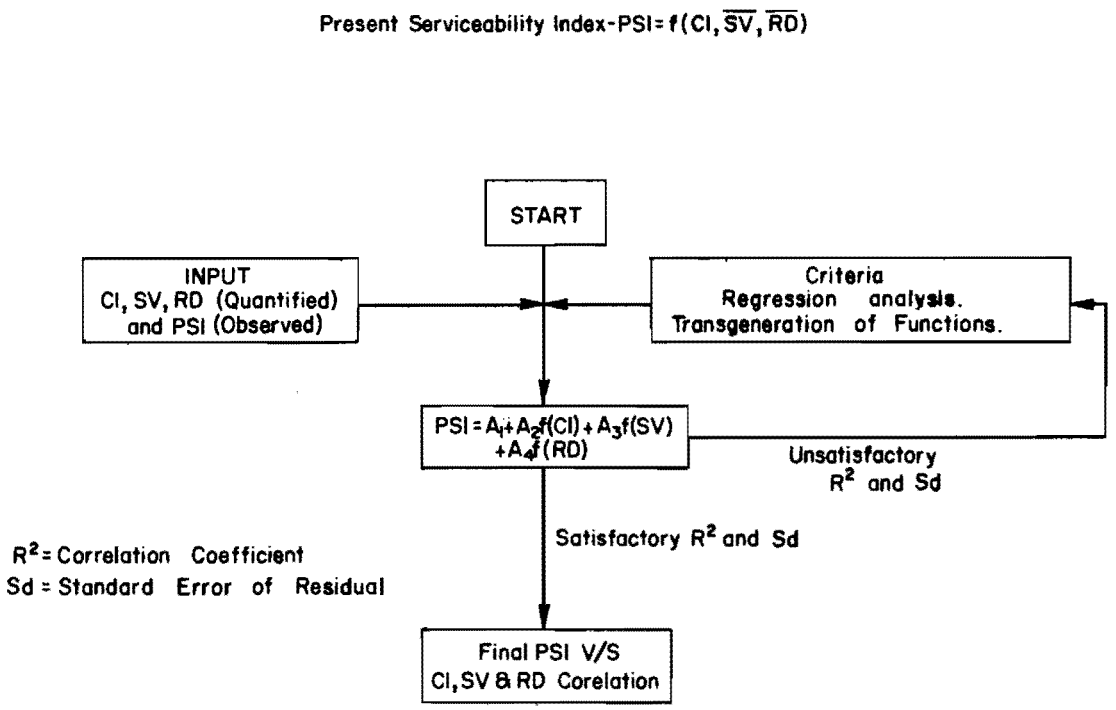

Fig 7.2. Flow chart for development of performance model.

Verification of the distress index models developed in this report is detailed in Chapter 11. A typical pavement performance curve is shown in Fig A7.1 of Appendix 7. An attempt has been made in this research to reproduce the observed performance curves of the AASHO Road Test.

CHAPTER 8. DEVELOPMENT OF CRACKING INDEX MODEL

In this chapter, a model for predicting the cracking index (CI) is developed, using the fatigue theory and Miner's hypothesis (Chapter 4), and stochastic concepts.

STOCHASTIC CONCEPTS APPLIED TO CRACKING INDEX IN FLEXIBLE PAVEMENTS

Generally, cracking in a pavement structure is considered to be a deterministic phenomenon occurring when the stress is greater than the strength. Both stress and strength in a pavement are subject to stochastic variations, which can be approximated by a continuous normal distribution (Ref 116). The fatigue phenomenon occurs in a pavement, following a predictable relationship between repetition of a load, stress or strain, and material properties. The modulus of elasticity and Poisson's ratio are subject to variations in both space and time, and generally variations of these properties could be approximated by a normal distribution. Therefore, statistical methods and probability theory are required to predict the amount of cracking or the cracking index. In the present model, stochastic concepts for variations in the material properties are applied only to the space variation. The time variation is considered in terms of monthly variations. Fatigue life tests for asphaltic concrete must be made to determine the distribution of fatigue life. The mean value and standard deviation of fatigue life and its relationship to induced strains must be obtained. As already discussed in Chapter 4, fatigue life variations can be approximated by a log normal distribution. Since in fatigue life (the number of stress repetitions N), a log normal distribution is applicable, it is reasonable to assume that the same is applicable to the ratio of actual to theoretical stress applications $\frac{n}{N}$.

According to Miner's hypothesis for no distress, the cumulative damage must be less than one, as given by

$$\sum_{0}^{t}\sum_{0}^{j}\frac{n_j}{N_j} \leq 1.0 \qquad (8.1)$$

where

n_j = the actual number of load applications of level j,

N_j = the number of load applications of level j which will cause failure in simple loading.

Using these values in a statistical analysis, the probability p of distress for cumulative damage being more than 1.0 in a given situation may be computed. In the case of a given area of roadway, it may be said that approximately p percent of the roadway area would experience cracking distress under the given conditions (Refs 78 and 116). Thus, the cracking index is calculated as the probability of $\sum_{0}^{t}\sum_{0}^{j} \frac{n_j}{N_j}$ exceeding one. This probability is represented by the area A beyond log 1.0 value of abcissa of a normal distribution curve, as shown in Fig 8.1. The cracking index represents the distress in a pavement at any time, in square feet of cracking per thousand square feet. Thus,

$$CI(x,t) = P\left(\sum_{0}^{t}\sum_{0}^{j} \frac{n_j}{N_j} > 1.0\right) \times 1000 \qquad (8.2)$$

where

$P\left(\sum_{0}^{t}\sum_{0}^{j} \frac{n_j}{N_j} > 1.0\right)$ = probability of total cumulative damage at any time for all load groups being more than one,

= area A (Fig 8.1).

Based on a normal distribution curve, this can be determined from the following equations:

$$\log (D)_{\alpha} = \log (D)_m + K \log \sigma_D \qquad (8.3)$$

and

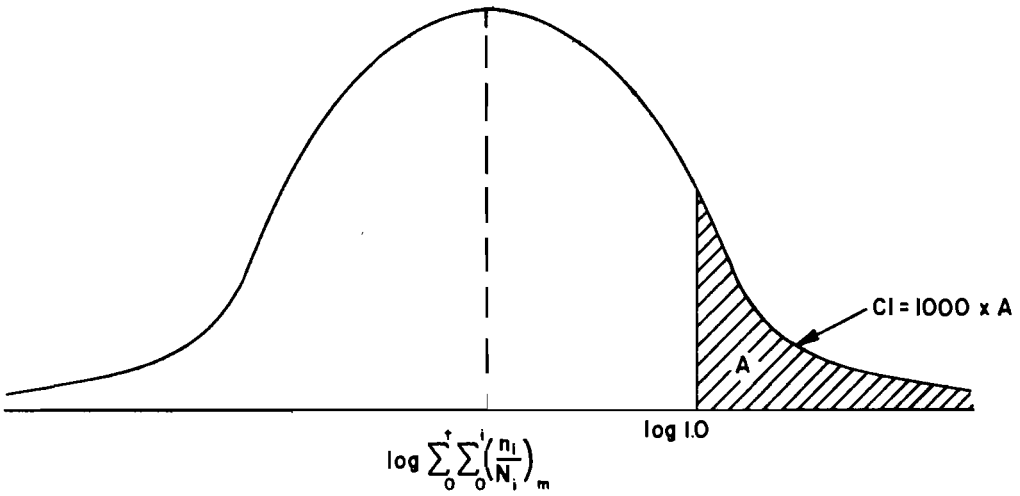

Fig 8.1. Log normal distribution curve for $\sum_0^t \sum_0^i \frac{n_i}{N_i}$

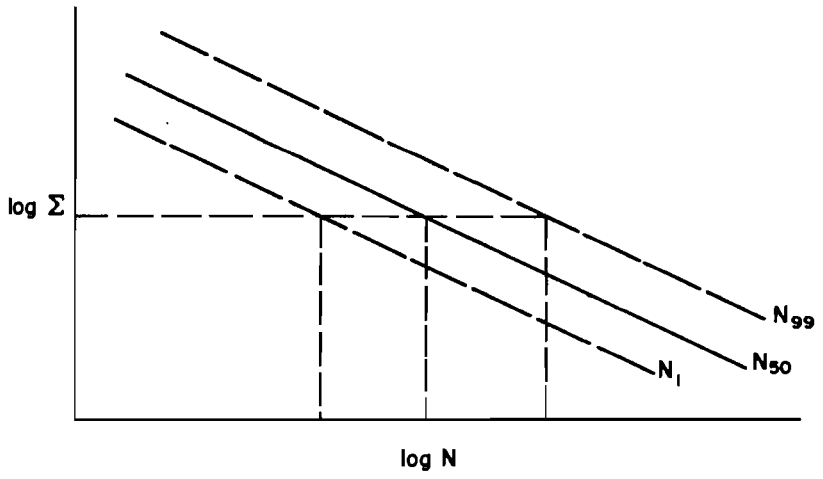

Fig 8.2. Asphaltic concrete fatigue curve.

$$\log (1.0) = \log (D)_m + K_{CI} \log \sigma_D \tag{8.4}$$

where

$(D)_\alpha$ = total damage at a confidence level $\alpha = \sum_0^t \sum_0^j \left(\frac{n_j}{N_j} \right)_\alpha$,

$(D)_m$ = mean total damage $= \sum_0^t \sum_0^j \left(\frac{n_j}{N_j} \right)_m$,

K = normal curve parameter corresponding to confidence level α,

σ_D = standard deviation for damage,

K_{CI} = normal curve parameter for σ_D corresponding to other parameters in Eq 8.4,

t = time,

x = position vector of a point referred to in a coordinate system.

From the computed values of other parameters, the value of log σ_D can be calculated from Eq 8.3. Then, from Eq 8.4, K_{CI} is computed. From the normal tables, the corresponding probability, that is, the area under the normal distribution curve A in Fig 8.1, is obtained. This area A when multiplied by 1000 gives the cracking index.

In staitstical terms, the modulus values of various layers in a pavement may be considered as random variables and can be treated as independent factors. With the special case of statistical independence, the probability of the modulus values of several layers occurring simultaneously is equal to the product of the probability of each occurring independently. Thus, the overall probability is

$$\alpha = \prod_{i=1}^{\ell} \alpha_i \tag{8.5}$$

where

α = the overall confidence level for modulus values in a pavement structure,

α_i = the confidence level of the modulus value in the i^{th} layer,

ℓ = number of layers in a pavement structure.

The stress and strain caused by a wheel load in a pavement structure, due to variation in modulus values and variation in the fatigue life of surface layer materials, are considered as mutually exclusive. Thus, the probability of the alternative events is equal to the sum of each occurring alone. The overall probability in this case is given by

$$\alpha_T = \alpha + \alpha_N \tag{8.6}$$

where

α_T = total confidence level for damage or failure load repetitions,

α = overall confidence defined by Eq 8.5,

α_N = confidence level assumed for calculation of fatigue life.

QUANTIFICATION OF CRACKING INDEX

The cracking index is calculated for a particular pavement on the basis of its structural components, expected traffic, the period for which the facility will be used, fatigue behavior, and stochastic variations in the material properties. Mathematically, this can be represented as

$$CI(x,t) = f\left[\sigma_j(x,t),\ \epsilon_j - N_j(x,t),\ n_j(t)\right] \tag{8.7}$$

where

$$\sigma_j(x,t) = f\left[E_i(x,t),\ \mu_i(x,t),\ D_i(x,t),\ W_j\right] \tag{8.8}$$

and

$$\left[\varepsilon_j - N_j(x.t)\right] = \text{the asphaltic concrete fatigue curve (Fig 8.2).}$$

From the equation of the asphaltic concrete fatigue curve, the mean fatigue life at any time t is given by

$$N_j(t) = A\left(\frac{1}{\varepsilon_j(t)}\right)^{\beta} \tag{8.9}$$

or

$$\log N_j(t) = \log A + \beta \log \left(\frac{1}{\varepsilon_j(t)}\right) \tag{8.10}$$

Assuming that the asphaltic concrete fatigue life variation in space x at any time t can be approximated by a log-normal distribution

$$\log N(x,t) = \log N_j(t) \pm K \log \sigma_N \tag{8.11}$$

Combining Eqs 8.10 and 8.11 for both space and time,

$$\log N_j(x,t) = \log A + \beta \log \left(\frac{1}{\varepsilon_j(t)}\right) \pm K \log \sigma_N \tag{8.12}$$

where

CI = cracking index of the surface material, measured in square feet per thousand square foot;

σ_j = stress in the surface material of level j, in psi units;

ε_j = flexural tensile strain in the surface material of level j, in inches per inch;

N_j = the number of load applications of level j to cause failure;

n_j = the number of actual load applications of level j ;

E_i = elastic modulus of the i^{th} layer in a pavement structure, in psi;

μ_1 = Poisson's ratio of the i^{th} layer in a pavement structure;

D_i = depth of the i^{th} layer in a pavement structure;

W_j = applied wheel load of level j on the pavement structure;

A = constant of asphaltic concrete fatigue equation;

β = constant of asphaltic concrete fatigue equation;

K = normal distribution curve parameter;

σ_N = standard deviation of fatigue curve;

(x,t) = function of space and time.

Modulus of Elasticity

For the elastic modulus values of the materials used in a pavement, the time variation is considered in terms of monthly variations. As explained in Chapter 5, the values of the modulus depend upon many factors and these values vary with time. Actually, the smaller the time interval considered, the better the simulation. However, to limit the computation work, a monthly variation was considered reasonable for the development of the cracking index model

$$E_i(t) = f\left[E_{i1}, E_{i2}, \ldots, \ldots, E_{i11}, E_{i12}\right] \qquad (8.13)$$

where

E_{i1} = average elastic modulus value of the i^{th} layer material for January,

E_{i2} = average elastic modulus value of the i^{th} layer material for February, etc.

Typical variations in monthly modulus values for pavement layers of AASHO Road Test sections are included in Chapter 5 and shown in Fig 8.3.

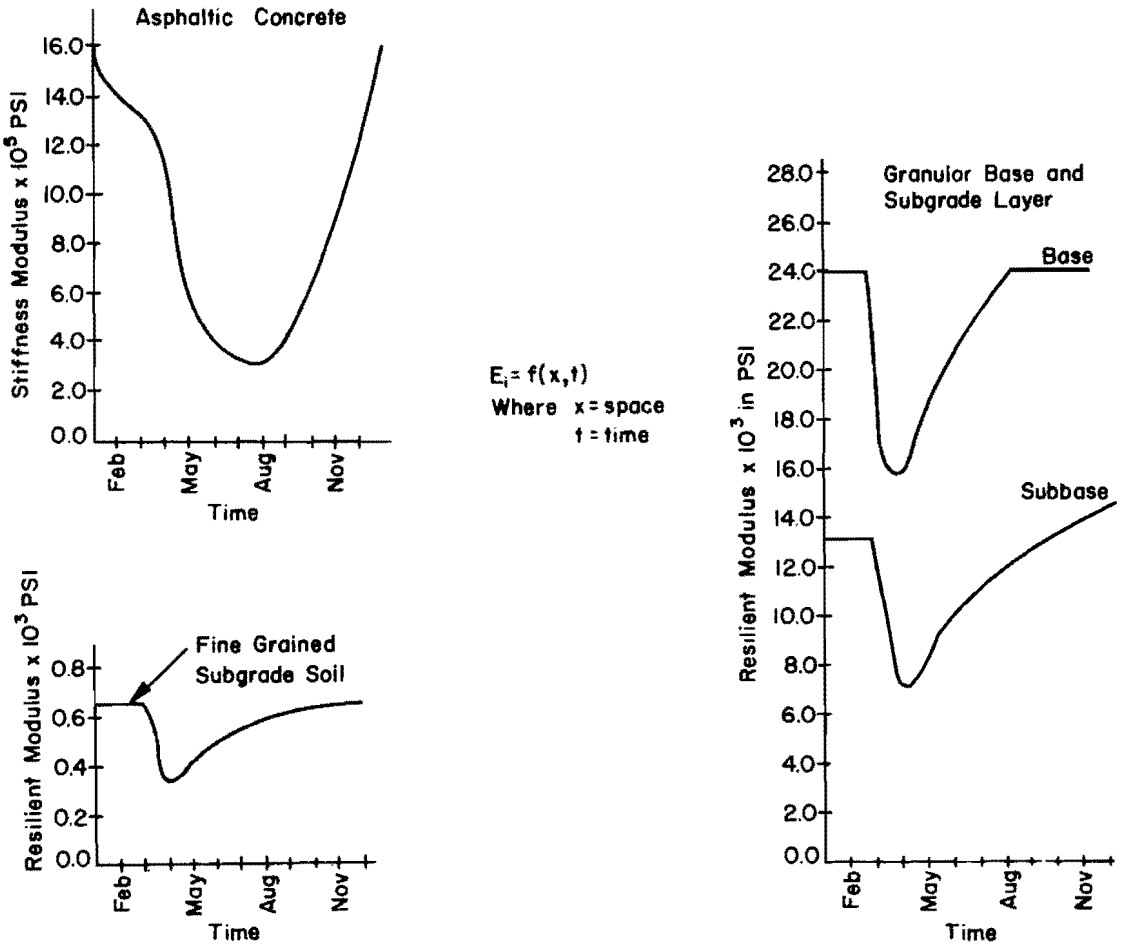

(a) Variation in time.

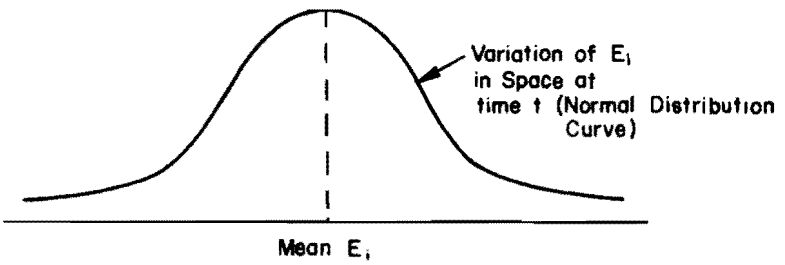

(b) Variation in space.

Fig 8.3. Conceptual diagram showing variation of modulus E_i in both space and time.

For the space variation, it is assumed that the modulus values are normally distributed and variation can be represented by a normal distribution curve (Fig 8.3). The density function of such a distribution in space is given by

$$f(E_i) = \frac{1}{\sigma_{Ei}\sqrt{2\pi}} \cdot e^{\frac{-(E_i - \bar{E}_i)^2}{2\sigma_{Ei}^2}} \tag{8.14}$$

and, based on Eq 8.14, the value of elastic modulus in space $E_i(x)$ is given by

$$E_i(x) = \bar{E}_i \pm K \cdot \sigma_{Ei} \tag{8.15}$$

where

$\bar{E}_i$ = arithmatic mean of the distribution,

σ_{Ei} = standard deviation of modulus values,

π = constant, and

e = constant.

To combine space and time variations, the final value of the modulus in both space and time is given by

$$E_i(x,t) = \bar{E}_{it} \pm K \cdot \sigma_{Eit} \tag{8.16}$$

Poisson's Ratio

In a sensitivity study, Buttler (Ref 15) found that magnitudes of the strain values in the surface layer calculated by the layered program are not significantly affected by variations in the Poisson's ratio. Therefore, this parameter is taken as a constant for each material in these developments.

$$\mu_i(x,t) = \mu_i \tag{8.17}$$

Layer Thickness

In a real-world situation, the thickness of any layer varies in both space and time. With the best construction control, small variations in thicknesses in space cannot be avoided. The load, environment, and variation in material properties can cause variation in this parameter with time. However, the variations in the layer thickness are not considered of much significance in these developments. Therefore,

$$D_i(x,t) = D_i \tag{8.18}$$

where

D_i = thickness of the i^{th} layer.

Applied Load

The effect of different wheel loads is considered by summation of the damage caused by each load group in Miner's hypothesis.

PROCEDURE FOR MODELING THE CRACKING INDEX

The flow chart for modeling the cracking index in a typical pavement structure (Fig 8.4) is shown in Fig 8.5. The various steps required are

(1) From the given monthly values of $\bar{E}_i$, σ_{Ei}, and the assumed confidence level α_i, calculate the $E_i(x,t)$ values of materials with Eq 8.16.

(2) Use the layered program and input $E_i(x,t)$ from step 1 and μ_i, axle load, tire pressure, and layer thicknesses to compute the tangential strains at the bottom of the surface layer.

(3) Calculate the overall confidence level α from Eq 8.5.

(4) From Eqs 8.10 and 8.11, calculate the theoretical values of N_j, both the mean and at some confidence level, considered.

(5) Calculate the overall confidence level for damage from Eq 8.6.

(6) From the given values of n_j, calculate cumulative damage $\sum_0^t \sum_0^j \frac{n_j}{N_j}$ for each month and for each load group. In the process, the mean, as well as the value at a certain confidence level, have been calculated.

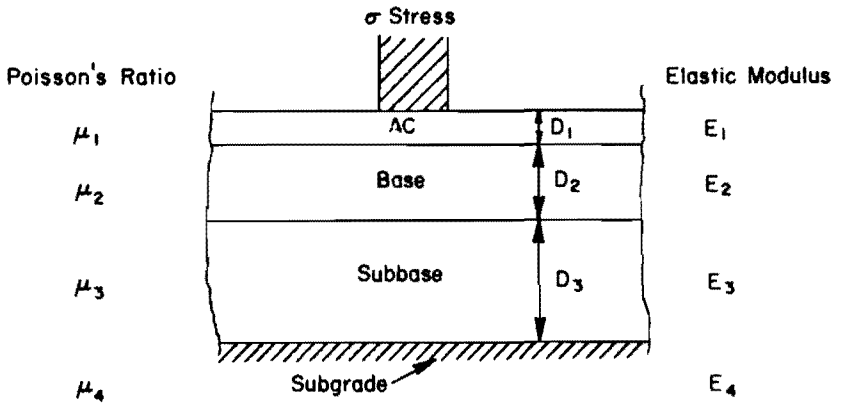

Fig 8.4. Typical flexible pavement section.

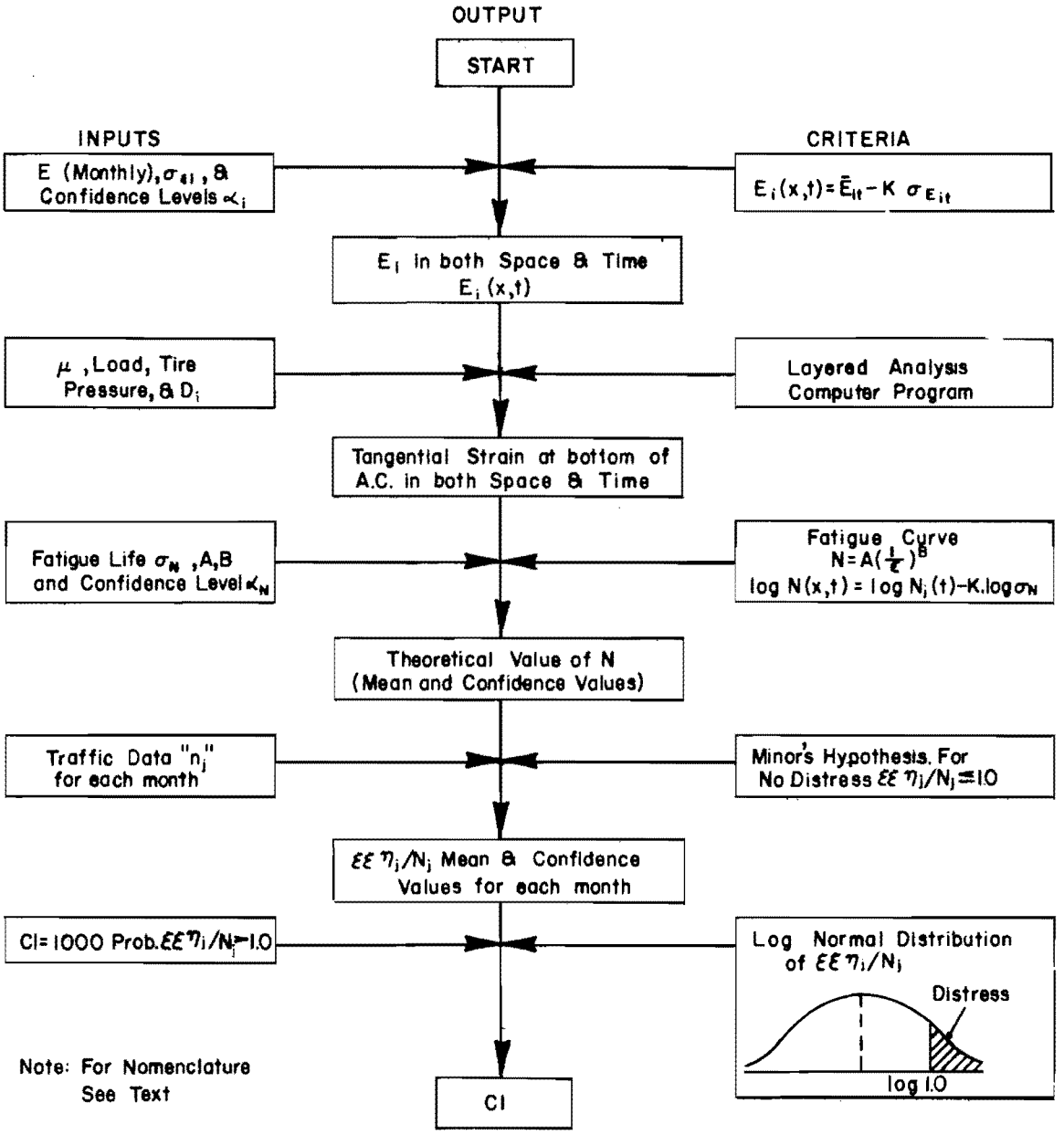

Fig 8.5. Flow chart for modeling the cracking index.

(7) Calculate the cracking index, as discussed earlier, from Eqs 8.2, 8.3, and 8.4.

COMPUTER PROGRAM

As can be seen, it is difficult to make all the necessary calculations by hand. Therefore, a computer program was developed to calculate the final cumulative cracking index values every month. The flow chart of the computer program is shown in Fig A4.1. The computer program follows the steps shown in Fig 8.5 in calculating the cracking index in a pavement structure. The input to the program consists of the parameters listed in the boxes on the left-hand side of this figure. The middle boxes show the sequence of the output based on the criteria in the right-hand boxes and the corresponding input. This computer program is written for the CDC 6600 computer in FORTRAN language. This computer program can be used directly for the design of flexible pavements and can also be included in the pavement system design computer program previously developed for the Texas Highway Department. However, efforts to make this computer program more efficient should continue.

CHAPTER 9. DEVELOPMENT OF RUT DEPTH INDEX MODEL

In this chapter, a model for predicting the rut depth index is presented. The vertical and radial stresses in a pavement system are computed from the layered analysis. The repeated load-deformation characteristics of the materials under triaxial testing are used. The rut depth may be represented as a permanent portion of the total deformation in a pavement structure due to repetition of loads. The deformation computations are made on the basis of mean values of the parameters, without considering the stochastic variations in space.

QUANTIFICATION OF RUT DEPTH INDEX MODEL

Figure 9.1 outlines the procedure developed to compute rut depth in a pavement structure. The rut depth is calculated in terms of permanent deformation in different layers due to repeated loading. The vertical deformation in an asphaltic concrete layer is very small relative to other layers and thus is not considered. The total deformation consists of the sum of the deformations in all the layers below the surface layer. Mathematically, rut depth in the pavement is represented as:

$$\text{Rut depth } \overline{RD}(t) = f\left[\sigma_{ij}(t),\ (\epsilon - n)_i,\ n_j(t)\right] \tag{9.1}$$

where

$$\sigma_{ij}(t) = f\left[E_i(t),\ \mu_i(t),\ D_i(t),\ W_j\right]; \tag{9.2}$$

(t) = function of time;

σ_{ij} = vertical and confining stresses in the i^{th} layer due to applied load W_j, in psi;

$\overline{RD} = f$ [applied load $, \eta_j, E_i, \mu_i$, repeated load v/s deformation curve]

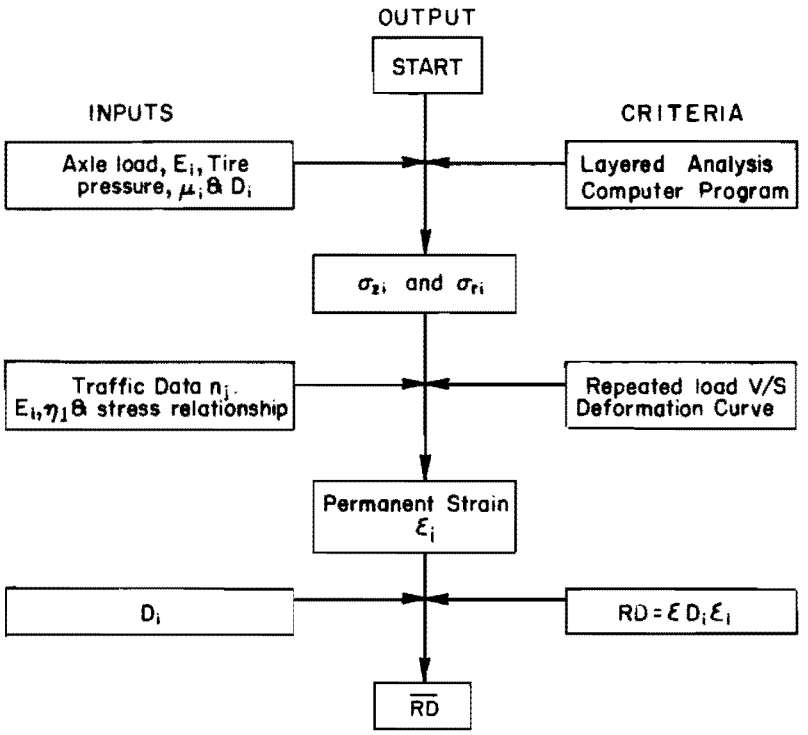

Fig 9.1. Flow chart for quantification of rut depth index.

n_j = number of load applications of level j ;

μ_i = Poisson's ratio of the i^{th} layer;

E_i = elastic modulus of the i^{th} layer, in psi;

D_i = depths of the i^{th} layer, in inches;

$(\epsilon - n)_i$ = repeated load deformation curve for the i^{th} layer;

ϵ_i = permanent vertical strain in the i^{th} layer.

Load Deformation Curves

In triaxial loading, the permanent deformation of a particular layer depends upon the number of load repetitions and vertical and confining stresses. Load deformation curves and regression equations developed from these curves, required to calculate the permanent deformation in various layers, were discussed in Chapter 5. These curves and regression equations give an estimate of the permanent strain and deformation in each layer in terms of vertical stress, confining stress, and number of stress repetitions.

Vertical and Confining Stresses

Vertical and confining stresses are considered in two catagories:

(1) Those due to wheel load, for which stresses are calculated from the layered program. The means of the stresses at the bottom and of those at the top of each layer represent the vertical and confining stresses due to wheel load.

(2) Those due to overburden, for which stresses in each layer are calculated as follows:

Layer	Effective Height of Overburden h_i, inches	Effective Weight of Overburden γ_{di}, pci
Base	$D_1 + D_2/2$	$\frac{1}{hi}(\gamma_{AC} \times D_1 + \gamma_{\beta} \times 0.5D_2)$
Subbase	$D_1 + D_2 + D_3/2$	$\frac{1}{hi}(\gamma_{AC} \times D_1 + \gamma_{\beta} \times D_2 + \gamma_{S\beta} \times 0.5 \times D_3)$
Subgrade	$D_1 + D_2 + D_3$	$\frac{1}{hi}(\gamma_{AC} \times D_1 + \gamma_{\beta} \times D_2 + \gamma_{S\beta} \times D_3)$

$$\sigma_{iro\beta} = \gamma_{di} \cdot h_i \cdot \frac{\mu_i}{1 - \mu_i} \tag{9.3}$$

$$\sigma_{izo\beta} = \gamma_{di} \cdot h_i \tag{9.4}$$

where

γ_{AC}, γ_{β} = unit weight of asphalt concrete, base, etc., pci;

$\sigma_{iro\beta}$ = radial stresses due to overburden in the i^{th} layer, psi;

$\sigma_{izo\beta}$ = vertical stresses due to overburden in the i^{th} layer, psi;

μ_i = Poisson's ratio of the i^{th} layer;

γ_{di} = effective weight of overburden, pci.

Final stresses to compute the deformation in each layer are obtained from the following equations:

$$\sigma_{ir} = \sigma_{izo\beta} + \sigma_{ir\ell} \tag{9.5}$$

$$\sigma_{iz} = \sigma_{izo\beta} + \sigma_{iz\ell} \tag{9.6}$$

where

σ_{ir} = total radial stress in the i^{th} layer, psi;

σ_{iz} = total vertical stress in the i^{th} layer, psi;

$\sigma_{ir\ell}$ = mean radial stress in the i^{th} layer due to wheel load, psi;

$\sigma_{iz\ell}$ = mean vertical stress in the i^{th} layer due to wheel load, psi.

Elastic Modulus

Elastic modulus for each layer is considered monthly; i.e.,

$$Ei(t) = f\left[E_{i1}, E_{i2}, \ldots, E_{i11}, E_{i12}\right] \tag{9.7}$$

where

E_{i1} = average modulus value of the i^{th} layer for January,

E_{i2} = average modulus value of the i^{th} layer for February, etc.

Applied Wheel Load

For various load groups, equivalent repetitions in terms of one single load group can be calculated as portrayed in Fig 9.2. Chan (Ref 20) found a linear relationship for total strain versus the log of the number of repetitions for several sands and gravel. Therefore, a straight-line relationship between the cumulative permanent strain ϵ and the logarithm of the number of load repetitions log N for materials of various pavement layers, other than the surface asphaltic concrete layer, is assumed. However, similar computations can be made if the straight-line relation is different from the assumed one. The equivalent repetitions are calculated in terms of the heaviest load group to give the least error in this computation. It is also assumed that load group h is the heaviest load group. For equivalent permanent strain (Fig 9.2),

$$\frac{\log N_i}{\epsilon_i} = \frac{\log n_h}{\epsilon_h} \tag{9.8}$$

or

$$N_i = 10.0^{\left(\frac{\log n_h}{\epsilon_h} \cdot \epsilon_i\right)} \tag{9.9}$$

Total equivalent repetitions in terms of h load group, say N_{ht}, is given by

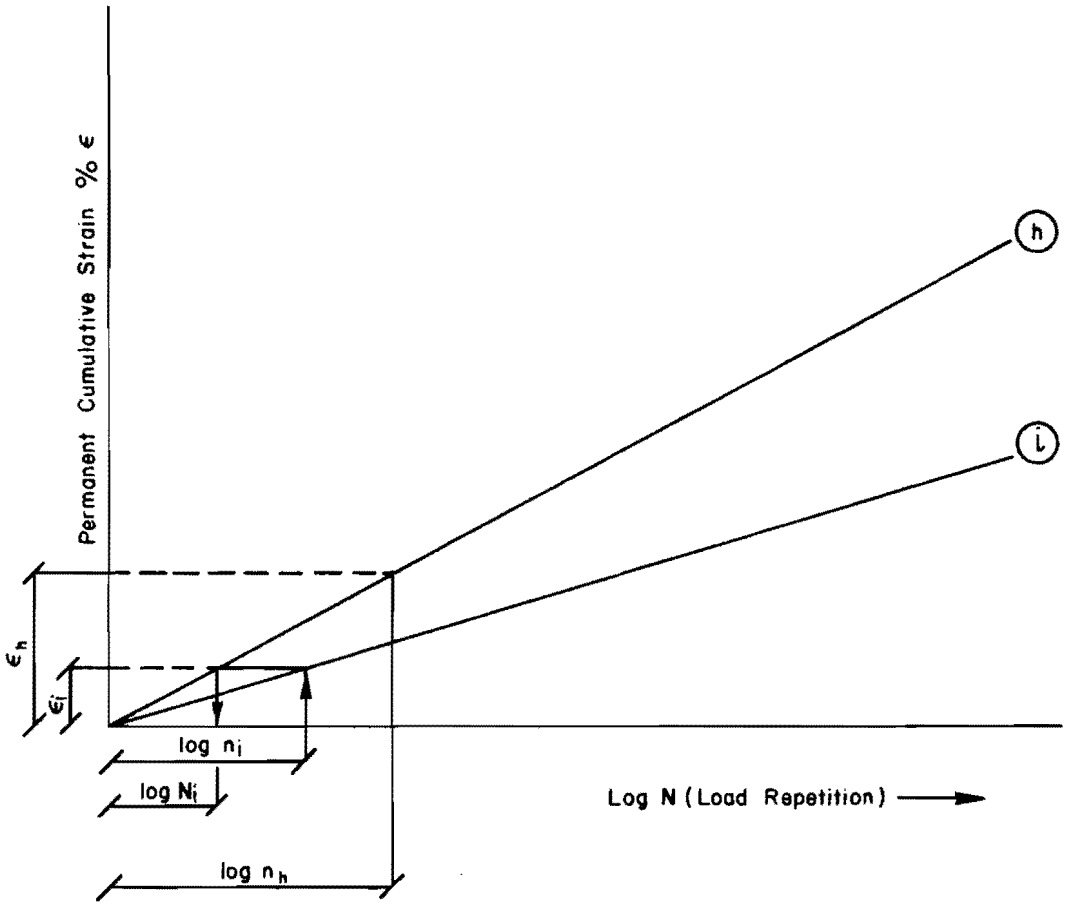

Note: The number on the curves represents the load group.

Fig 9.2. Development of equivalent load repetitions for one load group in terms of other load group.

$$N_{ht} = N_1 + N_2 + \ldots + N_h = \sum N_i \tag{9.10}$$

Combining Eqs 9.9 and 9.10,

$$N_{ht} = \sum 10.0^{\left(\frac{\log n_h \times \epsilon_i}{\epsilon_h}\right)} \tag{9.11}$$

where

N_i = equivalent number of load repetitions of load group of level i in terms of heaviest load group h,

n_i = actual load repetitions of load group of level i,

N_{ht} = total equivalent load repetitions in terms of heaviest load group,

ϵ_i = total permanent strain corresponding to load group n_i.

Permanent Strain in a Particular Month

Due to monthly variation in the material properties, the same load group creates different stress conditions in each layer each month. To find the cumulative deformation in each layer in a particular month, the net permanent strain caused by a particular load group in that month is required. This permanent strain in each layer, in percent inches per inch, is obtained from the difference of the permanent strain corresponding to the number of load repetitions at the beginning and at the end of that month.

$$\epsilon_{ip}(t) = \epsilon_{iE}(t) - \epsilon_{iB}(t) \tag{9.12}$$

where

$\epsilon_{ip}(t)$ = net permanent strain in the i^{th} layer for the t^{th} month;

$\varepsilon_{iB}(t)$ = permanent strain in the i^{th} layer for the t^{th} month and at the beginning of that month;

$\varepsilon_{iE}(t)$ = same as $\varepsilon_{iB}(t)$, but at the end of the month.

Permanent Deformation

The permanent deformation for each month in the pavement is calculated as

$$\Delta_i(t) = \varepsilon_{ip}(t) \cdot D_i \cdot \frac{1}{100} \tag{9.13}$$

$$\Delta(t) = \sum_{i=1}^{\ell} \Delta_i(t) \tag{9.14}$$

where

$\Delta_i(t)$ = permanent deformation in the i^{th} layer and t^{th} month, in inches;

$\Delta(t)$ = permanent deformation in the whole pavement structure in the t^{th} month, in inches;

ℓ = number of layers.

Cumulative Deformation or Rut Depth

The rut depth in a particular month is represented by the cumulative deformation of the pavement structure from the beginning of the pavement facility to the end of that month. Mathematically, the rut depth is given by:

$$\overline{RD}(t) = \sum_{o}^{t} \Delta(t) \tag{9.15}$$

Therefore, knowing the monthly deformations $\Delta(t)$, the rut depth is calculated by Eq 9.15.

PROCEDURE TO COMPUTE THE RUT DEPTH

The steps in the calculation of rut depth, shown in Fig 9.1, are

(1) From the axle load, modulus of elasticity of various layers, tire pressure, Poisson's ratio, and thickness of layers, compute the vertical and radial confining stresses at the top and bottom of each layer.

(2) Compute the total radial and vertical stresses in each layer due to overburden and wheel load from Eqs 9.5 and 9.6.

(3) Input the repeated load deformation curves obtained from the field for each layer except for the asphaltic concrete surface layer. Regression equations used in the computer program are developed in Chapter 5 from the repeated load-deformation data (Eqs 5.3, 5.4, and 5.5). Compute permanent strain corresponding to stress conditions and number of load repetitions at the beginning and end of each month for each load group.

(4) Calculate the equivalent repetitions in terms of the single heaviest load group, using Eq 9.9.

(5) Again compute the permanent strain from the regression equations at the beginning and end of each month (as in item 3), but only for the heaviest load group for the equivalent number of repetitions calculated in item 4.

(6) For each month, the permanent strain in each layer is calculated from the difference of the strain values corresponding to the number of load repetitions at the beginning and end of that month from Eq 9.12.

(7) From the permanent strain in each layer for each month, the total permanent deformation in the individual layers and for the whole pavement for each month is calculated with Eqs 9.13 and 9.14.

(8) Finally, cumulative deformation for each month, representing the rut depth in the pavement is calculated by Eq 9.15.

COMPUTER PROGRAM

The whole procedure for computing the expected rut depth is too lengthy to handle by hand calculations. Therefore, a computer program has been written which solves all the above mentioned steps and computes the values of the expected rut depth. To reduce the work of the designer, this part of the computer program is combined with the program developed for calculation of the cracking index in Chapter 8. The program has the alternative that either or both cracking index and rut depth values can be computed. Because most of the input data for calculation of rut depth and the cracking index are common to the combined program, manual as well as computer time is saved in solving a problem.

Moreover, this one computer program is easier to include in the existing flexible pavement system computer program. At present, the model does not consider the stochastic variations in space. This may be done at the time of detailed stochastic studies of various variables in the present flexible pavement system.

As indicated in Chapter 8, the computer program, flow chart, input guide, and sample input and output are enclosed in Appendix 4.

CHAPTER 10. DEVELOPMENT OF ROUGHNESS INDEX MODEL

In this chapter, a model for quantification of roughness index is developed. It is hypothesized that the trend in the cracking index is a good indicator of the trend in the roughness index, and a correlation is established between the cracking index and the roughness index. Thus, a model is presented for roughness index in terms of axle load, number of axles, depth of pavement layer, and cracking index.

THEORY

Cracking in an asphalt surface has long been used as a direct indication of a structural inadequacy somewhere in a pavement system, and cracking was used as the principal criterion of pavement failure at the WASHO Road Test (Ref 74). Cracking and patching were found to be of only minor significance in the performance model of a pavement at the AASHO Road Test (Ref 70), but that does not mean cracking is of minor structural importance. By the time fatigue cracking due to repeated loading has progressed enough to greatly impair the riding quality of a pavement, the pavement becomes very rough in terms of slope variance, and the slope variance or roughness index in the AASHO Road Test represented most of the detrimental effects of cracking (Ref 139). It can be assumed that fatigue cracking due to repeated loading is a good indicator of the roughness caused due to fatigue loading. Thus, a good correlation exists between the cracking index and the roughness index. The following comments of NCHRP Project 39 (Ref 42) support the above hypothesis very well:

> "Careful examination of the criterion and the basic measurements tends to indicate that a significant amount of the drop in riding quality must have been due to the longitudinal roughness associated with fatigue cracking."

A mathematical correlation between the roughness index, in terms of the cracking index, and pavement structural elements is hypothesized as:

$$RI(x,t) = f\left[CI(x,t),\ D_i,\ W_j,\ L_j\right] \tag{10.1}$$

where

RI = roughness index,

CI = cracking index,

(x,t) = function of space and time,

D_i = thickness of the i^{th} layer in a pavement,

W_j = axle load in kips of level j,

L_j = single or tandem axle of the load j.

In correlating slope variance and cracking-patching from observed data, it seems that each has a direct relationship with the number of repetitions of a particular load (Ref 139). Figure 10.1 shows a typical example of such a relationship. The relationship between cracking-patching and slope variance, depending upon the various values for structural elements of the pavement and the load, can be represented by the following equation.

$$SV = A + B\sqrt{CP} \tag{10.2}$$

The values of A and B will depend upon the pavement structural element and load group, or

$$A = f(C_i,\ D_i,\ W_j,\ L_j) \tag{10.3}$$

$$B = f(C_i,\ D_i,\ W_j,\ L_j) \tag{10.4}$$

where

SV = slope variance,

CP = measured crack-patching,

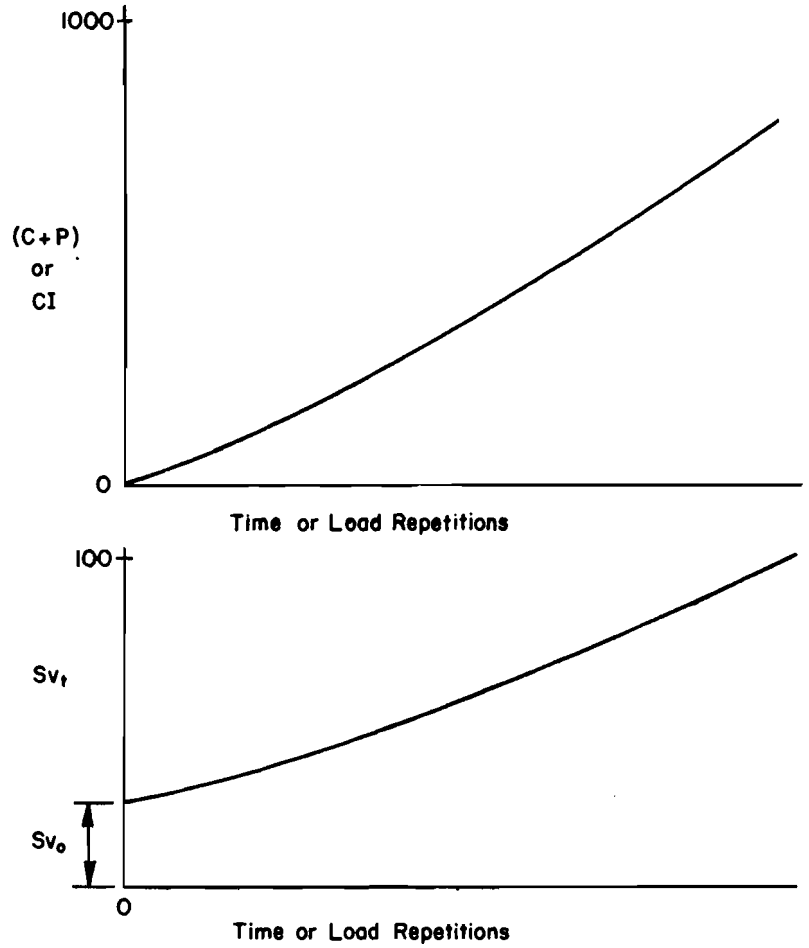

Sv_o = Initial Value of the Slope Variance
Sv_t = Slope Variance at any Time t
C + P = Cracking and Patching
CI = Cracking Index

Fig 10.1. Typical example of relationship between cracking-patching, slope variance and number of load repetitions of a particular load.

C_i = some coefficient to show the relative importance of various layers in a pavement.

and SV is given by

$$RI = \log (1 + SV) \tag{10.5}$$

Based on the above hypothesis (Eqs 10.1 and 10.2), AASHO Road Test data are analyzed later in this chapter to obtain a correlation between the roughness index based on measured values and cracking-patching. Only the load-associated distress is considered in the work reported here and thus, the AASHO Road Test data are used because they are primarily fatigue load data, with no significant effects of nonload-associated distress. The procedure and steps involved for the above analysis are shown in Fig 10.2. Through the regression analysis (Ref 18), trying various functions, a suitable model is obtained for a correlation between the dependent variable slope variance (to be predicted) and independent variables, cracking-patching, layer thicknesses, etc. (known).

QUANTIFICATION OF ROUGHNESS INDEX

Two approaches to quantification of the roughness index are discussed in this section, one based on literature and one on regression analysis.

Quantification Based on Literature

A literature review shows that the quantification of a roughness index is possible from the available information on AASHO Road Test results. The results of an analysis of AASHO Road Test data by the Asphalt Institute (Ref 139) include equations of the following forms:

$$\sqrt{SV_t} = \sqrt{SV_o} + bN_t \tag{10.6}$$

$$\overline{RD}^2 = bN_t \tag{10.7}$$

$$\sqrt{CP} = bN_t \tag{10.8}$$

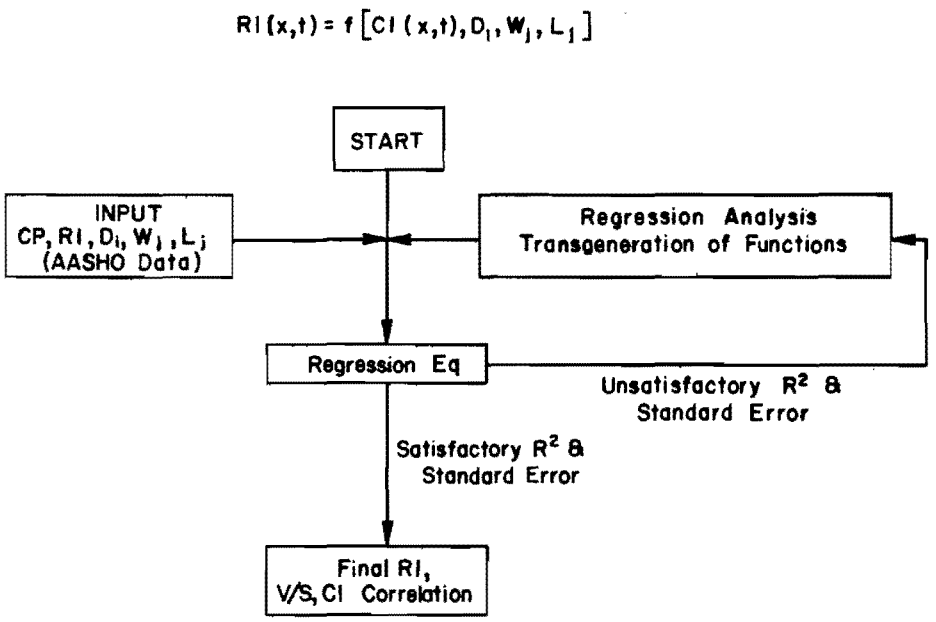

Fig 10.2. Flow chart for quantification of roughness index.

where

SV_t = slope variance at any time t,

SV_o = slope variance of the pavement at the time of construction,

b = rate of deterioration,

N_t = accumulated load applications to time t,

$\overline{RD}$ = rut depth.

The rate of deterioration b was shown to depend on the thicknesses and structural coefficients of different layers, subgrade strength, and load parameter:

$$\log b = a_o + a_i D_i + a_2 D_3 + a_4 L + a_6 WP \qquad (10.9)$$

where

a_o, a_1, etc. = constants representing some structural coefficient and depending upon the strength properties of pavement layers,

L = factor representing axle load group,

WP = factor for outer or inner wheel path.

Painter also obtained some numerical correlations for Eqs 10.6 to 10.9. Based on his work, the correlation between cracking-patching is

$$D_1 + 0.284D_2 + 0.228D_3 = 9.403 + 2.931 \log W_{18} - 1.466 \log CP + \log F \qquad (10.10)$$

and slope variance is

$$D_1 + 0.313D_2 + 0.2D_3 = 7.412 + 3.477 \log W_{18}$$

$$- 3.477 \log (\sqrt{SV} - \sqrt{SV_o}) + \log F \qquad (10.11)$$

where

W_{18} = millions of accumulated load applications of 18-kips load,

F = climate factor.

Combining Eqs 10.10 and 10.11 to eliminate $\log W_{18}$ and combining terms gives

$$\text{Log } (\sqrt{SV} - \sqrt{SV_o}) = 0.053D_1 + 0.007D_2 + 0.0201D_3$$

$$- 1.075 - 0.053 \log F + 0.5 \log (CP) \qquad (10.12)$$

In the Painter's analysis, the average value for F was found to be 4.0. Eliminating $\log F$ between Eqs 10.10 and 10.11:

$$0.029D_2 - 0.028D_3 = -1.991 + 0.546 \log W_{18}$$

$$- 3.477 \log (\sqrt{SV} - \sqrt{SV_o}) + 1.466 \log (CP) \qquad (10.13)$$

Thus, Eqs 10.12 and 10.13 can be used for predicting the slope variance from the known value of cracking-patching, thickness of pavement layers, and equivalent 18-kip load applications.

Quantification Based on Regression Analysis

In Eqs 10.10 and 10.11, the loads were converted to single-axle 18-kip equivalents (based on values in Ref 139, Table 3, and page 26); hence, no terms for load and number of axles appear in Eq 10.12. However, based on the discussion earlier in this chapter and Painter's analysis, a general relationship between roughness index and cracking-patching would be expected to be

$$\log\ (1 + \sqrt{SV} - \sqrt{SV_o}) = A_1 + A_2D_1 + A_3D_2 + A_4D_3$$

$$+ A_5W + A_6L + A_7\ \log\ (1 + CP) \qquad (10.14)$$

where

A_1, A_2, etc. = constants of the regression equation,

SV = slope variance at any value of cracking-patching (CP),

SV_o = initial slope variance of the pavement.

Using data for various AASHO Road Test sections (Table 10.1), a regression analysis was conducted. The data consist of representative sections, constituting various observations for the analysis which could be performed within a reasonable time and efforts under the scope of the project. The data for the analysis represent various loops, load groups, and combinations of thicknesses of various layers of the AASHO Road Test sections. In this analysis, computer program STEP-01 (Ref 18) was used. Input and output of the computer program, used for the regression analysis, are given in Appendix A4.5. Results of this analysis are consolidated in Table 10.2. On the basis of regression analyses alone, one term, $[\log\ (1 + CP)]^2$, i.e., first step, had a correlation coefficient R^2 of 0.9289 and should be considered best for the proposed correlation between cracking-patching and slope variance for interpolation of results within the data analyzed, because the additional terms did not improve the value of the correlation coefficient or standard error of residual. However, from the engineering point of view, based on the earlier discussions (Eq 10.14), and for extrapolation of results from the available information, the inclusion of other terms in the correlation may be considered desirable. During the analyses of data, it was also seen that the first step in the regression analysis produced seven points which are more than twice the standard error away from the desired value, as against four points in the case of the eighth step. Also, the highest error of prediction is lower in step 8 in comparison to step 1. Addition of a few terms in case of computation by computers does not involve any significant difference in time or labor. Moreover, during the

TABLE 10.1 SECTIONS CONSIDERED FOR REGRESSION ANALYSIS FOR RI V/S CP CORRELATION (AFTER REF 70)

Loop 1

Axle Load

Lane 1	Lane 2
None	None

Main Factorial Design Design 1

Surface Thickness	Base Thickness	Subbase Thickness	Test Section No. Lane 1	Test Section No. Lane 2
1	0	0	857	858
		8	867	868
		16	833	834
			841	842
	6	0	827	828
		8	847	848
		16	839	840
3	0	0	859	860
			863	864
		8	869	870
			829	830
		16	837	838
	6	0	825	826
			851	852
		8	875	876
			819	820
		16	821	822
5	0	0	823	824
		8	865	866
		16	877	878
	6	0	871	872
		8	849	850
		16	879	880
			873	874

Subsurface Studies Design 5

Surface Thickness	Base Thickness	Subbase Thickness	Test Section No. Lane 1	Test Section No. Lane 2
3	0	0	861	862
		8	831	832
			853	854
		16	817	818
	6	0	855	856
		8	845	846
		16	843	844
			835	836

Loop 2

Axle Load

Lane 1	Lane 2
2,000-S	6,000-S

Main Factorial Design Design 1

Surface Thickness	Base Thickness	Subbase Thickness	Test Section No. Lane 1	Test Section No. Lane 2
1	0	0	721	722
		4	727	728
	3	0	●743■	744■
		4	●717■	●718
	6	0	755	756
		4	719	●720■
2	0	0	771	772
		4	●729■	730
	3	0	759	●760
			731	732
		4	741	742■
			709	●710■
	6	0	775	776
			757	758
		4	737	738
			711	712
3	0	0	769	●770
		4	739	740
	3	0	773	●774
		4	745	746
	6	0	749	750
		4	763	764

Surface Treatment Study Design 6

Surface Thickness	Base Thickness	Subbase Thickness	Test Section No. Lane 1	Test Section No. Lane 2
Surface Treatment	0	0	733	734
			751	752
		4	753	754
			723	724
	3	0	725	726
			767	768
		4	765	766
			715	716
	6	0	747	748
			735	736
		4	761	762
			713	714

Loop 3

Axle Load

Lane 1	Lane 2
12,000-S	24,000-T

Main Factorial Design Design 1

Surface Thickness	Base Thickness	Subbase Thickness	Factorial Block	Test Section No. Lane 1	Test Section No. Lane 2
2	0	0	1	●165	166
		4	3	125	126
		8	2	143	144
			2	133	134
	3	0	3	113	114
		4	2	135	136
		8	1	●159■	160
	6	0	2	127	128
		4	1	157	158
		8	3	111	112
3	0	0	2	●137	138
		4	1	●163■	164
		8	3	109	110
	3	0	1	147	148
		4	3	107	108
			3	115	116
	6	8	2	129	130
		0	3	117	118
		4	2	131	132
		8	1	155	156
4	0	0	3	119	120
		4	2	141	142
		8	1	153	154
	3	0	2	145	146
		4	1	●151■	152
		8	3	121	122
	6	0	1	●161■	162
			1	149■	150
		4	3	123	124
		8	2	139	140

Shoulder Paving Study Design 2

Shoulder Paving	Surface Thickness	Base Thickness	Subbase Thickness	Test Section No. Lane 1	Test Section No. Lane 2
With	2	3	0	177	178
				179	180
	2	3	8	175	176
				183	184
	4	3	0	173	174
				181	182

Base Type Study Design 4

Base Type	Surface Thickness	Base Thickness	Subbase Thickness	Test Section No. Lane 1	Test Section No. Lane 2
Crush. Stone	3	2-14	0	169	170
				105	106
Gravel	3	2-14	0	171	172
				103	104
Bit. Treat.	3	2-11	0	167	168
				101	102

Loop 4

Axle Load

Lane 1	Lane 2
18,000-S	32,000-T

Main Factorial Design Design 1

Surface Thickness	Base Thickness	Subbase Thickness	Factorial Block	Test Section No. Lane 1	Test Section No. Lane 2
3	0	4	1	633	634
		8	2	●607■	●608
		12	3	571	572
			3	569	570
	3	4	2	599	●600
		8	3	573	●574
		12	1	617	618
	6	4	3	585	586
		8	1	●623■	624
		12	2	601	602
4	0	4	3	583	584
		8	1	619	620
		12	2	603	●604
	3	4	1	●627■	628
		8	2	589	590
			2	597	598
		12	3	575	576
	6	4	2	595	●596
		8	3	577	578
		12	1	●625■	626
5	0	4	2	605	606
		8	3	587	588
		12	1	621	622
	3	4	3	579	580
		8	1	631	632
		12	2	593	594
	6	4	1	629■	630
			1	●615■	616
		8	2	591	592
		12	3	581	582

Shoulder Paving Study Design 2

Shoulder Paving	Surface Thickness	Base Thickness	Subbase Thickness	Test Section No. Lane 1	Test Section No. Lane 2
With	3	0	4	637	638
				609	610
	3	6	4	635	636
				611	612
	5	0	4	639	640
				613	614

Base Type Study Design 4

Base Type	Surface Thickness	Base Thickness	Subbase Thickness	Test Section No. Lane 1	Test Section No. Lane 2
Crush. Stone	3	2-16	4	567	568
				561	562
Gravel	3	2-16	4	565	566
				559	560
Cem. Treat.	3	2-10	4	563	564
				557	558

Loop 5

Axle Load

Lane 1	Lane 2
22,400-S	40,000-T

Main Factorial Design Design 1

Surface Thickness	Base Thickness	Subbase Thickness	Factorial Block	Test Section No. Lane 1	Test Section No. Lane 2
3	3	4	1	485	486
		8	2	451	452
		12	3	415■	416
			3	429■	430
	6	4	2	449	450
		8	3	419	420
		12	1	487■	488
	9	4	3	413	414
		8	1	471	472
		12	2	441	442
4	3	4	3	411	412
		8	1	481	482
		12	2	443	444
	6	4	1	473	474
		8	2	455	456
			2	453■	454
		12	3	425	426
	9	4	2	437	438
		8	3	417	418
		12	1	477	478
5	3	4	2	439	440
		8	3	421	422
		12	1	479	480
	6	4	3	423	424
		8	1	469	470
		12	2	445	446
	9	4	1	475■	476
			1	483■	484
		8	2	447	448
		12	3	427	428

Shoulder Paving Study Design 2

Shoulder Paving	Surface Thickness	Base Thickness	Subbase Thickness	Test Section No. Lane 1	Test Section No. Lane 2
With	3	3	4	435	436
				407	408
	3	9	4	431	432
				405	406
	5	3	4	433	434
				409	410

Base Type Study Design 4

Base Type	Surface Thickness	Base Thickness	Subbase Thickness	Test Section No. Lane 1	Test Section No. Lane 2
Gravel	3	3-18	4	467	468
				457	458
Bit. Treat.	3	3-16	4	463	464
				459	460
Cem. Treat.	3	3-12	4	465	466
				461	462

Loop 6

Axle Load

Lane 1	Lane 2
30,000-S	48,000-T

Main Factorial Design Design 1

Surface Thickness	Base Thickness	Subbase Thickness	Factorial Block	Test Section No. Lane 1	Test Section No. Lane 2
4	3	8	3	269	270
		12	2	299	300
		16	1	317	318
			1	329	330
	6	8	2	303	304
		12	1	323■	324■
		16	3	253	254
	9	8	1	321	322
		12	3	267	268
		16	2	309	310
5	3	8	1	319	320
		12	3	261	262
		16	2	315	316
	6	8	3	259	260
		12	2	307■	308■
			2	305	306
		16	1	327	328
	9	8	2	313	314
		12	1	331	332
		16	3	265	266
6	3	8	2	297	298
		12	1	335	336
		16	3	255	256
	6	8	1	325	326
		12	3	257	258
		16	2	301	302
	9	8	3	263	264
			3	271	272
		12	2	311■	312
		16	1	333	334

Shoulder Paving Study Design 2

Shoulder Paving	Surface Thickness	Base Thickness	Subbase Thickness	Test Section No. Lane 1	Test Section No. Lane 2
With	4	3	8	291	292
				275	276
	4	3	16	293	294
				273	274
	6	3	8	295	296
				277	278

Base Type Study Design 4

Base Type	Surface Thickness	Base Thickness	Subbase Thickness	Test Section No. Lane 1	Test Section No. Lane 2
Crush. Stone	4	3-19	8	287	288
				279	280
Bit. Treat.	4	3-18	4	285	286
				283	284
Cem. Treat.	4	3-13	4	289	290
				281	282

NOTE:

Shaded sections are replicates. Dotted sections are considered for RI v/s CP correlation. Sections marked with squares are compared for RI observed and computed from proposed model.

TABLE 10.2. RESULT OF REGRESSION ANALYSIS FOR CRACKING-PATCHING (CP) VERSUS ROUGHNESS INDEX (RI)

Step Number	Variables	Residuals	R	R^2
1.	Constt. SQLCP	0.0680	0.9638	0.9289
2.	Constt. LCP SQLCP	0.0671	0.9651	0.9315
3.	Constt. LCP D_2 SQLCP	0.0669	0.9657	0.9325
4.	Constt. LCP D_2 L SQLCP	0.0670	0.9660	0.9332
5.	Constt. LCP D_2 W L SQLCP	0.0665	0.9669	0.9348
6.	Constt. LCP D_1 D_2 W L SQLCP	0.0668	0.9669	0.9350

(Continued)

TABLE 10.2. (Continued)

Step Number	Variables	Residuals	R	R^2
7.	Constt. LCP D_1 D_2 D_3 W L SQLCP	0.0670	0.9671	0.9353
8.	Constt. LCP D_1 D_2 D_3 W L CBLCP SQLCP	0.0674	0.9692	0.9354

INDEPENDENT VARIABLES

LCP = Log (1 + CP)

D_1 = Depth of A. concrete

D_2 = Depth of base

D_3 = Depth of subbase

W = Axle load

L = 1. For single axle
2. For tandum axle

SQLCP = $[\text{Log } (1 + CP)]^2$

CBLCP = $[\text{Log } (1 + CP)]^3$

DEPENDENT VARIABLES

Arctan. Log $(1 + \sqrt{SV_i} - \sqrt{SV_o})$

When:

SV_i = Slope variance at any time

SV_o = Initial slope variance

analysis, it was observed that at the higher values of cracking index, the values of the roughness index often tended to give results relatively lower than the observed values. Therefore, the term $[\log (1 + CP)]^3$ was also retained in the equation to help in predicting values closer to the actual values. Finally, Eq 10.15, which corresponds to step 8 in the regression program (Table 10.2), is adopted for the present analysis.

$$\begin{aligned}\text{Arctan } \log (1 + \sqrt{SV_i} - \sqrt{SV_o}) &= -0.09136 + 0.09108 \log (1 + CP) \\ &+ 0.02445 [\log (1 + CP)]^2 + 0.00778 [\log (1 + CP)]^3 \\ &+ 0.00837D_1 + 0.00458D_2 + 0.00175D_3 - 0.00386W \\ &+ 0.08325L \end{aligned} \qquad (10.15)$$

This regression correlation, developed on the 95 observed points, has nine coefficients with a correlation coefficient R^2 of 0.9354. For a mean value of 0.37 of the dependent variable, the standard error of the residuals is 0.0674 (coefficient of variation 18 percent), in comparison to the standard deviation in the variability of the SD Profilometer measurement of 0.0644 for assumed SV_o equal to one (Ref 155). Values of dependent variables in the analysis range from 0.0 to 1.0. The comparison of the predicted values from this model and the measured values from the AASHO Road Test is discussed in Chapter 11.

The AASHO Road Test measure of cracking-patching is theoretically obtained from the cracking index model and is defined as the cracking index, as explained in Chapter 8. Thus, for the performance calculation in the present report, the cracking-patching term in Eq 10.15 is replaced by the cracking index CI .

SELECTION OF MODEL

Equation 10.13 is given in terms of only equivalent 18-kip load group and is not suitable for the proposed design procedure which considers all load groups individually.

Figure 10.3 compares the actual data points with the predictions made by the equation obtained from Painter's analysis (Eq 10.12) and the regression model (Eq 10.15). Equations derived from literature (Eqs 10.12 and 10.13) are indeterminate at the zero value of CP . The regression model (Eq 10.15) predicts a mean value of $\log (1 + \sqrt{SV} - \sqrt{SV_o})$ as 0.52, while Eq 10.12 predicts 0.514 against the actual mean value of 0.525. The standard error of residuals for regression model (Eq 10.15) is found to be 0.09 against 0.138 for Eq 10.12. Thus, the regression model is seen to predict the points more accurately and is determinate at all values of cracking-patching.

Verification of the roughness index values predicted by the regression model also shows good agreement with observed values, as further discussed in Chapter 11. Moreover, the equations (Eq 10.12 and 10.13) developed from Painter's analysis are obtained by an indirect relationship (Eqs 10.10 and 10.11) and may not be considered accurate.

The proposed regression model is generalized for various load groups and number of axles, and the correlation between cracking-patching and roughness index is derived directly from AASHO Road Test data. Thus, for the analysis presented here, the regression model represented by Eq 10.15 was adopted.

PROCEDURE FOR COMPUTATION OF ROUGHNESS INDEX

The procedure for calculating the roughness index for any pavement section is:

(1) Calculate the cracking index values as detailed in Chapter 8.

(2) Based on engineering experience, assume certain values for the initial slope variance (SV_o) expected in a planned pavement. Initial values of slope variance, depending on the type of construction, generally vary from 1.0 to 3.0.

(3) Using the known values of pavement layer thickness, axle load, number of axles, and computed cracking index obtain the slope variance with Eq 10.15.

(4) Substitute the value of slope variance into Eq 10.5 to obtain the roughness index.

COMPUTER PROGRAM

The model selected for the roughness index contains several terms, and making the necessary calculations by hand is very time consuming. Moreover,

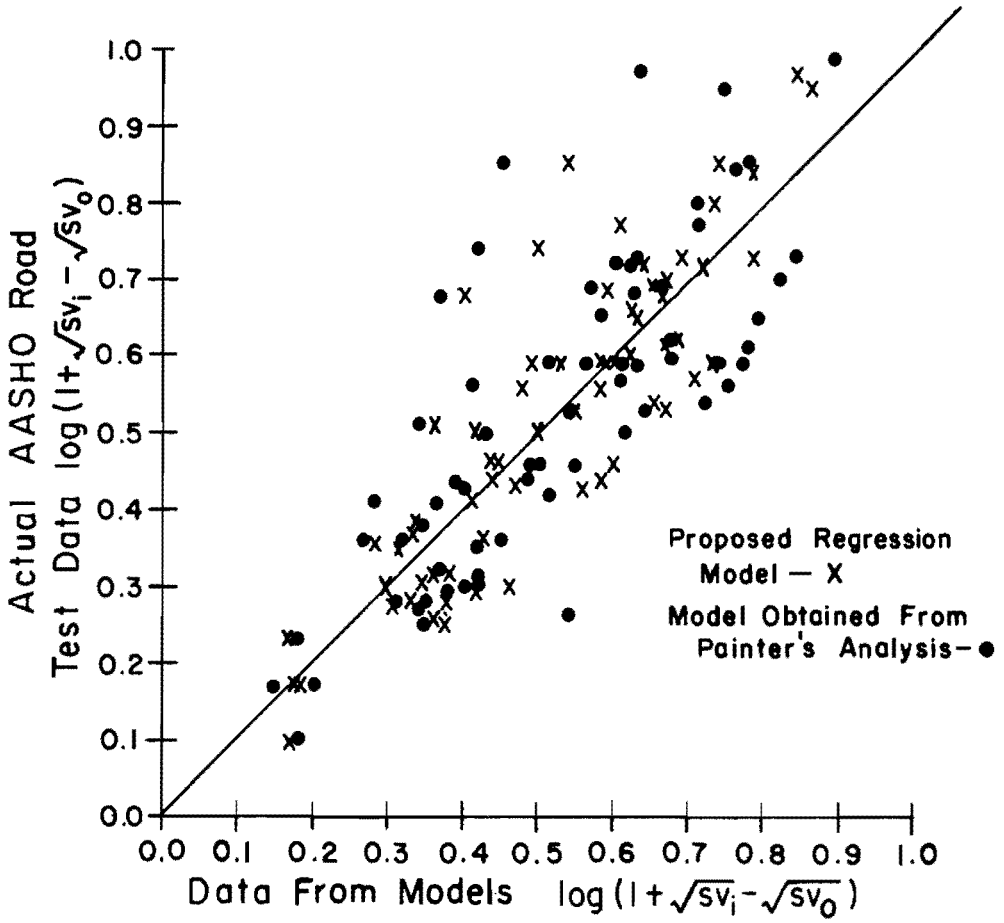

Fig 10.3. Comparison of log $(1 + \sqrt{SV_i} - \sqrt{SV_o})$ for various values of log (1 + CP) computed from the model of painters analysis with that predicted from the proposed model.

the whole procedure of pavement design developed here is to be included in an existing flexible pavement systems computer program. A computer program for the calculation of the cracking index and rut depth index has been developed, as explained in Chapters 8 and 9. A computer program for calculation of the roughness index has also been developed and is included in Appendix 4. This computer program, for the roughness index also calculates the present serviceability index. The input consists of the cracking index, rut depth index, pavement layer thicknesses, axle load, number of axles, and initial slope variance. A typical output is included in Appendix 4.

CHAPTER 11. VERIFICATION OF DISTRESS MODELS

The purpose of this chapter is to verify the distress index models which were developed in Chapters 7 through 10. This chapter is divided into four parts, each of which provides details of verification of one of the models developed for cracking index, slope variance, rut depth, and PSI with the AASHO Road Test data. The AASHO Road Test sections which are compared are shown in Fig 11.1. These 28 sections were selected based on the following criteria:

(1) to represent various load groups;

(2) to represent various loops;

(3) to represent various combinations of layer thicknesses;

(4) to represent some sections without base and some without subbase;

(5) considering the reasonable time to be spent, scope of the project, computer time involved in solving problems, and money involved consistent with the accuracy desired and obtained.

All 28 sections were carried over for all distress models. Overdesigned sections such as 763 were avoided in this selection because these were not of much value for comparison. Sections of loop 1 were not considered because this loop did not carry any load.

CRACKING INDEX MODEL

The detailed development of this model was discussed in Chapter 8. Figure 11.2 compares the calculated cracking index and actual measured values of cracking-patching of six AASHO Road Test sections. This comparison for the other 22 sections is included in Appendix 8 (Figs A8.1 through A8.18).

Computation of Cracking Index

In computing the cracking index values, the material properties characterized in Chapter 5 are used. Tables 5.2, 5.3, and 5.8 show the adopted monthly values of elastic modulus. The actual monthly traffic data of AASHO Road Test (Ref 70) and the computer program procedure detailed in Chapter 8

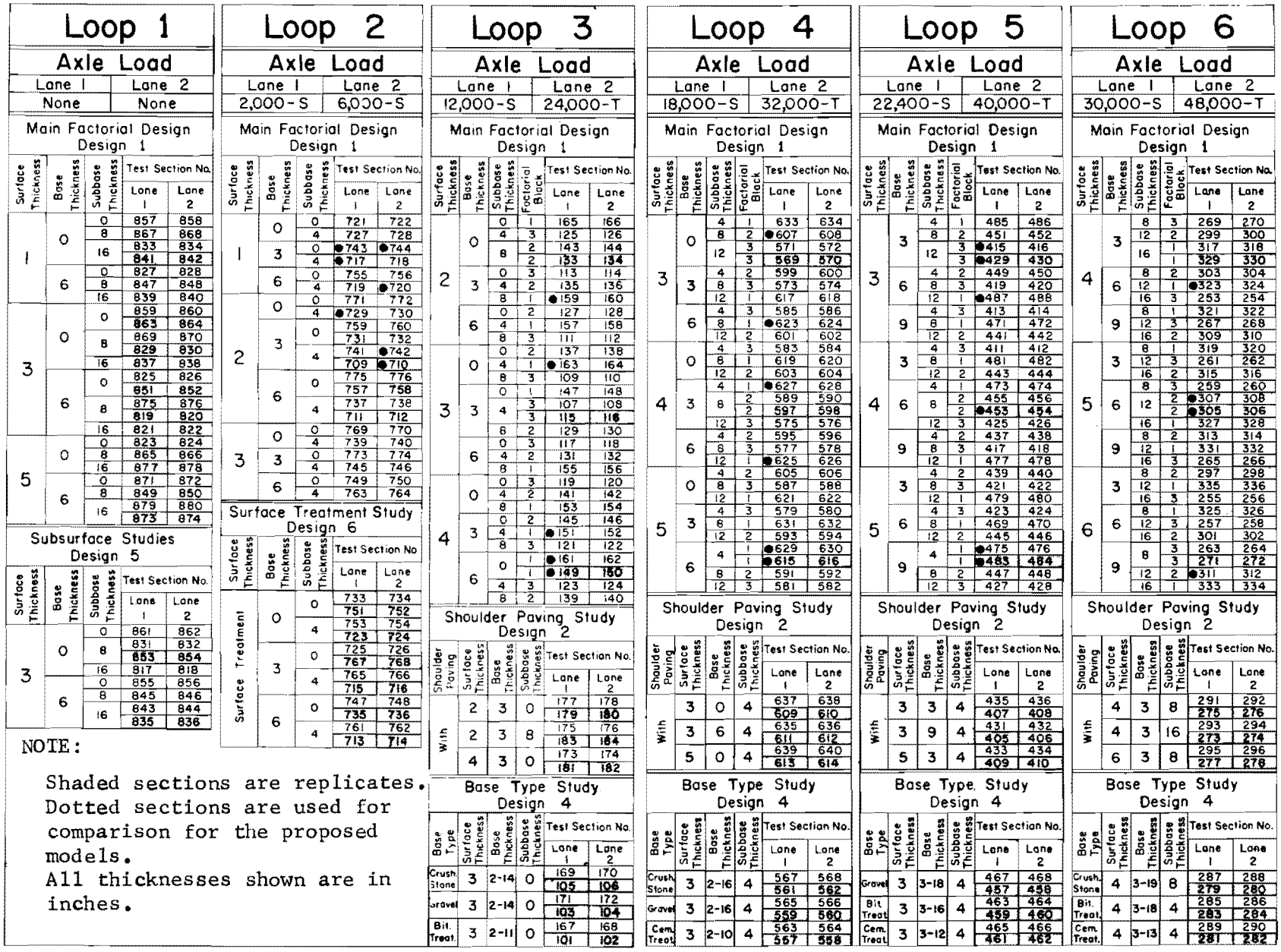

Fig 11.1. AASHO Road Test sections used for comparison of distress index and performance model (After Ref 70).

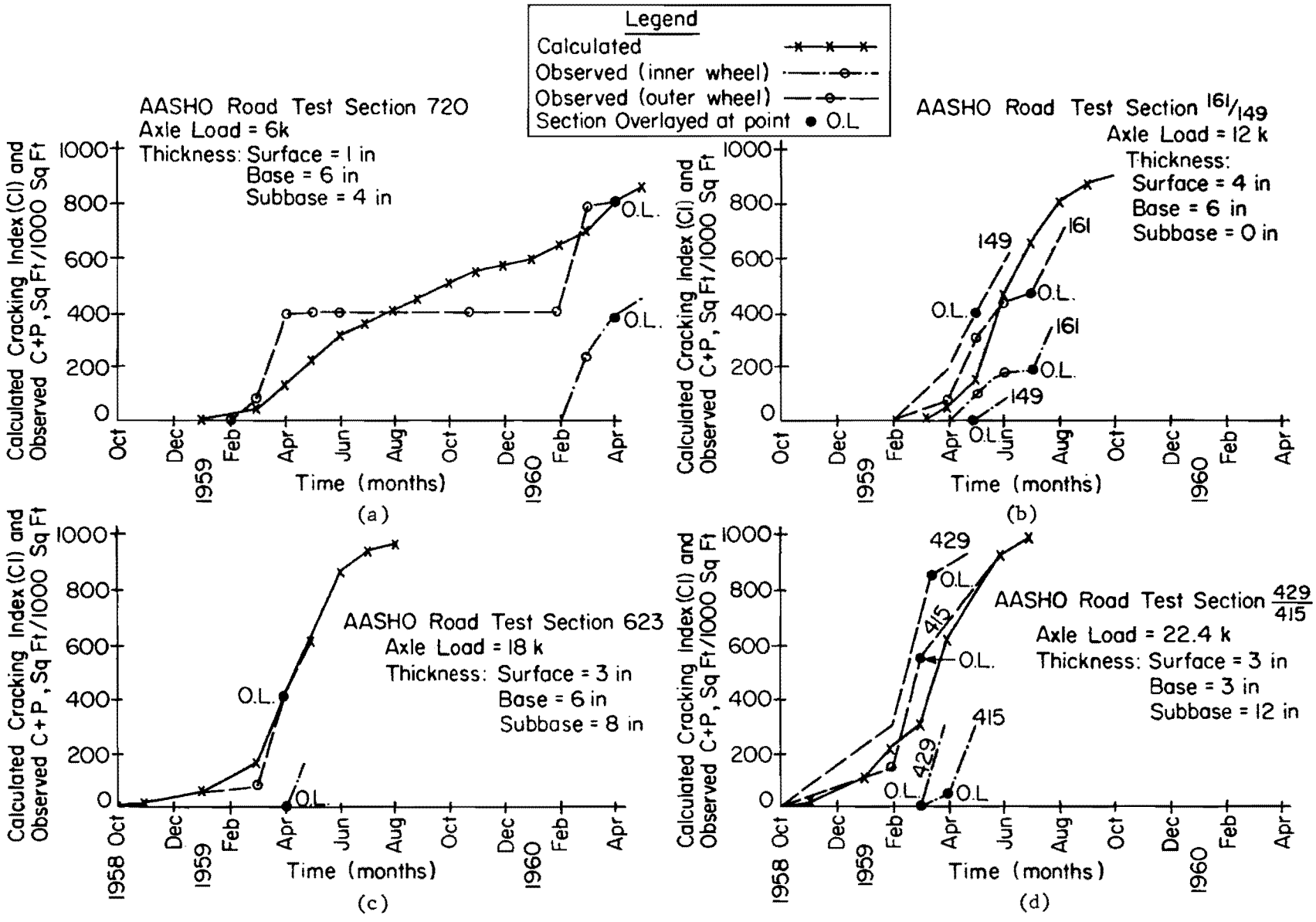

Fig 11.2. Computed cracking index (CI) versus observed cracking-patching (C + P).

to calculate the cracking index are used in these computations. Typical computer computations are shown in Appendix 4. The observed field values of cracking-patching are from the AASHO Road Test performance record for each test section (Ref 70). Typical performance records for a few sections are included in Appendix 5. The observed and computed values thus obtained are plotted and compared. For 2-kip axle loads (Figs A8.1 through A8.3) on loop 2 of the AASHO Road Test sections, the results based on the above mentioned material properties were quite conservative, for the following reasons:

(1) Small loads and low tire pressures resulted in a lower effective tire radius, which, for the same speed, gives a loading time that is about 50 percent of the average for all axle loads. The lower loading time can give asphalt concrete stiffness values for 2-kip axle loads that are up to 25 percent more than the stiffness values for higher loads. Moreover, a lower time of loading will increase the fatigue life of the pavement.

(2) The test results for the AASHO Road Test sections indicate that the outer wheel path generally showed more distress than the inner wheel path, but for lane 1 of loop 2 in many cases, and especially the sections under consideration, the inner wheel path showed more distress than the outer wheel path.

(3) Report 5 of the AASHO Road Test (Ref 70) shows that lane 1 of loop 2 always behaved differently from other loops; in most cases, when other lanes showed good correlation with certain parameters, lane 1 was dropped from consideration. In some cases the correlations were based on a minimum asphalt concrete thickness of 2 inches, which excluded quite a few sections of loop 2 (Ref 70, pp 37, 38, 40, 41, 42, 43. 60, and 66).

In view of the above, the cracking index values for 2-kip axle loads in loop 2 were recomputed with revised stiffness modulus and fatigue characteristics for asphalt concrete. The cracking index values thus calculated are plotted in Figs A8.1 through A8.3.

Comparison of Computed and Field Cracking Distress

A study of the comparison of observed and computed cracking index shows that most of the plots agree well, but in a few cases the calculated values are different than the observed values.

The reasons are not known, but even the replicate sections in the AASHO Road Test did not show the same cracking-patching history. Therefore, it can be expected that observed values of cracking-patching will deviate from any calculated with a theoretical model. A model that resulted in residual errors that averaged about the same as the deviations of the replicate observations

would be satisfactory. These replicate sections showed differences of up to 450 square feet per 1000 square feet in the cracking-patching measurements for the same month. Furthermore, for Sections 307 and 305 (Fig A8.16), there was a year's difference in failure, i.e., Section 305 had a failure pattern similar to that for 307, but it was one year sooner.

In comparing results, consideration must be given to the overall trends and quality of the plots, as specific points may differ for various reasons at different times.

Based on this criteria for expected variation and engineering judgment, for comparison and explanation, the plots of observed and computed cracking index (Figs 11.2 and A8.1 through A8.18) were divided into three categories as follows:

(1) Good fit. Calculated and observed plots match very closely. The plots have similar shapes and differences at any one point are seldom reach more than 300 square feet.

(2) Medium fit. Calculated and observed plots do not fit well, but the differences can be explained and do not affect the predicted pavement performance significantly. The difference, however, in a few cases may reach 450 square feet or more. This difference of 450 square feet in a particular month is equivalent to a difference of 0.21 in PSI which is not of much significance.

(3) Poor fit. Calculated and observed plots have considerable differences. Some of them may be explained; some are due to random variations.

The number of sections in each category is

(1) Good fit - 20

(2) Medium fit - 5

(3) Poor fit - 3

Thus, plots for more than 70 percent of the sections under study fit well. Results were good for all the sections in the 12-kip loop 3 group. In addition, other explanations given below show that the cracking index model gives very good results. For extreme conditions of loading and thickness, some deviation can be expected, but this is a normal statistical characteristic and is acceptable.

Discussion of Comparison

The comparison of observed and calculated values of cracking index and the above discussion shows that general discrepancies observed in the results for loop 2 may be resolved by proper material characterization. The

following discussion for all loops explains some apparent differences that are due to time phase and measurement discrepancies; some other differences can also be explained and discrepancies resolved as discussed hereafter. Only a few sections actually have notable differences between actual and predicted values.

(1) If for some reason a failure in the field did not occur one spring season, the whole cycle is likely to be shifted in the actual pavement sections in the field (Fig A8.16). In this case, the shape of the distress envelopes is the same, but the time phase difference will be apparent. Since the theoretical model does not consider this contingency, differences between field and computed values can arise in several cases. Figures A8.4, A8.11, A8.16, and A8.17 are examples of this situation. At first glance it may appear that the observed and calculated values are very different but a careful study shows that if the time phase shift may be considered, the values are in close agreement. Therefore, the sections put in the categories of poor or medium fit in fact had good fit, and confidence in the developed model is improved.

(2) In several cases not enough points are available to show the actual trend (Figs A8.10, A8.13, and A8.14).

(3) Monthly average variations in the modulus values were considered, in accordance with the procedure developed, but shorter periods might give closer results.

(4) Material characterization is a very important factor. Any discrepancy in the characterization of material properties can cause differences in the results. In this study the materials were characterized on an average basis not for specific sections.

(5) During hot months the rate of crack propagation is slow; the asphaltic concrete becomes softer and the cracks become temporarily invisible. Therefore, during these months inaccuracy in the measurements of observed data could occur and more discrepancy is likely to show up between calculated and observed values. In Section 305 (Fig A8.16) observed values decreased instead of increasing, which was not as expected. Moreover, during hot months, due to lower stiffness values, higher strains are expected; these may appear in the extreme end of the fatigue curve and show more distress, according to the design criteria, than actually happened and was observed. The sections in these periods may tend to behave under constant strain rather than constant stress conditions (assumed), making the calculated values more conservative. These facts are apparent from many sections (Figs A8.4, A8.11, A8.15, A8.16, and A8.17).

(6) The daily temperature cycling and other environmental effects when taken into account will also tend to give more realistic and better trends in all cases.

(7) Once the surface has distressed to some extent, impact and regenerated or progressive added distress effects may also influence the pavement condition. This result may be different for different axle loads.

(8) The slope of the fatigue curve may vary slightly for different axle load groups and temperature conditions, since the response of asphaltic concrete may be affected to some extent by time of loading and temperature. In this study average characteristics are assumed. Thus, the results for load groups other than 12 kips show comparatively more variation.

(9) From the discussion in Chapter 4, it appears that in thinner sections controlled-strain is more suitable. Therefore, for thinner sections the constant stress assumption is likely to give conservative results (Figs A8.1 through A8.4).

(10) Some of the unexplainable differences may be due to random statistical behavior of the test sections, especially extremely thin sections with small loads, for which extreme values of strain may show even more variation in fatigue curve and in which statistically more variation is expected.

The following comments from NCHRP Report 35 (Ref 164) support the use of the procedure explained herein.

> "It has been shown that tensile strains of a magnitude sufficient to initiate fatigue cracks occur on the road surface and theoretical considerations of a layered system indicate that even greater tensile strains occur on the under side of the top layers. These tensile strains will be a maximum when the overall stiffness of the entire structure is a minimum. The stiffness of bituminous materials is dependent on temperature and the critical condition is therefore likely to arise at high temperatures during the summer months.
>
> However, the fatigue tests at high temperatures show that although cracks initiate under these conditions, they propagate only slowly due to the lower stress, and thus failure will not necessarily be apparent at this time. But once the temperature falls and the stiffness of the bituminous layers increases, there will be an increase in the stress, particularly at the tip of the crack, owing to stress concentration effect. This will result in more rapid propagation of any fatigue cracks under winter conditions, but again it will not necessarily lead to failure owing to the freezing of the subbase and subgrade and the resultant increase in strength. During the thaw period, however, the fact that the surface layers are cracked increases greatly the likelihood of pavement deterioration from penetration of water and consequent local subgrade failure."

Summary

From the above discussion, it can be concluded that the difference in calculated and observed values, even in the cases of poor and medium fit plots, can reasonably be explained in all but one or two cases (Fig A8.14), which could not be explained because not enough data points are available. The model developed seems to give acceptable results, is based on a rational recognized approach, and can be used for design of flexible pavements. Any improvements,

as discussed above, in the model will further reduce the gaps between observed and calculated results.

RUT DEPTH INDEX MODEL

The details and development of the rut depth index model were discussed in Chapter 9. For the comparison of rut depth index values, the sections used for the cracking index model are considered here. Figure 11.3 shows a comparison of the calculated rut depth index and observed values of six selected AASHO Road Test sections. Other test sections so compared are included in Appendix 8 (Figs A8.19 through A8.36).

Computation of Rut Depth Index

In computing the rut depth index values also the material properties were characterized as in Chapter 5. The monthly values of elastic modulus contained in Tables 5.2, 5.3, and 5.8 are used. Equations 5.1, 5.2, and 5.4 are used for repeated load-deformation characteristics of materials. The actual monthly traffic data of the AASHO Road Test (Ref 70) are used. Typical computer computations are included in Appendix 4. The rut depth index computer program, discussed in Chapter 9, computes the total deformation as well as the deformations of the base, subbase, and subgrade layers. When the total calculated deformation was compared with the observed values of the AASHO Road Test sections, it was noted that the calculated values were generally higher initially but were approximately equal at the time of failure. In this regard, a study of the AASHO Road Test (Ref 70) showed that

(1) Rate of rut development decreased with load applications.

(2) Although pronounced rutting developed in both wheel paths of the pavement surface, very little was apparent in the embankment soil where the sections were maintained. This and other thickness and trend measurements of the AASHO Road Test sections were considered to be evidence that pavement layers were mainly responsible for rutting observed in the wheel paths of the pavement surface and that the subgrade makes almost no contribution toward rut depth.

(3) If the sections that were failing at a rapid rate were not maintained rutting or distortion of the pavement in the wheel paths extended into the embankment soil.

Based on the above observations, plots of observed and computed rut depth were made (Figs 11.3 and A8.19 through A8.36) without considering the effect of subgrade deformation unless the condition in item 3 above was encountered.

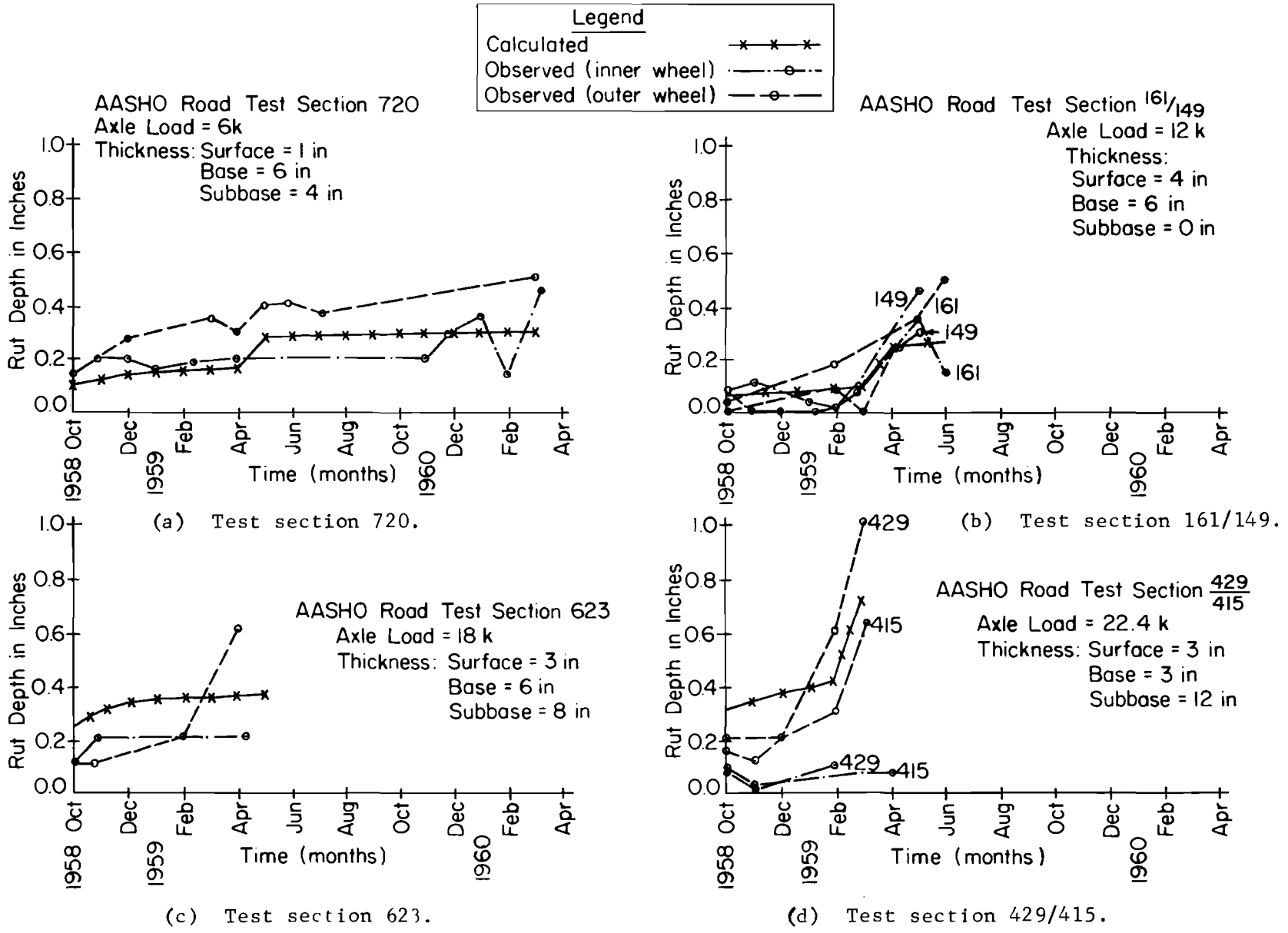

Fig 11.3. Observed versus calculated rut depth index.

In the present design procedure, the computer program computes the deformation in all the pavement layers separately. Therefore, the observation made in item 2 can be accounted for in the procedure easily.

Comparison of Computed and Field Rut Depth

Figures 11.3 and A8.19 through A8.36 show that there was close agreement between the observed and calculated values. Of 28 sections which were compared, about 23 showed a difference between the calculated and observed values of less than 0.2 inch and none of the sections has a difference of more than 0.3 inch.

Not even the replicate sections in the AASHO Road Test showed the same performance and rut depths; therefore, it can be expected that observed rut depths data will deviate from values of rut depths calculated from any theoretical model. A satisfactory model should give residual errors that average about the same as the deviations of replicate observations from their own mean. The rut depth differences in the observed values of the replicate sections have been noted as high as 0.3 or even more.

Discussion of Comparison

When observed and calculated values of rut depth are compared, the following points must be considered:

(1) For calculations of rut depth, not all the local climatic and other factors could be or were considered in detail; for example, certain rainfalls and snowfalls of short duration, non-load associated effect, and temperature stresses. Therefore, some differences are bound to occur. Comparison should be made of the general trend of the plots and their qualitative rather than exact quantitative agreements for each month. In some cases the observed values of rut depth decreased with increases in traffic load repetitions, instead of increasing. This is not correct and may be due to observation errors. In many cases corrections close the gap in observed and calculated values.

(2) Quantitative differences between observed and calculated values may be considered in the light of the effect on the PSI values of the sections. In the PSI and PSR observations of the AASHO Road Test data (Ref 70), a difference as large as 1.1 was observed and the mean value of the difference for 74 observations, on which PSI equation was based, was 0.3. The contribution of the rut depth in the PSI equation is $1.38\ \overline{RD}^2$ (Ref 70). Assuming that all the error in PSI is due to rut depth and that a correct average rut depth is about 0.25 inch, the reasonable acceptable value of the difference between computed and observed values of rut depth can be computed. It is seen that for a mean correct rut depth of 0.25 inch even a

value of rut depth between 0.0 and 0.53 and similarly at a mean value of 0.6 inch rut depth, values from 0.38 to 0.76 will be within the acceptable difference of 0.3 in the PSI values.

(3) At the AASHO Road Test a high level of correlation was found between deflections and performance. Performance is affected by degree of rutting. Thus, deflections were correlated with rutting (Ref 70, Fig 95). Dotted lines on the plots of deflection vs rut depth in Fig 95 in Ref 70 were located one standard error of the estimate from the regression line. For a creep speed deflection of 0.04 inch, for example, the corresponding values of rut depth for one standard deviation vary from 0.35 to 0.65. A model predicting a variation to this extent was acceptable for AASHO Road Test data. Therefore, any model of this accuracy should ordinarily be satisfactory.

(4) In the replicate sections (Ref 70, Appendix C) of the AASHO Road Test reports, the spring creep deflection data show a variation from 0.038 inch to 0.072 inch for loop 3, lane 2. The corresponding rut depths from Fig 95 of Ref 70 are

Axle Applications	Rut Depth in Inches
140,000	0.2 - 0.7
610,000	0.35 - 0.8
1,114,000	0.45 - 1.0

Deflections for 18-kip axle loads in loop 4, lane 1, for replicate sections measured 0.077 inch and 0.056 inch. The corresponding rut depths at 140,000 applications are 0.8 inch and 0.47 inch. These data show that in the replicate sections of the AASHO Road Test data the above order of variation in the rut depth can be expected and any model predicting with this accuracy should be satisfactory.

(5) For a few sections the difference between observed and calculated rut depth was relatively more in the beginning of the performance period and then evened out. This is not considered significant for the following reasons:

(a) A discrepancy in rut depth in the beginning affects the present serviceability much less. For example, a discrepancy of 0.2 inch between values of 0.1 and 0.3 will affect the PSI only by 0.1, while toward the end the same difference between rut depth values of 0.5 and 0.7 affect the PSI by 0.33.

(b) The computed values are in most cases conservative.

(c) From the design point of view, relatively more correct values for the level of service are required at some time other than the beginning, for example, at the time of overlay, and maintenance, when correct values of PSI are more important for decision criteria.

(d) In the beginning, when the ruts are not visibly well defined, measurement error in the observed values is likely to be relatively higher.

Summary

It is seen from the plots that in almost all cases the differences are much less than the expected minimum accuracy discussed above, and in most cases the predicted or calculated values are very close to the mean observed values for outer and inner wheel paths. From the above discussions, it can be concluded that rut depth prediction by the model and the method presented in this report are dependable and can be used in the design of the flexible pavements.

VERIFICATION OF ROUGHNESS INDEX MODEL

To estimate the value of slope variance, a roughness index model was developed (Chapter 10). This model predicted the roughness index values corresponding to the cracking index. In this section the computed values of roughness index are compared with the observed values of the selected 28 AASHO Road Test sections. These sections are the same as those selected for the cracking index and rut depth index models (Fig 11.1).

Computation of Roughness Index

Cracking index values are theoretically calculated equivalent values and represent the cracking-patching in the pavement. Therefore, from the cracking index values calculated from the cracking index model as discussed in the first section of this chapter for various AASHO Road Test sections, corresponding values of roughness index (RI) were calculated by the computer program (Appendix A4.4), as discussed in Chapter 10. In these calculations the regression analysis model (Eq 10.15) developed earlier in Chapter 10 is used.

Comparison of Computed and Field Roughness Index

Figure 11.4 shows a comparison with six selected AASHO Road Test sections. This comparison with the other 22 sections is shown in Figs A8.37 to A8.58. The computations were made for 28 AASHO Road Test sections. Careful scrutiny and engineering judgment will show that about 16 sections show very good predictions, six may be termed as showing medium fit, and six show comparatively poor results. However, it must be remembered that the calculated roughness index values were obtained from the calculated cracking index values. Any discrepancy in the observed cracking-patching and calculated cracking index, therefore, will also show up here. Such observed differences were explained

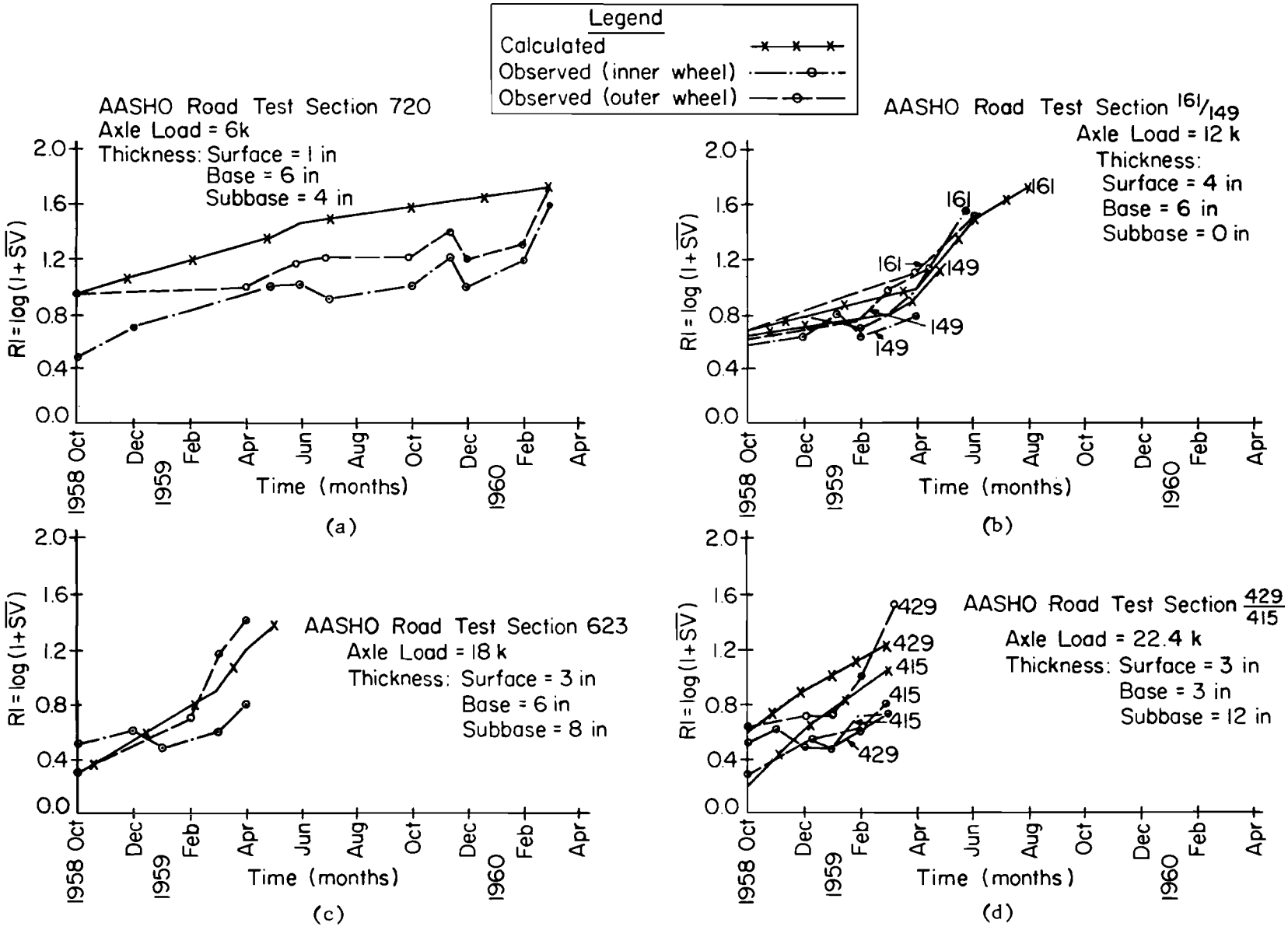

Fig 11.4. Calculated and observed roughness index, RI.

earlier, and it was noted that most discrepancies could be explained, and thus the calculated cracking index values were reliable and satisfactory. Once the cracking index value discrepancy is explained, the estimated roughness index value will also give satisfactory results, and the apparent differences noted above in the calculated and observed roughness index values will be reduced.

For plots with good fit, the differences are very small, with the greatest difference being 0.2. In the medium fit category the difference was occasionally as large as 0.4. For poor fit plots, the differences in calculated and observed roughness index values were sometimes as much as 0.6 to 0.7, although most differences were much less. However, with the explanation already offered for the cracking index these differences will be reduced. Moreover, even in these sections (poor fit), values at the beginning and end of the performance period compare very well, but observed values of roughness index either decreased or stayed the same at some other time resulting in apparent high differences in values during the performance period. The constant or decreased observed values of roughness index during the performance period are considered wrong for theory and/or logic. Proper corrections in the observed data will reduce the differences.

The replicate sections in the AASHO Road Test did not show the same performance and slope variance measurements, and it can be expected that observed performance data will deviate from calculated values from any theoretical model. For the AASHO Road Test sections, replicate differences in roughness index values as much as 0.40 and in some cases 0.7 were observed. These replicate differences in roughness index are equivalent to replicate differences of 0.76 and 1.33, respectively, in PSI. Moreover, even the standard deviation of the variability of the SD Profilometer measurements for roughness index has been observed as 0.37 (Ref 155). The final effect of any discrepancy of roughness index should be compared in terms of present serviceability index, and this is done in the last section of this chapter.

Figures 11.5 through 11.9 show the comparison of calculated and observed roughness index values for some additional AASHO Road Test sections. For these sections, values of roughness index were calculated, from the actual observed values of cracking-patching as well as from the computed cracking index. The calculated and observed values in both cases are found in close agreement for these sections also.

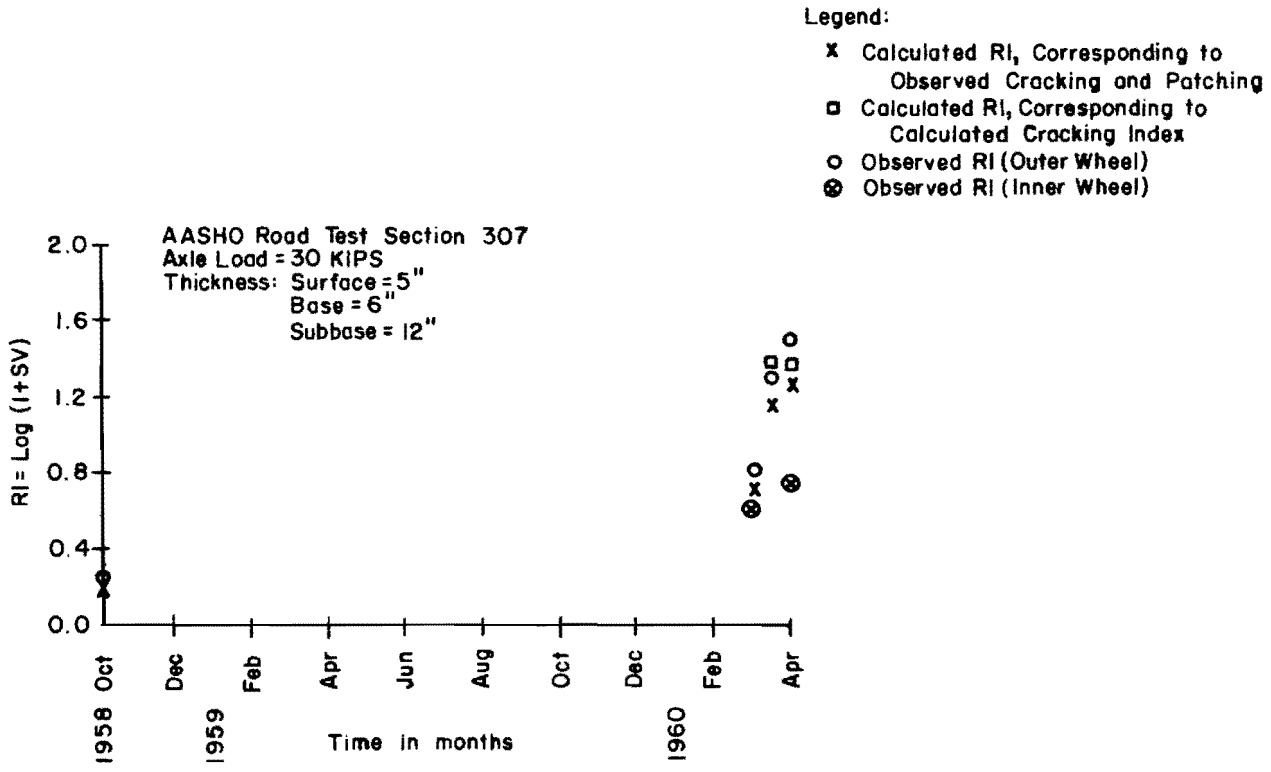

Fig 11.5. Verification of roughness index model.

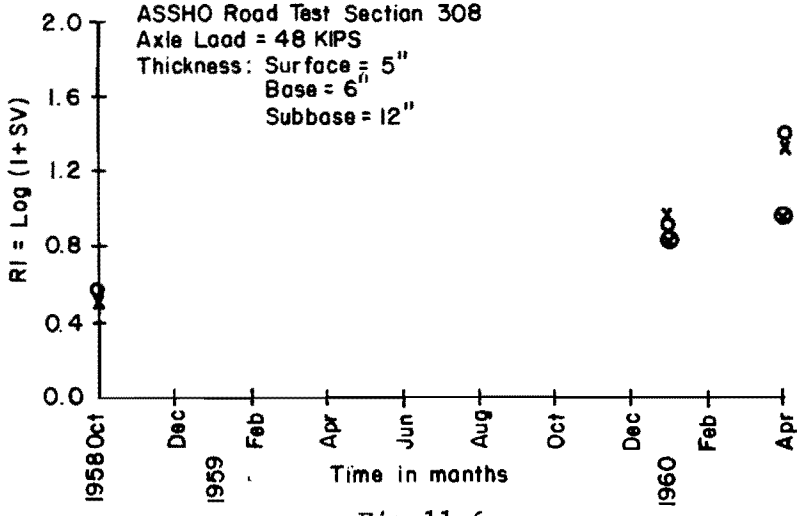

Fig 11.6.

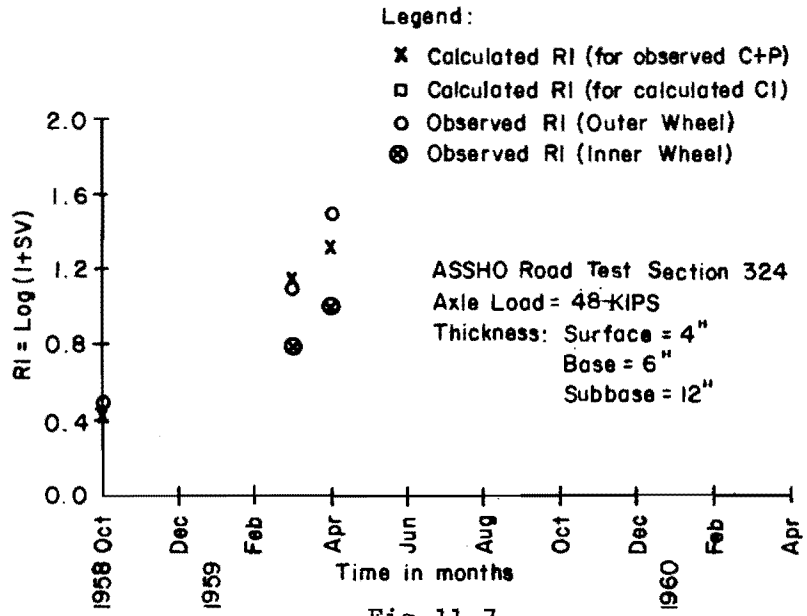

Fig 11.7.

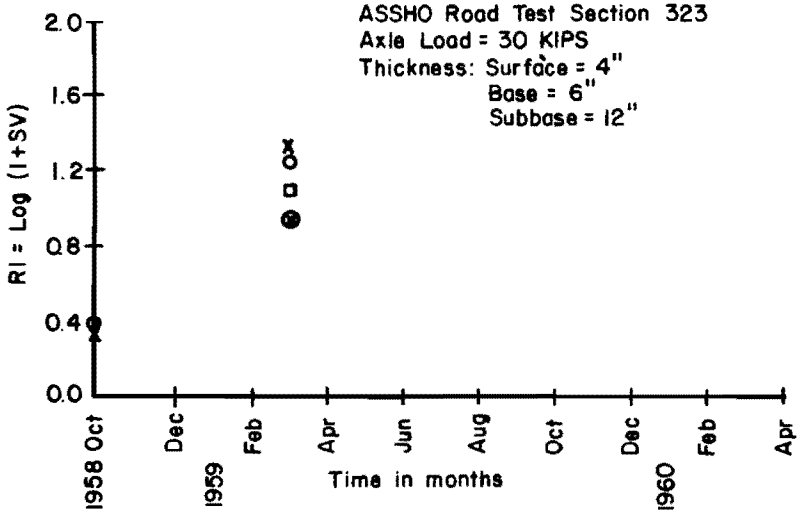

Fig 11.8.

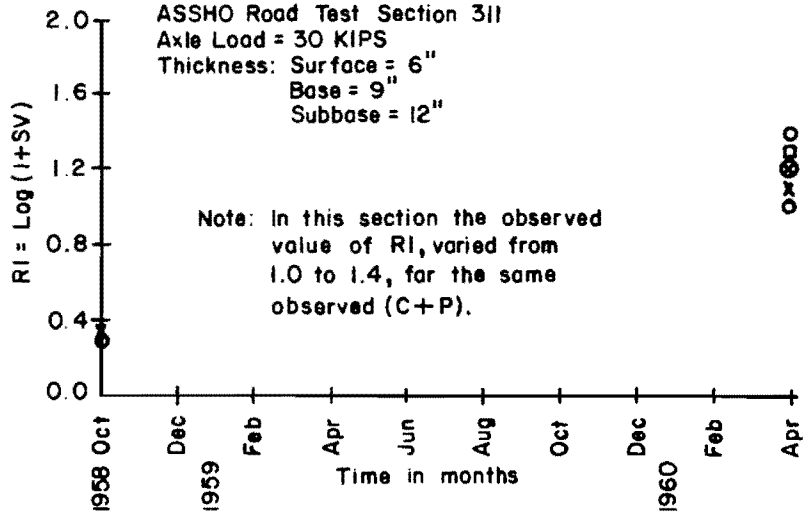

Fig 11.9.

Verification of roughness index model.

Summary

Generally the differences between calculated and observed values are within acceptable limits and the model presented herein gives satisfactory results and can be relied on in the design of flexible pavements.

VERIFICATION OF THE PERFORMANCE MODEL

The models for quantification of the cracking index (CI), rut depth (RD), and roughness index (RI) were developed in Chapters 8, 9, and 10, respectively. Verification of these models earlier in this chapter proved their applicability to the design procedure for flexible pavements. For comparison of the observed and calculated values of PSI, 28 sections selected for distress index models comparison are also utilized here.

Computation of PSI

For selected AASHO Road Test sections, the values of CI, RI, and RD were computed from the models developed in this report. Then PSI values for these sections were calculated from Eq 7.1. The computer program to calculate the cracking index and rut depth index values is given in Appendix A4.2. Another computer program, which calculates the roughness index and present serviceability index, is included in Appendix A4.4.

Comparison of the Performance Model

The calculated and observed values of present serviceability index for AASHO Road Test sections are compared as shown in Figs 11.10 and A8.59 through A8.80. In these figures, it can be observed that

(1) In general, the calculated and predicted values of PSI at the beginning are very close in almost all cases, as are those at the end.

(2) Fluctuations and some differences in calculated and observed values occur at times other than close to the beginning and end.

(3) The calculated values always show a decreasing trend, but in some cases the observed values of PSI increase with time for some periods, which is wrong theoretically as well as conceptually. Other than this discrepancy, the trend of loss in serviceability is computed and observed values is the same.

(4) Of 28 plots, 17 show a maximum difference in any month in calculated and observed values of PSI on the order of 0.3. This difference is about 0.7 in five cases while it is as much as 1.5 in six cases. The mean difference, however, is only 0.15.

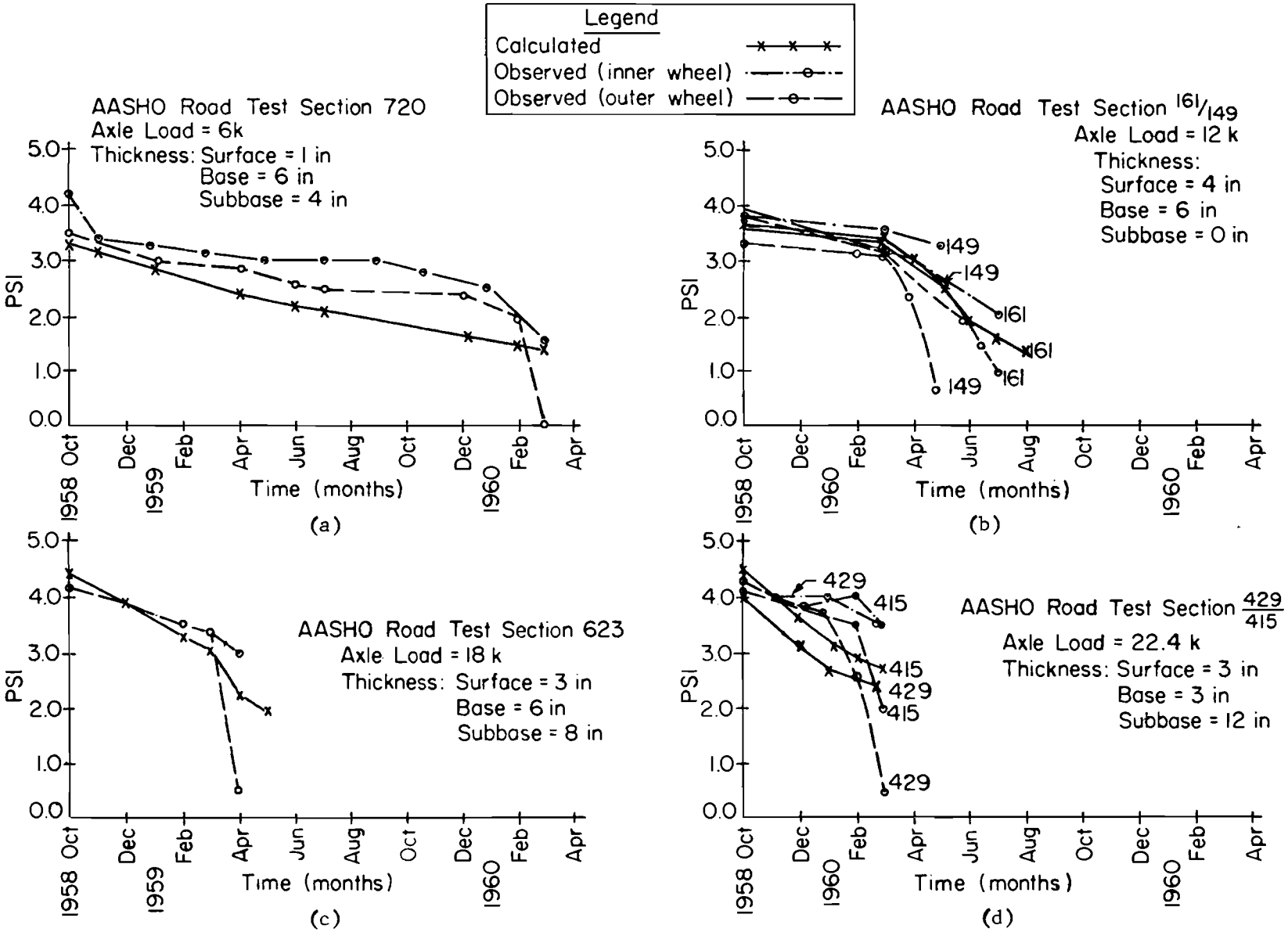

Fig 11.10. Observed versus calculated present serviceability index, psi.

For a comparison of calculated and observed values the following points should be considered:

(1) At the AASHO Road Test (Ref 70), where the original PSI equation was derived, based on the present serviceability ratings of 74 data points, the difference between PSR and PSI was as large as 1.1, with a mean value of 0.3. Therefore, it seems that any difference between calculated and observed values of ± 0.3 is not significant, and in some cases a difference as high as 1.1 can be tolerated.

(2) In the theoretical calculations, not all the local and temporary conditions affecting the PSI can be taken into account, for example, a brief local rainfall or snowfall. Therefore, large fluctuations at times other than at the beginning and end of the performance period are likely to occur.

(3) The effects of embankment swelling, nonload-associated effects, and temperature stresses were not taken into account. When these effects are included, closer predictions are expected. The work to quantify these effects is already in progress and is the subject of another report.

(4) The increase in PSI at any time in the performance period cannot be explained theoretically or logically. In observed measurements it increased very often, which may be due to errors in the measurements or, sometimes, to local and short smooth surfaces. When this discrepancy in the observation is removed, better agreement between the calculated and observed values will result.

(5) During certain times of the year, especially hot months, measurements of cracking are likely to be wrong (Ref 70) because of temporary invisibility of the cracks. This may lead to lower and false observed values of the PSI. During some periods the measured values of roughness index also decreased instead of increasing with load repetitions. Some of the large differences in observed and calculated values of PSI are in fact due to these discrepancies in observed values (Figs A8.63, A8.69, A8.70, A8.72, A8.74, A8.75, A8.78, and A8.79) and the observed values, instead of going down as expected, either went up or stayed the same, causing bigger differences. Correction of this situation will improve the agreement between observed and calculated values.

(6) The general trend of the performance curve and the values of PSI calculated and observed at the beginning and end are very close in most cases.

(7) Differences in some cases occurred in the field because of the time phase difference phenomenon, which was explained for the cracking index. Sections showing large differences in PSI are the same as those which showed large differences in cracking index.

(8) The replicate sections in the AASHO Road Test did not show the same performance (Figs 11.10, A8.63, A8.64, A8.69, A8.72, A8.74, A8.75, A8.77, and A8.78). Therefore, it can be expected that the observed performance data will deviate from the calculated performance values obtained from any theoretical model. However, a model may be

considered satisfactory which results in residual errors that average about the same as the deviations of the replicate observations from their mean. The same type of criteria were adopted in the AASHO Road Test for choosing a satisfactory model (Ref 70, p 43).

The performance model developed in the AASHO Road Test gave a mean prediction error in the performance value of PSI for various loops of 0.39 to 0.75, with an overall mean of 0.53 (Ref 70, Table 11). There is no mention of the extent of the maximum errors of predictions involved in the model. However, when the mean error in a loop is 0.75, the maximum prediction error can be more than 1.0 and up to 1.5.

For the AASHO Road Test, a mean replicate observed difference in PSI was reported as 0.46 (Ref 70, p 43). From the observation of various replicate sections in this report, the PSI values were different by even more than 1.0 at various times. This difference was 2.0 or greater at or close to the time of failure in some test sections.

The replication difference given by the panel in the PSR ranged as high as 0.5 (Ref 70, Table 1.F, pp 295 and 306). It was noted that this replicate difference was observed when ratings were made on successive days and it is possible that replicate PSR's would differ even more over a longer interval of time. The standard deviation of the individual PSR value for each section is 0.5, which shows that 3 ratings out of 10 will be even more than 0.5 rating points from the panel mean PSR.

(9) In the spring of 1971 a team of graduate students from the Center for Highway Research at The University of Texas at Austin was sent out to measure the performance data of some of the highways in Texas. They were also instructed to assign the rating values to these highways in accordance with the AASHO Road Test procedure. A difference between the ratings of the students as high as 1.1 was noted, and the difference in PSI and PSR was as high as 1.6. A difference in PSI and PSR up to 1.0 was very common.

(10) Figure 11.11 shows the calculated monthly values of the present serviceability index (PSI) against the observed values for all test sections shown in Fig 11.1. The overall mean values of observed and predicted PSI values are 3.28 and 3.13, respectively. The difference in mean values is only 0.15, as compared to 0.3 mean difference between PSR and PSI (paragraph (1) above) and a mean observed replicate difference of 0.46 (paragraph (8) above). Less than 10 percent of the points fall outside the ±0.75 lines (paragraph (8) above). The correlation coefficient between the predicted and observed values is 0.872 and the mean absolute residual is 0.43.

Summary

Based on the discussions in the previous section of this chapter and the results using the models developed in this report, it may be concluded that the predictions are well within the expected accuracy and discussed criteria.

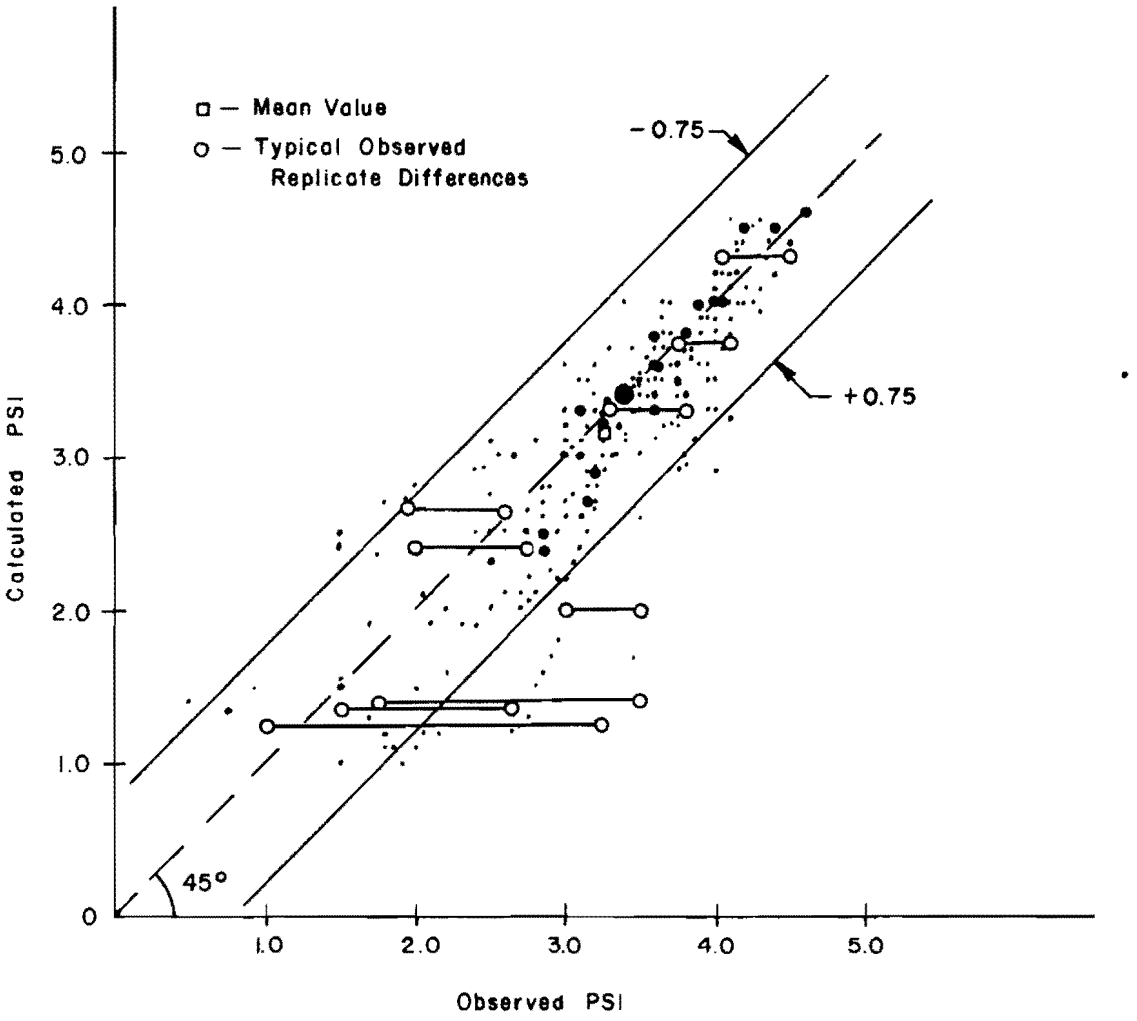

Fig 11.11. Comparison of observed and computed present serviceability index (psi) of various test sections.

Any major differences can be explained in all cases. Therefore, these models should be considered satisfactory for use in the design of the flexible pavements.

PART IV

VERIFICATION AND PROPOSED USE OF MODELS

CHAPTER 12. SENSITIVITY ANALYSIS

Verification of the developed models in Chapter 11, and predictions which compare well with observed data give confidence in the use of the proposed models. In this chapter, results of a sensitivity analysis for the cracking index model are reported. The purposes of the sensitivity analysis are to

(1) establish confidence and reliability in the models,
(2) improve the understanding of the models,
(3) debug the computer program,
(4) establish the relative significance of the input variables,
(5) simplify the computer program by eliminating or fixing variables, and
(6) establish guidelines and precautions for the use of the models.

It is recognized that a designer has only limited time and resources to spend in estimating the large number of inputs needed in the proposed procedure. Therefore, the more important inputs in determining the optimum cost and design should be estimated with greater precision and accuracy than the others. The conclusions in this chapter are based on broad general observation and do not hold in all cases. One effective method of determining the relative significance of the parameters in a complex model is to perform a sensitivity analysis by evaluating the amount of response in a model due to a unit change in the parameters. The interactions of the variables must be studied for a complete sensitivity analysis.

Description of Analysis

About 35 main parameters are involved in the present fatigue models developed in the report. Complete sensitivity analysis is a major task and is not considered herein, but it is recommended that it be made at the earliest opportunity. The most important and significant mathematical model developed in the present study is the cracking index model. Therefore, a

limited sensitivity analysis was made to study the effect of different parameters on cracking index values and verify the suitability of the model.

Results of detailed sensitivity analyses on FPS models reported in Refs 89, 92, and 93 provide background for such a study.

A complete sensitivity study would require an analysis of designs and costs at all levels of the possible ranges of the variables involved. Such an analysis of variance would have to be performed on a very large scale to cover the effects of individual variations of the variables as well as their variations in groups. To study all the possible interactions of variables, an experiment would have to be set up to solve the number of problems given by the full factorial of 35 variables. Such a large scale experiment is not feasible from either a solution time or a data analysis point of view.

Therefore, an experiment had to be formulated which could be done within reasonable time and with a reasonable amount of effort and would give the maximum information desired to effectively use the developed computer program and to attain the required confidence for using the proposed models for actual field problems. A five-level experiment (Fig 12.1), as discussed in Ref 93, is desirable for a sensitivity study of a model having a large number of variables, the type proposed in this report. However, for the sensitivity study of small magnitude reported herein, a three-level experiment (Fig 12.2) was selected. This experiment would isolate the effects of individual variables by varying one variable while the rest are held constant. The experiment was designed by giving each variable, based on engineering judgments, its low, average, and high magnitude value, as shown in Table 12.1. For example, in the present study the low and high values of the elastic modulus of different materials are varied by 25 percent, i.e., about one standard deviation, either way to study the effect of the variation. These elastic modulus values do not represent the real low and high values of this parameter. A detailed sensitivity study should consider the actual variation from low low values to high high values expected in real situations for all the parameters. One basic solution was then obtained keeping all the variables at the average level. The variations were then studied in the average cut, and two more problems were studied for every variable. These problems involved all the variables at their average levels except that the one under study was given its low and high value for the two problems. In a detailed three-level experiment similar studies should be made for the low

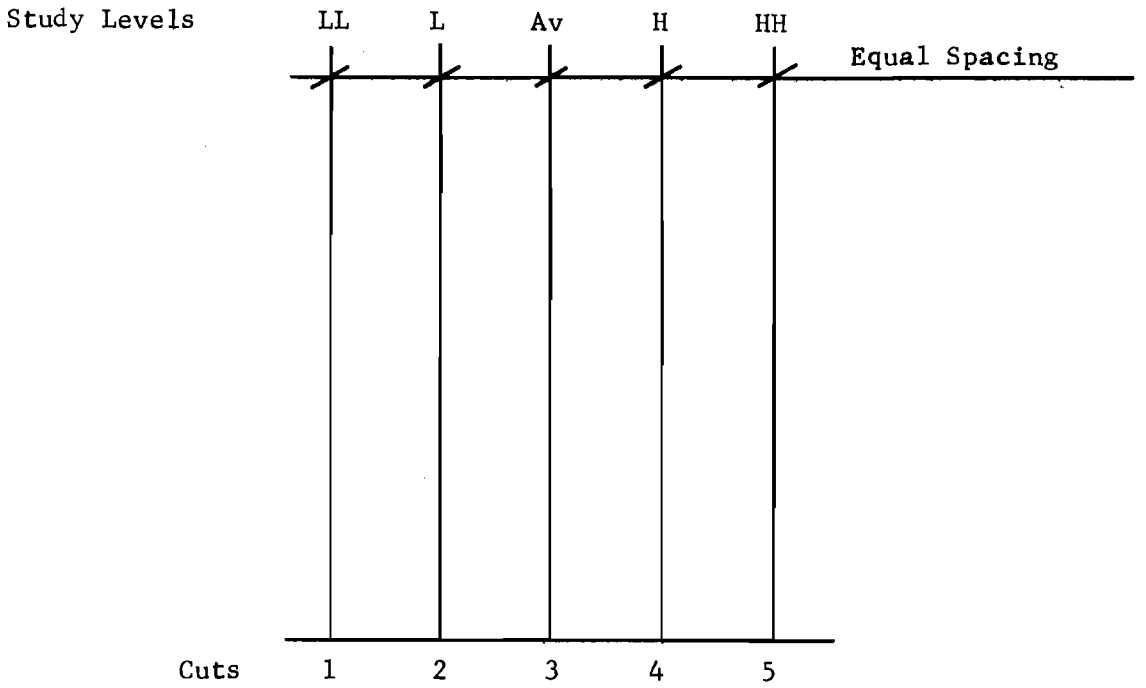

Where

LL = low low values

L = low values

Av = average values

H = high values

HH = high high values

Number of Problem Solutions N is given by

$$N = C + V \times C\ (S - 1)$$

where

C = number of cuts

V = number of variables

S = number of study levels

Fig 12.1. Typical five - level experiment for sensitivity analysis.

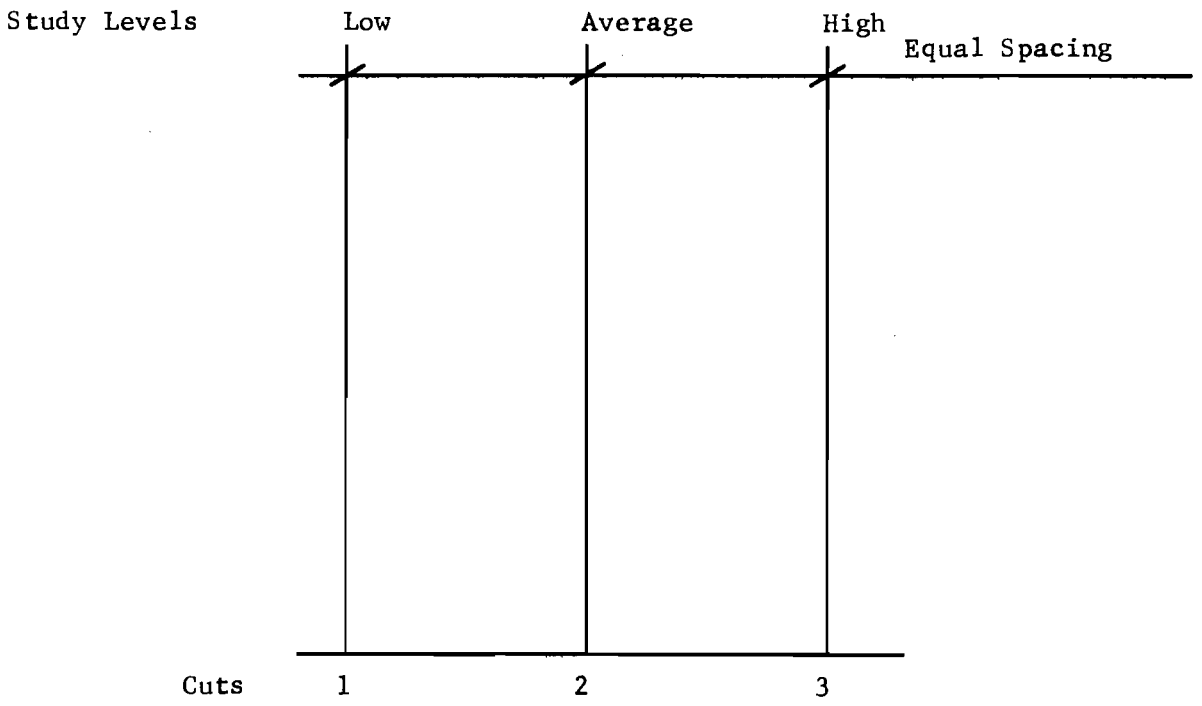

Where

L = low value

Av = average value

H = high value

Number of problem solutions N is given by

$$N = C + V \times C\ (S - 1)$$

where

V = number of variables

S = number of study levels

C = number of cuts

Note: In the present study the variables were studied at the average cut only (C = 1), for which the number of solutions are:

$$1 + V \times 1 \times 2 = 2V + 1$$

Fig 12.2. Typical three-level experiment for sensitivity analysis.

TABLE 12.1. ASSIGNED LOW, AVERAGE AND HIGH MAGNITUDE VALUES OF THE PARAMETERS

SR/NO	Variable	Value		
		Low	Average	High
1	Single Axle Load (Kip)	7	12	17
2	Tire Pressure (lbs/in^2)	42.3	65.7	67.5
3	Thickness (inches)			
	(a) A. Concrete	3.0	5.0	7.0
	(b) Base	3.0	6.0	9.0
	(c) Subbase	9.0	12.0	15.0
4	Mean Elastic Modulus E values (lbs/in^2)			
	(a) Concrete			
	Jan.	12.00×10^5	16.00×10^5	20.00×10^5
	Feb.	10.60×10^5	14.20×10^5	17.60×10^5
	Mar.	10.28×10^5	13.70×10^5	17.12×10^5
	Apr.	6.75×10^5	9.00×10^5	11.25×10^5
	May	4.50×10^5	6.00×10^5	7.50×10^5
	June	3.00×10^5	4.00×10^5	5.00×10^5
	July	2.62×10^5	3.50×10^5	4.37×10^5
	Aug.	2.25×10^5	3.00×10^5	3.70×10^5
	Sep.	3.15×10^5	4.20×10^5	5.25×10^5
	Oct.	4.92×10^5	6.50×10^5	8.12×10^5
	Nov.	6.27×10^5	8.30×10^5	10.37×10^5
	Dec.	9.82×10^5	13.10×10^5	16.37×10^5
	(b) Base			
	Jan.	18000	24000	30000
	Feb.	18000	24000	30000
	Mar.	18000	24000	30000

(Continued)

TABLE 12.1. (Continued)

SR/NO	Variable	Value		
		Low	Average	High
	Apr.	11700	15600	14500
	May	11000	18000	22500
	June	14700	19600	24500
	July	16200	21600	27000
	Aug.	17400	23200	29000
	Sep.	18000	24000	30000
	Oct.	18000	24000	30000
	Nov.	18000	24000	30000
	Dec.	18000	24000	30000
(c)	Subbase			
	Jan.	9900	13200	16500
	Feb.	9900	13200	16500
	Mar.	9900	13200	16500
	Apr.	5400	7200	9000
	May	6450	8600	10750
	June	7100	9800	12250
	July	8100	10800	13500
	Aug.	8700	11 00	15500
	Sep.	9150	12200	15250
	Oct.	9400	12400	15600
	Nov.	9600	12800	16000
	Dec.	9900	13200	16500
(d)	Subgrade			
	Jan.	4950	6600	8250
	Feb.	4950	6600	8250
	Mar.	4950	6600	8250
	Apr.	2700	3600	4500
	May	3225	4300	5375

(Continued)

TABLE 12.1. (Continued)

SR/NO	Variable	Value		
		Low	Average	High
	June	3675	4900	6125
	July	4050	5400	6750
	Aug.	4350	5800	7250
	Sep.	4575	6100	7625
	Oct.	4650	6200	7750
	Nov.	4800	6400	8000
	Dec.	4950	6600	8250
5	Poisson's Ratio (μ) held constant			
	(a) A. Concrete	0.3	0.3	0.3
	(b) Base	0.4	0.4	0.4
	(c) Subbase	0.45	0.45	0.45
	(d) Subgrade	0.5	0.5	0.5
6	Confidence α for E-values (E_α)			
	(a) A. Concrete	.095	.18	.265
	(b) Base	.095	.18	.265
	(c) Subbase	.095	.18	.265
	(d) Subgrade	.095	.18	.265
7	Coefficient of variation "V_v" of E values $\left(V_v = \frac{\sigma_E \times 100}{\bar{E}_v}\right)$*			
	(a) A. Concrete	12.5	20.0	27.5
	(b) Base	12.5	20.0	27.5
	(c) Subbase	12.5	20.0	27.5
	(d) Subgrade	12.5	20.0	27.5

(Continued)

TABLE 12.1. (Continued)

SR/NO	Variable	Value		
		Low	Average	High
8	Values for parameters in fatigue equations: $N = A\left(\frac{1}{\varepsilon}\right)^{\beta}$ ** and $N_{\alpha} = N_{50} - \log SD.K$			
	(a) "A" values	10^{-9}	10^{-8}	10^{-7}
	(b) "B" values	3.35	3.9	4.45
	(c) Log SD	0.25	0.3	0.35
	(d) Confidence α for "N"	0.095	0.18	0.265
9	Monthly load applications "N" Actual	20750	40500	60250

* $\overline{E}_v$ = Mean value of elastic modulus

σ_{E_v} = Standard deviations in elastic modulus

** See Chapters 4 and 9.

cut with the variable being studied given its average and high level and all the other variables kept at low levels. A similar procedure should be used for high cut, in which the variables are studied at their average and low values. A five-level experiment needs similar study at five cuts (Fig 12.1). In the present experiment the procedure required, in all, that 31 problems be solved for fifteen variables. One additional solution for the fatigue parameter B, considered to be most significant, was run for the value as 2.9. Two more solutions for all variables at their high and low values were also run. Thus the total number of solutions was 34. In Table 12.2 the cumulative final value of the cracking index (CI) of each problem after 36 months for the given monthly traffic is expressed as a percentage of the corresponding CI value of the average problem, with all parameters at the average level (Ref 171). These values of the cracking index were obtained using the computer program for cracking index, included in Appendix 4.

RESULTS

Figure 12.3 shows the plot, for each variable, of cracking index versus the percentage of the variable in terms of its average value (Table 12.2). The relative slopes of these plots indicate the comparative significance of each variable. The plots also help suggest the comparative qualitative significance of different variables and give an initial indication of the sensitivity or rating of the variables. For example, because the slope of the curve for fatigue parameter B (Curve No. 23-24) is steepest on both sides of the average value (100), this parameter is considered most significant (significance 1) at both levels. Similarly thickness of subbase (Curve No. 7-8) is considered 14 in significance, one level above the least significant variable.

A more quantitative approach to assigning the significance of various parameters is shown in Table 12.3. For many plots in Fig 12.3, it is difficult to define any regular trend of slopes from the low side to the high side, i.e., from one end of the plot to the other. Therefore, it seems reasonable at this stage to define a constant variation in two parts, i.e., from low to average and from average to high. The plots are not always uniform and straight but in most cases, based on this subdivision, reasonable indication of the relative significance of the various variables is expected. Cracking index values for a one percent increase or decrease in average value of a particular parameter are calculated (col 4, Table 12.3) representing the slope of the

TABLE 12.2. CRACKING INDEX VALUES FOR VARIOUS PROBLEMS

No.	Variable	Final Value of CI in sq ft per 1000 sq ft with Variable at		CI Expressed as Percent of Average Value = $\frac{(2) \text{ or } (3)}{40.7} \times 100$		Curve Number Figs 12.3 & 12.4
		Low	High	Low	High	
	1	2	3	4	5	6
1	Axle Load	0.322	107.0	0.7	260.0	1-2
2	Thickness of Asphalt Concrete	251.0	1.22	610.0	2.0	3-4
3	Thickness of Base	56.3	24.0	138.0	58.0	5-6
4	Thickness of Subbase	47.2	35.9	115.0	88.0	7-8
5	Elastic Modulus E of Concrete	88.3	19.7	216.0	48.0	9-10
6	Elastic Modulus E of Base	60.9	27.9	149.0	68.0	11-12
7	Elastic Modulus E of Subbase	48.5	34.9	119.0	85.0	13-14
8	Elastic Modulus E of Subgrade	42.9	14.3	105.0	35.0	15-16
9	Confidence Value for Elastic Modulus E α	85.7	17.5	210.0	42.0	17-18
10	Coefficient of Variation for Elastic Modulus E α	12.6	79.4	30.0	195.0	19-20
11	Fatigue Parameter "A"	397.0	0.633	975.0	1.5	21-22

(Continued)

TABLE 12.2. (Continued)

No.	Variable	Final Value of CI in sq ft per 1000 sq ft with Variable at		CI Expressed as Percent of Average Value = $\frac{(2) \text{ or } (3)}{40.7} \times 100$		Curve Number Figs 12.3 & 12.4
		Low	High	Low	High	
	1	2	3	4	5	6
12	Fatigue Parameter "B"*	905.0	0.00686	2220.0	0.01	23-24
13	Log Standard Deviation of Fatigue Curve	29.9	52.4	70.0	120.0	25-26
14	Confidence Level for Fatigue Curve N α	18.3	82.3	40.0	202.2	27-28
15	Actual Number of Load Repetitions "N"	14.9	68.5	36.6	168.3	29-30

Notes:

1. Value of cracking index (CI) for the case when
   a. all variables are at their average value is 407,
   b. all variables are at their low values is 1000,
   c. all variables are at their high values is 1.46×10^{-5}.
2. For typical pavement under consideration see Fig 8.4.

* Final value of CI for value of B as 2.9 is 1000.

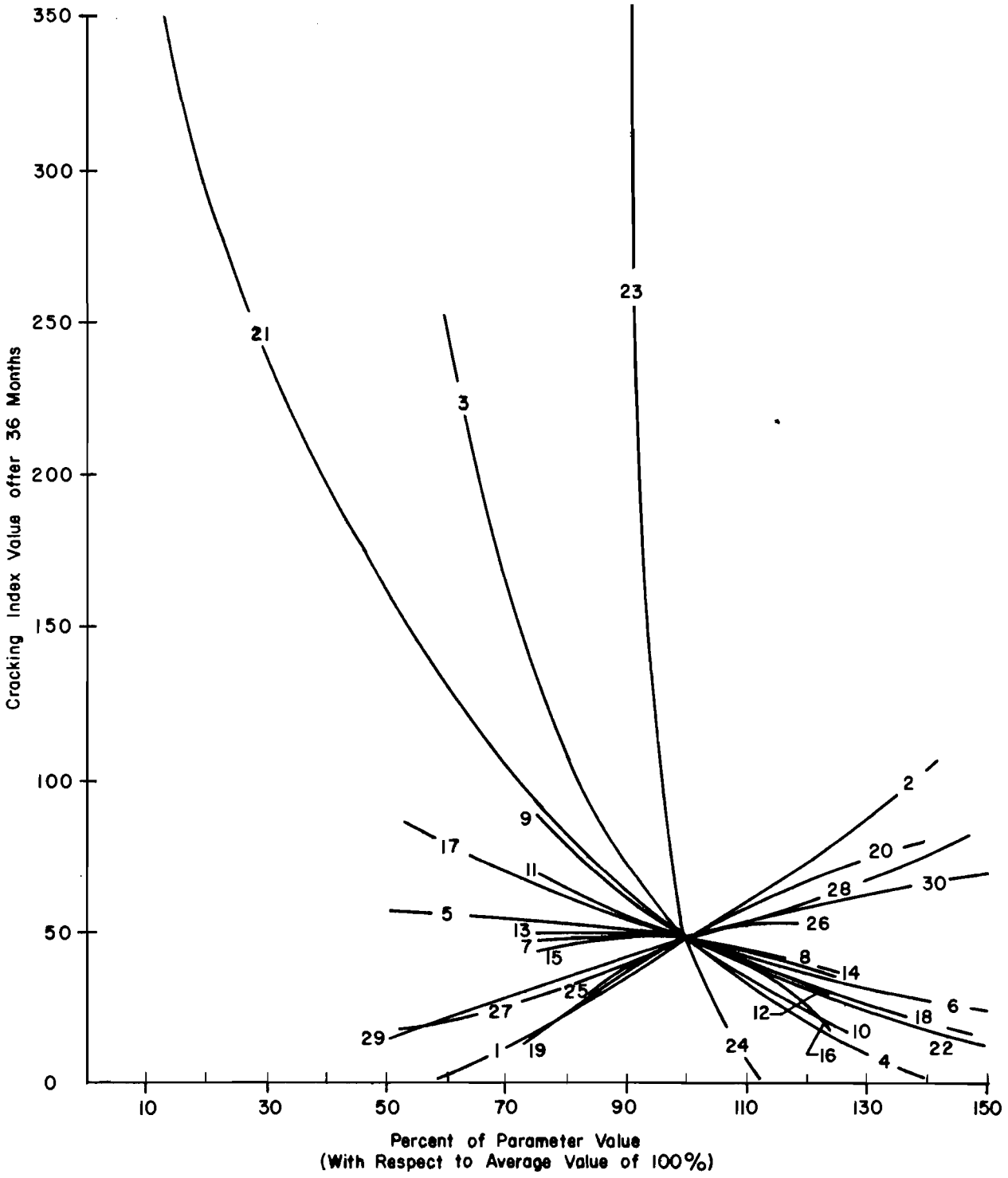

Fig 12.3. Plots showing relative significance of various parameters.

TABLE 12.3. PROCEDURE TO GET THE RELATIVE SIGNIFICANCE OF VARIABLES

Parameter's Name	X = % Increase or Decrease in Parameter Value From Average 100.0	Y = Final CI of the Problem-Final CI of Average (CI = 40.7)	CI Value per 1% of Increase or Decrease in Average Parameter Value Slope = Y/X	Sequence Nos. in Order of Decreasing Slope		Curve or Problem No. (Fig 12.3)
				Lowside of Average Value of Para.	Highside of Average Value of Para.	
1	2	3	4	5	6	7
Axle Load (L)	-41.8	-40.378	0.970	5		1
Axle Load (H)	+41.8	+66.3	1.586		2	2
Thickness AC (L)	-40.0	+210.3	-5.260	2		3
Thickness AC (H)	+40.0	-39.48	-0.987		5	4
Thickness Base (L)	-50.0	+15.60	-0.312	12		5
Thickness Base (H)	+50.0	-16.70	-0.334		12	6
Thickness Subbase (L)	-25.0	+6.50	-0.260	14		7
Thickness Subbase (H)	+25.0	-4.80	-0.192		14	8
Elastic Modulus E_{AC} (L)	-25.0	+47.60	-1.905	4		9
Elastic Modulus E_{AC} (H)	+25.0	-21.00	-0.840		7	10
Elastic Modulus E_{Base} (L)	-25.0	+20.20	-0.808	7		11
Elastic Modulus E_{Base} (H)	+25.0	-12.80	-0.5115		10	12

(Continued)

TABLE 12.3. (Continued)

Parameter's Name	X = % Increase or Decrease in Parameter Value From Average 100.0	Y = Final CI of the Problem-Final CI of Average (CI = 40.7)	CI Value per 1% of Increase or Decrease in Average Parameter Value Slope = Y/X	Sequence Nos. in Order of Decreasing Slope		Curve or Problem No. (Fig 12.3)
				Lowside of Average Value of Para.	Highside of Average Value of Para.	
1	2	3	4	5	6	7
Elastic Modulus $E_{Subbase}$ (L)	-25.0	+7.80	-0.312	13		13
Elastic Modulus $E_{Subbase}$ (H)	+25.0	-5.80	-0.232		13	14
Elastic Modulus $E_{Subgrade}$ (L)	-25.0	+2.20	-0.0879	15		15
Elastic Modulus $E_{Subgrade}$ (N)	+25.0	-26.40	-1.056		3	16
Confidence Value for Elastic Modulus E_{α} (L)	-47.3	+45.00	-0.9515	6		17
Confidence Value for Elastic Modulus E_{α} (H)	+47.3	-23.20	-0.4910		11	18
Coefficient of Variance (L)	-37.5	-28.10	+.07490	8		19

(Continued)

TABLE 12.3. (Continued)

Parameter's Name	X = % Increase or Decrease in Parameter Value From Average 100.0	Y = Final CI of the Problem-Final CI of Average (CI = 40.7)	CI Value per 1% of Increase or Decrease in Average Parameter Value Slope = Y/X	Sequence Nos. in Order of Decreasing Slope		Curve or Problem No. (Fig 12.3)
				Lowside of Average Value of Para.	Highside of Average Value of Para.	
1	2	3	4	5	6	7
Coefficient of Variance (H)	+37.5	+38.70	+1.033		4	20
Fatigue Parameter A-Value (L)	-90.0	+356.3	-3.962	3		21
Fatigue Parameter A-Value (H)	+90.0	-40.067	-0.044519		15	22
Fatigue Parameter B-Value (L)	-14	+864.30	-61.700	1		23
Fatigue Parameter B-Value (H)	+14	-40.693	-2.908		1	24
Standard Deviation of Fatigue Curve Log SD (L)	-16.6	-10.80	+0.650	9		25
Standard Deviation of Fatigue Curve Log SD (H)	+16.6	+11.70	+0.705		8	26

(Continued)

TABLE 12.3. (Continued)

Parameter's Name	X = % Increase or Decrease in Parameter Value From Average 100.0	Y = Final CI of the Problem-Final CI of Average (CI = 40.7)	CI Value per 1% of Increase or Decrease in Average Parameter Value Slope = Y/X	Sequence Nos. in Order of Decreasing Slope		Curve or Problem No. (Fig 12.3)
				Lowside of Average Value of Para.	Highside of Average Value of Para.	
Confidence Level for Fatigue Curve Number of Load Rep.: N_α (L)	-47.3	-22.40	+0.474	11		27
Confidence Level for Fatigue Curve Number of Load Rep.: N_α (H)	+47.3	+41.60	+0.8805		6	28
Actual Number of Load Repetitions "N" (L)	-48.5	-25.80	-0.528	10		29
Actual Number of Load Repetitions "N" (H)	+48.5	+27.80	+0.5725		9	30
Fatigue Parameter B-Value (LL)	-28.2	+959.3	-30.00			31

curves in Fig 12.3. The relative values of this slope then represent the relative significance of each parameter as entered in cols 5 and 6. The variables are arranged in order of decreasing significance in Table 12.4.

These procedures not only give the qualitative and quantitative importance of each variable, but also give the relative order of importance of the variables. However, these results are considered to be limited since they do not consider all the interactions between the different variables. A complete factorial experiment for all interactions is not possible because of the large number of variables. However, the detailed sensitivity study recommended earlier is expected to give more dependable results in a wide variety of situations. In some cases it may be advisable to run a sensitivity analysis for each design problem. It may further be advisable to compare the variation in the output due to one standard deviation in each variable rather than on the basis of 1% increase or decrease and assign the significance on this basis. However, before this can be done a study of the expected variations to calculate the standard deviation for each variable is required and is a field opened for future research.

Figure 12.4 shows curves for all parameters at various levels against the cracking index expressed as a percent of average value. For true high and low values the ranges shown would represent 100 percent variations and the actual relative significance of the various parameters would be shown. However, extreme high and low values were not considered in this study and the relative significance of the parameters shown is only for the specific values of the parameters considered in this experiment. In the detailed sensitivity study of the five-level experiment, low low and high high values represent true extreme variations of each parameter.

OBSERVATIONS

The following tentative observations are made from this short sensitivity study:

(1) Fatigue parameter B in the fatigue equation 4.1, is the most significant variable and has the maximum effect on the CI values. Other important parameters are thickness of asphaltic concrete fatigue parameter A, axle load, and modulus of subgrade.

(2) The effect of the resilient modulus of subgrade is least on the low side and is quite significant on the high side.

TABLE 12.4. RELATIVE SIGNIFICANCE OF THE VARIABLES

Sequence Number	Parameters Arranged in the Order of Effect	
	Low Side (L)	High Side (H)
1	Fatigue Parameter "B"	Fatigue Parameter "B"
2	Thickness of Asphalt Concrete	Axle Load
3	Fatigue Parameter "A"	Elastic Modulus Subgrade
4	Elastic Modulus Asphaltic Concrete	Coefficient of Variation in Modulus Values
5	Axle Load	Thickness - A.C.
6	Confidence Value for Elastic Modulus	Confidence for Fatigue Curve $N\alpha$
7	Elastic Modulus for Base	Elastic Modulus Asphaltic Concrete
8	Coefficient of Variation in Modulus Values	Log SD for Fatigue Curve
9	Log SD for Fatigue Curve	Actual Traffic Repetitions $N\alpha$
10	Actual Traffic Repetitions "N"	Elastic Modulus for Base
11	Confidence for Fatigue Curve $N\alpha$	Confidence Value for Elastic Modulus
12	Thickness - Base	Thickness - Base
13	Elastic Modulus for Subbase	Elastic Modulus for Subgrade
14	Thickness - Subbase	Thickness - Subbase
15	Elastic Modulus for Subgrade	Fatigue Parameter "A"

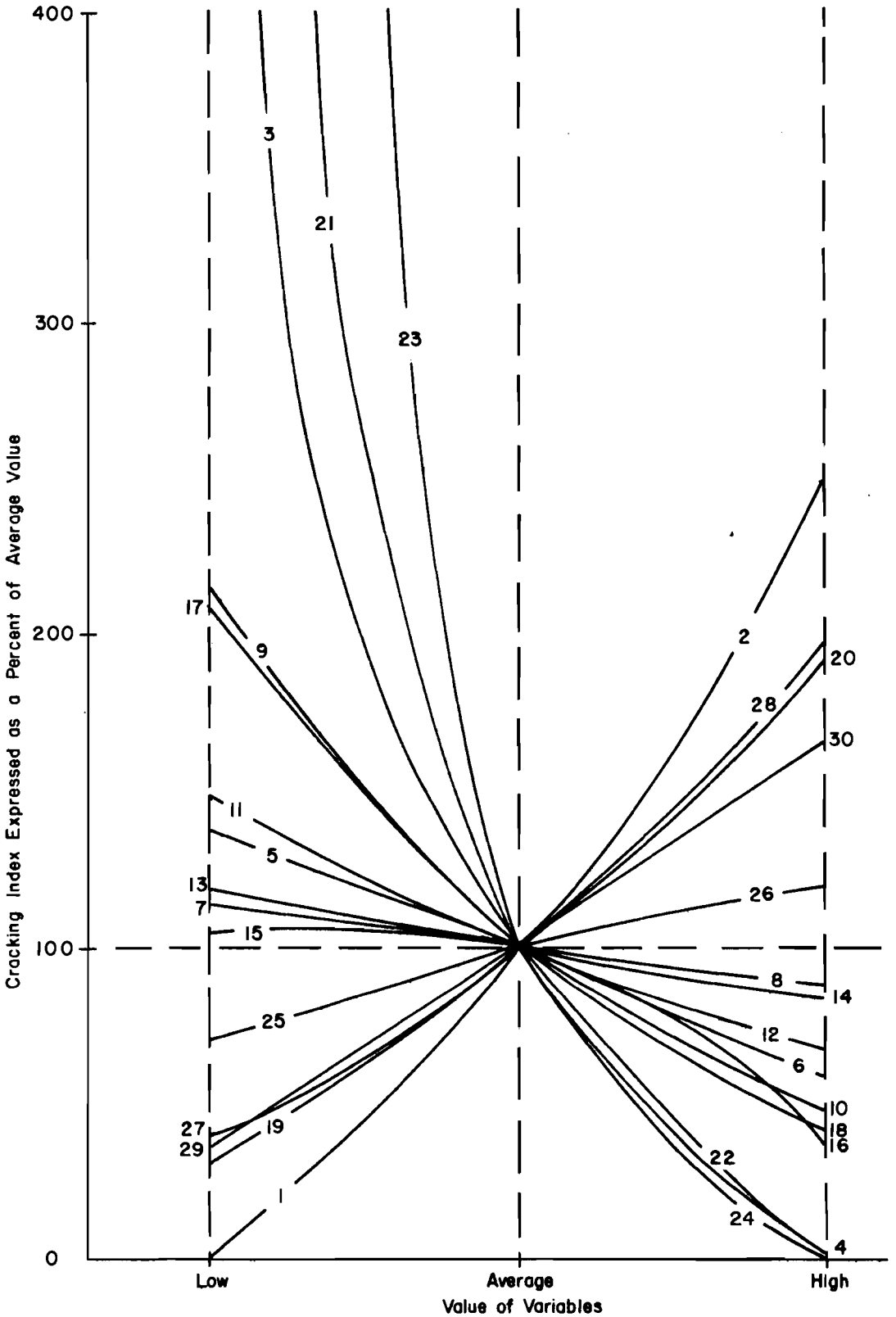

Note: Number on the curves correspond to the numbers given in Table 12.2.

Fig 12.4. Variation of parameters versus cracking index expressed as a percent of average value.

(3) The thickness of asphalt concrete, fatigue parameter A in Eq 4.1, the stiffness modulus of concrete, the confidence level of modulus values, the thickness of base, and the resilient modulus of base have a more pronounced effect on the low side than on the high side.

(4) Axle load, coefficient of variation for modulus values, confidence value for fatigue curve, standard deviation of fatigue life log SD, and number of actual load repetitions have a more pronounced effect on the high side than on the low side.

The present analysis, which was conducted using only the average values, may not give a true picture of the actual significance of the parameters, and problems with all low values and high values should also be run. For complete analysis, a five-level experiment is recommended. To examine the behavior of the models, a complete sensitivity analysis of all the models should be conducted at the earliest opportunity.

The large number of solutions run during this study not only gave a better understanding of the cracking index model, but also more confidence in the use of the model. The various runs also helped in debugging the computer program at various stages.

The magnitude of this small sensitivity analysis makes it difficult to draw any definite conclusions regarding fixing or eliminating the less important variables. From this study, all the parameters considered variable contributed significantly and none can be fixed or eliminated at this stage. However, this study establishes a criterion of relative significance which can be used to determine the precision which should be applied in estimating each variable. Fatigue parameter B is relatively significant and should be estimated very accurately. The relative significance of various parameters based on the range of values for each variables (Table 12.1) and relative effect on the output for one percent change in the average value of the parameter established on the basis of this study is shown in Table 12.4. Such relative significance is liable to change in certain cases because this type of analysis does not consider complete interaction between parameters.

Detailed criteria for using the cracking index models in the most economical way can be established only on the basis of the complete sensitivity study. In the meantime, several alternate solutions should be run to obtain the most economical design based on the procedure established in the next chapter.

SUMMARY

In this chapter, a general format for a complete sensitivity analysis was discussed. The results of a sensitivity analysis of the cracking index model were discussed and the relative significance of the variables established, as shown in Table 12.4. Based on this study it is noted that fatigue parameter B is very sensitive and should be estimated very accurately. It is recommended that a detailed sensitivity study of all the models developed in this report should be made as soon as possible.

Verification of the proposed models in Chapter 11 and the sensitivity study in this chapter prove the applicability of these models for design of flexible pavements. The design procedure based on the proposed fatigue models is prescribed in Chapter 13. This design procedure should be used until some parameters can be fixed or eliminated and the amount of computation time reduced, based on a detailed sensitivity study.

CHAPTER 13. SUMMARY OF PROPOSED FATIGUE MODEL

The theoretical background of the proposed distress index models was explained in earlier chapters, and these models were developed in Chapters 7 to 10. The computer program to calculate the distress indices and pavement performance is included in Appendix 4. The verification of these models with AASHO data that was made in Chapter 11 proved that these models predict the distress indices and performance of a pavement satisfactorily and that the procedure can be used for the design of flexible pavements. In this chapter a summary of the proposed design procedure is presented. Revision of the FPS model for a second generation model is discussed. A comparison of the existing flexible pavement systems computer program with the present design procedure is made by solving example problems.

PROPOSED FATIGUE MODEL

This section describes direct use of the proposed procedure for the design of flexible pavements. Use of the procedure in the existing FPS is discussed in the next section. The steps required to solve a design problem by the proposed design procedure (Fig 13.1) are:

(1) Collect data on traffic, materials, and environment. A list of all the input data required is included in Appendix 4. The traffic volume and design period are decided from the traffic record and project planning.

(2) Characterize Materials: Material characterization is an important part of the whole design process. Material parameters should be ascertained on the basis of laboratory test results, as explained in Chapter 5 and Appendix 2.

(3) Initial Pavement Condition: The design and performance of the pavement require assumption of the initial slope variance SV and initial and final values of the pavement PSI. Through an engineering judgment an evaluation is made of these parameters in advance. For example, just after the construction of pavements, the initial value of the roughness index, log (1 + SV), generally varies from 0.3 to 0.6 and the PSI from 4.5 to about 3.8, depending upon the importance of the highway. The terminal PSI varies from 3.0 to 1.5, at which stage either an overlay or a reconstruction will be required.

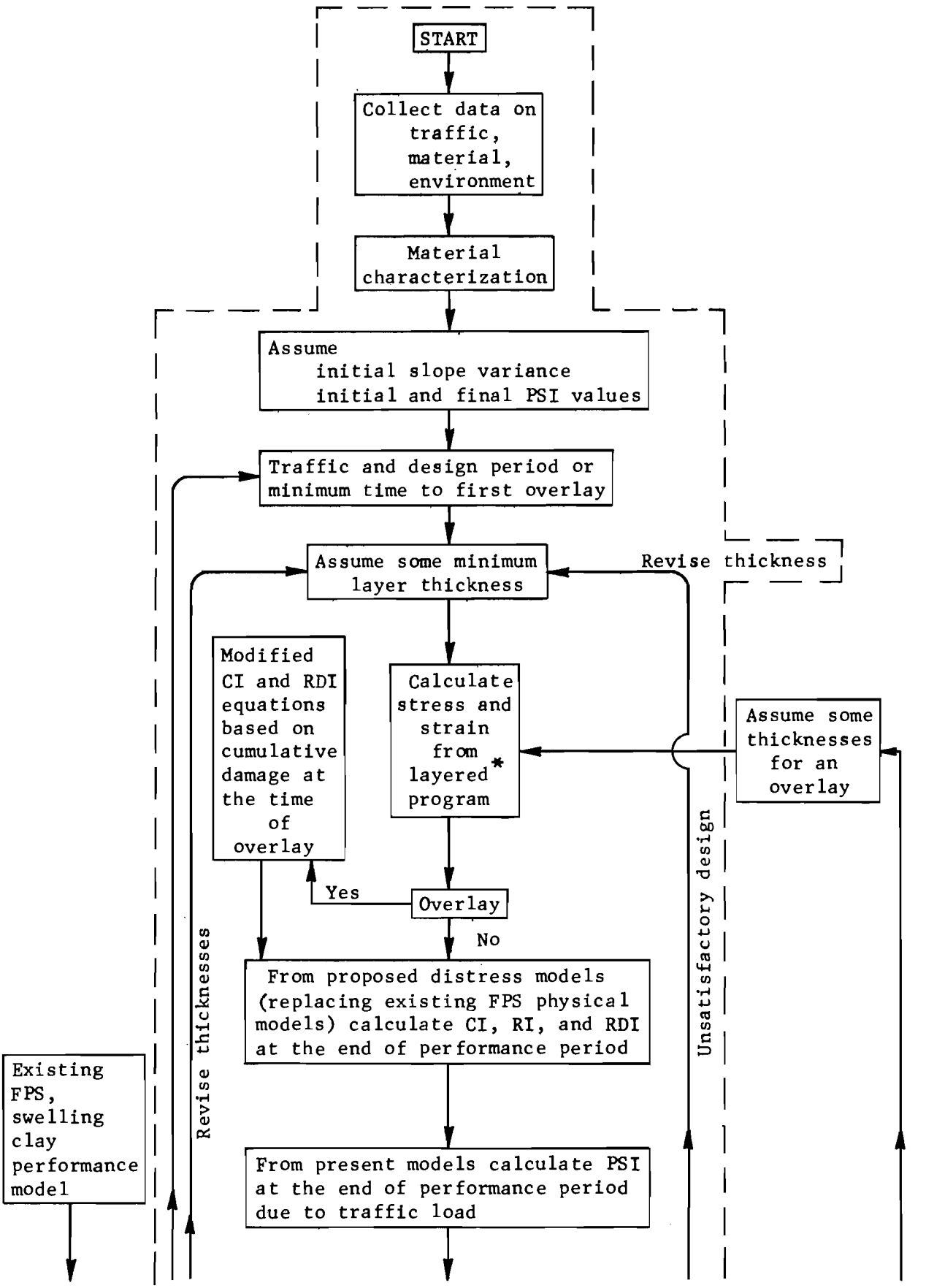

Fig 13.1. Flow diagram for present design procedure and FPS second generation. (Continued)

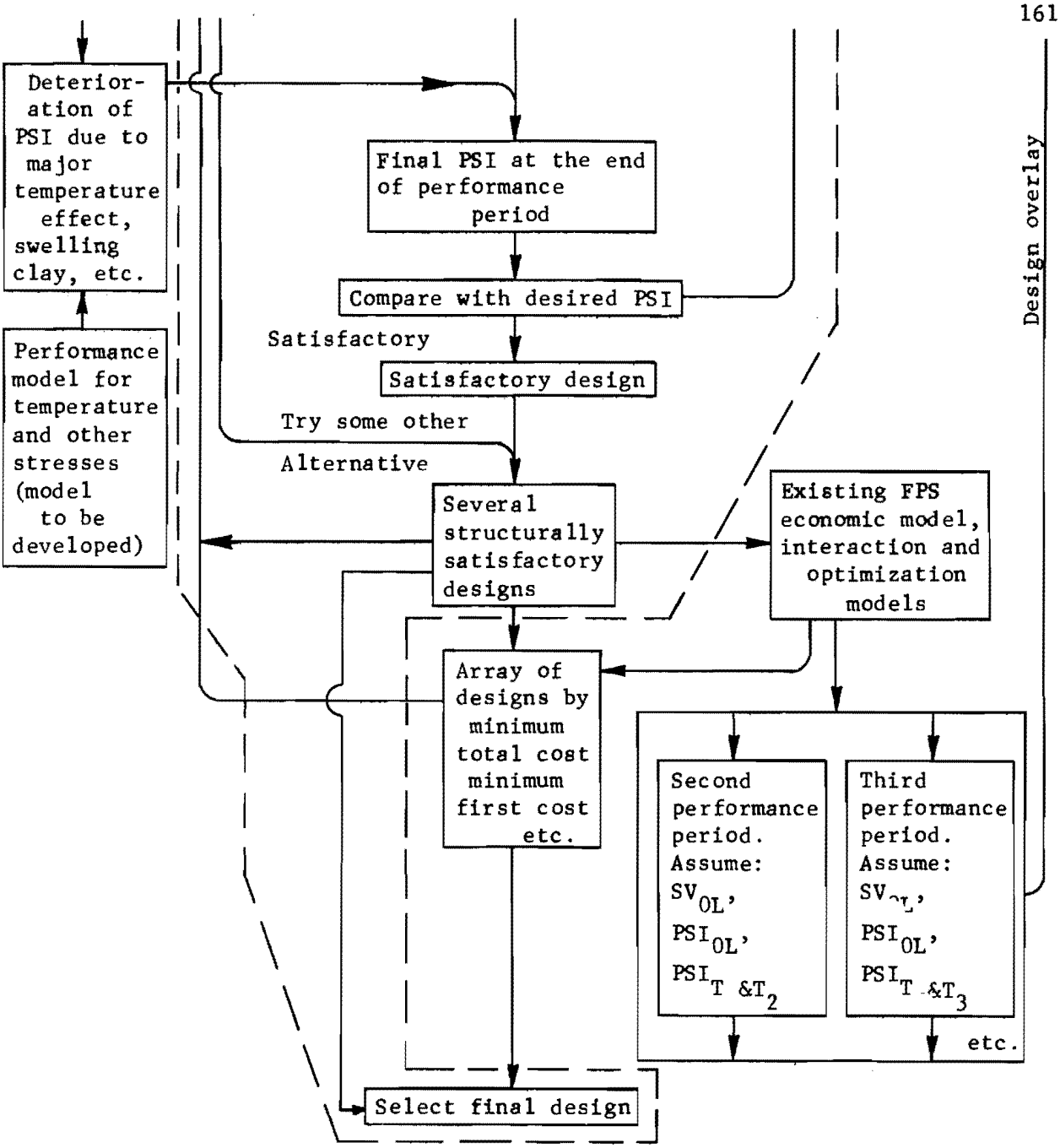

CI - Cracking index
RI - Roughness index
RDI - Rut depth index
PSI - Present serviceability index
SV_{OL} - Slope variance just after an overlay
PSI_{OL} - Present serviceability index just after an overlay
PSI_T - Present serviceability index at the end of performance period

T_i - Performance period

* To be replaced later by a more efficient technique for stress-strain calculations

[ ] Shows steps for direct use of the present procedure

Fig 13.1. (Continued).

(4) Assume Minimum Layer Thickness: Based on engineering judgment, trial layer thicknesses for the pavement section are assumed.

(5) Calculate Distress Index: Based on the above data and information, the distress index values (CI, RDI, and RI) and pavement performance PSI for the trial traffic and design period are calculated with the distress models and computer program developed in this report (Appendix 4).

(6) Compare Final PSI: The computed terminal PSI is compared with the desired value. If the values compare within the desired accuracy, the assumed design is satisfactory; otherwise, the layer thickness assumed is revised and another trial comparison is made, until a satisfactory solution is reached. Layer thickness combinations may have to be tried also to find the most economical design. Although several designs, with different layer thickness combinations, may be structurally equal, only one is economically best.

PROPOSED FPS SECOND GENERATION

The flow diagram of the proposed FPS second generation (Fig 13.1) shows the proposed procedure included in the existing FPS programs. Mainly, it is a question of replacement of the physical models of the existing FPS. From the new distress index models, PSI due to traffic load is computed at the end of an assumed performance period. Adjustments are made to this PSI for the existing swelling clay model of the FPS and for other nontraffic associated PSI models to be added later. This adjusted PSI is compared with the desired PSI and a satisfactory design is obtained. Several other structurally satisfactory designs can be obtained, and these designs are optimized by the existing FPS economic and other models to get the array of designs for final selection for the no-overlay case. The computations for overlays are made for several performance periods, as shown in Fig 13.1 and all satisfactory designs are again optimized by the existing FPS models to give the final array of design from which final selection is made.

Figure 13.2 shows the existing and proposed generation of working pavement systems. The modified and replaced items are marked. The deflection coefficients have been replaced by elastic constants, fatigue properties, and stochastic variations in these parameters. The deflection term is replaced by stress and strain computations. Instead of a direct empirical deflection versus performance equations in the existing procedure, the distress indices are computed and from the PSI versus distress indices correlation the performance of the pavement is obtained. The overlay computations are made as shown in

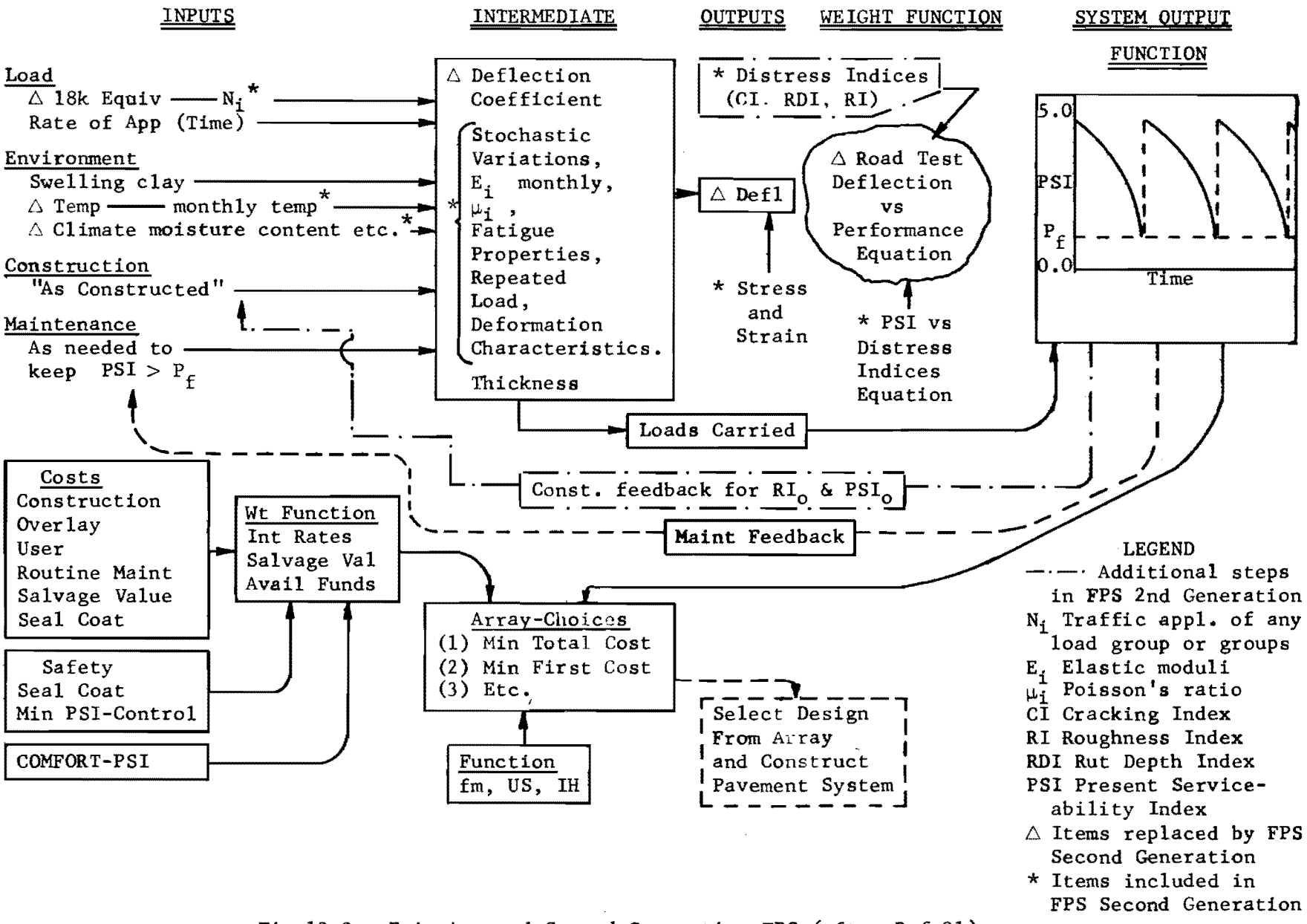

Fig 13.2. Existing and Second Generation FPS (after Ref 81).

Fig 13.1, with proper consideration of fatigue damage at the time of the overlay. The cost models, which compute the array-choices, are not changed.

Computation of Stress and Strain

At present, the computer program developed in this report takes about 60 seconds to solve one problem. In solving one problem the computation for strain is made 24 times while the computation for stresses goes through the layered subroutine 12 times. Therefore, most of the computer time is spent on these computations. To make the computer program more efficient, it is necessary to find an efficient way to calculate stresses and strains and to replace the layered subroutine. The simplest way would be to solve some factorial problems for various combinations of important parameters (E_i , D_i , and W_i) in the layered program, and to get regression equations to determine stresses and strains. It is seen that a direct factorial of the important parameters involved gives an unfeasible number of problems to be solved. Therefore, some simplified procedure needs to be adopted. During a study of the analysis of layered program it was found that stress in the layers is a function of the modular ratios of the layers rather than their absolute values (Ref 131). This is verified and reported by Shahin (Ref 166). Furthermore, Heukelom and Klomp (Ref 60) found from field observation that the modular ratios of untreated pavement layers do not exceed 1.5 to 2.5. For a fixed modular ratio, the number of variables in the layered program is reduced, thereby considerably reducing the number of factorial solutions. This or some other suitable approach should simplify the stress and strain computation in a layered system. Scrivner, at the Texas Transportation Institute, is also working to simplify this problem. Once efficiency in stress and strain calculation is achieved, the problem of computer time in the present procedure is solved.

Application of Damage Theory for Overlay Design

In the existing FPS models, it is assumed that after an overlay the resulting total thickness of asphalt concrete behaves as one layer, with the original material properties of all layers. Although in reality some allowance is required to take into account the change in material properties due to traffic loads and time, no such allowance is made in the existing FPS. In the proposed procedure, for layers other than the surface layer, it is planned to account for this change in material properties in the calculations of the rut depth index. The cumulative net rut depth index after an overlay is calculated by subtracting the rut depth index at the time of the overlay from the cumulative

rut depth index at any time after an overlay. After damage to the surface layer, a new layer is added but the old surface layer is cracked. At present there is no rational method available to take this damage into account. An advantage of the proposed procedure, which is based on fatigue and damage hypotheses, is that this damage to the pavement can be taken into account. In a pavement layer, according to Minor's hypothesis, failure is considered to occur when the cumulative damage exceeds 1.0 because initial damage for a new facility is zero. Thus, for a new pavement the cracking index is computed based on the probability of cumulative damage exceeding one. However, when a pavement is overlaid it has already experienced some cumulative damage $\left(\Sigma_o^t \Sigma_o^j \frac{n_j}{N_j}\right)$. Thus, for an overlaid pavement, an estimate of the mean initial damage x due to traffic already experienced by the pavement should be made and subtracted from 1.0 (Ref 116). After an overlay, the cracking index should be computed based on the probability that cumulative damage due to new traffic will exceed (1.0 - x). This procedure should be adopted in the second generation FPS. An overlay example problem based on this criteria is shown in Fig 13.3. A pavement with layer thicknesses of 3.5, 9, and 8 inches is considered. For a terminal PSI of 2.5, this pavement lasts for 5.5 months. After an overlay of 1-1/2 inches, for the same constant traffic, the pavement lasts for 13 months as compared to 16 months based on the criteria of the existing FPS.

EXAMPLE PROBLEM - COMPARISON OF THE PRESENT FPS AND PROPOSED FATIGUE MODELS

To develop confidence in the procedure presented in this report, example problems were run comparing the proposed model with the existing FPS method. Since the comparisons were carried out with AASHO Road Test data, in these example problems high traffic values corresponding to the AASHO Road Test data are adopted. Thus, short time periods for the pavement performance are the result due to high traffic. However, in actual problems, the lower traffic values will result in corresponding increase in the actual performance time periods.

In the first example problem, AASHO Road Test Section 623, which carried 18-kip single axle applications, is designed using the AASHO FPS model. The strength coefficient values assumed are the same as developed in the AASHO Road Test. The input and output are shown in Tables A9.1 and A9.2, respectively.

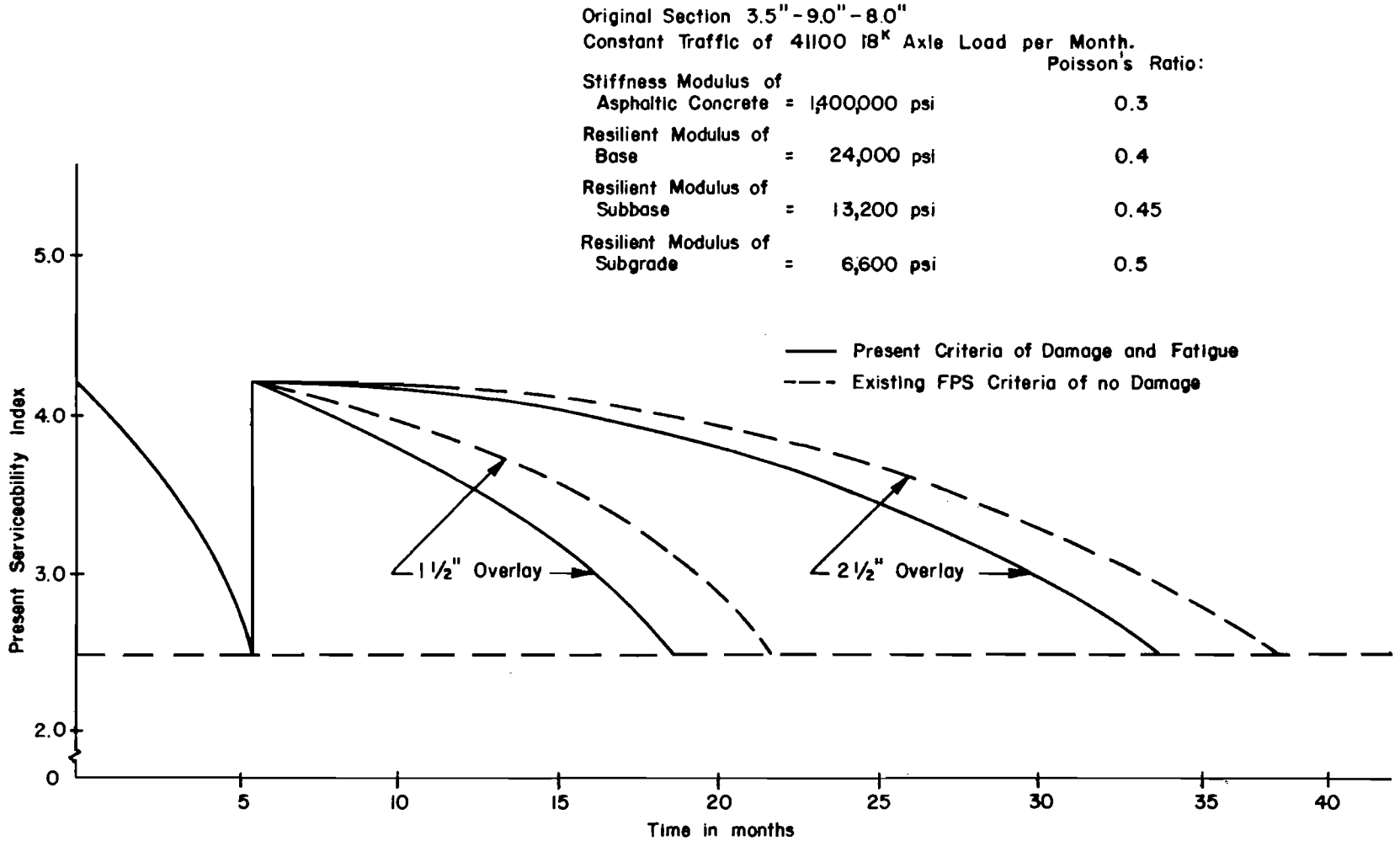

Fig 13.3. Typical overlay design based on fatigue and damage criteria.

To simulate the design for the AASHO Road Test section, no swelling effect was assumed. The initial present serviceability index was assumed as 4.2, which corresponds to the initial observed value of the AASHO Road Test Section 623. The average daily traffic values at the beginning and end including accumulated 18-kip axle applications are based on average values of traffic used on the above AASHO Road Test section. The maximum and minimum layer thicknesses are restricted to 3, 6, and 8 inches for surface, base, and subbase, respectively, and minimum and maximum time for the overlay are restricted to obtain the design life for this thickness combination without an overlay and for an assumed terminal PSI of 1.5.

A few trial solutions established the stiffness coefficient of the FPS deflection model giving the same performance as that predicted by the FPS AASHO model. Figure 13.4 shows performance curves for the pavement section under consideration from various methods, as detailed in the figure. The performance curves are quite close and give confidence in the present procedure.

In the second example, with 18-kip axle load repetitions of the AASHO Road Test data, problems are run with FPS, AASHO and deflection model computer program to obtain a set of structurally equal designs. The input to the program for the FPS AASHO model is shown in Table A9.3 while output is shown in Table A9.4. The input and output for the deflection model are similar. The stiffness coefficients for deflection models are the same as those used in the first example.

The data for swelling clay, traffic, and PSI are the same as taken for the first example. However, the maximum and minimum layer thicknesses are input to get some feasible designs. The minimum and maximum times of overlay are made equal to the performance period to get structural designs to last for approximately the time of the AASHO Road Test period, 2.2 years without an overlay.

These computations have given several designs with different layer thickness combinations, but with the same performance, i.e., the same structural number in the AASHO model and the same surface curvature index (SCI) in the deflection model of FPS. Therefore, as far as FPS is concerned all these combinations have the same structural performance. For comparison the following combinations are considered:

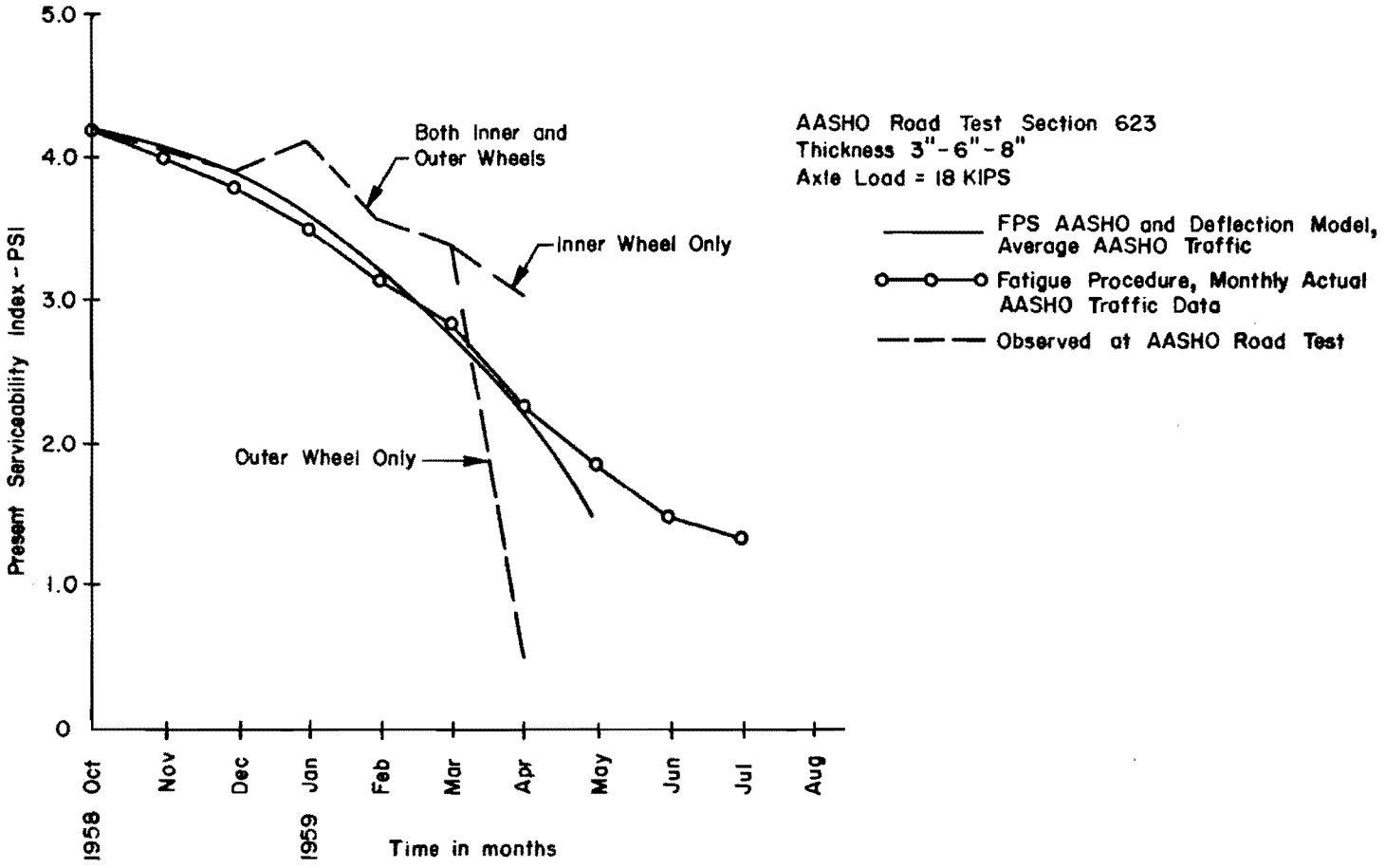

Fig 13.4. Comparison of fatigue method with FPS.

Concrete	Base	Subbase
2.75"	9"	11"
3.5"	9"	8"
4.5"	9"	4"

Figure 13.5 shows that, though the FPS predicts the same performance, the different thickness combinations do influence the performance of a pavement. It is shown that the 3.5, 9, and 8-inch thickness combination has the same performance in the FPS and fatigue procedures, but the performance of the other combinations is significantly different in the fatigue procedure.

The third example (Fig 13.6) shows the effect of support variations. In the FPS, a constant support condition throughout the year is assumed, which is not the real world situation. The performance curves for the FPS deflection model for 50 percent and 80 percent confidence are also shown. The fatigue procedure with some material properties assumed constant throughout the year shows the same performance as FPS. The effect of change in the material properties is shown. The figure also shows the performance when account is taken of monthly variations in the material properties. The figure shows that the assumption of a constant support condition in FPS can give designs which fail much earlier than predicted.

For FPS, the month when the pavement is opened for traffic and monthly traffic distributions are immaterial when no monthly variations in the material properties are taken into account. However, for the proposed fatigue procedure the opening month and monthly traffic distributions and material properties variations are important because the performance and the deterioration in the PSI of the pavement at particular time depend upon the material properties at that time. The effect of monthly traffic distribution and of opening month, for short design period, is shown in Fig 13.7. This is a more realistic approach since, generally, in practice failures have been observed in the spring months.

Figure 13.8 shows the performance curves, for the three combinations of layer thicknesses, as computed by FPS and the proposed fatigue procedure. The proposed procedure is more realistic because, as expected, the performance curves for the three thickness combinations are different in the case of the proposed procedure as compared to the one and same performance curve in case of existing FPS. In this particular example, the design life for different combinations varied by 50 percent. It is also observed that increasing the

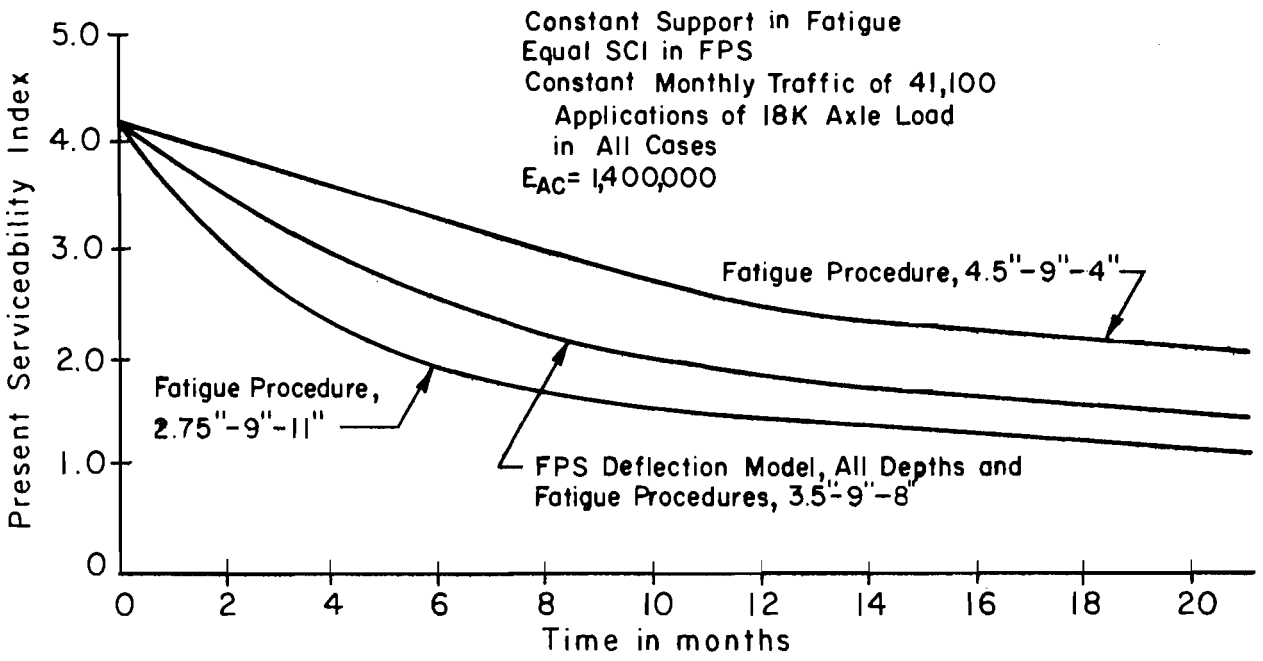

Fig 13.5. Thickness combinations influence performance.

Note: For typical pavement section see Fig 8.4.

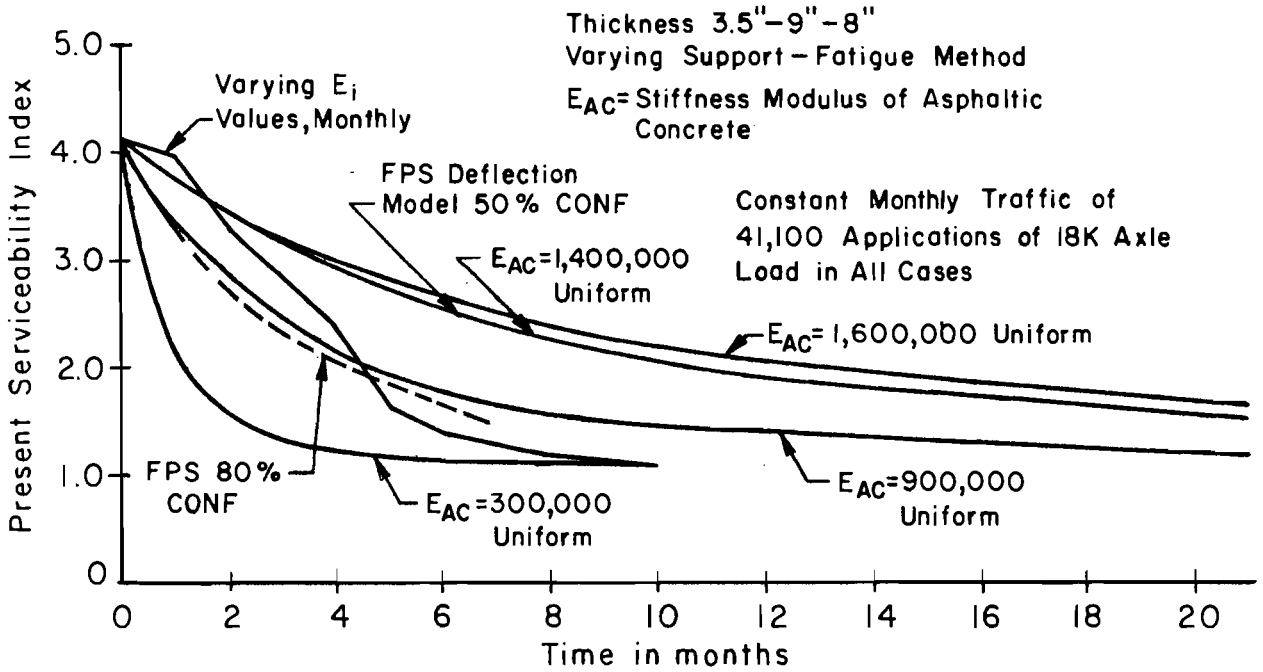

Fig 13.6. Effect of support variation in fatigue procedure.

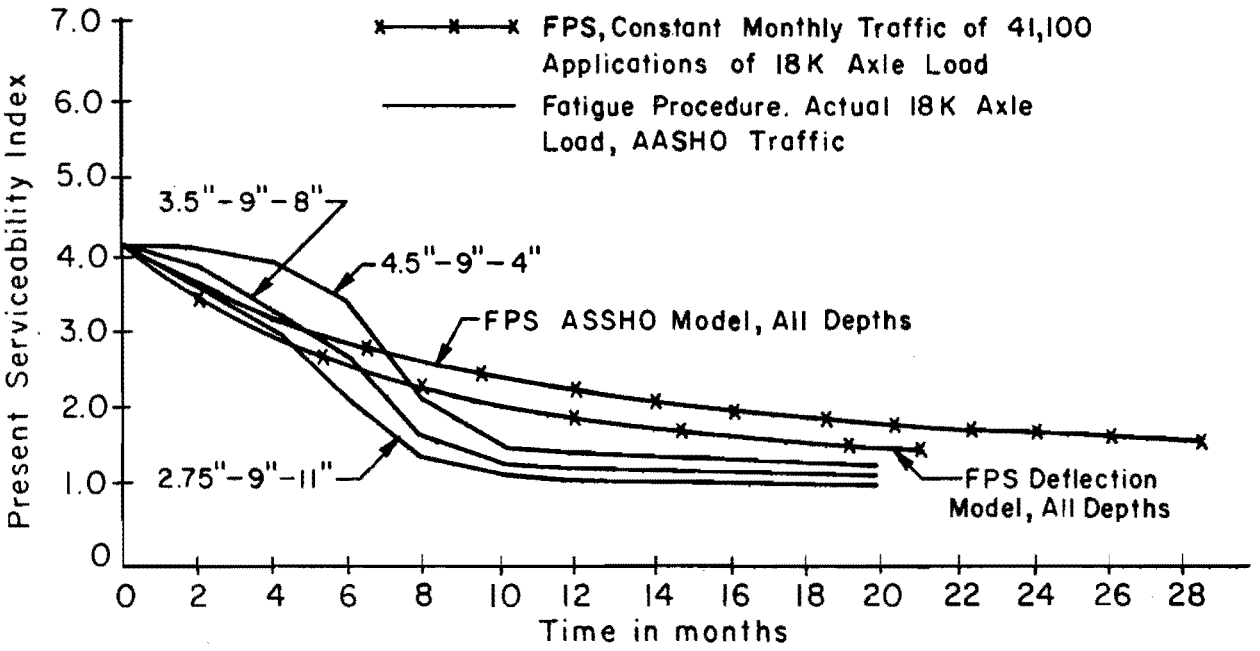

Fig 13.7. Performance curve - fatigue procedure for different starting time.

Note: For typical pavement section see Fig 8.4.

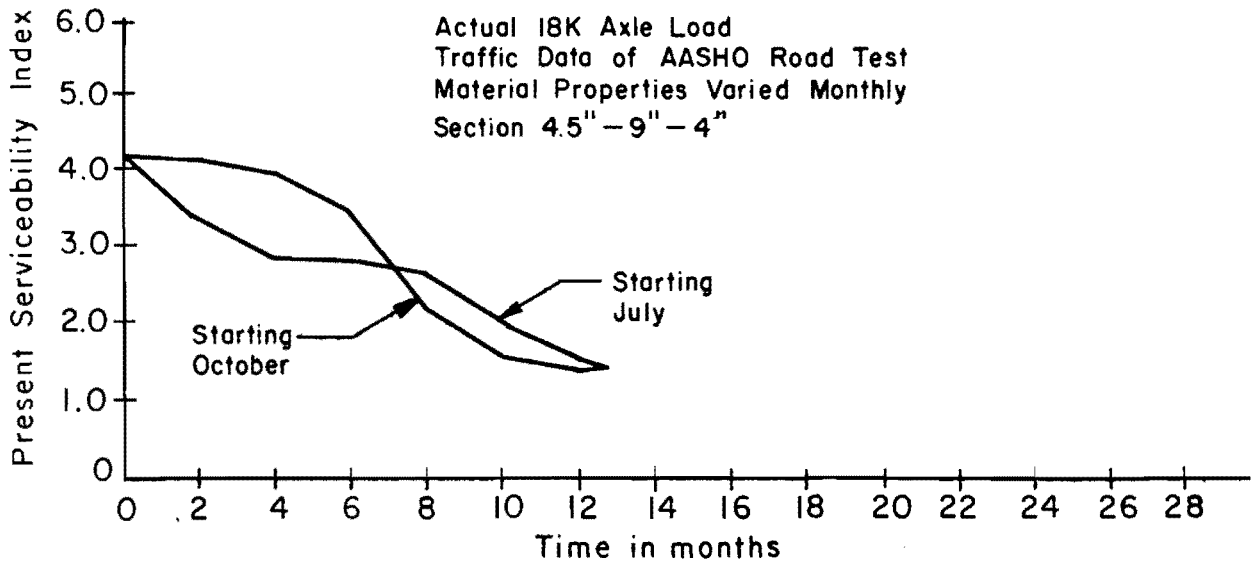

Fig 13.8. Performance curve - FPS vs fatigue procedure.

layer depths from 3, 6, and 8 inches to 3.5 - 9 - 8 inches increased (Figs 13.4 and 13.8) the life of the pavement in FPS from 7 to 21 and 29 months for deflection and AASHO models, respectively, which does not seem reasonable. However, for the proposed fatigue procedure the life increased by 16 percent.

From the results discussed herein the fatigue design procedure seems to give better and more realistic designs of flexible pavements than based on the existing FPS models.

CHAPTER 14. IMPLEMENTATION

The verification of the models developed in this report and their accurate predictions of the observed data in Chapter 11 along with the results of the sensitivity study in Chapter 12 give confidence in using the proposed procedure for the design of flexible pavements and in including this procedure in the existing FPS. In Chapter 13, revision of the existing FPS was discussed. Including the present design procedure and making the revision to the existing FPS led to the second generation FPS. In its implementation, new inputs are required (see Appendix 4). Implementation of the proposed procedure is discussed in this chapter.

STRESS AND STRAIN COMPUTATIONS

In the proposed procedure stresses and strains are calculated from the layered program. The inputs for this analysis include the elastic modulus, Poisson's ratio, and stochastic variations in modulus for each material. These properties of the materials are characterized as in Chapter 5. In the previous chapter it was noted that stress and strain calculations in the present analysis, by the direct use of the layered subroutine, should be improved and replaced by a more efficient approach. An alternate approach was discussed and further research to make the present procedure more efficient was recommended. The work on distress due to major temperature cyclic effects is also to be included in FPS second generation and is expected to take additional time at the Center for Highway Research. During this time the research efforts may also be continued to reduce the computation time in the proposed procedure and revision of the present FPS may be made to include the present procedure as well as the major temperature effects. To help with the problem of long computation time only the limited number of designs predicted as the most optimum by the existing FPS should be checked by the present design procedure for correct performance. This will avoid the time used for computations on infeasible and unacceptable designs. Once an array of most suitable designs from the existing FPS is known they are checked by the proposed procedure and

final selection is made. It may be necessary once more to run the cost analysis for these revised designs through the FPS cost models. This tentative design procedure, shown in Fig 14.1, is expected to reduce the computation time considerably.

OVERLAY DESIGN

Revision of the existing FPS overlay design procedure is proposed, following the procedure discussed in the previous chapter, which is based on the fatigue theory and cumulative damage hypothesis. The computer program developed for the present design procedure needs a small change for overlay designs. For computation of the cracking index after an overlay, the log 1.0 term in Eq 8.5 needs to be changed to log(1.0 - x), where x is the cumulative damage $\left(\sum_{0}^{t}\sum_{0}^{j}\frac{n_j}{N_j}\right)$ up to the time of overlay. For the rut depth index the change for an overlay design requires that the rut depth index at the time of an overlay RDI_{oL} should be subtracted from the rut depth index at any time after an overlay RDI_L to get the correct net rut depth index after an overlay RDI_C. The effect of swelling clay is already considered by the existing FPS.

REPEATED LOAD-DEFORMATION DATA

The regression models for computing the permanent strain in a pavement (Eqs 5.1, 5.2, and 5.4) are based on the typical characteristics of coarse-grained base and subbase materials and fine-grained subgrade materials of the AASHO Road Test. Characteristics of the coarse-grained materials of the AASHO Road Test are similar to those of materials tested at the Texas Transportation Institute (Ref 35), as mentioned in Chapter 5. These regression models are only used for computations of the rut depth index. Any small variation in the rut depth index is not comparatively important in the performance equation (Chapters 7 and 11) and does not affect the PSI significantly. In addition, any change in the above typical regression models based on actual materials used in a particular pavement probably does not affect the rut depth appreciably. Thus, though these regression models should be revised for accurate computations, based on actual repeated load-deformation characteristics of a

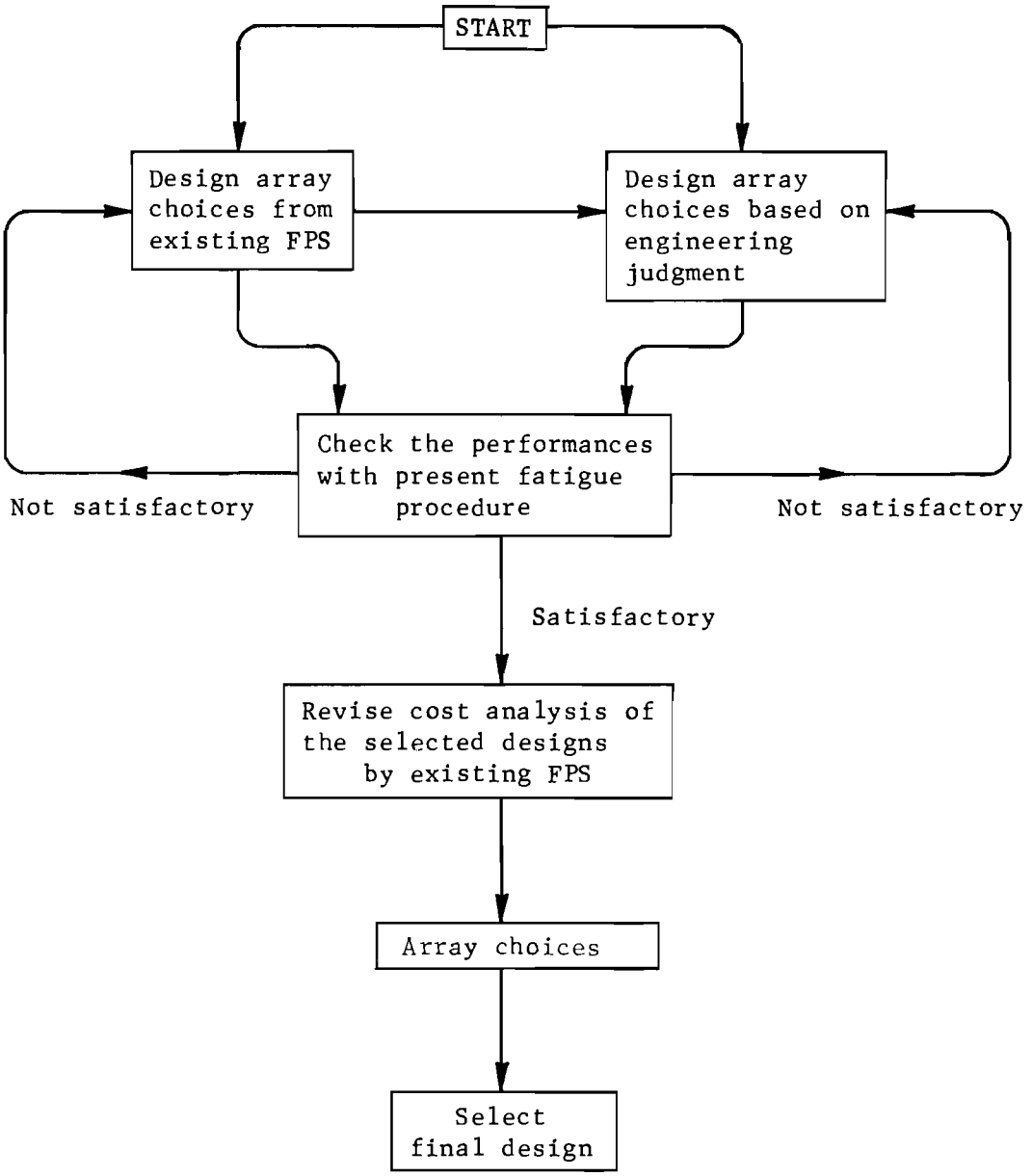

Fig 14.1. Tentative design procedure utilizing existing FPS.

particular material used in a particular pavement as discussed in Chapter 5, even these models are expected to give results which do not affect the final PSI significantly.

EQUIVALENCIES

The present procedure has the capability to compute the distress for various single axle load groups of any load intensity, and it is not necessary to change into equivalent 18-kip axle applications as in the existing FPS. However, it is seen that separate computations for various load groups consume much computer time. Thus, to save computation time it is suggested that equivalencies to convert the various load groups into one should be used. The present procedure was developed based on the verification of the AASHO Road Test data. Moreover, in the HRB Asphalt Concrete Structural Design Workshop, 1970 (Ref 63 and Appendix 1), it was suggested that the load equivalency factors developed from the AASHO Road Test equations be used for the present. These equivalencies are based on fatigue and damage criteria. Thus, it is recommended that the equivalencies based on the AASHO Road Test for different load groups and axle combinations be utilized in the design procedure to reduce computation time.

PRESENT SERVICEABILITY INDEX

The computation of present serviceability index with the proposed procedure and the modifications needed in the existing FPS performance equation were discussed in Chapter 3. With slight modifications in Eq 3.2, the proposed procedure can be included in the FPS.

TRAFFIC COMPUTATIONS

In the existing FPS, Eq 3.3 is utilized for traffic computations. In the proposed procedure the actual load repetitions for each load group or Eq 3.4 is utilized for traffic instead of 18-kip equivalent repetitions. However, existing Eq 3.3 can also be utilized in the second generation FPS with slight modifications in the proposed procedure, by including this equation in addition to Eq 3.4 or replacing Eq 3.4.

TIME SUBROUTINE

The time subroutine of the existing FPS can be utilized in a modified form for the convergence process of performance time for the desired PSI, traffic, layer thicknesses, and distresses based on material properties.

LABORATORY INVESTIGATIONS

Test procedures required to characterize the material properties which are used in the present design procedure are discussed in Chapters 4 and 5. Laboratory testing programs should be initiated at the earliest opportunity to characterize the fatigue material properties properly and to include the determination of the parameters needed in this development, so that reliable data may be created for implementation of this procedure for use of specific materials in a particular pavement. In the meantime, the design may have to rely on data in the literature or from other sources to obtain values for all variables used in the present method. The fatigue parameters B and A are very sensitive variables, and their values need accurate determination. Thus an immediate testing program to create accurate data is important.

LIMITATIONS FOR SURFACE TREATMENT AND THIN ASPHALTIC CONCRETE SURFACES

The proposed models for cracking index and roughness index are derived based on the following hypotheses:

(1) The cracking index in a pavement system is caused by the repeated flexural tensile strain developed in the asphaltic concrete surface layer due to applied wheel loads.

(2) The constant stress mode of loading conditions is most logical to determine the fatigue response of asphalt concrete for flexible pavement design.

(3) The roughness index represents most of the detrimental effects of cracking and that cracking is a good indicator of roughness in a pavement.

Under the above logical hypotheses, the proposed cracking index and roughness index models are not applicable in case of the surface treatments. For thin asphalt concrete surfaces less than 1 inch thick the models are not expected to give satisfactory results, and therefore the models may not be directly used for these cases. Further research work is needed to modify the models for their use for thin surfaces.

PREDICTION ERRORS IN THE MODELS

The prediction errors in the proposed models were discussed in Chapter 11 and results of a short sensitivity analysis were discussed in Chapter 12 to create a confidence in use of the proposed models. However, for the variations in the performance predictions at various confidence levels under different combinations of input variables and for determining the relative significance of these variables a detailed sensitivity analysis shall have to be performed.

PART V

CLOSURE

CHAPTER 15. SUMMARY, CONCLUSIONS, AND RECOMMENDATIONS

In Chapter 1, the general study objective of development of new design models for flexible pavement system second generation, based on best available technology, to update the existing FPS model, was mentioned. The author feels, in his opinion, that this objective has been achieved successfully herein by development of the various distress models and quantifying the present serviceability index value from these models. The inclusion of this procedure in FPS requires revisions in only the structural design portion and corresponding material characterization of the systems, while the user's cost and other economic models will continue to remain the same.

SUMMARY

In the first few chapters, the existing design methods and theories were discussed and need for a new systems design procedure, considering the fatigue theory, linear elastic layered theory, and probability theory, was established. The concept of distress and failure in the pavement, along with the AASHO concept of performance and present serviceability index, was discussed. Based on these concepts, the distress models for cracking index, roughness index, rut depth index, and overall present serviceability index were developed in terms of elastic and fatigue material properties (which can be predicted in the laboratory) and their stochastic variations with space and time, loading, environmental conditions, and load-deformation characteristics. These distress models are proposed to replace the empirical relationship used at present to simulate the transformation between the input variables and performance of a pavement.

Similarity and accurate predictions of the distresses actually observed for the AASHO Road Test sections and sensitivity analyses performed for the cracking index models give the confidence in the use of the models and procedure developed in this report. The development and the use of the computer program makes it easy to handle the calculations involved in the systems.

The proposed models can be used directly and can also be included in the existing FPS models leading to the flexible pavement system second generation. To reduce the computer time, the proposed models may be used to provide an independent check on current design procedures. The present method of overlay design is proposed to be replaced by the method which is based on fatigue theory and damage criteria. The example problems are solved which show the improvements of the proposed method and add to the confidence in use of the proposed models for the design of flexible pavements.

The concept of fatigue and probability theory in pavement design presented herein, though recent, is well recognized now. Their proper use in the design of flexible pavements for the first time, in the present form, adds a new dimension to the pavement design field.

The need of (1) proper relationship between distress mechanism, performance, and serviceability; (2) considerations of stochastics in pavement design; (3) distress due to fatigue in the pavement; and (4) applicability of linear theories to predict stress and strains in the pavement was recognized in the first few priority items for research by the HRB Workshop in January 1970, held at Austin, Texas (Appendix 1). The author feels that this report is a first successful attempt in this direction.

In summary, a comparison of various field observations with the predicted distress values gives a large degree of initial confidence in the design models and, in the author's opinion, the method is ready for immediate practical application, although it is only long-term observation and feedback process that will truly verify the models.

CONCLUSIONS

The flexible pavement design models presented in this report are based on sound fundamentals using the best state-of-the-art information available. The author feels that the specific objective of this study, detailed in Chapter 1, has been well accomplished.

Following are the specific conclusions for this study.

(1) A study of the development of the design methods of flexible pavement shows the need of a rational method of design which can predict the performance of a pavement under various sets of conditions to update the existing FPS.

(2) The review of current procedures and methods of flexible pavement design reveals that only a few bona-fide procedures exist and those in practice now certainly need improvements in various ways. The proposed design method will go a long way to fulfill these needs.

(3) The characterization of materials is a very important part of the whole design procedure. Proper laboratory techniques need to be extended for material testing. In the meantime, the engineer may have to rely on data in the literature or from other sources to obtain values for all variables used in the present method.

(4) The use of linear layered elastic theory may be considered as the most appropriate method for the calculations of stress and strains in various layers, although some more efficient approach to make these computations is needed.

(5) The development of the proposed method in the present form gives a new added dimension in the pavement design field and gives the realization of the importance of stochastic principles over the deterministic models.

(6) The proposed distress models have been verified successfully with the AASHO Road Test data which gives the confidence in the use of these methods. Example problems show the improvements of the proposed method over the existing FPS.

(7) This method shows some combinations to be unacceptable, which are acceptable with the present design.

(8) The new design models are more realistic and are based on sound and latest state-of-the-art. The models can be easily included in the existing flexible pavement systems model without many changes except in the structural design portion of the systems program. The proposed method can also be used directly for design of flexible pavements.

(9) Since the conventional hand solutions are a physical impossibility in solving the problems with these new models, the necessary computer programs have been developed to aid the design process.

(10) The developed design models are considered to be ready for an immediate application in the field.

(11) Deteriorated condition of the pavement should be adequately considered at the time of the overlay construction, based on fatigue principal. The proposed method of overlay design, based on fatigue theory, damage hypotheses, and stochastic concepts, presented in this report, adds a new dimension to the overlay design.

RECOMMENDATIONS

The author recommends that

(1) The models developed in this report may be put to immediate application for the design of flexible pavements and procedure included in the existing systems model to create FPS second generation.

(2) Research efforts should be continued to include the fatigue effects of the nontraffic-associated temperature cycles and foundation movements.

(3) The existing FPS model may be revised to include the developed models for traffic-associated distress and for nontraffic-associated distress when such models are ready.

(4) Laboratory testing programs should be initiated to characterize the material properties properly and to include the determinations of the parameters needed in this development.

(5) Necessary feedback data banks should be created and kept up-to-date to update the method as and when required.

(6) It is also important that necessary efforts are continued to make the developed computer program more efficient.

(7) A sensitivity study of the parameters involved should be made and their significance in the program should be evaluated.

(8) Consideration of the variability and probability may be extended for other parameters in the systems design not considered in these developments.

(9) Maintenance and other models in the FPS may be updated.

(10) The swelling clay effect needs to be considered in some more rational way in the systems design model.

(11) Cracking index distress model, presented herein, has been based on the constant stress conditions in the pavement. This is a conservative situation in some cases in comparison to the constant strain conditions, especially for thin pavements. Further research efforts are needed as to the application of these two cases in different situations.

(12) The proposed cracking index and roughness index models are not applicable in case of the surface treatments. For thin asphalt concrete surface of less than 1-inch thickness, the models are not expected to give satisfactory results. Further research efforts may be extended to modify the models for their use in these cases.

(13) The principles of design and development of models discussed in this report should be extended for the existing rigid pavement system.

(14) Efforts should be continued to make the present method of layered computer program to calculate stress and strain more efficient and/or replaced by a more efficient approach.

(15) The proposed models could be used to give better evaluation of some of current blackbases being proposed for pavements by the Texas Highway Department.

REFERENCES

1. Alden, H. L., and E. B. Roessler, Introduction to Probability and Statistics, Freeman & Sons, 1964.

2. American Society for Testing Materials, Revision of Section II, Manual on Fatigue Testing, STP No. 91, Philadelphia, 1959.

3. Avramesco, A., "Dynamic Phenomena in Pavements Considered as Elastic Layered Structures," Proceedings, Second International Conference on the Structural Design of Asphalt Pavements, August 1967, Braun-Brumfield, Inc., Ann Arbor, Michigan, 1968.

4. Bateman, John H., Highway Engineering, Fifth Edition, John Wiley & Sons, Inc., New York, 1948.

5. Bazin, P., and J. B, Saunier, "Deformability, Fatigue, and Healing Properties of Asphalt Mixes," Proceedings, Second International Conference on the Structural Design of Asphalt Pavements, August 1967, Braun-Brumfield, Inc., Ann Arbor, Michigan, 1968.

6. Barksdale, R. D., and A. H. Leonards, "Predicting Performance of Bituminous Surfaced Pavements," Proceedings, Second International Conference on the Structural Design of Asphalt Pavements, August 1967, Braun-Brumfield, Inc., Ann Arbor, Michigan, 1968, pp 321-340.

7. Benkelman, A. C., R. I. Kingham, and H. Y. Fang, "Special Deflection Studies on Flexible Pavements," Special Report 73, Highway Research Board, 1962.

8. Boussinesq, J., "Application des potentials a l'etude de l'equelibre et de mouvement des solids elastique," Gauthier-Villars, Paris, 1885.

9. Bradbury, Royall D., "Reinforced Concrete Pavement," Washington Wire Reinforcement Institute, 1938.

10. Brown, James L., Larry J. Buttler, and Hugo E. Orellana, "A Recommended Texas Highway Department Pavement Design System Users' Manual," Research Report No. 123-2, Texas Highway Department, March 1970.

11. Brown, S. F., and P. S. Pell, "An Experimental Investigation of the Stresses, Strains, and Deflections in a Layered Pavement Structure Subjected to Dynamic Loads," Proceedings, Second International Conference on the Structural Design of Asphalt Pavements, August 1967, Braun-Brumfield, Inc., Ann Arbor, Michigan, 1968, pp 487-504.

12. Bureau of Public Roads, "Quality Assurance in Highway Construction," by Edwin C. Granley, Public Roads, August 1969.

13. Burmister, D. M., "Evaluation of Pavement Systems of the WASHO Road Test by Layered System Methods," Bulletin 177, Highway Research Board, 1958.

14. Burmister, D. M., "The Theory of Stresses and Displacements in Layered Systems and Application to the Design of Airport Runways," Proceedings, Vol 23, Highway Research Board, 1943.

15. Buttler, Larry Jack, "Sensitivity Study of a Design System for Determining Thickness of Asphaltic Concrete Overlay in Rigid Highway Pavement," M.S. Thesis, The University of Texas at Austin, May 1971.

16. Carey, W. N., Jr., and P. E. Irick, "The Pavement Serviceability-Performance Concept," Bulletin 250, Highway Research Board, January 1960.

17. Center for Highway Research, "FAOV-01 Statistical Computer Program for the Analysis of Variance with Factorial Treatment Combinations," The University of Texas at Austin, 1968.

18. Center for Highway Research, "STEP-01 Statistical Computer Program for Stepwise Multiple Regression," The University of Texas at Austin, 1968.

19. Chan, C. K., and H. B. Seed, "A Study of the Deformation Characteristics of the AASHO Road Test Subgrade Under Repeated Loading," unpublished report to the AASHO Road Test staff, 1960.

20. Chan, L. S., "An Investigation of Stress-Strain and Strength Characteristics of Cohesionless Soils," Proceedings, Second International Conference on Soil Mechanics and Foundation Engineering, Rotterdam, Vol V, 1948.

21. Chen, H. H., and R. G. Hennes, "Dynamic Design of Bituminous Pavements," The Trend in Engineering, Vol 2, No. 1, January 1950, pp 22-25.

22. Coffman, Bonner S., David C. Kraft, and Jorge Tamayo, "A Comparison of Calculated and Measured Deflections for the AASHO Road Test," Proceedings of the Association of Asphalt Paving Technologists, Vol 33, 1964.

23. Committee E-9 on Fatigue, American Society for Testing and Materials, A Guide for Fatigue Testing and the Statistical Analysis of Fatigue Data, STP No. 91-A, Second Edition, Philadelphia, 1963.

24. Deacon, John Allen, "Fatigue of Asphalt Concrete," Ph.D. Dissertation, University of California, Berkeley, 1965.

25. Deacon, J. A., and C. L. Monismith, "Laboratory Flexural-Fatigue Testing of Asphalt Concrete with Emphasis on Compound-Loading Tests," a paper presented at the Annual Meeting of the Highway Research Board, Washington, D. C., January 1966.

26. Deacon, John A., "Material Characterization-Experimental Behavior," a paper presented at the Workshop on Structural Design of Asphalt Concrete Pavement Systems, The University of Texas at Austin, December 7-10, 1970.

27. Dehlen, G. L., "Flexural of a Road Surfacing, Its Relations to Fatigue, and Factors Determining Its Severity," Bulletin 321, Highway Research Board, 1962.

28. Design Manual for Controlled Access Highways, Texas Highway Department, January 1960.

29. Dolan, T. J., Basic Concepts of Fatigue Damage in Metals, Metal Fatigue, McGraw-Hill, New York, 1959.

30. Dommasch, D. O., and C. W. Laudeman, Principles Underlying Systems Engineering, Pitman Publishing Corporation, New York, 1962.

31. Dorman, G. M., "The Extension of Practice of a Fundamental Procedure for the Design of Flexible Pavements," Proceedings, International Conference on the Structural Design of Asphalt Pavements, Braun-Brumfield, Inc., Ann Arbor, Michigan, 1963, pp 785-793.

32. Dorman, G. M., and J. M. Edwards, "Developments in the Application in Practice of a Fundamental Procedure for the Design of Flexible Pavements," Proceedings, Second International Conference on the Structural Design of Asphalt Pavements, August 1967, Braun-Brumfield, Inc., Ann Arbor, Michigan, 1968, pp 99-109.

33. Drake, W. B., and James H. Havens, "Kentucky Flexible Pavement Design Studies," Bulletin No. 52, Engineering Experiment Station, University of Kentucky, June 1959.

34. Duncan, J. M., Carl L. Monismith, and E. L. Wilson, "Finite Elements Analysis of Pavements," Highway Research Record No. 228, Highway Research Board, 1968.

35. Dunlap, A. Wayne, "Deformation Characteristics of Granular Materials Subjected to Rapid, Repetitive Loading," Research Report No. 27-4, Texas Transportation Institute, Texas A&M University, College Station, Texas, November 1966.

36. Ellis, D. O., and F. J. Ludwig, Systems Philosophy, Prentice-Hall, Inc., Englewood Cliffs, New Jersey, 1962.

37. "Engineering and Design - Flexible Air Force Pavements," Corps of Engineers' Manual EM1110-45-302, August 15, 1958.

38. Epps, Jone Albert, "Influence of Mixture Variables on the Flexural Fatigue and Tensile Properties of Asphalt Concrete," Ph.D. Dissertation, University of California at Berkeley, September 1968.

39. Epremian, E., and R. F. Mehl, "The Statistical Behavior of Fatigue Properties and the Influence of Metallurgical Factors," Symposium on Fatigue with Emphasis on Statistical Approach, Part II, STP No. 137, American Society for Testing Materials, Philadelphia, 1953, pp 25-57.

40. Fang, H. Y., and J. H. Schaub, "Analysis of the Elastic Behavior of Flexible Pavement," Proceedings, Second International Conference on the Structural Design of Asphalt Pavements, August 1967, Braun-Brumfield, Inc., Ann Arbor, Michigan, 1968, pp 719-729.

41. Ferrari, P., "The Behavior of Asphalt Pavements Under Variable Repeated Loads," Proceedings, Second International Conference on the Structural Design of Asphalt Pavements, August 1967, Braun-Brumfield, Inc., Ann Arbor, Michigan, 1968.

42. Finn, F. N., "Factors Involved in the Design of Asphalt Pavement Surfaces," NCHRP Report 39, Highway Research Board, 1967.

43. Finn, F. N., W. R. Hudson, B. F. McCullough, and K. Nair, "An Evaluation of Basic Material Properties Affecting Behavior and Performance of Pavement Systems," a paper presented at the meeting of the Highway Research Board, Washington, D. C., January 1968.

44. Freudenthal, A. M., and E. J. Gumbel, "Distribution Functions for the Prediction of Fatigue Life and Fatigue Strength," Proceedings, International Conference on Fatigue of Metals, Institution of Mechanical Engineers, London, 1956, pp 262-271.

45. Freudenthal, A. M., and R. A. Heller, "On Stress Interaction in Fatigue and a Cumulative Damage Rule," Journal of the Aero-Space Sciences, Vol 26, No. 7, July 1959, pp 431-442.

46. Gallaway, T. M., "Implied Fatigue Life of Cement Treated Base," unpublished term project for C.E. 391P.1, The University of Texas at Austin, May 1970.

47. Gardner, L. J., and E. L. Skok, Jr., "Use of Viscoelastic Concepts to Evaluate Laboratory Test Results and Field Performance of Some Minnesota Asphalt Mixtures," Proceedings, Second International Conference on the Structural Design of Asphalt Pavements, August 1967, Braun-Brumfield, Inc., Ann Arbor, Michigan, 1968.

48. Garrison, W. A., "Three-Year Evaluation of Shell Avenue Test Road," Highway Research Record No. 117, Highway Research Board, 1965.

49. Gray, W. H., "A Study of the Fatigue Properties of Lightweight Aggregate Concrete," Purdue University Joint Highway Research Project, Lafayette, Indiana, 1960.

50. Grumm, Fred J., "Designing Foundation Courses for Highway Pavements and Surfaces," California Highways and Public Works, Vol 20, No. 3, March 1942, pp 6-9, 20.

51. Haas, R. C. G., "Developing a Pavement Feedback Data System," Research Report No. 123-4, Center for Highway Research, The University of Texas at Austin, August 1970.

52. Haas, R. C. G., "The Performance Behavior of Flexible Pavements at Low Temperatures," Ph.D. Dissertation, University of Waterloo, June 1968.

53. Hagerup, E., "Flexural Fatigue Testing of Polyesters," Journal of Applied Polymer Science, Vol 7, No. 3, May 1963, pp 1093-1116.

54. Hank, R. J., and F. H. Scrivner, "Some Numerical Solutions of Stresses in Two and Three Layered Systems," Proceedings, Vol 28, Highway Research Board, 1948.

55. Harris, Frederick A., "Selection and Design of Semi-Flexible and Conventional Type Pavements," Proceedings, Vol 35, Highway Research Board, 1956.

56. Hansen, Torben C., "Notes from a Seminar on Structure and Properties of Concrete," Department of Civil Engineering, Stanford University, Stanford, California, September 1966.

57. Haynes, J. H., and E. J. Yoder, "Effects of Repeated Loading on Gravel and Crushed Stone Base Course Materials Used in the AASHO Road Test," Highway Research Record No. 39, Highway Research Board, 1964, pp 82-96.

58. Heukelom, W., "Observations on the Rheology and Fracture of Bitumens and Asphalt Mixes," Proceedings of the Association of Asphalt Paving Technologists, 1966.

59. Heukelom, W., and A. J. G. Klomp, "Consideration of Calculated Strains at Various Depths in Connection with the Stability of Asphalt Pavements," Proceedings, Second International Conference on the Structural Design of Asphalt Pavements, August 1967, Braun-Brumfield, Inc., Ann Arbor, Michigan, 1968, pp 155-168.

60. Heukelom, W., and A. J. G. Klomp, "Dynamic Testing as a Means of Controlling Pavements During and After Construction," Proceedings, International Conference on the Structural Design of Asphalt Pavements, Braun-Brumfield, Inc., Ann Arbor, Michigan, 1963, pp 667-678.

61. Heukelom, W., and A. J. G. Klomp, "Road Design and Dynamic Loading," Proceedings of the Association of Asphalt Paving Technologists, Vol 33, 1964.

62. Hicks, R. G., "Fatigue of Asphalt Concrete," Thesis, Master of Science in Mechanical Engineering, University of California, 1965.

63. Highway Research Board, "Structural Design of Asphalt Concrete Pavement Systems," Proceedings of Workshop held 7-10 December 1970, Austin, Texas.

64. Highway Research Board, "AASHO Interim Guide for Design of Flexible Pavement Structures," AASHO Committee on Design, April 1962.

65. Highway Research Board, "AASHO Interim Guide for Design of Flexible Pavements," AASHO Committee on Design, October 1961.

66. Highway Research Board, "AASHO Road Test Technical Staff Papers," AASHO Road Test technical staff, Special Report 66, 1961.

67. Highway Research Board, "The AASHO Road Test: Report 2, Materials and Construction," Special Report 61B, 1962.

68. Highway Research Board, "The AASHO Road Test: Report 3, Traffic Operations and Pavement Maintenance," Special Report 61C, 1962.

69. Highway Research Board, "The AASHO Road Test: Report 4, Bridge Research," Special Report 61D, 1962.

70. Highway Research Board, "The AASHO Road Test: Report 5, Pavement Research," Special Report 61E, 1962.

71. Highway Research Board, "The AASHO Road Test: Report 6, Special Studies," Special Report 61F, 1962.

72. Highway Research Board, "The AASHO Road Test: Report 7, Summary Report," Special Report 61G, 1962.

73. Highway Research Board, "The AASHO Test History and Description of Project," Special Report 61A, 1961.

74. Highway Research Board, "The WASHO Road Test, Part 1, Design, Construction, and Testing Procedure," Special Report 18, 1954.

75. Hong, H., "State of the Art Theory and Application of Sonic Testing for Bituminous Mixtures," Special Report 94, Highway Research Board, 1968.

76. Howkins, S. D., "Measurement of Pavement Thickness by Rapid and Nondestructive Methods," NCHRP Report 52, Highway Research Board, 1968.

77. Hudson, W. R., "Discontinuous Orthotropic Plates and Pavement Slabs," Ph.D. Dissertation, The University of Texas, Austin, August 1965.

78. Hudson, W. R., F. N. Finn, B. F. McCullough, K. Nair, and B. A. Vallerga, "Systems Approach to Pavement Design," Interim Report NCHRP Project 1-10, submitted to National Cooperative Highway Research Program, Highway Research Board, March 1968.

79. Hudson, W. R., and B. F. McCullough, "An Extension of Rigid Pavement Design Methods," Highway Research Record No. 60, Highway Research Board, 1963.

80. Hudson, W. R., B. F. McCullough, and Fred N. Finn, "Factors Affecting Performance of Pavement Systems," Transportation Engineering Journal, Vol 95, No. TE3, American Society of Civil Engineers, August 1969.

81. Hudson, W. Ronald, B. Frank McCullough, F. H. Scrivner, and James L. Brown, "A Systems Approach Applied to Pavement Design and Research," Research Report 123-1, Center for Highway Research, The University of Texas at Austin, March 1970.

82. Hutchinson, B. G., and R. C. G. Haas, "A System Analysis of the Pavement Design Process," Highway Research Record No. 239, Highway Research Board, 1968.

83. Hveem, F. N., "Devices for Recording and Evaluating Pavement Roughness," Bulletin 264, Highway Research Board, 1960.

84. Hveem, F. N., "Pavement Deflections and Fatigue Failures in Design and Testing of Flexible Pavements," Bulletin 114, Highway Research Board, 1955.

85. Hveem, F. N., "Types and Causes of Failure in Highway Pavements," Bulletin 187, Highway Research Board, 1958, pp 1-52.

86. Hveem, F. N., and R. M. Carmany, "Factors Underlying the Rational Design of Pavements," Proceedings, Vol 28, Highway Research Board, 1948.

87. Hveem, F. N., Earnest Zube, Robert Bridges, and Raymond Forsyth, "The Effect of Resilience-Deflection Relationship on the Structural Design of Asphaltic Pavements," Proceedings, International Conference on the Structural Design of Asphalt Pavements, Braun-Brumfield, Inc., Ann Arbor, Michigan, 1963, pp 649-666.

88. Irick, P. E., "An Introduction to Guidelines for Satellite Studies of Pavement Performance," NCHRP Report 2, Highway Research Board, 1964.

89. Jain, S. P., "Significance of Different Variables in FPS-7," Research Report, Center for Highway Research, The University of Texas at Austin, in progress.

90. Jain, S. P., "Application of Traffic Data of Texas Highway Department to Determine the Load Distribution Factor," Technical Memorandum 123-01, Center for Highway Research, The University of Texas at Austin, November 1969.

91. Jain, S. P., "Effect on Value of the Modulus of the Subgrade Reaction (K) Due to Variations in Soil Support or Erodability," Technical Memorandum 123-04, Center for Highway Research, The University of Texas at Austin, April 1970.

92. Jain, S. P., "Rating of the Variables in FPS-2," Technical Memorandum 123-07, Center for Highway Research, The University of Texas at Austin, July 1970.

93. Jain, S. P., "Sensitivity Analysis on FPS-6 (AASHO Model)," Technical Memorandum 123-08, Center for Highway Research, The University of Texas at Austin, July 1970.

94. Jain, S. P., "An Extension of AASHO Flexible Design Method," Technical Memorandum 123-11, Center for Highway Research, The University of Texas at Austin, November 1970.

95. Jimenez, R. A., and B. M. Gallaway, "Behavior of Asphalt Concrete Diaphragms to Repetitive Loading," Proceedings, International Conference on the Structural Design of Asphalt Pavements, University of Michigan, 1963.

96. Jones, A., "Tables of Stresses in Three-Layer Elastic Systems," Bulletin 342, Highway Research Board, 1962, pp 176-215.

97. Jones, R., and E. N. Gatfield, "Fatigue Effects in Concrete Under Vibratory Stress," Research Note No. RN/3891/RJ. ENG., Department of Scientific and Industrial Research, Road Research Laboratory, January 1961.

98. Kang, Nai C., "Systems of Pavement Design and Analysis," Highway Research Record No. 239, Highway Research Board, 1968.

99. Kaplan, M. F., "Strains and Stresses of Concrete at Initiation of Cracking and Near Failure," Journal of the American Concrete Institute, July 1963.

100. Kasianchuk, D. C., "Fatigue Consideration in the Design of Asphalt Concrete Pavement," Ph.D. Dissertation, University of California at Berkeley, August 1968.

101. Kelley, James A., "Quality Assurance in Highway Construction, Part 5, Summary of Research for Quality Assurance Aggregate," Public Roads, Vol 35, No. 10, October 1969, pp 230-237.

102. Kersten, M. S., and Eugene L. Skok, "Application of AASHO Road Test Results to Design of Flexible Pavement in Minnesota," Investigation Number 183 - Interim Report, Minnesota Department of Highways, 1968.

103. Kesler, Clyde E., "Effect of Speed of Testing on Flexural Fatigue Strength of Plain Concrete," Proceedings, Vol 32, Highway Research Board, 1953, pp 251-258.

104. Kher, Ramesh K., and W. R. Hudson, "A Systems Analysis of Rigid Pavement Design," Research Report 123-5, Center for Highway Research, The University of Texas at Austin, September 1970.

105. Kirk, J. M., "Analysis of Deflection Data From the AASHO Test," Proceedings, Second International Conference on the Structural Design of Asphalt Pavements, August 1967, Braun-Brumfield, Inc., Ann Arbor, Michigan, 1968, pp 151-154.

106. Klomp, A. J. G., and T. H. W. Niesman, "Observed and Calculated Strains at Various Depths in Asphalt Pavements," Proceedings, Second International Conference on the Structural Design of Asphalt Pavements, August 1967, Braun-Brumfield, Inc., Ann Arbor, Michigan, 1968, pp 671-688.

107. Kondner, Robert L., and Raymond J. Krizer, "Factors Influencing Flexible Pavement Performance," NCHRP Report 22, Highway Research Board, 1966.

108. Kriege, H. F., and L. C. Gilbert, "Some Factors Affecting the Resistance of Bituminous Mixtures to Deformation Under Moving Wheel Loads," Proceedings of the Association of Asphalt Paving Technologists, 1933, pp 73-84.

109. Kung, Kuang-Yuan, "A New Method in Correlation Study of Pavement Deflection and Cracking," Proceedings, Second International Conference on the Structural Design of Asphalt Pavements, August 1967, Braun-Brumfield, Inc., Ann Arbor, Michigan, 1968, pp 1037-1046.

110. Lazan, B. J., and A. Yorgiadis, "The Behavior of Plastics Under Repeated Stress," Symposium on Plastics, STP No. 59, American Society for Testing Materials, Philadelphia, 1944, pp 66-94.

111. Lewis, W. C., "Fatigue of Wood and Glued-Wood Constructions," Proceedings, Vol 46, American Society for Testing Materials, 1946, pp 814-835.

112. Lister, N. W., and R. Jones, "The Behavior of Flexible Pavements Under Moving Wheel Loads," Proceedings, Second International Conference on the Structural Design of Asphalt Pavements, Braun-Brumfield, Inc., Ann Arbor, Michigan, 1968, pp 1021-1036.

113. Lytton, R. L., "A Method of Decreasing the Computer Running Time for FPS," Technical Memorandum, Texas Transportation Institute, Texas A&M University, College Station, Texas, July 13, 1971.

114. Marco, S. M., and W. L. Starkey, "A Concept of Fatigue Damage," Transactions, Vol 76, American Society of Mechanical Engineers, 1954, pp 627-632.

115. McCall, John T., "Probability of Fatigue Failure of Plain Concrete," Journal of the American Concrete Institute, Vol 30, No. 2, August 1958.

116. McCullough, B. F., "A Pavement Overlay Design System Considering Wheel Loads, Temperature Changes, and Performance," Ph.D. Dissertation, University of California at Berkeley, July 1969.

117. McCullough, B. F., C. J. Vantil, B. A. Vallerga, and R. G. Hicks, "Evaluation of AASHO Interim Guide for Design of Pavement Structures," NCHRP Project 1-11, submitted to National Cooperative Highway Research Program, Highway Research Board, December 1968.

118. Metcalf, C T., "Field Measurement of Dynamic Elastic Moduli of Materials in Flexible Pavement Structures," Proceedings, Second International Conference on the Structural Design of Asphalt Pavements, August 1967, Braun-Brumfield, Inc., Ann Arbor, Michigan, 1968, pp 521-536.

119. Miner, Milton A., "Estimation of Fatigue Life with Particular Emphasis on Cumulative Damage," Metal Fatigue, George Sines and J. L. Waisman, editors, McGraw-Hill Book Company, Inc., New York, 1959, pp 278-289.

120. Miner, Milton A., "Cumulative Damage in Fatigue," Transactions, Vol 66, American Society of Mechanical Engineers, 1945, pp A159-A164.

121. Monismith, Carl L., "Asphalt Paving Mixtures, Properties, Design and Performance," course notes, The Institute of Transportation and Traffic Engineering, University of California at Berkeley, 1961.

122. Monismith, C. L., "Flexibility Characteristics of Asphaltic Paving Mixtures," Proceedings of the Association of Asphalt Paving Technologists, Vol 27, 1958, pp 74-106.

123. Monismith, C. L., "Effect of Temperature on the Flexibility Characteristics of Asphaltic Paving Mixtures," Symposium on Road and Paving Materials, STP No. 277, American Society for Testing Materials, Philadelphia, 1960, pp 89-108.

124. Monismith, C. L., "Asphalt Mixture Behavior in Repeated Flexure," Report No. TE-63-2, Institute of Engineering Research, University of California at Berkeley, November 1963.

125. Monismith, C. L., "Symposium on Flexible Pavement Behavior as Related to Deflection, Part II - Significance of Pavement Deflections," Proceedings of the Association of Asphalt Paving Technologists, Vol 31, 1962, pp 231-260.

126. Monismith, C. L., and J. A. Deacon, "Fatigue of Asphalt Paving Mixtures," Transportation Engineering Journal of ASCE, Vol 95, No. TE2, May 1969.

127. Monismith, C. L., and K. E. Secor, "Thixotropic Characteristics of Asphaltic Paving Mixtures with Reference to Behavior in Repeated Loading," Proceedings of the Association of Asphalt Paving Technologists, Vol 29, 1960, pp 114-140.

128. Monismith, C. L., H. B. Seed, F. G. Mitry, and C. K. Chan, "Prediction of Pavement Deflections from Laboratory Tests," Proceedings, Second International Conference on the Structural Design of Asphalt Pavements, August 1967, Braun-Brumfield, Inc., Ann Arbor, Michigan, 1968, pp 109-141.

129. Monismith, C. L., K. E. Secor, and E. W. Blackmer, "Asphalt Mixture Behavior in Repeated Flexure," Proceedings of the Association of Asphalt Paving Technologists, Vol 30, 1961, pp 188-222.

130. Monismith, C. L., D. A. Kasianchuk, and J. A. Epps, "Asphalt Mixture Behavior in Repeated Flexure: A Study of an In-Service Pavement Near Morro Bay, California," Report No. TE 67-4, University of California, Berkeley, December 1967.

131. Morgan, J. R., and A. J. Scala, "Flexible Pavement Behavior and Application of Elastic Theory: A Review," Australian Road Research Board Fourth Conference, 1968.

132. Murdock, John W., "A Critical Review of Research on Fatigue," Bulletin 475, Engineering Experiment Station, College of Engineering, University of Illinois, 1965.

133. Nichols, F. P., "A Practical Approach to Flexible Pavement Design," Proceedings, Second International Conference on the Structural Design of Asphalt Pavements, August 1967, Braun-Brumfield, Inc., Ann Arbor, Michigan, 1968, pp 769-780.

134. Nielsen, J. P., "Implications of Using Layered Theory in Pavement Design," Transportation Engineering Journal of ASCE, Vol 96, No. TE4, 1970.

135. Nijboer, L. W., "Mechanical Properties of Asphalt Materials and Structural Design of Asphalt Roads," Proceedings, Vol 33, Highway Research Board, 1954.

136. Nijboer, L. W., "Mechanical Properties of Bituminous Road Mixtures," Proceedings of the Symposium on Vibration Testing of Roads and Runways, Koninklijke/Shell-Laboratorium, Amsterdam, April 20-24, 1959.

137. Nijboer, L. W., and C. T. Metcalf, "Dynamic Testing at the AASHO Road Test," Proceedings, International Conference on the Structural Design of Asphalt Pavements, Braun-Brumfield, Inc., Ann Arbor, Michigan, 1963, pp 713-721.

138. Nordby, Gene M., "Fatigue of Concrete - A Review of Research," presented at the ACI 54th Annual Convention, from a symposium sponsored by ACI Committee 215, Chicago, Illinois, February 26, 1958.

139. Painter, L. J., "Analysis of AASHO Road Test Asphalt Pavement Data by the Asphalt Institute," Highway Research Record No. 71, Highway Research Board, 1965.

140. Palmer, L. A., and E. S. Barber, "Soil Displacement Under a Circular Loaded Area," Proceedings, Vol 20, Highway Research Board, 1940, pp 279-286.

141. Papazian, H. S., and R. F. Baker, "Analysis of Fatigue Type Properties of Bituminous Concrete," Proceedings of the Association of Asphalt Paving Technologists, Vol 28, 1959, pp 179-210.

142. Paris, P. C., M. P. Gomez, and W. E. Anderson, "A Rational Analytic Theory of Fatigue," The Trend in Engineering, Vol 13, No. 1, January 1961, pp 9-14.

143. Pavement Design and Evaluation Committee, "Field Performance Studies of Flexible Pavements," Proceedings, Second International Conference on the Structural Design of Asphalt Pavements, August 1967, Braun-Brumfield, Inc., Ann Arbor, Michigan, 1968, pp 1087-1101.

144. Peattie, K. R., "Stress and Strain Factors for Three-Layered Elastic Systems," Bulletin 342, Highway Research Board, 1962, pp 215-252.

145. Peattie, K. R., "A Fundamental Approach to the Design of Flexible Pavements," Proceedings, International Conference on the Structural Design of Asphalt Pavements, Braun-Brumfield, Inc., Ann Arbor, Michigan, 1963, pp 403-411.

146. Pell, P. S., "Fatigue of Asphalt Pavement Mixes," Proceedings, Second International Conference on the Structural Design of Asphalt Pavements, August 1967, Braun-Brumfield, Inc., Ann Arbor, Michigan, 1968.

147. Pell, P. S., "Fatigue Characteristics of Bitumen and Bituminous Mixes," Proceedings, International Conference on the Structural Design of Asphalt Pavements, Braun-Brumfield, Inc., Ann Arbor, Michigan, 1963.

148. Pell, P. S., "Fatigue of Bituminous Materials in Flexible Pavements," Proceedings, Vol 31, Institute of Civil Engineering, 1965.

149. Pell, P. S., P. F. McCarthy, and R. R. Gardner, "Fatigue of Bitumen and Bituminous Mixes," International Journal of Mechanical Sciences, Vol 3, 1961, pp 247-267.

150. Pister, K. S., and R. A. Westmann, "Analysis of Viscoelastic Pavements Subjected to Moving Loads," Proceedings, International Conference on the Structural Design of Asphalt Pavements, Braun-Brumfield, Inc., Ann Arbor, Michigan, 1963, pp 522-529.

151. Porter, O. J., "Foundations for Flexible Pavements," Proceedings, Vol 22, Highway Research Board, 1942, pp 100-143.

152. Plunkett, Robert, "Statistical Analysis of Fatigue Data," Symposium on Statistical Aspects of Fatigue, STP No. 121, American Society for Testing Materials, Philadelphia, 1951, pp 45-53.

153. Richmond, Samuel B., Statistical Analysis, Second Edition, the Ronald Press Company, New York, January 1964.

154. Road Research Laboratory, "Bituminous Materials in Road Construction," Her Majesty's Stationery Office, London, 1962.

155. Roberts, Freddy L., "Pavement Serviceability Equation Using the Surface Dynamics Profilometer," Special Report 116, Highway Research Board, 1971.

156. Saal, R. N. J., and P. S. Pell, "Fatigue of Bituminous Road Mixes," Kolloid Zeitschrift (Darmstadt), Vol 171, 1960.

157. Saal, R. N. J., and P. S. Pell, "Fatigue Characteristics of Bituminous Road Mixes," British Society of Rheology, 1959.

158. Scrivner, F. H., and Chester H. Michalak, "Flexible Pavement Performance Related to Deflections, Axle Applications, Temperature, and Foundation Movements," Research Report 32-13, Texas Transportation Institute, Texas A&M University, College Station, Texas, 1969.

159. Scrivner, F. H., and W. M. Moore, "An Empirical Equation for Predicting Pavement Deflections," Research Report 32-12, Texas Transportation Institute, Texas A&M University, College Station, Texas, 1968.

160. Scrivner, F. H., and W. M. Moore, "Some Recent Findings in Flexible Pavement Research," Research Report 32-9, Texas Transportation Institute, Texas A&M University, College Station, Texas, 1967.

161. Scrivner, F. H., and W. M. Moore, "An Electro-Mechanical System for Measuring the Dynamic Deflection of a Road Surface Caused by an Oscillating Load," Research Report 32-4, Texas Highway Department - Texas Transportation Institute Cooperative Research, December 1964.

162. Scrivner, F. H., W. M. Moore, and G. R. Carey, "A Systems Approach to the Flexible Pavement Design Problem," Research Report 32-11, Texas Transportation Institute, Texas A&M University, College Station, Texas, 1968.

163. Sebastyan, G. Y., "Pavement Deflection and Rebound Measurements and Their Application to Pavement Design and Evaluation," Proceedings of the Association of Asphalt Paving Technologists, Vol 32, 1962.

164. Seed, H. B., F. G. Mitry, C. L. Monismith, and C. K. Chan, "Prediction of Flexible Pavement Deflection from Laboratory Repeated-Load Test," NCHRP Report 35, Highway Research Board, 1967.

165. Seed, H. B., C. K. Chan, and C. E. Lee, "Resilience Characteristics of Subgrade Soils and Their Relation to Fatigue Failures in Asphalt Pavements," Proceedings, International Conference on the Structural Design of Asphalt Pavements, Braun-Brumfield, Inc., Ann Arbor, Michigan, 1963, pp 611-636.

166. Shahin, M. Y., "Two Layered Systems Analyses," unpublished term project for CE 391.P1, The University of Texas at Austin, 1971.

167. Shahin, Mohammed Y., "Outlines of Computer Program Available for Analyses of Stresses and Strains, and Displacement in a Five Layered Elastic System Under a Load Uniformly Distributed on a Circular Area," Technical Memorandum, Center for Highway Research, October 13, 1970.

168. Shook, James F., and H. Y. Fang, "Cooperative Materials Testing Program at the AASHO Road Test," Special Report 66, Highway Research Board, 1961.

169. Skok, Eugene L., Jr., and Fred N. Finn, "Theoretical Concepts Applied to Asphalt Concrete Pavement Design," Proceedings, International Conference on the Structural Design of Asphalt Pavements, Braun-Brumfield, Inc., Ann Arbor, Michigan, 1963, pp 412-440.

170. Standard Specifications of Road and Bridge Construction, Texas Highway Department, January 2, 1962.

171. Sutaria, T. C., "Sensitivity of Various Parameters in Cracking-Index Program," unpublished term project for CE 391P.L, The University of Texas at Austin, 1971.

172. Symposium on Fatigue with Emphasis on Statistical Approach, II, STP No. 137, American Society for Testing Materials, Philadelphia, 1953.

173. Takeshita, H., "Considerations on the Structural Number," Proceedings, Second International Conference on the Structural Design of Asphalt Pavements, August 1967, Braun-Brumfield, Inc., Ann Arbor, Michigan, 1968, pp 407-412.

174. Teller, W., An Introduction to Probability Theory and Its Applications, John Wiley & Sons, Inc., New York, 1961.

175. Texas Highway Department, Flexible Pavement Designer's Manual, Part I, March 1970.

176. Texas Highway Department, "Triaxial Compression Test for Disturbed Soils and Base Materials," Manual of Testing Procedures, Vol 1, Tex-1171E, Revised Edition, September 1965.

177. Thenn de Barros, S., "A Critical Review of Present Knowledge of the Problem of Rational Thickness Design of Flexible Pavements," Highway Research Record No. 71, Highway Research Board, 1965.

178. Thomas, T. W., "The Testing of Asphalt Paving Specimens Upon a Flexible Spring Base," Proceedings of the Association of Asphalt Paving Technologists, Vol 17, 1948, pp 174-183.

179. Timoshenko, S., Theory of Elasticity, McGraw-Hill Company, Inc., New York, 1934.

180. Vallerga, B. A., "On Asphalt Pavement Performance," Proceedings of the Association of Asphalt Paving Technologists, Vol 24, 1955, pp 79-102.

181. Vallerga, B. A., F. N. Finn, and R. G. Hicks, "Effect of Asphalt Aging on the Fatigue Properties of Asphalt Concrete," Second International Conference on the Structural Design of Asphalt Pavements, August 1967, Braun-Brumfield, Inc., Ann Arbor, Michigan, 1968.

182. Van der Poel, C., "A General System Describing the Viscoelastic Properties of Bitumen and Its Relation to Routine Test Data," Journal of Applied Chemistry, May 4, 1954.

183. Vesic, Aleksander S., William H. Perloff, and Carl L. Monismith, editors, "Review of Existing Theories and Methods of Pavement Design," Circular Number 112, Highway Research Board, October 1970.

184. Vesic, Aleksander Sedmak, and Leonard Domaschuk, "Theoretical Analysis of Structural Behavior of Road Test Flexible Pavements," NCHRP Report 10, Highway Research Board, 1964.

185. Walker, Roger S., Freddy L. Roberts, and W. Ronald Hudson, "A Profile Measuring, Recording, and Processing System," Research Report No. 73-2, Center for Highway Research, The University of Texas at Austin, April 1970.

186. Weibull, W., Fatigue Testing and Analysis of Results, Pergamon Press, New York, 1961.

187. Witt, Arthur W., III, and B. Frank McCullough, "Characterization of the Swelling Clay Parameter Used in the Pavement Design System," Research Report No. 123-3, Center for Highway Research, The University of Texas at Austin, August 1970.

188. Yoder, E. J., Principles of Pavement Design, John Wiley & Sons, Inc., New York, 1959.

189. Zimpfer, W. H., T. L. Bransford, and William Gartner, Jr., "A Tentative Flexible Pavement Design Method for the State of Florida," Research Bulletin No. 22-A, Division of Research and In-Service Training, State Road Department of Florida, January 1960.

190. Zube, Ernest, and Raymond Forsyth, "Flexible Pavement Maintenance Requirements as Determined by Deflection Measurements," Highway Research Record No. 129, Highway Research Board, 1966.

APPENDIX 1

SUMMARY OF RESEARCH NEEDS, ADVISORY COMMITTEE, HRB WORKSHOP ON STRUCTURAL DESIGN OF ASPHALT CONCRETE PAVEMENT SYSTEMS HELD IN AUSTIN, TEXAS, DECEMBER 7-10, 1970 (REF 63)

APPENDIX 1. SUMMARY OF RESEARCH NEEDS, ADVISORY COMMITTEE, HRB WORKSHOP ON STRUCTURAL DESIGN OF ASPHALT CONCRETE PAVEMENT SYSTEMS HELD IN AUSTIN, TEXAS, DECEMBER 7-10, 1970 (REF 63)

To make engineers more effective in bringing developments to the profession quickly and in helping to direct research efforts by improving the interaction between engineers and researchers, a workshop was held at The University of Texas during the period December 7-10, 1970, under the auspices of the Highway Research Board and sponsored by the Federal Highway Administration.

The following list represents ten major research items required to develop additional methodology for problems currently not solvable. These items have been obtained from the deliberations of the nine discussion groups and have been ranked by the Advisory Committee (Ref 63). This committee has prepared statements which reflect the extent of these research areas.

It should be noted that there are many items included in the discussion group reports which have not been included in this listing.

1. Relationship Between Pavement Distress and a Performance or Failure Function

There is no mechanistic way to relate pavement distress to pavement failure except for specific conditions (e.g., excess of rutting levels related to safety).

2. Determine Applicability of Linear Theories to Predict Stress, Strain, Deflections and Fatigue Distress in Pavements

This research is intended to determine how accurately the linear theories of elasticity and viscoelasticity (applied to layered systems) can predict the stress and strain states, and surface deflections. The predicted stress and/or strain state in conjunction with fatigue data is to be used to estimate the cracking of pavements subjected to repeated loads. In addition the viscoelasticity theory is to be used to predict surface rutting. In all cases the predictions will be compared with closely controlled and thoroughly instrumented laboratory and field experiments.

3. Mechanical Characterization of Granular Materials

Although unbonded granular materials have been used as components of pavements for many years, there are as yet no generally accepted constitutive equations by which they may be represented in the stress analysis or which will reflect their cumulative deformation under repeated loadings. Sensitivity to confining pressure, the modification of response due to various degrees of saturation, the "conditioning" which occurs under early applications of load, and the cumulative densification or distortion which is produced by many cycles of load well below failure levels, must be considered. Relationships which approximate these effects under the three dimensional states of stress typical of those occurring in pavement systems are required. Since rigorous representation is not immediately attainable, the emphasis should be placed on the permissible deviations from linear viscoelastic systems which are tractable in analysis. After acceptable parameters are selected to characterize such materials, test procedures must be developed for use by engineers on a production basis which permit measurement of these parameters on granular materials in a state representative of their in-situ condition in the pavement system.

4. Effect of Environment on Pavement System Condition and Response

To provide the ability to predict the equilibrium conditions which will prevail in a given pavement system under local moisture and temperature environments and the effects of these conditions on materials' properties, differential surface deformations, and pavement performance.

5. Treating Pavement Design as a Stochastic Process

A procedure needs to be developed which will predict variations in the system response due to statistical variations in load, environment, geometry, and material properties. In addition, an error analysis is required to estimate the variations in the predictions arising from inaccuracy of the analytical model and inconsistency in testing procedures.

This would provide the designer with the ability to evaluate the risk involved in arriving at a particular design value by the selection of various assumed values for parameters based on statistical considerations.

6. Fracture Mechanisms

The mechanistic approach to fatigue-crack prediction utilizes fracture-mechanics principles to explain the initiation, propagation, and accumulation

of cracks. It offers many potential advantages as compared with the phenomenological approach primarily in terms of its ability to handle both mode of loading and areal cracking as well as in terms of its ability to explicitly treat the stochastic nature of the process. Following the successful completion of current research programs, additional research that is anticipated includes the effects of random loading, the phenomenon of localized plastic flow due to occasional heavy loadings, and continuing field verification.

7. Mechanical Characterization of Pavement Materials (Other than Granular)

While considerable progress has been made in the identification and measurement of properties of asphaltic concrete required for insertion into the linear viscoelastic and other procedures of stress analysis, there still remain important questions in the characterization of these materials and of asphalt-treated base materials, cement-treated base materials, and cohesive soils. In all cases, the degree of departure of these materials from the linear response model must be determined to identify any deviations large enough to require special analysis. Further, the deformation and fracture response of these materials to repeated loading under states of stress representative of critical states in pavement systems must be determined. The effects of the environmental variables of temperature and moisture, where appropriate, must be evaluated. After appropriate characterizations are obtained, production type tests capable of use by highway engineers must be developed, and typical ranges of values determined.

8. Identification of Loading

(a) Determine accuracy of weight and volume data presently being obtained and reported in the W-4 loadometer tables by extending the studies.

(b) Gather data to check accuracy of past predictions of design loadings.

9. Reflection Cracking - Method of Prediction

Current systems of overlay design do not provide adequate guidance in designing overlays to prevent reflection cracking. This is particularly true in the case of large random or thermal cracks found in older Portland Cement Concrete or cement-treated base structures. In addition, current design methods do not recognize that cracking can initiate in the base course due to

shrinkage or other environmental changes. Such a crack can then reflect through the surface layer leading to distress.

It is believed that the possibility of developing a mechanistic model should be explored with the purpose of providing a rational approach to these design problems.

With portions of the Interstate as well as other Federal and State Highways approaching the end of their structural design life, it is important that work on the problem be started at an early date so that it will be available to help in the designs which will be facing the states in the next few years.

10. Information Data Base for the Pavement System

Development of rational pavement design methods is an iterative process which involves observation and subsequent improvement bases on analysis of observed data. Validation or modification of system and sub-system models lends emphasis to the need for selecting of proper variables and compatible ways of measurement. The numbers of the possible candidates for inclusion in the system requires that effective information management techniques be applied to the data handling process. This involves; selection of parameters to be stored, sampling plan (i.e., how, when, where to take data), data processing, input, storage, and output techniques. The pilot model of such a system probably involves selected pavement sections rather than an entire pavement inventory.

Service-Performance Measurements, or subjective ratings, must be used to bridge this gap and thus to establish a way of defining pavement failure and unserviceability for combined levels of distress in terms of the pavement function and the user.

Studies must define important distress factors involved in pavement failure (including weighting functions for these factors) in terms of time, traffic, or other usable factors. Concepts of "value", such as Utility Theory, should be studied to see if such work can be applied to this function.

A crude estimate of man-years necessary to accomplish bringing research needs to the true implementation state was compiled by the Advisory Committee. There was not time to make any considered judgments, therefore these should only be viewed as an expression of magnitude.

1. 10-50 2. 10 3. 12 4. 10 5. 5 6. 10 7. 12 8. 2 9. 5
10. 5-50

APPENDIX 2

DETAILS OF MATERIAL CHARACTERIZATION

APPENDIX 2. DETAILS OF MATERIAL CHARACTERIZATION

Introduction

The need for and technical aspect of the material characterization along with the details of the material properties required for the present flexible pavement design procedure were discussed in Chapter 5. Consolidated statements on the properties of the AASHO Road Test materials which were adopted for the present analysis were also included in Chapter 5. Details of the procedure to characterize these material properties which were not included in Chapter 5 are given in this appendix.

Elastic Modulus

The elastic modulus is one of the most important material properties to be considered in the proposed fatigue model. Its determination should be based on a close simulation of expected field conditions. The computations required for such a determination are given in the following paragraphs.

Asphalt Concrete. Various parameters and mix properties required for determination of the stiffness modulus of asphalt concrete are listed in Chapter 5. The procedure to determine these parameters is detailed below.

Monthly Temperature. For the present design procedure, to determine the monthly values of stiffness modulus of asphalt concrete, a temperature representative of each month is required. This can be obtained from weather data. For the present analysis, this information (Table A2.1) was obtained from the AASHO Road Test Report 5 (Ref 70).

Time of Loading. Several axle loads were used in the AASHO Road Test. The axle load as well as the tire pressures in each case was different. However, a constant speed of 35 miles an hour was maintained for the test traffic (Ref 70). Time of loading is required to calculate suitable values of the stiffness modulus for asphalt concrete. For this report, an average time of loading was calculated as shown in Table A2.2, which is self-explanatory. On this basis, a mean value of 0.02 seconds was adopted for all calculations.

TABLE A2.1. MONTHLY TEMPERATURES

Month	Temperature, ^{o}F
January	21
February	25
March	27
April	41
May	54
June	66
July	70
August	75
September	65
October	51
November	43
December	28

Mix Properties. The following average values were adopted from the AASHO Road Test Report 2, SR61B (Ref 67):

Ring and ball temperature	117^{o} F
Penetration at 77^{o} F	91
Voids	3-5%
Asphalt content	5.4% based on total weight of mixture
Density of surface course mix	146.8 lbs per cu ft

From the above data,

$$\text{Volume concentration } C_v = \frac{\text{Volume of compacted aggregate}}{\text{Volume of aggregate + asphalt}}$$

$$\text{Volume of asphalt per cu ft} = \frac{146.8 \times 5.4}{100 \times 62.4} = 0.127 \text{ cu ft}$$

(assuming specific gravity of asphalt as unity).

$$C_v = \frac{1}{1 + 0.127} = 0.89$$

Making Van Draat and Sommer corrections for voids of more than 3 percent (Ref 38),

$$\text{Corrected volume concentration } C_v' = \frac{C_v}{1 + \Delta H}$$

ΔH = difference between actual air void content and the value of 3 percent (expressed in decimal form)

$$C_v' = \frac{C_v}{1 + \Delta H} = \frac{0.89}{1 + \frac{5 - 3}{100}} = 0.87$$

$$\frac{C_v'}{1 - C_v'} = 6.7$$

From PI charts (Ref 121), assume PI = 0 .

Time of loading from Table A2.2 = 0.02 seconds.

Values of Stiffness Modulus. Values of the stiffness modulus of asphaltic concrete were calculated by the Heukelom and Klomp (Table A2.3), and the Nijboer method (Table A2.4).

Table A2.5 gives a consolidated statement of the stiffness values calculated by the above two methods at various temperatures. Columns 5 to 9 in this table give the stiffness values of asphalt concrete adopted in various references. Column 10 gives the practical observation values of stiffness in a pavement at various temperatures from a plot reported in Highway Research Record No. 71, pp 70-73. This plot was developed by use of the results of subgrade stress measurements at different pavement temperature. It may be observed that the values of stiffness calculated by Nijboer are very low as compared to the Heukelom and Klomp method. The literature review shows that the Heukelom and Klomp method has been given enough recognition to make the results based on this method more reliable, although it has been observed (Ref 42) that this method tends to give higher values. The Nijboer method has not been used much. To get a reasonable value of stiffness consistent with the values in Column 10, the following criteria were adopted for the present analysis.

(1) A weighted average stiffness value was calculated at all temperatures by weighting the Heukelom and Klomp method, twice as compared to the Nijboer method.

(2) After the stiffness values were recalculated by the method in the preceeding paragraph, it was found that values agreed reasonably well with Column 10 except at high temperatures. At a temperature of 77^{o} F the values given by the Nijboer method as well as by the Heukelom and Klomp method are lower than the values of Columns 5 to 10 obtained at this temperature from the indicated references. Therefore, to get a consistent value, an average of all the values in Cols 5 to 10 was taken and this value was assumed reasonable.

Based on paragraphs (1) and (2) above, a plot was made as shown in Fig A2.1 to represent the stiffness values of asphalt concrete of the AASHO Road Test. The monthly temperature values (Table A2.1) for the present analysis are taken from AASHO Road Test Report 5 (Ref 70). The monthly temperature and stiffness modulus thus obtained are tabulated in Table A2.6.

Untreated Granular Base and Subbase Materials. Monthly values of the resilient modulus for these AASHO Road Test materials are not available. However, proper analysis of the existing data could give the desired information.

TABLE A2.2. TIME OF LOADING

Wheel Load, lb	Tire Pressure, lb/in^2	Contact Area, in^2	Diameter of Contact Area, in.	Time of Loading, seconds
1,000	29.1	34.4	6.6	.0107
3,000	42.3	71.0	9.5	.0162
6,000	65.7	91.5	10.8	.0175
6,000	65.7	91.5	10.8	.0175
9,000	67.5	133.3	13.0	.0210
8,000	69.5	115.0	12.1	.0196
11,200	66.4	169.9	14.7	.0240
10,000	66.4	151.0	13.9	.0225
15,000	69.7	216.0	16.6	.0270
12,000	69.8	172.0	14.8	.0240
			MEAN	0.02

Average Adopted Time of Loading = 0.02 seconds

Speed of Vehicles at AASHO Road Test = 35 mph
= 51.3 fps

TABLE A2.3. CALCULATION OF MONTHLY STIFFNESS MODULUS OF AASHO ASPHALT CONCRETE BY HEUKELUM & KLOMP METHOD REF NCHRP REPORT 39 (Ref 42)

Temp ^{o}F	Temp Below R&B		Stiffness of Bitumen (S_b) kg/cm^2	$n = \frac{}{0.83 \times \log \frac{4 \times 10^5}{S_b}}$	$\frac{S_m}{S_b} = \left(1 + \frac{2.5}{n} \cdot \frac{cv'}{1-cv'}\right)^n = X^n$		Stiffness of mix (S_m) kg/cm^2	S_m psi $\times 10^5$
	^{o}F	^{o}C			X	X^n		
1	2	3	4	5	6	7	8	9
20	97	54	2000	1.91	9.75	77.5	155000	22.1
23	94	52	1600	1.95	9.6	82.3	131680	18.8
29	88	49	1200	2.08	9.0	96.7	116040	16.6
41	76	42	500	2.41	7.9	146.0	73000	10.5
52	65	36	300	2.59	7.5	184.0	55200	8.0
64	53	29	100	2.95	6.6	285.0	28500	4.0
67	50	28	90	3.03	6.5	290.0	26100	3.7
71	46	26	60	3.18	6.3	348.0	20880	3.0
74	43	24	50	3.24	6.2	370.0	18500	2.6
75	42	23	40	3.32	6.0	383.0	15320	2.2

TABLE A2.4. CALCULATION OF MONTHLY STIFFNESS MODULUS VALUES OF AASHO ASPHALT CONCRETE BY THE NIJOBOER METHOD (Ref 173)

$$E_{60} = 16 \frac{p}{f}$$

where

E_{60} = modulus of deformation (kg/cu^2) at 60^o C and time of loading of 5 sec,

p = Marshall stability (kg) of mix,

f = flow value (unit 1/100 cm).

For AASHO asphalt concrete p = 900 kg

f = 28

$$E_{60} = 16 \frac{p}{f} = 16 \times \frac{900}{28} = 514 \text{ kg/cu}^2$$

Coefficient for 0.02 time of loading = 4.0

Hence $E_{60}, t = 0.02 = 514 \times 4.0 = 2056 \text{ kg/cu}^2 = 29362$ lbs/sq in.

Temp. ^oF	Temp. ^oC	Coefficient	E lbs/sq in. x 10^5
1	2	3	4
20	-6.7	19	5.6
23	-5.0	18	5.3
29	-1.7	16	4.7
41	5.0	12.5	3.7
52	11.1	8	2.4
64	17.7	6.5	1.9
67	19.4	6.0	1.8
71	21.7	5.8	1.7
74	23.3	5.0	1.6
75	23.9	5.0	1.5

TABLE A2.5. STIFFNESS MODULUS OF ASPHALTIC CONCRETE OF AASHO ROAD TEST BY VARIOUS METHODS

Temp. ° F	Values of Stiffness Modulus by Various Methods psi x 10^5								
						Finn in Ref (169) pp 418			
	Heukelom & Klomp Method	Nijoboer Method	Adopted Values*	Coffman et al AAPT 1964 pp 87-89 Dynamic Test	NCHRP 1-10	Based on Vanderpoel Method	Baker & Papazian	Adopted by Finn	HRR 71 pp 70
1	2	3	4	5	6	7	8	9	10
20°	22.1	5.6	16.6						15.0
23°	18.8	5.3	14.3						14.0
29°	16.6	4.7	12.6						13.0
41°	10.5	3.7	8.2	17.0 at 40° F					10.0
52°	8.0	2.4	6.1						8.0
64°	4.0	1.9	3.3						6.0
67°	3.7	1.8	3.1						6.4
71°	3.0	1.7	2.6						5.0
74°	2.6	1.6	2.3						4.5
75°	2.2	1.5	2.0	6.0 at 77°F	1.5	3.4 at 77°F	4.6 at 77°F	1.5	4.3

*Adopted Values Calculated by $\frac{\text{Col (2)} \times 2 + \text{Col (3)}}{3}$

TABLE A2.6. MONTHLY TEMPERATURES AND VALUES OF STIFFNESS

Month	Temp. ^{o} F	Stiffness Modulus psi x 10^5
January	21^{o}	16.0
February	25^{o}	14.2
March	27^{o}	13.7
April	41^{o}	9.0
May	54^{o}	6.0
June	66^{o}	4.0
July	70^{o}	3.5
August	75^{o}	3.0
September	65^{o}	4.2
October	51^{o}	6.5
November	43^{o}	8.3
December	28^{o}	13.1

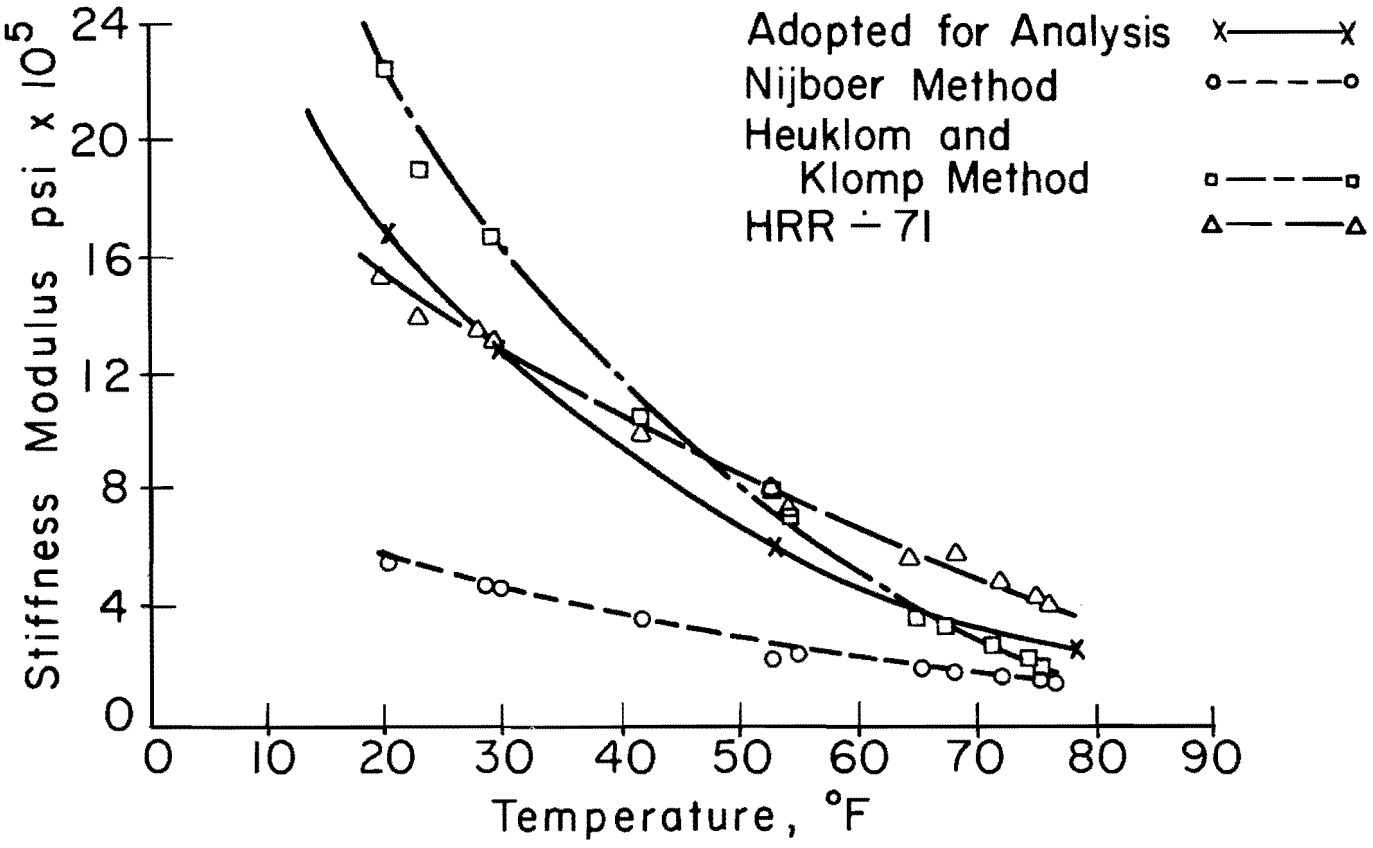

Fig A2.1. Plot of temperature versus stiffness modulus.

Figures 96 and 97 of AASHO Road Test Report 5 (Ref 70) show the moisture content and CBR values of the pavement components during various months. These values are entered in Columns 1 to 3 of Tables A2.7 and A2.8. NCHRP Report 1-11 (Ref 117) gives an approximate correlation between CBR and resilient modulus for these materials. Estimated values of resilient modulus based on this criterion are entered in Column 4. Special Report 66 (Ref 66) gives the test results of the AASHO Road Test materials as reported by various agencies. An average resilient modulus value of 15,000 psi for base and 8,000 psi for subbase are reported in this reference. Based on the AASHO Road Test results, a correlation between the AASHO Road Test strength coefficients and resilient modulus was developed (Ref 94). This criterion gives an expected variation in resilient modulus from 48,000 to 9,000 psi for base and 9,300 to 6,200 psi for subbase materials used in the AASHO Road Test. Heukelom and Klomp (Ref 60) observed that the modular ratio of the untreated material layers in the pavement in a stable condition are not expected to be more than 1.5 to 2.5. The expected values of resilient modulus for base and subbase based on this observation and assuming an average modular ratio of 2 are entered in Column 8. Special Report 66 (Ref 66) gives some CBR test values corresponding to the observed moisture contents. Corresponding values of resilient modulus estimated from NCHRP Report 1-11 (Ref 117) are entered in Column 11. Haynes and Yoder (Ref 57) have reported a range of modulus for base material as 33,500 psi to 39,500 psi. The plots of moisture content versus resilient modulus are shown in Figs A2.2 and A2.3.

From the above discussion, it is seen that it is difficult to pinpoint an absolute value of the resilient modulus for these materials. However, the modulus values for subbase were adopted on the basis of Heukelom and Klomp (Ref 60) criteria given in Column 8. These values are also about an average of the values given by other criteria. The modulus values of base were also based on Heukelom and Klomp criteria except that some adjustments, as shown in Column 12, were made because of very little change in the base CBR values during the months from September to March.

Fine Grained Subgrade Materials. No direct information regarding the monthly resilient modulus of the AASHO Road Test subgrade material is available from the test results. However, an indirect estimation of monthly resilient modulus is possible by use of available information (consolidated in Table A2.9) of the test results of this material.

TABLE A2.7. MODULUS OF RESILIENCE FOR AASHO ROAD TEST BASE MATERIAL

Month	AASHO Road Test Report 5 (Ref 70)		NCHRP 1-11 (Ref 117)	Average Value of	Jain Model (Ref 94)**		Heuklom & Klomp (Ref 60)	Page 89 of Ref 66** Test Results of AASHO Base Material by Various Agencies			Values Adopted
	CBR	M.C. Corresponding to CBR Test	E lbs/sq in.	E reported in Ref 66	Strength Coefficients A_2	E lbs/sq in.	$E_{base}=2 \times E_{subbase}$ (1.5 to 2.5)	Moisture Content	CBR	NCHRP 1-11	E lbs/sq in.
1	2	3	4	5	6	7	8	9	10	11	12
Jan.	36*	4.2*	21,000		0.25	48,000	26,400	1. 7.3	72	28,000	24,000
Feb.	36*	4.2*	21,000				26,400	2. 6.1	170	-	24,000
March	36*	4.2*	21,000				26,400	3. 6.8	120	-	24,000
April	19	6.7	14,000		0.11	9,300	14,400	4. 6.6	80	28,500	15,600
May	22	6.0	16,000				17,200	5. 6.8	87	29,000	18,000
June	25	5.3	17,500				19,600	6. 10.0	92	30,000	19,600
July	28	4.8	18,500	15,000**			21,600	7. 7.0	34	19,500	21,600
Aug.	32	4.6	19,000				23,200	8. 6.3	93	30,000	23,200
Sep.	34	4.5	19,500				24,400	9. 12.5	3	-	24,000
Oct.	35	4.4	20,000				24,800				24,000
Nov.	36	4.3	20,500				25,600				24,000
Dec.	36	4.3	21,000				26,400				24,000

* Assumed Values

** Values do not correspond to any particular month

According to the material specifications (AASHO Road Test Report 2 pp 64) the CBR for the base material was specified as 75, which according to NCHRP 1-11 will correspond to an E value of 28,000 psi.

Haynes and Yoder (Ref 57) reported values ranging from 33,500 to 39,500 psi.

TABLE A2.8. MODULUS OF RESILIENCE FOR AASHO ROAD TEST SUBBASE MATERIAL

Month	AASHO Road Test Report 5 (Ref 70)		NCHRP 1-11 (Ref 117)	Average Value of	Jain Model (Ref 94)**		Heuklom & Klomp (Ref 60)	Page 79, Table 17 of Ref 66 Test Results of AASHO Subbase Materials by Various Agencies**			Values Adopted
	M.C.	CBR	E lbs/sq in.	E reported in Ref 66	Strength Coefficients A3	E lbs/sq in.	$2xE_{subgrade}$	M.C.	CBR	E From NCHRP 1-11	E lbs/sq in.
1	2	3	4	5	6	7	8	9	10	11	12
Jan.	5.0*	26	14,000				13,200	1. 11.7	45	17,000	13,200
Feb.	5.0*	26	14,000		0.11	9,300	13,200	2. 7.3	27	13,500	13,200
March	5.0*	26	14,000				13,200	3. 8.0	28	14,000	13,200
April	7.6	12	10,800		0.09	6,200	7,200	4. 6.8	66	18,000	7,200
May	7.0	15	11,200				8,600	5. 5.7	16	11,400	8,600
June	6.2	17	11,500				9,800	6. 7.2	40	16,000	9,800
July	5.7	19	12,300	8,000**			10,800	7. 7.9	42	16,500	10,800
Aug.	5.4	21	13,000				11,600	8. 7.4	47	17,500	11,600
Sep.	5.3	22	13,200				12,200	9. 8.3	41	16,000	12,200
Oct.	5.2	23	13,400				12,400				12,400
Nov.	5.1	25	13,700				12,800				12,800
Dec.	5.0*	26	14,000				13,200				13,200

* Assumed Values
** Values do not correspond to any particular month

TABLE A2.9. MODULUS OF RESILIENCE FOR AASHO ROAD TEST SUBGRADE MATERIALS

Month	AASHO Road Test Report 5 (Ref 70)		NCHRP 1-11 (Ref 117)	Average Values of E Reported in	Heuklom & Klomp (Ref 60)	Page 70, Ref 66. Test Results of Subgrade Material by Various Agencies**			Fig 16 Page 555 (HRB Proc Vol 34) & Fig 5 (C.K. Chan & S.B. Seed) AASHO Subgrade & Vicksburg Clay Test Results ***					NCHRP 35 Page 15 and Table 5			Values Adopted
	M.C.	CBR	E lbs/sq in.	Ref 66**	E=1420x CBR	M.C.	CBR	E NCHRP 1-11	M.C.	Stress	Strain	E Vicksburg	E AASHO	M.C.	Coffman et al psi	Seed et al psi	E lbs/sq in.
1	2	3	4	5	6	7	8	9	10	11	12	13	14	15	16	17	18
Jan.	15.0*	3.7*	4700	5500	5300	15.9	2.8	4000						13.5	6200	13000	6600
Feb.	15.0*	3.7*	4700		5300	16.2	2.6	3700	14.0	80	.01	8000	6400				6600
March	15.0*	3.7*	4700		5300				15.1	80	.0125	6400	5000	15	4900	8000	6600
April	16.9	2.0	3000	1300	2840	14.8	3.7	4700	16.7	80	.042	1900	1500	16	4500	6600	3600
May	16.5	2.4	3500		3400	14.5	3.8	4800	17.2	80	.05	1200	1000				4300
June	16.1	2.8	4000		4000												4900
July	15.8	3.1	4100		4400	16.1	1.5	2500									5400
Aug.	15.5	3.3	4300		4700	13.4	4.5	5200									5800
Sep.	15.3	3.4	4400		4800									Nijboer & Metcraft give values:			6100
Oct.	15.2	3.5	4500		5000	12.7	7.2	7500									6200
Nov.	15.1	3.6	4600		5100												6400
Dec.	15.0*	3.7*	4700		5300									After frost = 8500 psi			6600
														Before frost = 21000 psi			

* Assumed values

** Values do not correspond to any particular month

*** For the same strain AASHO soil required about 80 percent stress of Vicksburg clay

Reference AASHO Subgrade Test results page 616 of First Conference on Structural Design of Asphalt Pavement, at M.C. of 15.3 the value of E varied from 3000 to 12000 psi.

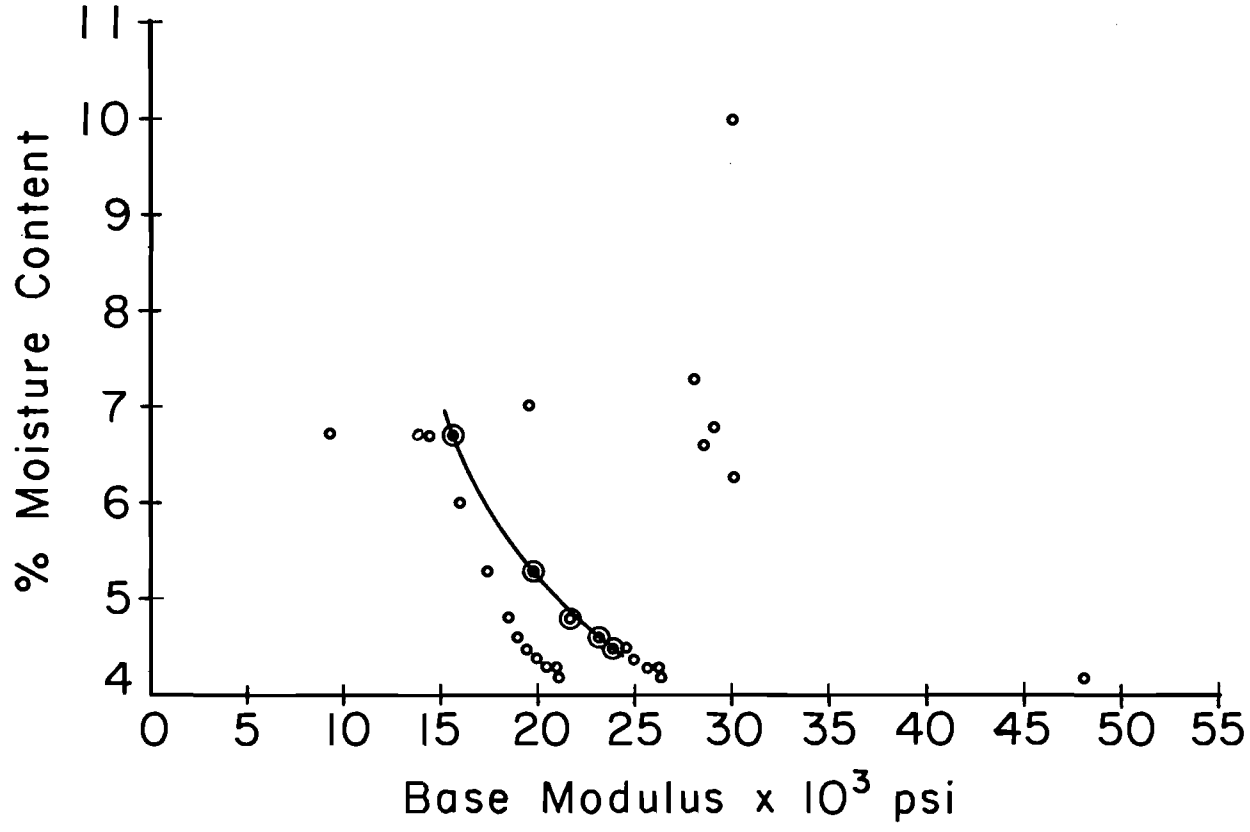

Fig A2.2. Base modulus versus moisture content.

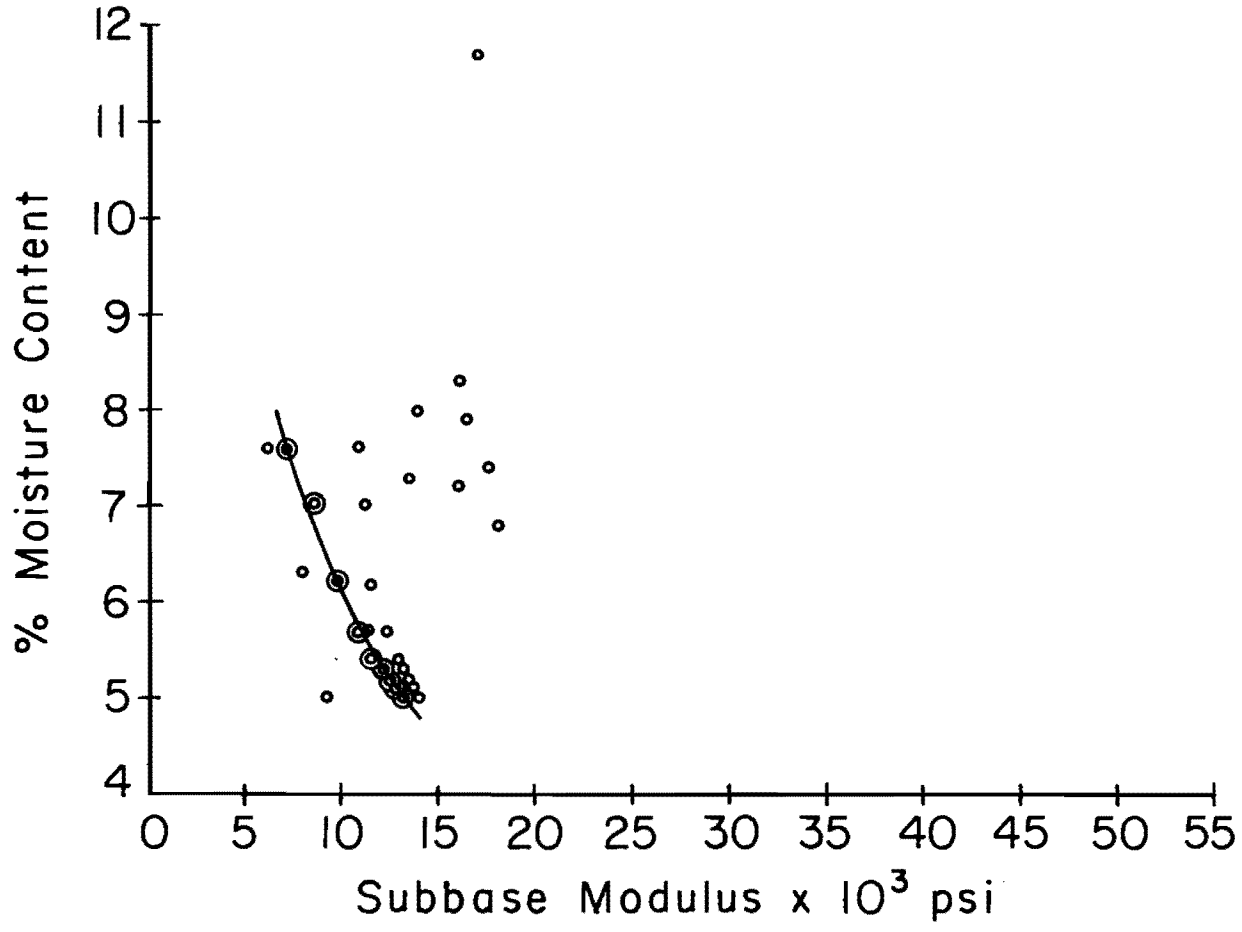

Fig A2.3. Subbase modulus versus moisture content.

TABLE A2.10. VARIATION IN THE STIFFNESS VALUES OF ASPHALT CONCRETE
(Ref Table 2, NCHRP-39 pp 12)

Stiffness Modulus E lbs/sq in. x 10^5	Std Deviation E_{sd} lbs/sq in. x 10^5	Coefficient of Variation % 1/2	Number of Samples	Product 3 x 4	Remarks
6.80	1.53	22.5	19	427.5	
7.03	1.91	27.2	20	544.0	
7.12	1.41	19.8	20	396.0	
5.90	1.11	18.8	19	357.2	
1.79	0.42	23.4	19	444.6	
1.65	0.39	23.6	20	472.0	
1.52	0.41	27.0	20	540.0	
1.34	0.37	27.6	19	524.4	
5.95	1.54	25.9	12	310.8	
4.40	0.90	20.4	8	163.2	
4.96	1.22	24.6	10	246.0	
1.57	0.42	26.8	12	321.6	Avg. Coeff. of variation $\frac{5490}{228}=24.0$
1.39	0.26	18.7	12	224.4	
1.47	0.41	27.8	8	222.4	
1.42	0.42	29.6	10	296.0	
		Total	228	5490.1	

TABLE A2.11. VARIATION IN THE STIFFNESS MEASUREMENTS ON PAVEMENT SAMPLES (Ref Page 136 2nd International Conference on Structural Design of Asphalt Pavements)

Location	No. of Specimens	Measured Stiffness, psi x 10^5						Mean Coefficient of Variation %
		68° F			40° F			
		Mean	Standard Deviation	Coefficient of Variation %	Mean	Standard Deviation	Coefficient of Variation %	
Surface Course	20	1.52	0.41	27.0	7.12	1.41	20.0	23.5
Base Course	8	1.47	0.41	28.0	4.40	0.90	20.0	24.0

AASHO Road Test Report 5 (Ref 70), in Figs 96 and 97, gives the moisture content and CBR value, of the AASHO Road Test pavement subgrade for various months. This information is entered in Columns 1 to 3 of Table A2.9. Based on NCHRP Report 1-11 (Ref 117) Column 4 contains the estimated value of resilient modulus. Special Report 66 (Ref 66) contains the test results of the AASHO Road Test material. The reported values of resilient modulus vary from 1,300 psi to 5,500 psi. The test results in this report also show the CBR values for various moisture contents. These values of CBR with corresponding estimated values (based on NCHRP Report 1-11) of resilient modulus are shown in Column 9. Heukelom and Klomp (Ref 60) have given an approximate relation between CBR and resilient modulus. An evaluation of modulus values based on this criterion is entered in Column 6. In Highway Research Board proceedings Vol 34, Chan and Seed have reported the stress-strain test results on AASHO subgrade and Vicksburg clay at various moisture contents. From these test results it was observed that for the same strain AASHO subgrade clay needed about 80 percent stress in comparison to the Vicksburg clay. Based on this information estimated values of resilient modulus of AASHO subgrade soil are given in Column 14. NCHRP Report 35 (Ref 165) also contains some test results on the AASHO Road Test subgrade soil. These are tabulated in Columns 15 to 17. Fluctuations in resilient modulus values based on different criteria are apparent from Table A2.9. However, based on such information a decision on values to be adopted for design purposes is not difficult, at least for an experienced designer. Based on averaging out the available information the values adopted for the present analysis are obtained from Fig A2.4 and tabulated in Column 18 of Table A2.9.

Stochastic Variations in Elastic Modulus. Direct observations are not available to estimate the expected variations in the elastic modulus values of the subgrade, subbase, base materials, and surface asphalt concrete used in the AASHO Road Test. However, some indirect information was utilized to determine the expected statistical variations in the elastic modulus of the AASHO Road Test materials.

Asphalt Concrete. In NCHRP Report 39 (Ref 42), some test data are available for various field specimens. These are shown in Table A2.10. A weighted mean calculation of the test results of the specimens shows a coefficient of variation of about 24 percent. Table A2.11 is an extract of

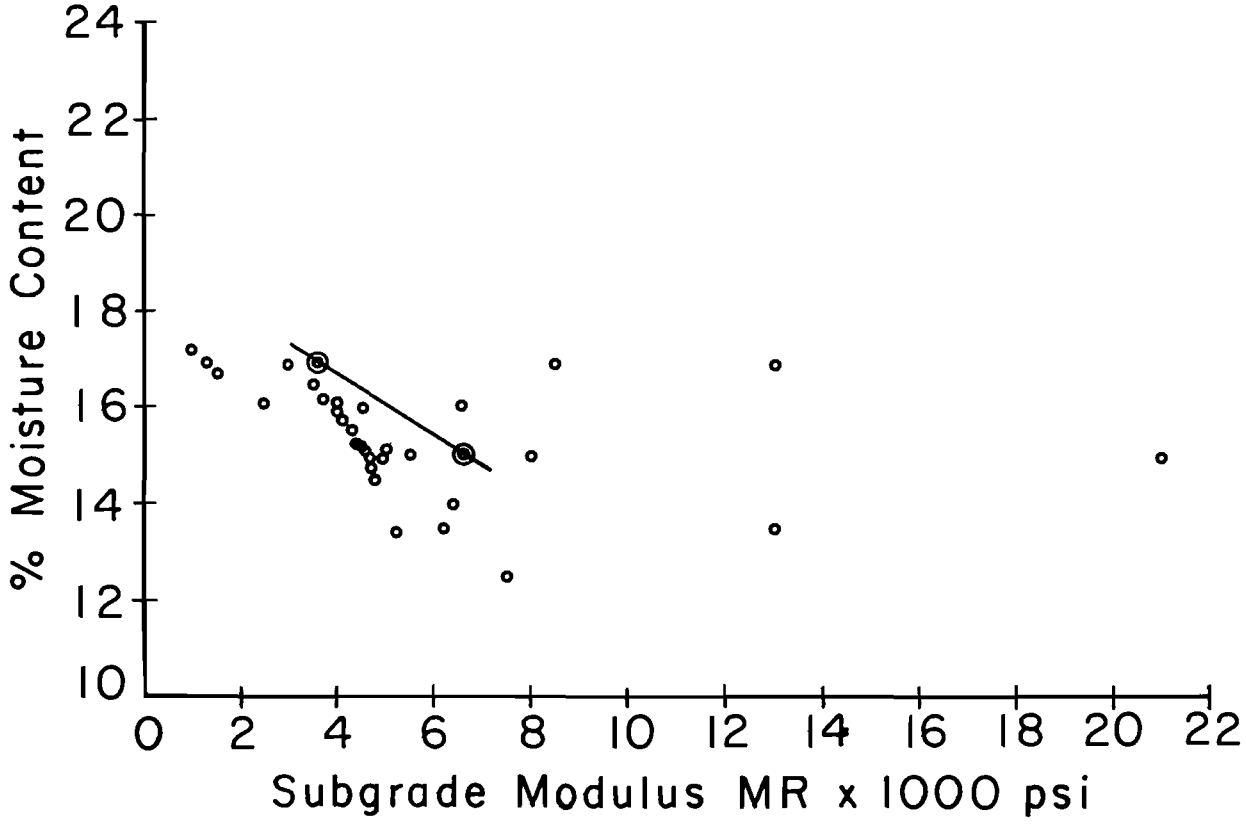

Fig A2.4. Subgrade modulus versus moisture content.

stiffness measurements of some pavement samples taken from page 136 of the Proceedings of the Second International Conference on Structural Design of Asphalt Pavements. This table gives an approximate value of coefficient of variation as 24 percent of the mean value. Table A2.12 shows the observed variations in the test results of the "stability test" performed on some asphalt concrete sample and reported in Public Roads, August 1969. The coefficient of variation in these test results varied from 12.2 to 23 percent. Based on this information, a value of coefficient of variation of 25 percent is assumed for analysis in this report.

Untreated Granular Base Material. Test results on AASHO Road Test materials for CBR values as reported in Special Report 66 (page 96 of Ref 66) are reproduced below with the statistical calculations made for the coefficient variation (page 40, Statistical Methods, by Snedecor).

Item	Number of Samples	Mean Value	Range	Expected Standard Deviation	Coefficient of Variation, %
CBR	5	100	83 - 140	$57 \times 0.53 = 30$	30

The coefficient of variation is about 30 percent of mean value. The other test results (Ref 66, page 90) show that the coefficient of variation was observed as 3 percent for maximum density and 16 percent for optimum moisture content. The results of 24 tests on the gravel base mixture (Ref 66, page 73) gave an average liquid limit of 18.9 and an average plasticity index of 3.1 with corresponding standard deviations of 2.1 and 1.9 which will give coefficients of variation of 11 percent and 60 percent, respectively. While other test results may not give a direct value of statistical variations expected in resilient modulus, the CBR has a direct correlation with this parameter. A 30 percent coefficient of variation calculated above for CBR may also be expected for the resilient modulus. However, this information is based on five samples and can only be treated as approximate. For the analysis in this report, a value of 25 percent for the coefficient of variation was adopted.

TABLE A2.12. HOT MIX MARSHALL TEST DATA "VARIATION IN STABILITY TEST VALUES"
(Ref "Public Roads" August 1969)

Test	Project Nos.	States Nos.	Average Standard Deviation	Average Mean	Coefficient of Variation %
Marshall Stability lbs	18	4	283.00	2305.00	12.2
Marshall Flow 100/in	15	2	1.29	8.62	15.0
Marshall Air Voids Pct	18	4	1.00	4.33	23.0

Untreated Granular Subbase. The results of the CBR test in Special Report 66, Ref 66) are given below.

Item	Number of Samples	Mean Value	Range	Expected Standard Deviation	Coefficient of Variation, %
CBR	5	58	32 - 86	54 x 0.53 = 29	50

The Computed Coefficient of Variation for the CBR value from the above test results is 50 percent.

Also, Fig 60 of AASHO Road Test Report 2 (Ref 67) gives the results of CBR determinations on 80 test samples. This shows a mean value as 34.7 and standard deviation 9.3. The coefficient of variation works out as 26.8 percent. Page 90 of Special Report 66 (Ref 66) gives the coefficient of variation in the measurement of maximum density as 2.5 percent, while in optimum moisture content it was 13 percent. Thus, based on the above results, the subbase coefficient of variation is expected to be of the same order as for the base material. Therefore, for analysis in this report, a 25 percent value for the coefficient of variation for the AASHO Road Test Subbase is adopted.

Fine Grained Subgrade. The data for CBR are given below, according to page 96 of Special Report 66.

Item	Number of Samples	Mean Value	Range	Expected Standard Deviation	Coefficient of Variation, %
CBR	8	5.0	4 - 6.7	.351 x 2.7 = 1.0	20

Figure 49 of AASHO Road Test Report 2 (Ref 67) gives the CBR determination of 80 test samples. The test shows a mean value of CBR as 2.9 and its standard deviation as 1.28. The coefficient of variation on this basis works out as 44 percent of the mean value. Page 90 of Ref 66 gives the coefficient of variation for optimum moisture content as 7.4 percent and for maximum density as 1.8 percent. Page 32 of AASHO Road Test Report 2 (Ref 67) shows statistical variations found for the Atterbergs limit test results, as follows:

Test	Coefficient of Variation, %
Liquid limit	19.5
Plastic limit	11.5
Plasticity index	31.0
Optimum moisture content	14.2
Maximum dry density	2.5

Based on the above test results it is seen that the average statistical variations in the test results of the subgrade are expected to be about the same order as for the base and subbase. Therefore, for the analysis in this report, a value of 25 percent for coefficient of variation is adopted.

TABLE A2.13. VARIABLES AFFECTING MATERIAL RESPONSE

I. Loading variables
- A. Stress history (nature of prior loading)
  - 1. Non-repetitive loading (such as preconsolidation)
  - 2. Repetitive loading
    - a. Nature
      - (1) Simple
      - (2) Compound
    - b. Number of repetitive applications
- B. Initial stress state (magnitude and direction of normal and shear stresses)
- C. Incremental loading
  - 1. Mode of loading
    - a. Controlled stress (or load)
    - b. Controlled strain (or deformation)
    - c. Intermediate modes
  - 2. Intensity (magnitude and direction of incremental normal and shear stresses)
  - 3. Stress path (relation among stresses - both normal and shear - as test progresses)
  - 4. Time path
    - a. Static
      - (1) Constant rate of stress (or load)
      - (2) Constant rate of strain (or deformation)
      - (3) Creep
      - (4) Relaxation
    - b. Dynamic
      - (1) Impact
      - (2) Resonance
      - (3) Other
        - (a) Sinusoidal (rate of loading is variable)
        - (b) Pulsating (duration, frequency, and shape of load curve are variables)
  - 5. Type of behavior observed
    - a. Strength (limiting stresses and strains)
    - b. Deformability
  - 6. Homogeneity of stresses
  - 7. Drainage (drained or undrained)

II. Mixture variables
- A. Mineral particles
  - 1. Maximum and minimum size
  - 2. Gradation
  - 3. Shape
  - 4. Surface texture
  - 5. Angularity
  - 6. Mineralogy
  - 7. Adsorbed ions
  - 8. Quantity

(Continued)

TABLE A2.13. (Continued)

- B. Binder
  - 1. Type
  - 2. Hardness
  - 3. Quantity
- C. Water
  - 1. Quantity
- D. Voids
  - 1. Quantity
  - 2. Size
  - 3. Shape
- E. Construction Process
  - 1. Density
  - 2. Structure
  - 3. Degree of anisotrophy
  - 4. Temperature
- F. Homogeneity

III. Environmental variables
- A. Temperature
- B. Moisture
- C. Alteration of material properties
  - 1. Thixotropy
  - 2. Aging
  - 3. Curing
  - 4. Densification

TABLE A2.14. TEST CONFIGURATIONS

I. Tension
   A. Uniaxial tension
   B. Indirect tension
      1. Splitting tension
      2. Cohesiometer

II. Compression
   A. Unconfined, uniaxial compression
   B. Triaxial compression
      1. Open system
         a. Conventional triaxial compression
            (1) Normal
            (2) Vacuum
            (3) High pressure
         b. Box with cubical specimen
      2. Closed system
         a. Oedometer
         b. Cell
         c. Hveem stabilometer

III. Flexure
   A. System
      1. Revolving bar
      2. Simple flexural
   B. Loading
      1. Cantilever
      2. Simple beam
         a. Point supports
         b. Uniform supports

IV. Direct shear
   A. Direct shear (rigid split box)
   B. Double direct shear
   C. Uniform direct shear (rigid caps with confined rubber membrane and split rings for lateral restraint)
   D. Uniform strain direct-shear (hinged box)
   E. Punching shear

V. Torsion
   A. Pure torsion
   B. Triaxial torsion
   C. Specimen shape
      1. Solid cylinder
      2. Thick-walled, hollow cylinder

TABLE A2.15. SPECIMEN SHAPE

I. Rectangular parallelepiped
   A. Short
   B. Long
   C. Cubic

II. Cylinder
   A. Solid
      1. Short
      2. Long
   B. Thick-walled, hollow
      1. Short
      2. Long

III. Plate

IV. Other

TABLE A2.16. SUMMARY OF CHARACTERISTICS OF RESEARCH MATERIALS

Designation	Description	Gradation	Compaction Characteristics*		Actual Unit Weight, D_A 100% Compaction Ratio pcf	Texas Triaxial Test			
			Optimum Moisture %	Maximum Unit Weight pcf		Average Moisture After Capillarity %	Failure Stress At Indicated Lateral Pressure, psi		Triaxial Class
							0 psi	15 psi	
HP-27-8	Rounded	Fine	7.3	133.9	-----	7.4	18.1	147.7	3.0
		Medium	6.8	135.4	133.8	7.0	23.8	158.7	2.8
		Coarse	6.7	135.2	-----	7.3	23.2	161.9	2.7
HP-27-9	Angular	Fine	7.3	133.9	-----	7.0	42.1	223.2	1**
		Medium	7.0	136.0	136.0	6.8	62.1	246.9	1***
		Coarse	6.8	137.7	-----	5.9	57.7	270.7	1****
HP-27-10	Soft	Fine	11.9	124.2	-----	11.5	28.8	169.5	2.5
		Medium	11.9	124.2	124.3	11.6	52.0	167.8	2.1
		Coarse	11.9	124.2	-----	11.3	48.2	175.4	2.1

* Compactive effort = 13.26 ft lbs per cu in.
** Lowest classification of HP-27-9
*** Medium classification of HP-27-9
**** Highest classification of HP-27-9

(Continued)

TABLE A2.16. (Continued)

Designation	Description	Gradation	Plasticity: Liquid Limit Liquid Class	Plasticity: Plasticity Index	Plasticity: Linear Shrinkage	Los Angeles Abrasion ("A" Grading): 100 rev.	Los Angeles Abrasion ("A" Grading): 500 rev.	Texas Wet Ball Mill	Classification: Texas	Classification: Unified	Specific Gravity	Permeability ft/day
HP-27-8	Rounded	Fine	21.3	7.4	5.6	7.2	27.3	37.2	Type B, Grade 3	GMd	2.64	-----
		Medium						36.2	Type B, Grade 3	GMd	2.63	0.006
		Coarse						32.0	Type B, Grade 3	GMd	2.65	-----
HP-27-9	Angular	Fine	17.8	2.3	2.4	6.8	25.3	39.0	Type A, Grade 2	GMu	2.64	-----
		Medium						36.1	Type A, Grade 1	GMu	2.63	0.003
		Coarse						33.5	Type A, Grade 1	GMu	2.64	-----
HP-27-10	Soft	Fine	20.2	4.8	2.7	19.0	57.9	50.3	Type A, Grade 2	GMu	2.67	-----
		Medium						47.8	Type A, Grade 2	GMu	2.67	0.002
		Coarse						48.1	Type A, Grade 2	GMu	2.67	-----

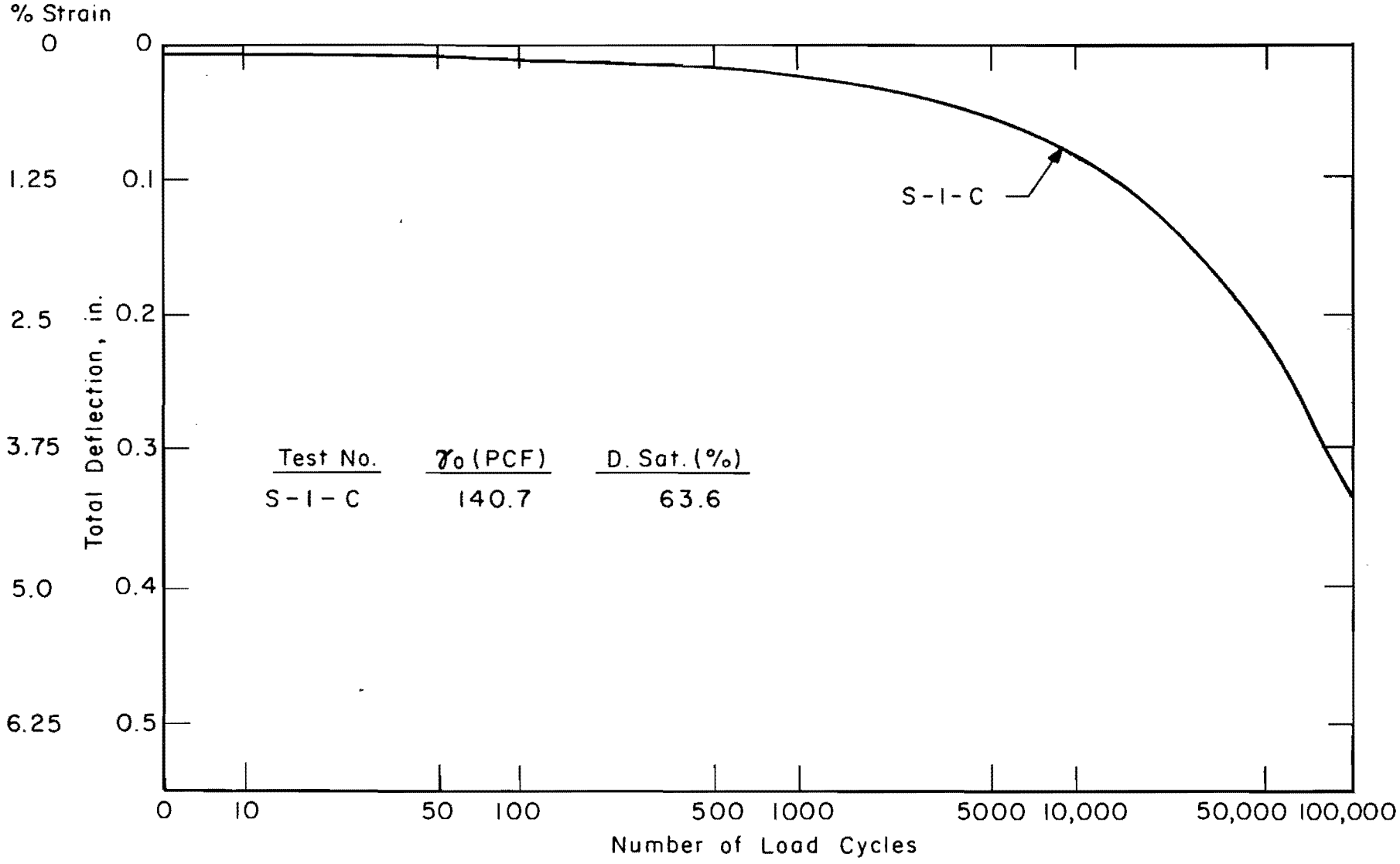

Fig A2.5. Deflection history of crushed stone specimens 11.5 percent passing No. 200 sieve (after Ref 57).

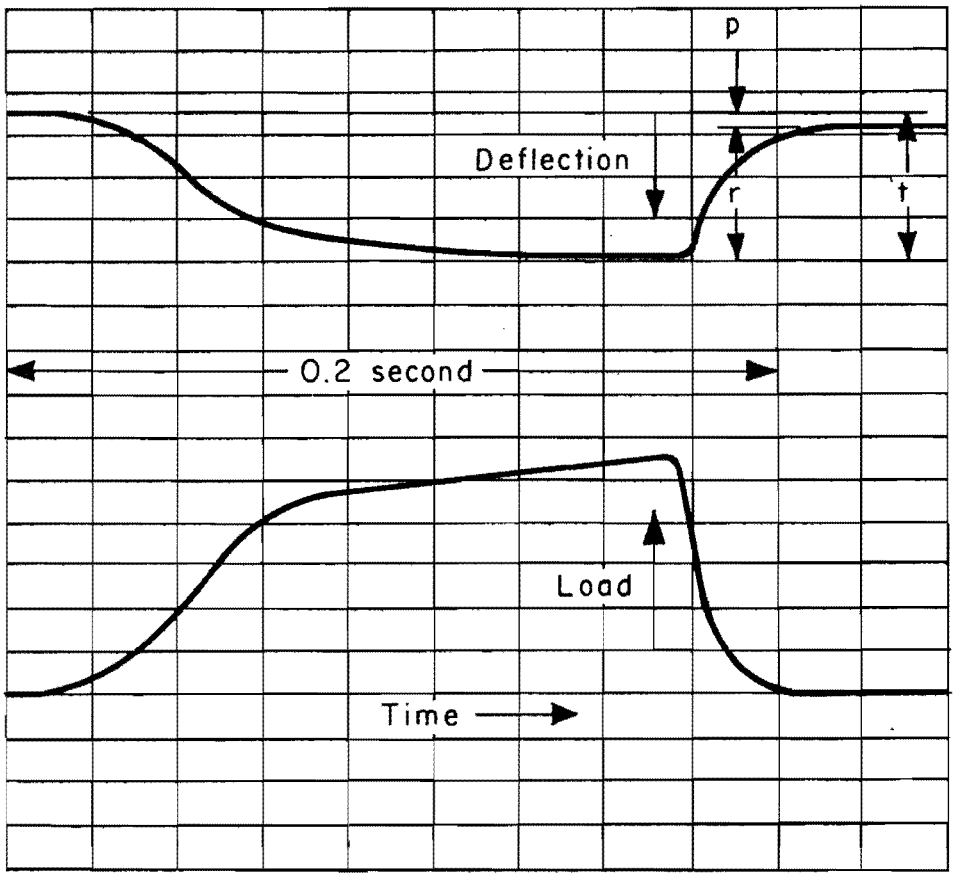

Fig A2.6. A typical load-deformation oscillograph (A&M material) (after Ref 35).

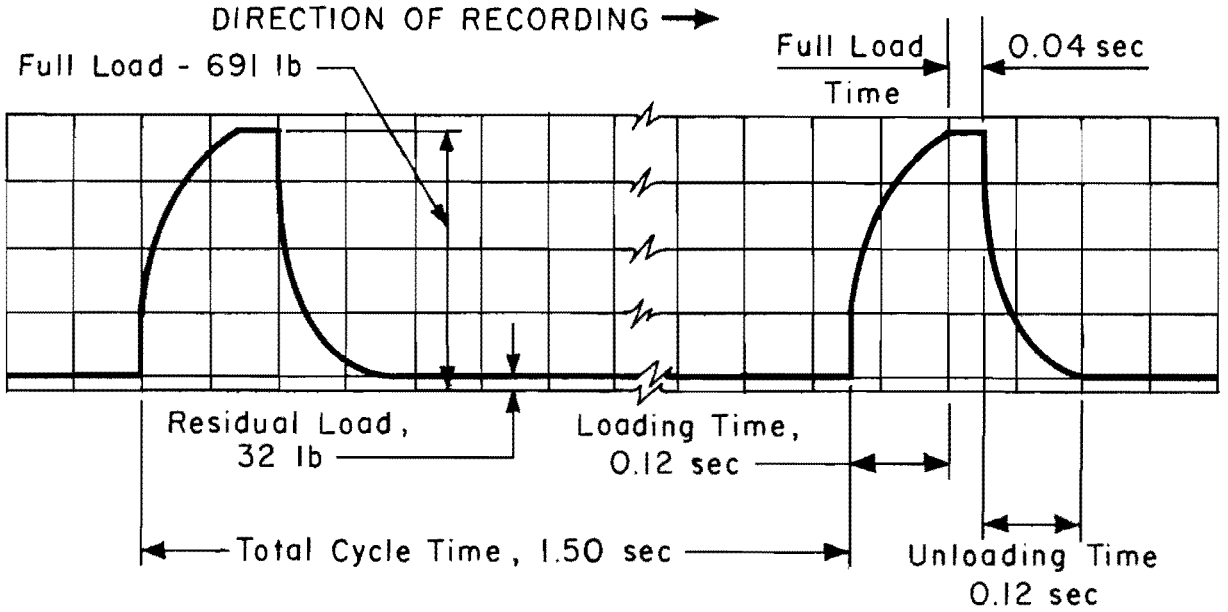

Fig A2.7. Typical load-time trace for two load cycles (AASHO material) (after Ref 57).

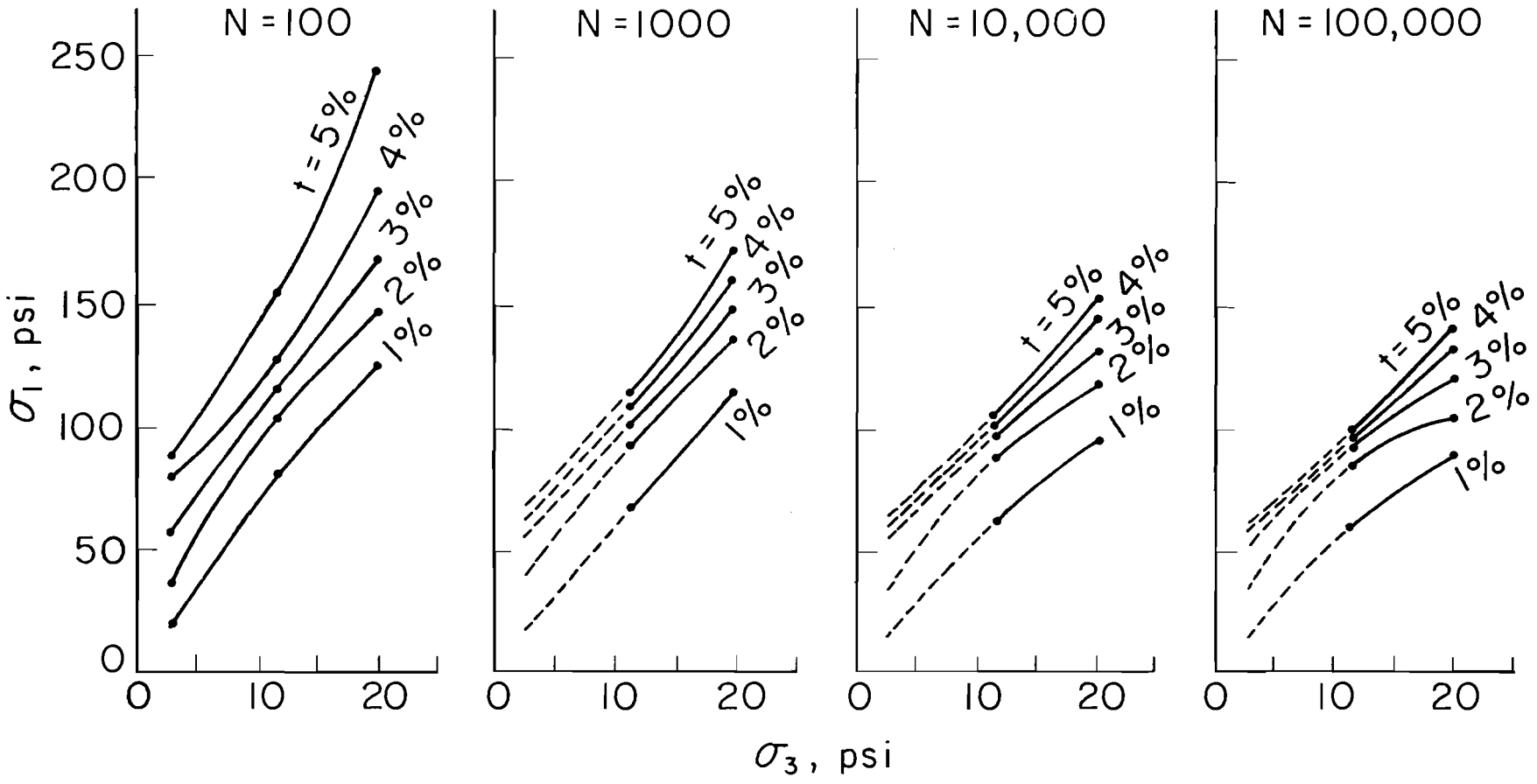

Fig A2.8. Angular medium aggregate similar to AASHO base material (after Ref 35).

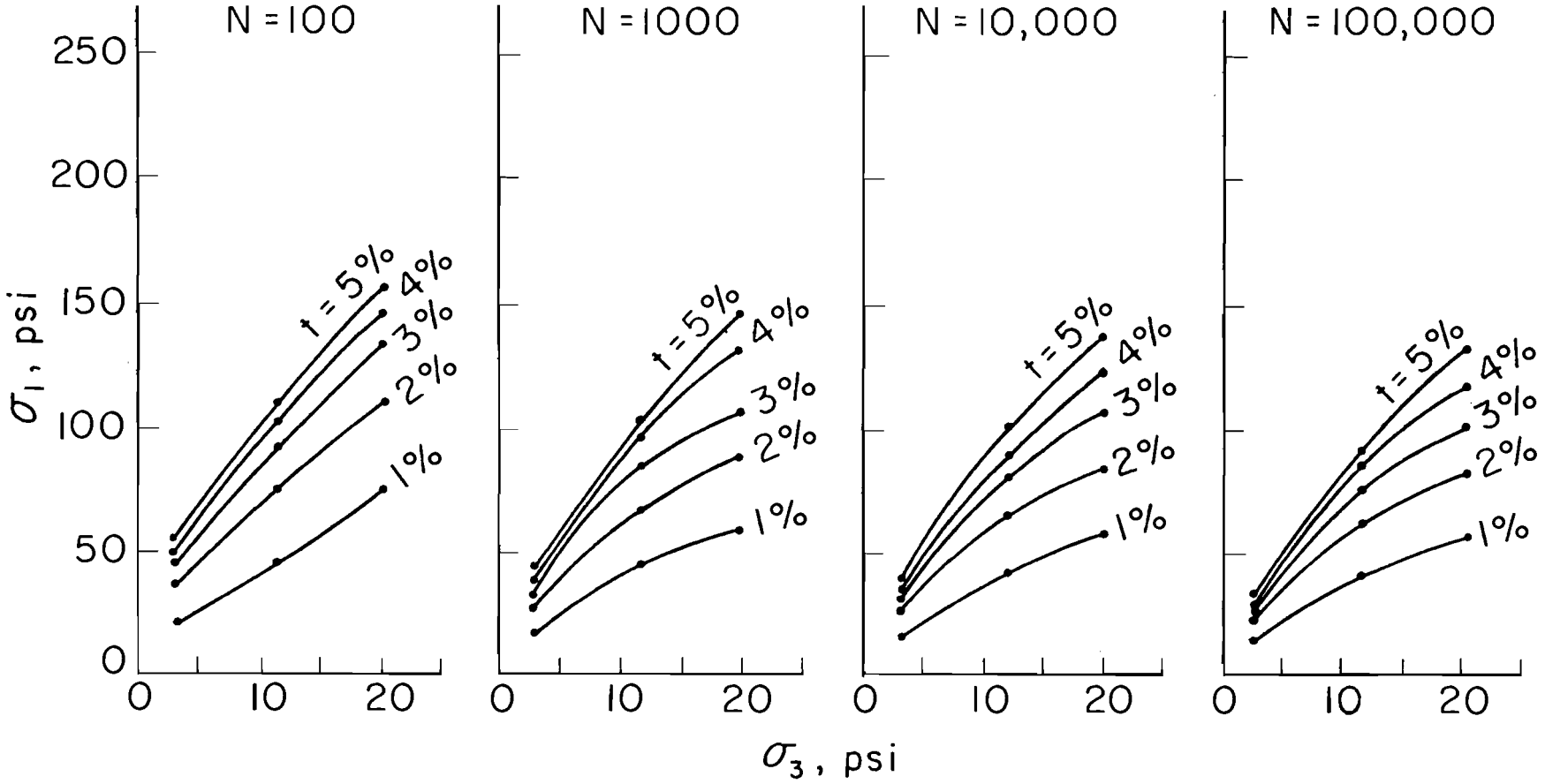

Fig A2.9. Rounded fine aggregate similar to AASHO subbase material (after Ref 35).

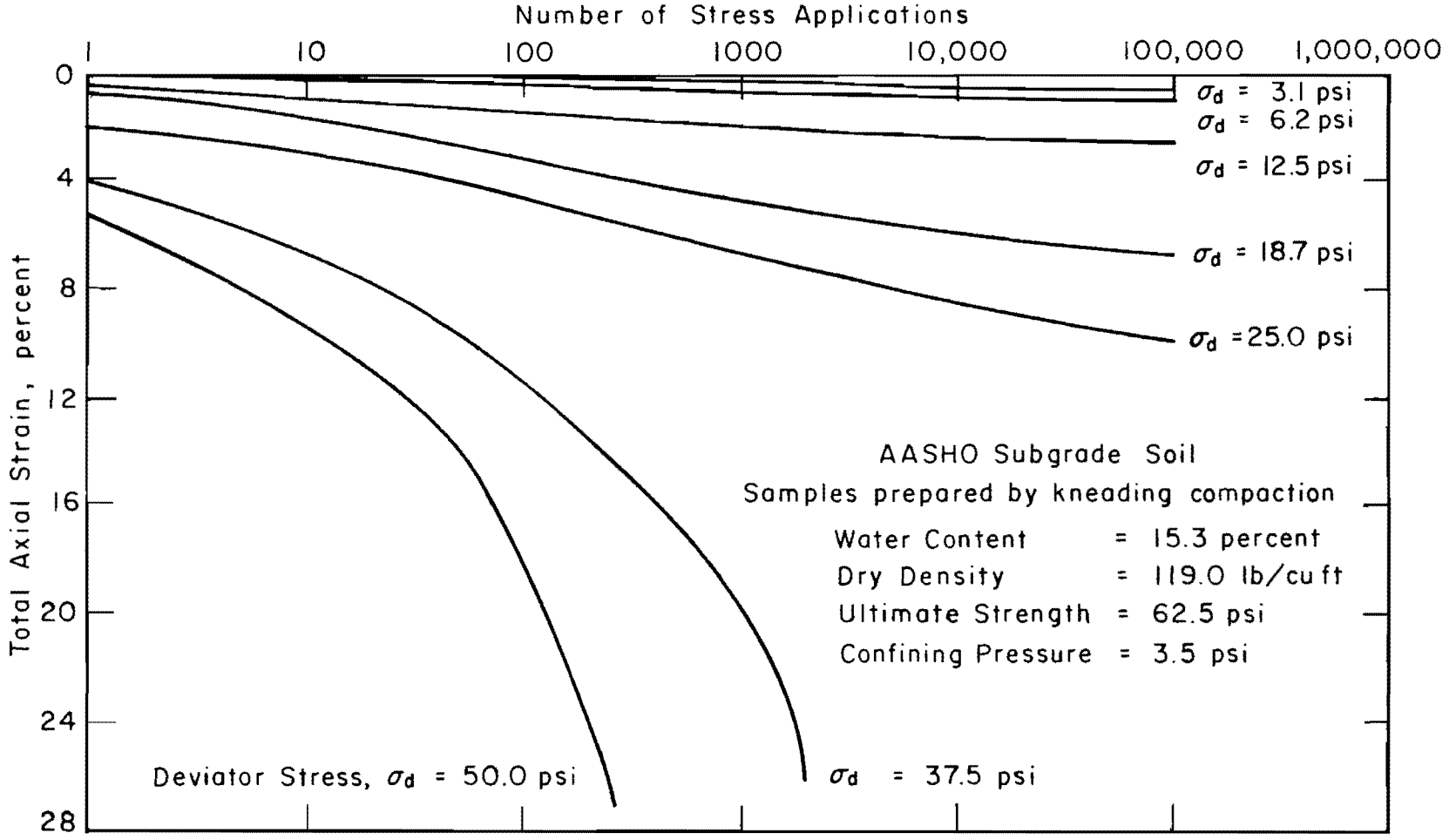

Fig A2.10. Deformation characteristics - AASHO Road Test subgrade soil (after Ref 165).

APPENDIX 3

OUTLINE OF COMPUTER PROGRAM AVAILABLE FOR ANALYSIS OF STRESSES, STRAINS, AND DISPLACEMENTS IN A FIVE-LAYERED ELASTIC SYSTEM UNDER A LOAD UNIFORMLY DISTRIBUTED ON A CIRCULAR AREA

APPENDIX 3. OUTLINE OF COMPUTER PROGRAM AVAILABLE FOR ANALYSIS OF STRESSES, STRAINS, AND DISPLACEMENTS IN A FIVE-LAYERED ELASTIC SYSTEM UNDER A LOAD UNIFORMLY DISTRIBUTED ON A CIRCULAR AREA

This program was developed by H. Warren and W. L. Dieckmann of California Research Corporation, Richmond, California, in 1963 and is based on the solution which was used by Mr. J. Michelow (California Research Corporation) in his analysis of multi-layered asphalt pavement system. The following is the outline of the computer program (after Ref 167).

Introduction

A. The program computes the following items numerically at any point in the layered system for a given load on a circular area of the free surface:

   1. vertical, tangential, radial, shear, and bulk stress;
   2. vertical displacement;
   3. radial, tangential, and shear strain.

   Note that a cylindrical system of coordinates is used.

B. The following input data should be provided:

   1. the wheel load (total load);
   2. tire pressure;
   3. load radius (= total load/$\pi \times$ tire pressure);
   4. for each layer, layer number, modulus of elasticity, Poisson's ratio, and thickness.

Description of the Layered System

The system consists of (5) layers of different homogeneous, ideally elastic materials. Each layer is of uniform thickness and infinite dimensions in all horizontal directions, stratified vertically over the semi-infinite bottom layer. Figure A3.1 shows complete details of the system.

Limitations

A. There are no body forces or couples present and inertia forces are neglected.

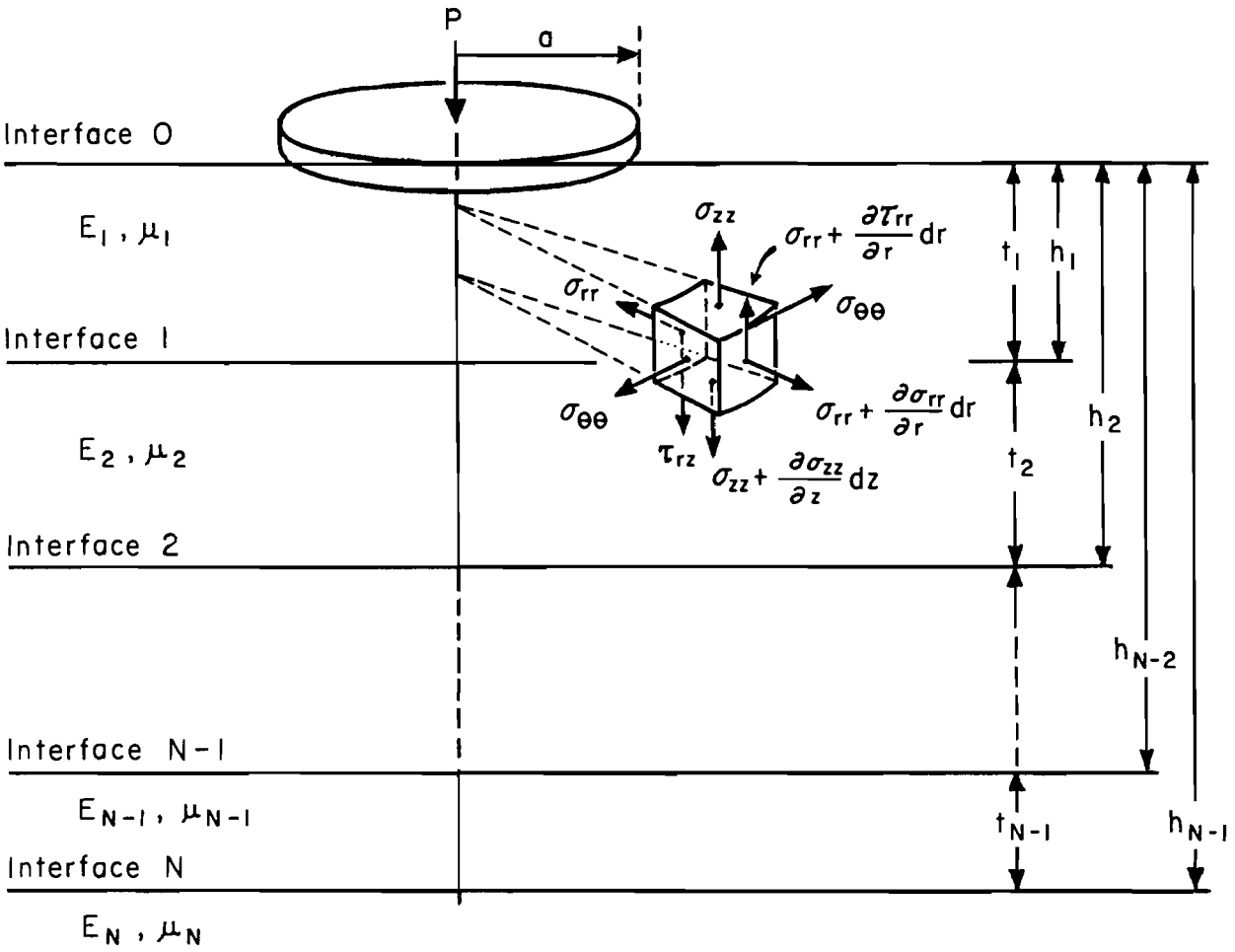

Fig A3.1. Stresses in a multi-layer system.

B. Stresses and strains small enough to be described in an infinitesimal elastic theory.

C. The load is uniformly distributed over a circular area.

D. The system is axisymmetric (z is axis of symmetry), which requires that each layer is uniform, homogeneous, and isotropic.

Summary of the Mathematical Model

For a cylindrical system of coordinates, the components of stress are:

σ_z = vertical stress

σ_r = radial stress

σ_θ = tangential stress

τ_{zr} , $\tau_{r\theta}$, $\tau_{z\theta}$ = shear stresses.

and the components of displacement are:

u = the radial displacement

v = the tangential displacement, and

w = the vertical displacement.

Because of the symmetry of the system under consideration (z axis is an axis of symmetry):

$$\tau_{r\theta} = \tau_{z\theta} = v = 0$$

Satisfying equilibrium and compatibility conditions and solving for the stresses, strains, and displacements, one finds that with each layer there are four unknowns (A, B, C, and D).

In total there are 4N unknowns to be solved from 4N boundary conditions.

Boundary Conditions

A. The assumption that adjacent layers are bonded and no slip occurs at the interfaces (rough interface) gives (4N-4) boundary conditions, i.e.;

1. $\underset{i}{\overset{i}{\sigma}}_z = \underset{i}{\overset{i+1}{\sigma}}_z$

2. $\underset{i}{\overset{i}{w}} = \underset{i}{\overset{i+1}{w}}$

3. $\underset{i}{\overset{i}{\tau}}_{rz} = \underset{i}{\overset{i+1}{\tau}}_{rz}$

4. $\underset{i}{\overset{i}{u}} = \underset{i}{\overset{i+1}{u}}$

Super- and sub-prefixes refer to the layer number and the interface number in the system, respectively.

B. The load situation at the surface gives two boundary conditions:

1. $\sigma_z = -p \quad 0 \leq r < a \,, \quad z = 0$

2. $\tau_{rz} = 0 \quad 0 \leq r < \infty \,, \quad z = 0$

C. The two last boundary conditions result from the requirement that the stresses, strains, and displacements are finite at infinite depth. This will lead to the fact that two of the unknowns of the bottom layers are zero.

1. $A_N = 0$

2. $B_N = 0$

At this point one has 4N unknowns and 4N boundary conditions.

APPENDIX 4

COMPUTER PROGRAM AND ANALYSIS

APPENDIX 4.1

FLOW CHART

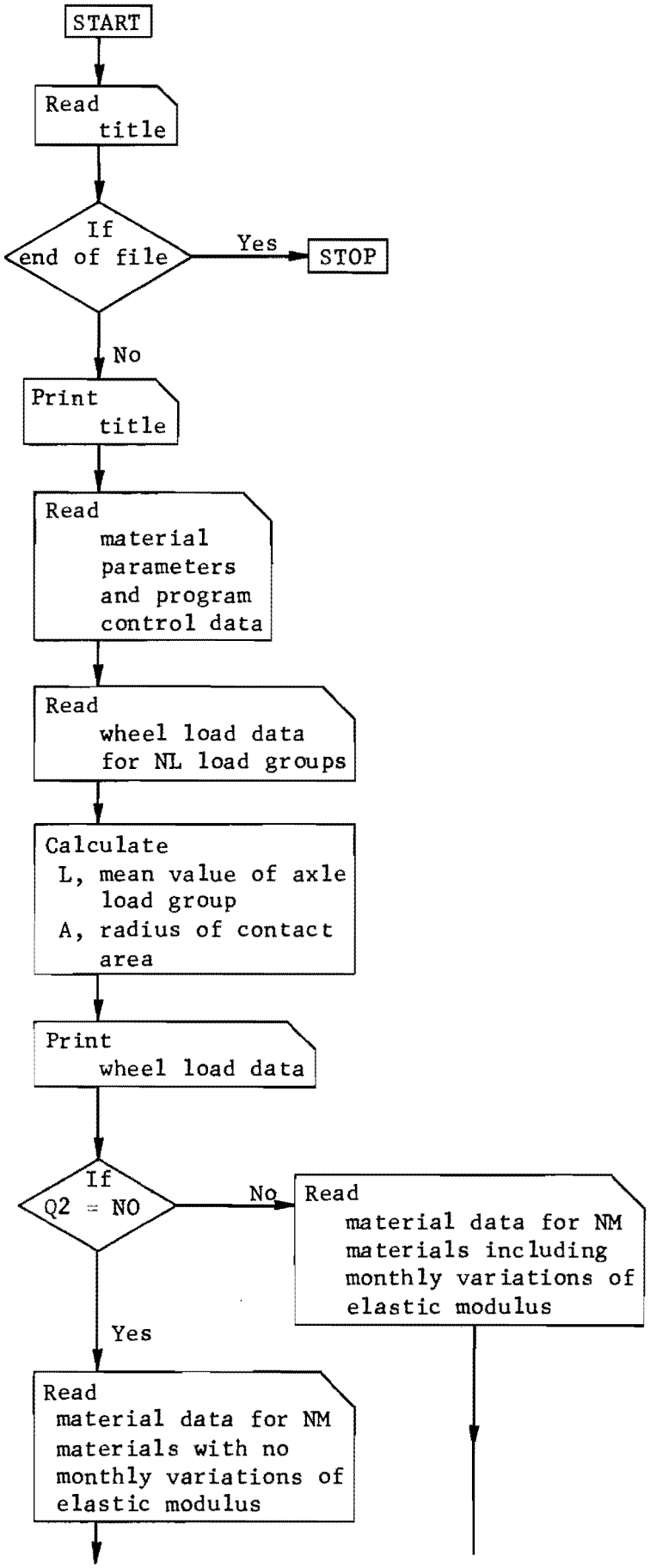

Fig A4.1. Flow chart.

(Continued)

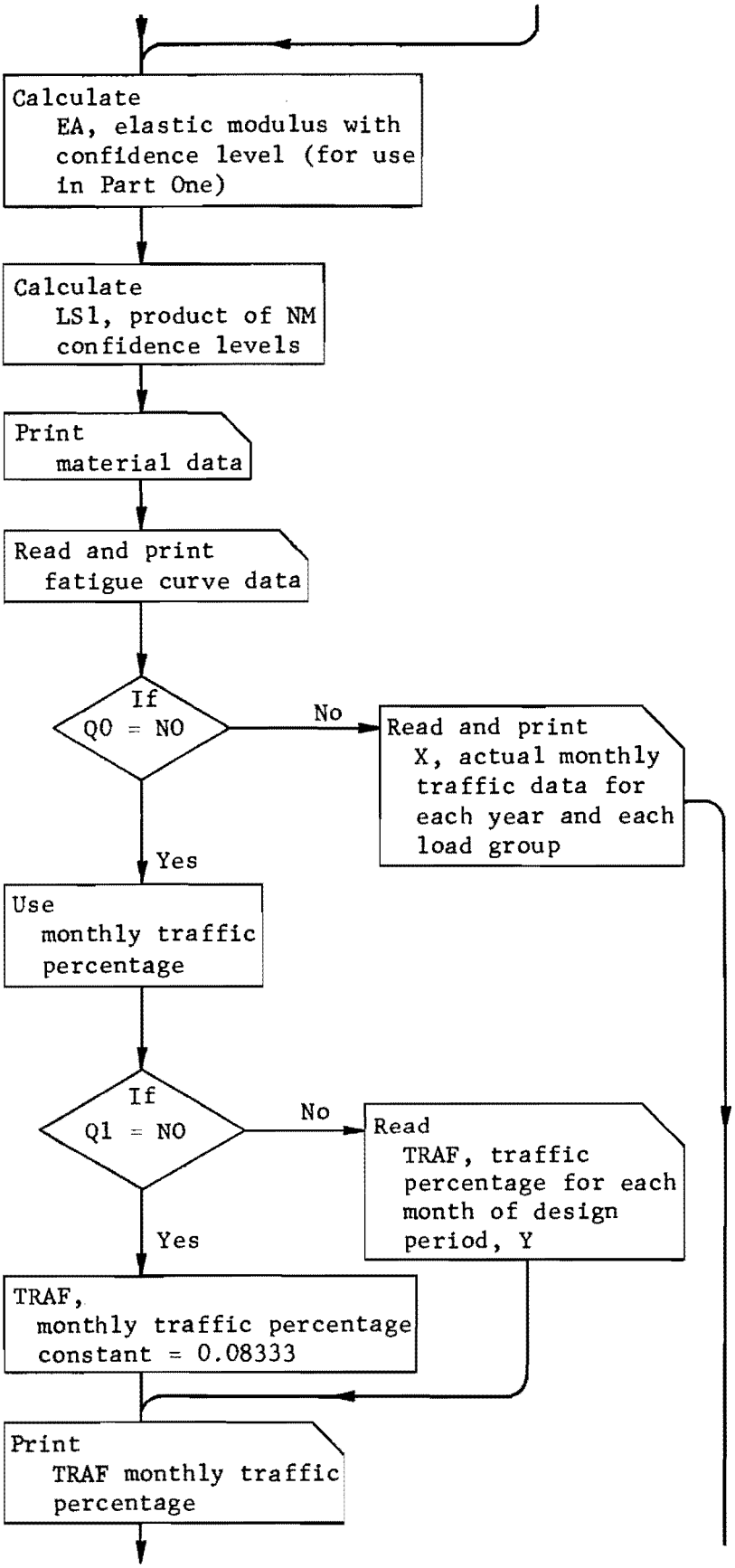

Fig A4.1. (Continued)

(Continued)

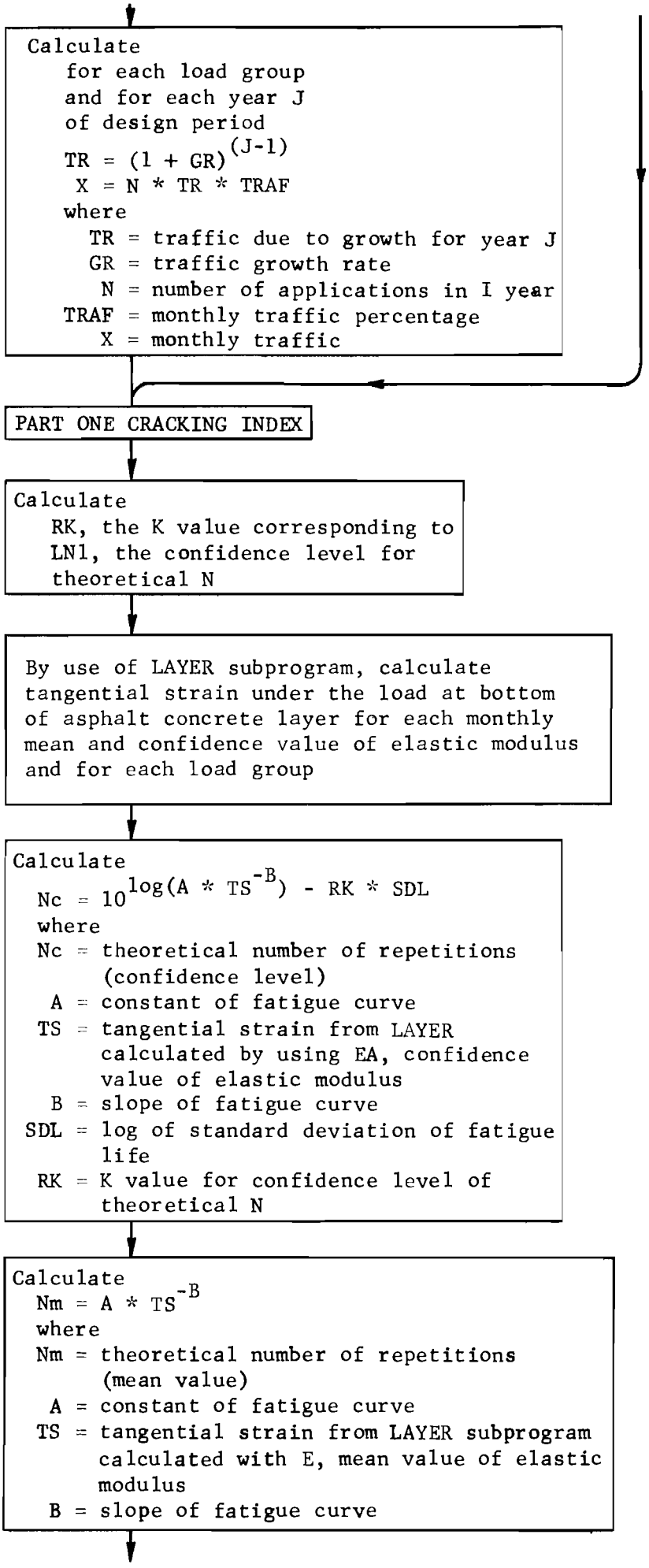

Fig A4.1. (Continued)

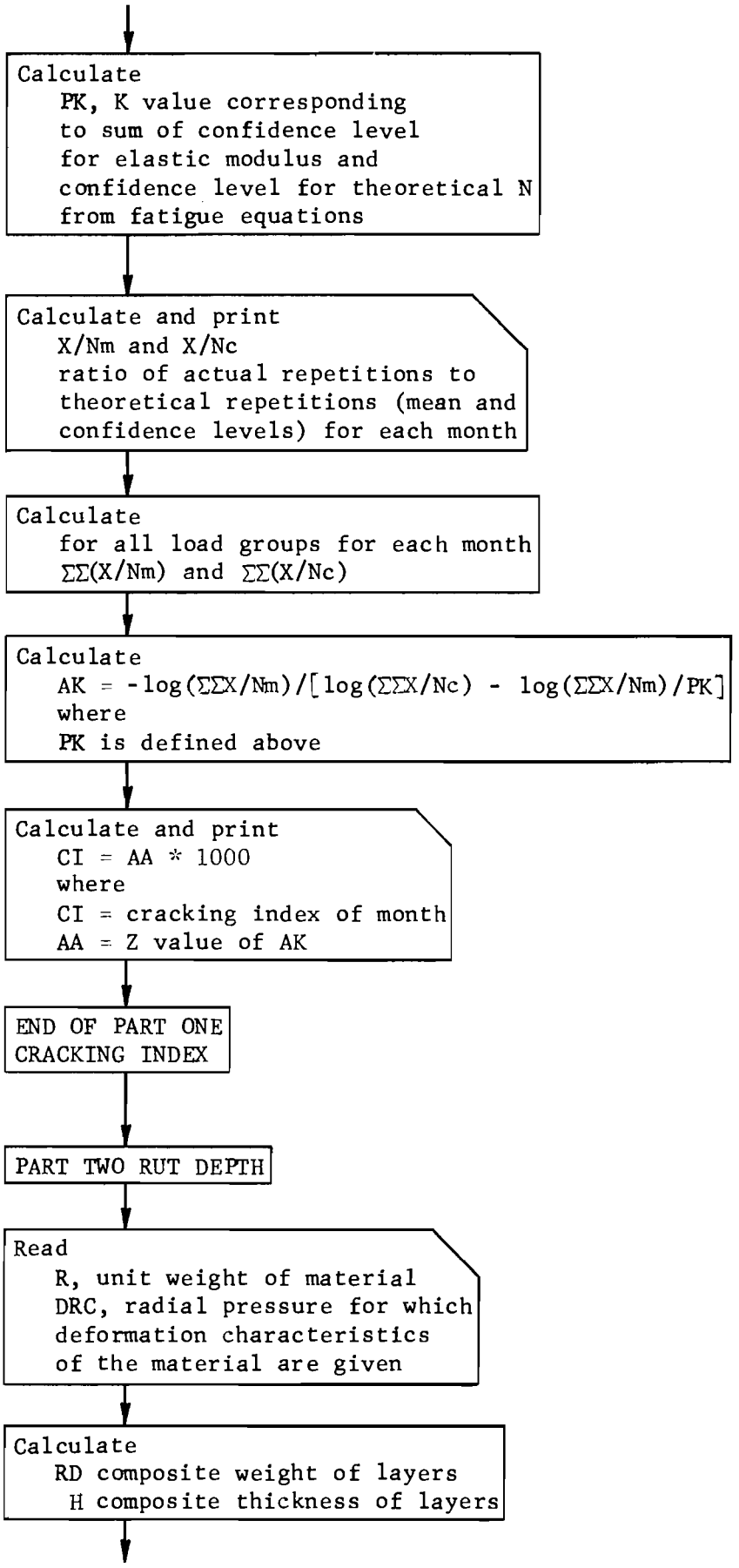

Fig A4.1. (Continued)

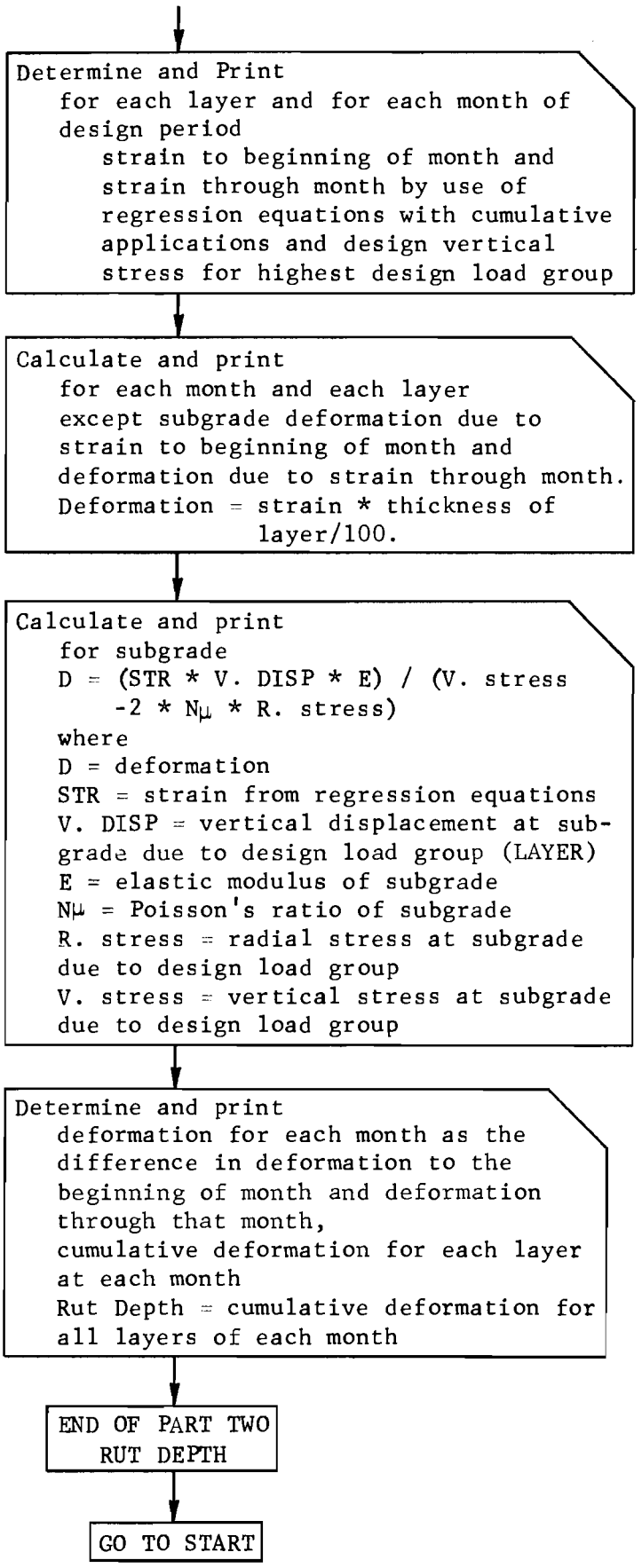

Fig A4.1. (Continued)

(Continued)

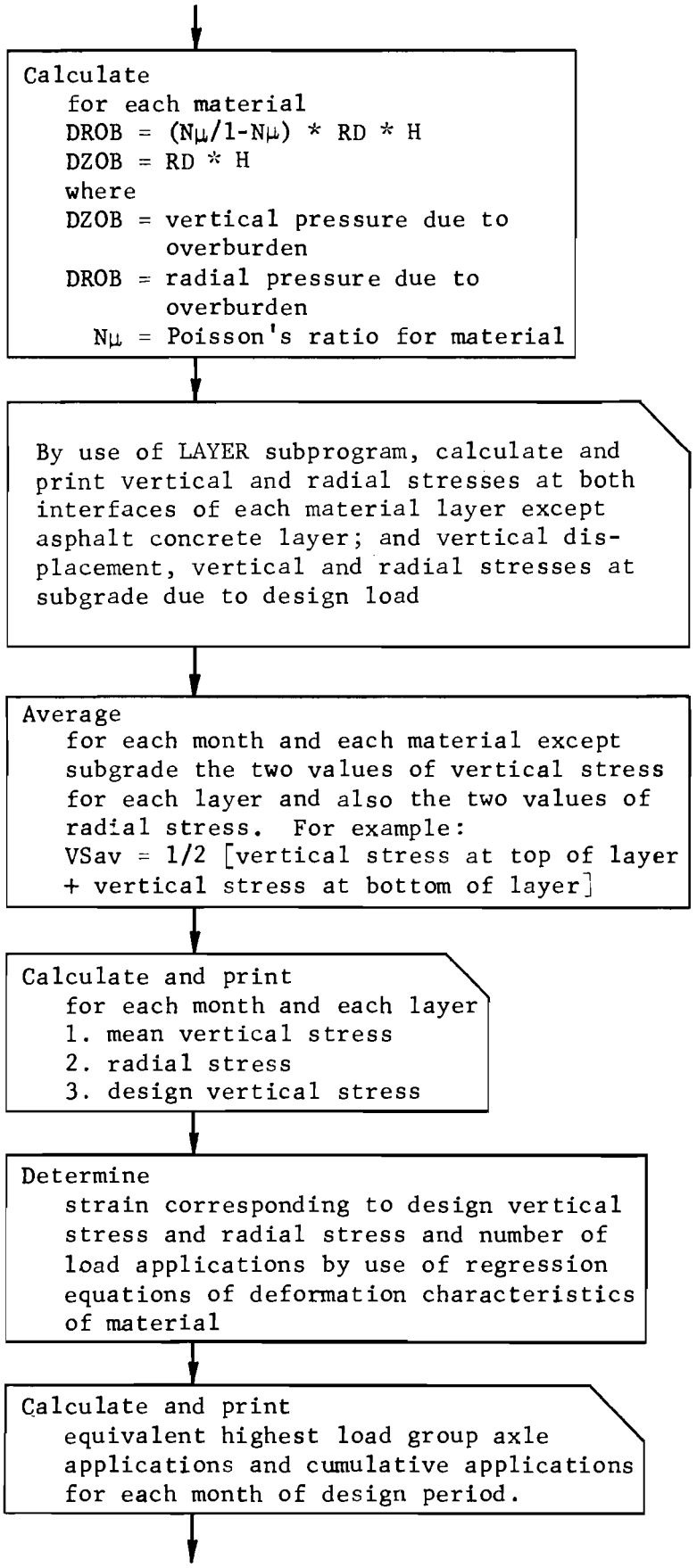

Fig A4.1. (Continued)

APPENDIX 4.2

LISTING OF COMPUTER PROGRAM FOR CRACKING INDEX AND RUT DEPTH INDEX

```
      PROGRAM CRKDEX(INPUT, OUTPUT, TAPE5=INPUT, TAPE2, TAPE3, TAPE4)      CRK   1
      COMMON /LAY/ E(5, 12), NU(5), NM, TMIN(5), IM, NL, A(20),            CRK   2
     1       TIRE(20), EA(5, 12), DROB(5), DZOB(5), RO(5), EM(5),          CRK   3
     2       DRC(5)                                                        CRK   4
      COMMON /PRIN/ AN1(13, 5, 20), AN2(13, 5, 20), AN3(13, 5, 20),        CRK   5
     1       DSP(12, 3), N18, L(20), MAT(5), MONTH(12)                     CRK   6
      COMMON /DUMMY/ L1(20), L2(20), N(20), TR(20), X(20), ANS(12),        CRK   7
     1       TITLE(8), TRAF(12), CONF(5), SIG(5), EN(2, 12), ENNT(480),    CRK   8
     2       DEF(12, 5), DEFD(12, 5), DEFC(12, 5), DEFTOT(12), DEFN(12,    CRK   9
     3       5), STRAIN(12, 5,2), CM(4, 12), EQ(4, 12), M(5), R(5),        CRK  10
     4       XX(12, 20), THN(20), ITH(400), IAC(400)                       CRK  11
      DATA NO/2HNO/                                                        CRK  12
      COMMON /CAL/ IW, IDX(20)                                             CRK  13
      DATA MONTH /10H  JANUARY  , 10H FEBRUARY  ,10H   MARCH   ,           CRK  14
     1            10H   APRIL   , 10H    MAY    , 10H    JUNE   ,          CRK  15
     2            10H    JULY   , 10H  AUGUST   , 10H SEPTEMBER ,          CRK  16
     3            10H OCTOBER   , 10H NOVEMBER  , 10H DECEMBER  /          CRK  17
      INTEGER Q0, Q1, Q2                                                   CRK  18
      REAL L, L1, L2, N, NU, LN1, LS1, LSN                                 CRK  19
   10 CONTINUE                                                             CRK  20
      DO 11 I = 1, 12                                                      CRK  21
         TRAF(I) = 0.08333                                                 CRK  22
   11    DEFTOT(I) = 0.0                                                   CRK  23
      DO 12 I = 1, 48                                                      CRK  24
         CM(I) = 0.0                                                       CRK  25
   12    EQ(I) = 0.0                                                       CRK  26
      DO 13 I = 1, 60                                                      CRK  27
         DEF(I) = 0.0                                                      CRK  28
         DEFD(I) = 0.0                                                     CRK  29
         DEFC(I) = 0.0                                                     CRK  30
         DEFC(I) = 0.0                                                     CRK  31
         STRAIN(I) = 0.0                                                   CRK  32
   13    STRAIN(I+60) = 0.0                                                CRK  33
      DO 14 I = 1, 480                                                     CRK  34
   14    ENNT(I) = 0.0                                                     CRK  35
      DO 15 I = 1, 1300                                                    CRK  36
         AN1(I) = 0.0                                                      CRK  37
         AN2(I) = 0.0                                                      CRK  38
   15    AN3(I) = 0.0                                                      CRK  39
      READ (5,980) TITLE                                                   CRK  40
         IF (EOF, 5) 970,20                                                CRK  41
   20 PRINT 990, TITLE                                                     CRK  42
C                                                                          CRK  43
         IW = 0                                                            CRK  44
C     READ  MATERIAL PARAMETERS                                            CRK  45
      READ (5,1000) NL, NM, LDOF, LNDF, Y, GR, Q0, Q1, Q2, TEST            CRK  46
C        NL          NUMBER OF AXLE  LOAD GROUPS                         CRK  47
C        NM          NUMBER OF MATERIALS (MAXIMUM OF FIVE)               CRK  48
C        LDDF        LOAD DISTRIBUTION FACTOR, RATIO                     CRK  49
C        LNDF        LANE DISTRIBUTION FACTOR, RATIO                     CRK  50
C        Y           DESIGN PERIOD, YEARS                                CRK  51
C        GR          TRAFFIC GROWTH RATE, RATIO                          CRK  52
C        Q0          PROVIDE  NO  IF THE ACTUAL TRAFFIC DATA FOR         CRK  53
C                    EACH MONTH IS NOT GIVEN                             CRK  54
C        Q1          PROVIDE  NO  IF THE MONTHLY TRAFFIC                 CRK  55
C                    PERCENTAGE DOES NOT VARY                            CRK  56
C        Q2          PROVIDE  NO  IF THE ELASTIC MODULUS VALUE           CRK  57
C                    OF THE DIFFERENT MATERIALS DO NOT VARY MONTHLY      CRK  58
C        TEST        LEAVE BLANK IF CALCULATIONS FOR BOTH CRACKING       CRK  59
C                    INDEX AND RUT DEPTH                                 CRK  60
C                    PROVIDE  1  FOR CRACKING INDEX ONLY                 CRK  61
C                    PROVIDE  2  FOR RUT DEPTH ONLY                      CRK  62
C                                                                        CRK  63
C     READ AND CALCULATE WHEEL LOAD DATA                                 CRK  64
         M = 1                                                           CRK  65
         N18 = 0                                                         CRK  66
      DO 30 I = 1, NL                                                    CRK  67
   READ (5,1010) L1(I), L2(I), N(I), TIRE(I)                             CRK  68
C        L1-L2       AXLE LOAD RANGE, KIPS                             CRK  69
C        N           NUMBER OF AXLE APPLICATIONS IN WHEEL LOAD GROUP I   CRK  70
C                    IN FIRST YEAR OF ANALYSIS                           CRK  71
C        TIRE        TIRE PRESSURE, PSI                                  CRK  72
C                                                                        CRK  73
         L(I) = (L1(I)+L2(I))/2.                                         CRK  74
      IF (L(I) .GT. L(M)) M = I                                          CRK  75
      IF (L(I) .EQ. 18.0) N18 = I                                        CRK  76
C        N18         INDEX OF 18-KIP LOAD GROUP                        CRK  77
C                    OR INDEX OF HIGHEST LOAD GROUP IF 18K NOT           CRK  78
C                    AVAILABLE                                           CRK  79
   30    A(I) = SQRT(318.3097/2.*L(I)/TIRE(I))                           CRK  80
      IF (N18 .EQ. 0) N18 = M                                            CRK  81
C                                                                        CRK  82
C        L           MEAN VALUE OF AXLE LOAD GROUP, KIPS                 CRK  83
C        A           RADIUS OF CONTACT AREA                              CRK  84
C                                                                        CRK  85
      PRINT 1020, (L1(I), L2(I), L(I), TIRE(I), N(I), I = 1, NL)         CRK  86
      PRINT 1030, LDOF, LNDF, Y                                          CRK  87
      IF (GR.NE.0.0)  PRINT 1035, GR                                     CRK  88
C                                                                        CRK  89
         IM = 1                                                          CRK  90
C        IM          1  IF ELASTIC MODULUS DOES NOT VARY MONTHLY         CRK  91
C                    12  IF ELASTIC MODULUS DOES VARY MONTHLY             CRK  92
         LS1 = 1.                                                        CRK  93
      DO 70 M = 1, NM                                                    CRK  94
      IF (Q2-NO) GO TO 40                                                CRK  95
   READ (5,1040) MAT(M), TMIN(M), NU(M), CONF(M), SIG(M), E(M, 1)        CRK  96
      GO TO 50                                                           CRK  97
   40    IM = 12                                                         CRK  98
   READ (5,1050) MAT(M), TMIN(M), NU(M), CONF(M), SIG(M), (E(M,          CRK  99
     1       I), I = 1, IM)                                              CRK 100
C        MAT         MATERIAL IDENTIFICATION                           CRK 101
C        TMIN        MINIMUM ALLOWABLE THICKNESS, INCHES                 CRK 102
C        NU          POISSONS RATIO                                    CRK 103
C        CONF        CONFIDENCE LEVEL FOR ELASTIC MODULUS                CRK 104
C        SIG         STANDARD DEVIATION OF ELASTIC MODULUS               CRK 105
C                    EXPRESSED AS A PERCENTAGE OF THE MEAN VALUE         CRK 106
C                    ALSO EQUAL TO THE COEFFICIENT OF VARIATION          CRK 107
C        E           ELASTIC MODULUS VALUE.  EITHER PROVIDE ONE          CRK 108
C                    VALUE FOR EACH MONTH OR ONE CONSTANT VALUE          CRK 109
C                    IF  Q2 = NO                                         CRK 110
C                                                                        CRK 111
C                                                                        CRK 112
   50 CONTINUE                                                           CRK 113
         LS1 = LS1*CONF(M)                                               CRK 114
C        LS1         PRODUCT OF ALL CONFIDENCE LEVELS                    CRK 115
```

```
      IF (TEST .EQ. 2.0) GO TO 70                                       CRK 116
      DO 60 I = 1, NM                                                   CRK 117
   60     EA(M, I) = E(M, I)-ALPHA(CONF(M))*SIG(M)/100.*E(M, I)         CRK 118
C     EA        ELASTIC MODULUS AT CONFIDENCE LEVEL                     CRK 119
   70 CONTINUE                                                          CRK 120
C                                                                       CRK 121
C     PRINT MATERIAL PARAMETERS                                         CRK 122
      PRINT 1060, (MAT(I), I = 1, NM)                                   CRK 123
           NS = NM-1                                                    CRK 124
      PRINT 1070, (TMIN(I), I = 1, NS)                                  CRK 125
      PRINT 1080, (NU(I), I = 1, NM)                                    CRK 126
      IF (TEST .NE. 2.0) PRINT 1160, (SIG(J), J = 1, NM)                CRK 127
C                                                                       CRK 128
      IF (Q2 .EQ. NO) GO TO 100                                         CRK 129
      PRINT 1090, MONTH                                                 CRK 130
      IF (TEST .EQ. 2.0) GO TO 90                                       CRK 131
      DO 80 I = 1, NM                                                   CRK 132
      PRINT 1100, MAT(I), CONF(I), (EA(I, J), J = 1, 12)                CRK 133
   80 PRINT 1110, (E(I, J), J = 1, 12)                                  CRK 134
      GO TO 110                                                         CRK 135
   90 PRINT 1120, (MAT(I), (E(I, J), J = 1, 12), I = 1, NM)             CRK 136
      GO TO 110                                                         CRK 137
  100 PRINT 1130, (E(J, 1), J = 1, NM)                                  CRK 138
      IF (TEST .EQ. 2.0) GO TO 120                                      CRK 139
      PRINT 1140, (EA(J, I), J = 1, NM)                                 CRK 140
      PRINT 1150, (CONF(J), J = 1, NM)                                  CRK 141
  110 CONTINUE                                                          CRK 142
  120 CONTINUE                                                          CRK 143
      PRINT 990, TITLE                                                  CRK 144
C                                                                       CRK 145
C                                                                       CRK 146
C     READ AND PRINT FATIGUE CURVE DATA                                 CRK 147
      READ (5,1010) A1, B, SDLOG, LN1                                   CRK 148
C     A1        CONSTANT OF FATIGUE CURVE                               CRK 149
C     B         SLOPE OF FATIGUE CURVE                                  CRK 150
C     SDLOG     STANDARD DEVIATION OF FATIGUE LIFE (LOG)                CRK 151
C     LN1       CONFIDENCE LEVEL FOR THEORETICAL N                      CRK 152
C                                                                       CRK 153
C     TEST = 2  SKIP CALCULATIONS IN PART ONE                           CRK 154
      IF (TEST .EQ. 2.) GO TO 150                                       CRK 155
      PRINT 1170, A1, B, SDLOG, LN1                                     CRK 156
C                                                                       CRK 157
C                                                                       CRK 158
C     CALCULATE TANGENTIAL STRAIN FOR EACH LOAD GROUP AND               CRK 159
C     LAYER THICKNESS(CONF. AND MEAN VALUE)                             CRK 160
C                                                                       CRK 161
      IF (Q2 .NE. NO) GO TO 130                                         CRK 162
      PRINT 1190                                                        CRK 163
  130 CALL LAYER (IM, 1)                                                CRK 164
  150 CONTINUE                                                          CRK 165
C                                                                       CRK 166
           IY = Y                                                       CRK 167
           IR = 0                                                       CRK 168
      IF (Q0-NO) 260,160,260                                            CRK 169
C     READ TRAFFIC PERCENTAGES FOR  EACH MONTH                          CRK 170
C     *** ONLY *** IF ACTUAL TRAFFIC DATA IS NOT GIVEN                  CRK 171
C                                                                       CRK 172
C                                                                       CRK 173
C     IF TRAFFIC PERCENTAGES ARE CONSTANT FOR EACH DESIGN YEAR.         CRK 174
C     THESE VALUES MAY BE OMITTED IF  Q1 = NO                           CRK 175
  160 CONTINUE                                                          CRK 176
      IF (Q1-NO) READ (5,1200) TRAF                                     CRK 177
C     TRAF      TRAFFIC PERCENTAGE OF MONTH                             CRK 178
           SUM = 0.0                                                    CRK 179
      DO 170 I = 1, 12                                                  CRK 180
  170      SUM = SUM+TRAF(I)                                            CRK 181
      PRINT 1210, (MONTH(I), TRAF(I), I = 1, 12), SUM                   CRK 182
C                                                                       CRK 183
C     CALCULATE  YEARLY TRAFFIC GROWTH                                  CRK 184
      DO 180 J = 1, IY                                                  CRK 185
           TR(J) = (1.+GR)**(J-1)                                       CRK 186
  180 CONTINUE                                                          CRK 187
C     TR        TRAFFIC DUE TO GROWTH FOR YEAR                          CRK 188
C                                                                       CRK 189
C                                                                       CRK 190
C                                                                       CRK 191
C     PRINT TRAFFIC DATA  CALCULATED FROM TRAFFIC PERCENTAGES           CRK 192
C     AND TRAFFIC GROWTH RATE AND AXLE APPLICATIONS                     CRK 193
      IF (Q1-NO) 200,190,200                                            CRK 194
  190 PRINT 1220                                                        CRK 195
      GO TO 210                                                         CRK 196
  200 PRINT 1230, MONTH                                                 CRK 197
  210 DO 250 J = 1, NL                                                  CRK 198
      IF (Q1-NO) PRINT 1240, L(J)                                       CRK 199
      DO 250 K = 1, IY                                                  CRK 200
      DO 220 K = 1, 12                                                  CRK 201
  220      X(K) = A(J)*TR(M)*TRAF(K)                                    CRK 202
C     X         MONTHLY TRAFFIC CALCULATED FROM PERCENTAGES,            CRK 203
C               GROWTH RATE, AND LOAD                                   CRK 204
           IR = IR+1                                                    CRK 205
C     IR        INDEX FOR IOBIN WRITE OF TRAFFIC FOR YEAR               CRK 206
      CALL IOBIN (6HWRITER, 3, X(1), 12, IAC(IR))                       CRK 207
      IF (Q1-NO) 230,230,240                                            CRK 208
  230 PRINT 1250, L(J), M, X(1)                                         CRK 209
      GO TO 250                                                         CRK 210
  240 PRINT 1260, M, (X(K), K = 1, 12)                                  CRK 211
  250 CONTINUE                                                          CRK 212
      GO TO 271                                                         CRK 213
  260      Q1 = 2M                                                      CRK 214
      PRINT 1230, MONTH                                                 CRK 215
      DO 270 J = 1, NL                                                  CRK 216
      PRINT 1235, L(J)                                                  CRK 217
      DO 270 K = 1, IY                                                  CRK 218
C                                                                       CRK 219
C     IF  Q0 IS NOT NO, READ ACTUAL TRAFFIC DATA                        CRK 220
C     GIVE MONTHLY VALUES FOR EACH YEAR FOR FIRST LOAD                  CRK 221
C     GROUP.  THEN REPEAT SET FOR ADDITIONAL LOAD GROUPS                CRK 222
C                                                                       CRK 223
      READ (5,1270) YR, (X(I), I = 1, 12)                               CRK 224
C     X         MONTHLY TRAFFIC VALUE                                   CRK 225
C     YR        IDENTIFICATION VARIABLE                                 CRK 226
      PRINT 1280, YR, (X(I), I = 1, 12)                                 CRK 227
           IR = IR+1                                                    CRK 228
      CALL IOBIN (6HWRITER, 3, X(1), 12, IAC(IR))                       CRK 229
  270 CONTINUE                                                          CRK 230
  271 CONTINUE                                                          CRK 231
C
```

```
      IF (TEST .EQ. 2.0) GO TO 500
C
C     CALCULATE THEORETICAL REPETITIONS BY STRAINS FROM
C     LAYER SUBROUTINE
          RK = ALPHA(LN1)
          IT = 0
C     RK        K VALUE CORRESPONDING TO LN1
C     IT        INDEX FOR IOBIN WRITE OF THEORETICAL TRAFFIC
C
          IM1 = IM*1
      DO 480 I = 2, IM1, 2
          I2 = (I+1)/2
      IF (IM-1) GO TO 280
      PRINT 1290, LN1
      GO TO 290
  280 CONTINUE
      PRINT 1300, L(I2), MONTH
  290 CALL IOBIN (7HREADSKP, 2, ANS(1), IM, IDX(I))
C     IW          INDEX FOR IOBIN READ OF STRAINS ANS
C     ANS         TANGENTIAL STRAIN AT BOTTOM OF ASPHALT
C                 CONCRETE CALCULATED IN SUBROUTINE LAYER
C                 USING CONFIDENCE LEVEL OF ELASTIC MODULUS
C
      DO 300 J = 1, IM
  300     THN(J) = 10.**(ALOG10(A1*ANS(J)**(-B))-RK*SDLOG)
C     THN         THEORETICAL NUMBER OF REPETITIONS FROM
C                 INPUT FATIGUE EQUATION AT SOME SPECIFIED
C                 CONFIDENCE LEVEL
      IF (IM-1) 320,320,310
  310 PRINT 1310, LN1, (THN(J), J = 1, I2)
      GO TO 340
C
C     IF MODULUS IS CONSTANT, THN IS CONSTANT
  320     SAV = THN(1)
      DO 330 J = 2, 12
  330     THN(J) = SAV
C
C
C     IT          INDEX FOR IOBIN WRITE OF THN
  340     IT = IT+1
      CALL IOBIN (6HWRITER, 4, THN(1), 12, ITH(IT))
          I1 = I-1
C     I - 1  IS USED BECAUSE IN THE LAYER SUBPROGRAM, THE
C     STRAINS ARE WRITEN ON TAPE2 IN ALTERNATING ORDER --
C     MEAN LEVEL AND CONFIDENCE LEVEL
      CALL IOBIN (7HREADSKP, 2, ANS(I), IM, IDX(I1))
C     ANS         TANGENTIAL STRAIN AT BOTTOM OF ASPHALT
C                 CONCRETE CALCULATED IN SUBROUTINE LAYER
C                 USING MEAN VALUE OF ELASTIC MODULUS
      DO 350 J = 1, IM
  350     THN(J) = A1*ANS(J)**(-B)
C     THN         THEORETICAL NUMBER OF REPETITIONS FROM
C                 INPUT FATIGUE EQUATION AT SOME SPECIFIED
C                 MEAN LEVEL
      IF (IM-1) 370,370,360
  360 PRINT 1320, (THN(J), J = 1, I2)
      GO TO 390
  370 DO 380 J = 2, 12
  380     THN(J) = THN(1)
      PRINT 1330, L(I2), SAV, THN(I)
  390     IT = IT+1
      CALL IOBIN (6HWRITER, 4, THN(I), 12, ITH(IT))
  400 CONTINUE
C
C
          LSN = LS1*LN1
          RK = ALPHA(LSN)
C     LSN         SUM OF CONFIDENCE LEVELS OF ELASTIC MODULUS
C                 AND FATIGUE EQUATION
C     RK          K VALUE CORRESPONDING TO LSN
      PRINT 990, TITLE
          NLN = 0
          NN = 0
          MM = 0
C
C     CALCULATE RATIO OF N ACTUAL TO N THEORETICAL
      DO 430 I = 1, NL
      PRINT 1340, L(I), MONTH
          IR = 0
          NN = NN+1
      CALL IOBIN (7HREADSKP, 4, LI(1), 12, ITH(NN))
          NN = NN+1
      CALL IOBIN (7HREADSKP, 4, THN(1), 12, ITH(NN))
      DO 430 MO = 1, IT
          MM = MM+1
      CALL IOBIN (7HREADSKP, 3, X(1), 12, TAC(MM))
      DO 410 II = 1, 12
          EN(1, II) = X(II)/LI(II)
          EN(2, II) = X(II)/THN(II)
C     EN(I)       RATIO OF MONTHLY TRAFFIC TO MEAN REPITITIONS
C     EN(2)                                TO CONF. REPITITIONS
          IR = IR+1
          ENNT(IR) = ENNT(IR)+EN(1, II)
          IR = IR+1
  410     ENNT(IR) = ENNT(IR)+EN(2, II)
C     ENNT        CUMULATIVE SUM OF EN
      PRINT 1360, MO, LSN, ((EN(J1, II), II = 1, 12), J1 = 1, 2)
C     NLN         PAGE SKIP CONTROL
          NLN = NLN+4
          IF (NLN-44) 430,420,420
  420     NLN = 0
      PRINT 990, TITLE
      PRINT 1340, L(I), MONTH
  430 CONTINUE
      DO 440 I = 3, IR, 2
          ENNT(I) = ENNT(I)+ENNT(I-2)
  440     ENNT(I+1) = ENNT(I+1)+ENNT(I-1)
      PRINT 1370
          NLN = 1
      DO 490 J = 1, IR, 2
      IF (NLN-44) 460,450,450
  450     NLN = NLN-44
      PRINT 990, TITLE
      PRINT 1370
  460     NLN = NLN+1
          J2 = (J+1)/2
```

```
      DO 470 JJ = 1, 2                                                  CRK 348
           L1(JJ) = ENNT(J+JJ-1)                                        CRK 349
      IF (L1(JJ)) 470,480,470                                           CRK 350
470        L2(JJ) = ALOG10(L1(JJ))                                     CRK 351
           SDL = (L2(1)-L2(2))/PK                                       CRK 352
           AK = -L2(2)/SDL                                              CRK 353
           AA = XNORM(AK, 0, 1)                                         CRK 354
           CI = AA*10**3                                                CRK 355
      PRINT 1380, J2, LSN, L1(1), L2(1), SDL, AK, AA, CI, L1(2),        CRK 356
     1    L2(2)                                                         CRK 357
      GO TO 490                                                         CRK 358
480        ZERO = 0.0                                                  CRK 359
      PRINT 1390, J2, LSN, (ZERO, III = 1, 4)                           CRK 360
490   CONTINUE                                                          CRK 361
500   CONTINUE                                                          CRK 362
      IF (TEST .EQ. 1.0) GO TO 970                                      CRK 363
C                                                                       CRK 364
C                                                                       CRK 365
C                                                                       CRK 366
C                          PART TWO                                     CRK 367
C                                                                       CRK 368
C                                                                       CRK 369
C     IZ          NUMBER OF DEPTHS FOR CALCULATIONS                     CRK 370
           IZ = NM-1                                                    CRK 371
      IF (IM .EQ. 1) PRINT 1400                                         CRK 372
      CALL LAYER (IM, IZ)                                               CRK 373
C                                                                       CRK 374
C     CALCULATIONS OF CONFINING AND VERTICAL PRESSURES                  CRK 375
C     DUE TO OVERBURDEN                                                 CRK 376
C                                                                       CRK 377
C                                                                       CRK 378
C     R           UNIT WEIGHT OF MATERIAL (LB/CU IN)                    CRK 379
C     DZOB        VERTICAL PRESSURE DUE TO OVERBURDEN                   CRK 380
C     DROB        RADIAL PRESSURE DUE TO OVERBURDEN                     CRK 381
C     DRC         INPUT RADIAL PRESSURE FOR WHICH CURVES ARE            CRK 382
C                 GIVEN FOR MATERIALS                                   CRK 383
C     EM          INPUT PARAMETER TO CALCULATE CORRECT RADIAL           CRK 384
C                 PRESSURE FOR GIVEN CURVE. VALUE IS 0 WHEN             CRK 385
C                 REGRESSION EQN IN N,Z1,Z3 AND E IS GIVEN              CRK 386
C                                                                       CRK 387
C                                                                       CRK 388
C                                                                       CRK 389
C                                                                       CRK 390
C                                                                       CRK 391
C                                                                       CRK 392
      READ (5,1410) (R(I), EM(I), DRC(I), I = 1, NM)                    CRK 393
           RD(1) = (R(1)+R(2)*0.5)/1.5                                  CRK 394
           RD(2) = (R(1)+R(2)+R(3)*0.5)/2.5                             CRK 395
           RD(3) = (R(1)+R(2)+R(3))/3.                                  CRK 396
C     RD          COMPOSITE WEIGHT                                      CRK 397
C     H           COMPOSITE THICKNESS                                   CRK 398
      DO 510 I = 1, NM                                                  CRK 399
           EM(I) = ABS(EM(I))                                           CRK 400
510   IF (DRC(I) .EQ. 0.0) DRC(I) = 1.                                  CRK 401
           H(1) = TMIN(1)+TMIN(2)*0.5                                   CRK 402
           H(2) = TMIN(1)+TMIN(2)+TMIN(3)*0.5                           CRK 403
           H(3) = TMIN(1)+TMIN(2)+TMIN(3)                               CRK 404
      DO 520 I = 1, NS                                                  CRK 405
           K = 1+I                                                      CRK 406
           DRCB(I) = NU(K)/(1.-NU(K))*RD(I)*H(I)                        CRK 407
520        DZCB(I) = RD(I)*H(I)                                        CRK 408
      DO 540 I = 1, NL                                                  CRK 409
      DO 540 K = 1, IM                                                  CRK 410
      DO 530 J1 = 2, NS                                                 CRK 411
           J = J1-1                                                     CRK 412
C                                                                       CRK 413
C     BASE AND SUBBASE CALCULATIONS                                     CRK 414
C                                                                       CRK 415
           AN1(K, J, I) = AN1(K, J, I)-DZOB(J1)                         CRK 416
C     MEAN VERTICAL STRESS                                              CRK 417
           AN3(K, J, I) = AMIN1(-1.0, (AN3(K, J, I)-DROB(J1)))          CRK 418
C     RADIAL STRESS                                                     CRK 419
           SI = (ABS(AN3(K, J, I)))**EM(J1))                            CRK 420
           AN2(K, J, I) = AN1(K, J, I)*(DRC(J1))/SI                     CRK 421
530        AN2(K, J, I) = SIGN(AN2(K, J, I), AN1(K, J, I))              CRK 422
C     DESIGN VERTICAL STRESS                                            CRK 423
C                                                                       CRK 424
C                                                                       CRK 425
C     SUBGRADE CALCULATIONS                                             CRK 426
           AN1(K, NS, I) = AN1(K, NS, I)*2.0-DZOB(NS)                   CRK 427
C     MEAN VERTICAL STRESS                                              CRK 428
           AN3(K, NS, I) = AMIN1(-1.0, (AN3(K, NS, I)*2.0-DROB(NS)))    CRK 429
C     RADIAL STRESS                                                     CRK 430
540        AN2(K, NS, I) = AN1(K, NS, I)*DRC(NM)-AN3(K, NS, I)          CRK 431
C     DESIGN VERTICAL STRESS                                            CRK 432
C                                                                       CRK 433
C                                                                       CRK 434
C     IM = 1    ELASTIC MODULUS VALUE CONSTANT MONTHLY                  CRK 435
      IF (IM-1) 550,550,580                                             CRK 436
550   DO 570 M = 2, 12                                                  CRK 437
      DO 560 N = 1, NS                                                  CRK 438
           E(N, M) = E(N, 1)                                            CRK 439
      DO 560 I = 1, NL                                                  CRK 440
           AN1(M, J, I) = AN1(1, J, I)                                  CRK 441
           AN2(M, J, I) = AN2(1, J, I)                                  CRK 442
560        AN3(M, J, I) = AN3(1, J, I)                                  CRK 443
           E(NM, M) = E(NM, 1)                                          CRK 444
      DO 570 IJ = 1, 3                                                  CRK 445
           DSP(M, IJ) = DSP(1, IJ)                                      CRK 446
570   CONTINUE                                                          CRK 447
580   CONTINUE                                                          CRK 448
C                                                                       CRK 449
C                                                                       CRK 450
C     PRINT DESIGN CONFINING PRESSURE AND VERTICAL PRESSURE             CRK 451
C                                                                       CRK 452
           NLN = 0                                                      CRK 453
C     NLN         NUMBER OF LINES PRINTED -- PAGE SKIP CONTROL          CRK 454
      DO 660 II = 1, NL                                                 CRK 455
C                                                                       CRK 456
C     ANI (MONTH,MATERIAL,LOAD GROUP)                                   CRK 457
C     I = 1  VERTICAL STRESS MEAN                                       CRK 458
C     I = 2  VERTICAL STRESS DESIGN                                     CRK 459
C     I = 3  RADIAL STRESS                                              CRK 460
      IF (NLN-45) 600,590,590                                           CRK 461
590   PRINT 990, TITLE                                                  CRK 462
           NLN = 0                                                      CRK 463
```

```
600           NLA = NLA+NS*3                                          CRK 464
              NS1 = NS - 1                                            CRK 465
      PRINT 1420, MONTH(1), MONTH(2), L(II), (MAT(K+1),               CRK 466
     1       (AN1(I, K, II), AN2(I, K, II), AN3(I, K, II), I = 1,    CRK 467
     2       2), K = 1, NS1)                                         CRK 468
      PRINT 1421, MAT(NN), DRC(NN), ((AN1(I, NS, II), AN2(I, NS, II),CRK 469
     1      AN3(I, NS, II), I = 1, 2)                                CRK 470
C                                                                     CRK 471
C                                                                     CRK 472
C         MONTHS 3 THROUGH 11 IN GROUPS OF THREE                      CRK 473
          DO 630 JJ = 1, 3                                            CRK 474
               J3 = JJ*3                                              CRK 475
               J5 = J3+2                                              CRK 476
          IF (NLN-45) 620,610,610                                     CRK 477
610   PRINT 990, TITLE                                                CRK 478
               NLA = 0                                                CRK 479
620           NLA = NLA+NS*3                                          CRK 480
630   PRINT 1430, (MONTH(J), J = J3, J5), ((AN1(J, K, II), AN2(J,     CRK 481
     1       K, II), AN3(J, K, II), J = J3, J5), K = 1, NS)           CRK 482
C                                                                     CRK 483
C         MONTH 12                                                    CRK 484
C                                                                     CRK 485
          IF (NLN-45) 650,640,640                                     CRK 486
640   PRINT 990, TITLE                                                CRK 487
               NLA = 0                                                CRK 488
650           NLA = NLA+NS*3                                          CRK 489
      PRINT 1440, MONTH(12), ((AN1(12, K, II), AN2(12, K, II), AN3(12,CRK 490
     1       K, II)), K = 1, NS)                                      CRK 491
660       CONTINUE                                                    CRK 492
C                                                                     CRK 493
C                                                                     CRK 494
C                                                                     CRK 495
C         DETERMINE STRAIN CORRESPONDING TO DESIGN VERTICAL           CRK 496
C         STRESS ACCORDING TO INPUT FATIGUE CURVES                    CRK 497
C                                                                     CRK 498
C                                                                     CRK 499
C                                                                     CRK 500
          DO 960 II = 1, IY                                           CRK 501
          DO 670 JJ = 1, NL                                           CRK 502
               J = (JJ-1)*(IY)+II                                     CRK 503
      CALL IOBIN (7HREADSKP, 3, X(1), 12, TAC(J))                     CRK 504
          DO 670 K = 1, 12                                            CRK 505
670            XX(JJ, K) = X(K)                                       CRK 506
C         XX(LOAD GROUP, MONTH)  TRAFFIC                              CRK 507
C                                                                     CRK 508
C         LOOP WHICH INCLUDES SIX MONTHS FOR PRINTOUT PURPOSES ONLY   CRK 509
          DO 960 JJ = 1, 12, 6                                        CRK 510
          DO 680 I = 1, 12                                            CRK 511
          DO 680 J = 1, 5                                             CRK 512
680            AN1(13, J, I) = 0.0                                    CRK 513
               J = JJ+5                                               CRK 514
C                                                                     CRK 515
C         AN1 (MONTH,MATERIAL,LOAD GROUP) IS NOW THE STRAIN           CRK 516
C         APPROPIATE TO THE CORRESPONDING DESIGN VERTICAL STRESS      CRK 517
C         AN1(13,MATERIAL,MONTH) IS THE CUMMULATIVE STRAIN            CRK 518
      PRINT 1450, II, (MONTH(I), I = JJ, J)                           CRK 519
          DO 790 I = JJ, J                                            CRK 520
          IF (XX(1, I)) 690,690,720                                   CRK 521
690       IF (II-1) 790,790,700                                       CRK 522
700       DO 710 K = 1, NS                                            CRK 523
               EQ(K, I) = 0.0                                         CRK 524
          IF (I .NE. 1) CM(K, I) = CM(K, I-1)                         CRK 525
          IF (I .EQ. 1) CM(K, I) = CM(K, 12)                          CRK 526
710       CONTINUE                                                    CRK 527
          GO TO 790                                                   CRK 528
720       CONTINUE                                                    CRK 529
          DO 780 K = 1, NS                                            CRK 530
          DO 750 M = 1, NL                                            CRK 531
               AN1(I, K, M) = POLY(XX(M, I), AN2(I, K, M), K, AN3(I,  CRK 532
     1              K, M))                                           CRK 533
          IF (AN1(I, K, N18)) 730,750,730                             CRK 534
730       IF (XX(N18, I)) 740,750,740                                 CRK 535
740            AN1(13, K, I) = AN1(13, K, I)+10.**(AN1(I, K, M)       CRK 536
     1            *ALOG10(XX(N18, I))/AN1(I, K, N18))                CRK 537
750       CONTINUE                                                    CRK 538
          IF (AN1(13, K, I)) EQ(K, I) = AN1(13, K, I)                 CRK 539
C         EQ        EQUIVALENT 18-KIP APPLICATIONS                    CRK 540
          IF (I-1) 760,760,770                                        CRK 541
C         CM        CUMULATIVE EQUIVALENT 18-KIP APPLICATIONS         CRK 542
760            CM(K, I) = EQ(K, I)+CM(K, 12)                          CRK 543
          GO TO 780                                                   CRK 544
770            CM(K, I) = EQ(K, I)+CM(K, I-1)                         CRK 545
780       CONTINUE                                                    CRK 546
790       CONTINUE                                                    CRK 547
C                                                                     CRK 548
C         PRINT EQUIV 18-KIP APPLICATIONS AND CUMULATIVE APPLICATIONS CRK 549
      PRINT 1460, (MAT(K+1), (EQ(K, I), I = JJ, J), K = 1, NS)        CRK 550
      PRINT 1470                                                      CRK 551
      PRINT 1460, (MAT(K+1), (CM(K, I), I = JJ, J), K = 1, NS)        CRK 552
C                                                                     CRK 553
C                                                                     CRK 554
C         DETERMINE STRAIN CORRESPONDING TO CUMULATIVE 18-KIP         CRK 555
C         AXLE APPLICATIONS AND DESIGN VERTICAL STRESS                CRK 556
C                                                                     CRK 557
      PRINT 1480                                                      CRK 558
          DO 920 K = 1, NS                                            CRK 559
          DO 910 I = JJ, J                                            CRK 560
          IF (I-1) 800,800,850                                        CRK 561
800       CONTINUE                                                    CRK 562
          IF (II-1) 810,810,820                                       CRK 563
810            STRAIN(1, K, 1) = 0.0                                  CRK 564
               GO TO 880                                              CRK 565
820       IF (CM(K, 12)) 830,830,840                                  CRK 566
830            STRAIN(1, K, 1) = 0.0                                  CRK 567
               GO TO 880                                              CRK 568
840            STRAIN(1, K, 1) = POLY(CM(K, 12), AN2(I, K, N18),      CRK 569
     1              K, AN3(I, K, N18))-(ABS(AN2(I, K, N18)-2.0       CRK 570
     2            *AU(K+1)*AN3(I, K, N18))/E(K+1, 1))*100.           CRK 571
               GO TO 880                                              CRK 572
850       IF (CM(K, I-1)) 860,860,870                                 CRK 573
860            STRAIN(1, K, 1) = 0.0                                  CRK 574
               GO TO 880                                              CRK 575
870            STRAIN(I, K, 1) = POLY(CM(K, I-1), AN2(I, K, N18),     CRK 576
     1              K, AN3(I, K, N18))-(ABS(AN2(I, K, N18)-2.0       CRK 577
     2            *AU(K+1)*AN3(I, K, N18))/E(K+1, 1))*100.           CRK 578
880       CONTINUE                                                    CRK 579
```

```
      IF (CM(K, I)) 890,890,900                                          CRK 580
  890     STRAIN(I, K, 2) = 0.0                                          CRK 581
      GO TO 910                                                          CRK 582
  900 CONTINUE                                                           CRK 583
          STRAIN(I, K, 2) = POLY(CM(K, I), AN2(I, K, N18),               CRK 584
     1         K, AN3(I, K, N18))-(ABS(AN2(I, K, N18)-2.0              CRK 585
     2       *NU(K-1)*AN3(I, K, N18))/E(K-1, I))*100.                   CRK 586
  910 CONTINUE                                                           CRK 587
C                                                                        CRK 588
      PRINT 1490, MAT(K-1), (STRAIN(M, K, 2), M = JJ, J)                 CRK 589
  920 CONTINUE                                                           CRK 590
      PRINT 1500                                                         CRK 591
      PRINT 1490, (MAT(K-1), (STRAIN(M, K, 2), M = JJ, J), K = 1, NS)    CRK 592
C                                                                        CRK 593
C         PRINT DEPTH OF LAYERS                                          CRK 594
      PRINT 1510, ((MAT(I), THIN(I)), I = 2, NS), MAT(NM)                CRK 595
C                                                                        CRK 596
C     PRINT 1520, ((DSP(I, K), I = JJ, J), K = 1, 3)                     CRK 597
C         CALCULATE DEFORMATION                                          CRK 598
          DO 925  I = 1, 12                                              CRK 599
  925         DEFTOT(I) = 0.0                                            CRK 600
          DO 950 NN = 2, NM                                              CRK 601
              I = NN-1                                                   CRK 602
C                                                                        CRK 603
C         DEF       DEFORMATION AT MONTH N DUE TO REPETITIONS THROUGH    CRK 604
C                   MONTH N                                              CRK 605
C         DEFN      DEFORMATIONS AT MONTH N DUE TO REPITIONS THROUGH     CRK 606
C                   MONTH (N-1)                                          CRK 607
C         DEFD      DIFFERENCE BETWEEN DEFORMATION DEF-DEFN              CRK 608
C         DEFC      CUMULATIVE DEFORMATION THROUGH MONTH N               CRK 609
C         DEFTOT    TOTAL CUMULATIVE DEFORMATION                         CRK 610
C                                                                        CRK 611
          DO 950 K = JJ, J                                               CRK 612
          IF (NN .EQ. 2) DEFTOT(K) = 0.0                                 CRK 613
C                                                                        CRK 614
C         THIN(NM)  THEORETICAL THICKNESS OF SUBGRADE BASED ON           CRK 615
C                   VERTICAL DISPLACEMENT, POISSONS RATIO,               CRK 616
C                   ELASTIC MODULUS, VERTICAL AND RADIAL STRESS ...      CRK 617
C                                                                        CRK 618
          IF (I .EQ. NS) THIN(NN) = ABS(DSP(K, 1)*E(NM, K)/(DSP(K,       CRK 619
     1         2)-2.0*NU(NM)*DSP(K, 3)))                                 CRK 620
C         DSP(MONTH, I)    VALUE AT SUBGRADE DUE TO 18-KIP LOAD          CRK 621
C                   I = 1      VERTICAL DISPLACEMENT                     CRK 622
C                   I = 2      VERTICAL STRESS                           CRK 623
C                   I = 3      RADIAL STRESS                             CRK 624
C                                                                        CRK 625
              DEF(K, I) = STRAIN(K, I, 2)*THIN(NN)/100.                  CRK 626
              DEFN(K, I) = STRAIN(K, I, 1)*THIN(NN)/100.                 CRK 627
          IF (K-1) 940,940,930                                           CRK 628
  930     CONTINUE                                                       CRK 629
              DEFD(K, I) = DEF(K, I)-DEFN(K, I)                          CRK 630
              DEFC(K, I) = DEFC(K-1, I)+DEFD(K, I)                       CRK 631
              DEFTOT(K) = DEFTOT(K)+DEFC(K, I)                           CRK 632
          GO TO 950                                                      CRK 633
  940     CONTINUE                                                       CRK 634
              DEFD(1, I) = DEF(1, I)-DEFN(1, I)                          CRK 635
              DEFC(K, I) = DEFC(12, I)+DEFD(K, I)                        CRK 636
              DEFTOT(1) = DEFTOT(1)+DEFC(K, I)                           CRK 637
  950     CONTINUE                                                       CRK 638
C                                                                        CRK 639
C         PRINT DEFORMATION AT MONTH N                                   CRK 640
      PRINT 1530                                                         CRK 641
      PRINT 1490, (MAT(I+1), (DEF(K, I), K = JJ, J), I = 1, NS)          CRK 642
      PRINT 1540                                                         CRK 643
      PRINT 1490, (MAT(I+1), (DEFN(K, I), K = JJ, J), I = 1, NS)         CRK 644
      PRINT 1550                                                         CRK 645
      PRINT 1490, (MAT(I+1), (DEFD(K, I), K = JJ, J), I = 1, NS)         CRK 646
      PRINT 1560                                                         CRK 647
      PRINT 1490, (MAT(1+1), (DEFC(K, I), K = JJ, J), I = 1, NS)         CRK 648
      PRINT 1570, (DEFTOT(K), K = JJ, J)                                 CRK 649
  960 CONTINUE                                                           CRK 650
      GO TO 10                                                           CRK 651
  970 CONTINUE                                                           CRK 652
C                                                                        CRK 653
  980 FORMAT    (8A10)                                                   CRK 654
  990 FORMAT    ( *1* 15X, 8A10 )                                        CRK 655
 1000 FORMAT    ( 2I10, 4F10.0, 3(A2, 3X) ,F5.0)                         CRK 656
 1010 FORMAT    ( 4F10.0 )                                               CRK 657
 1020 FORMAT    ( 3(/), 10X *AXLE LOAD      AXLE LOAD       TIRE       N  *CRK 658
     1           *INITIAL *                                              CRK 659
     2             /, 10X *RANGE*KIPS    MEAN*KIPS     PRESSURE    AXL* CRK 660
     3            *E APPL * /                                            CRK 661
     4           ( 9X, F4.0, * -*,  F4.0, 5X, F7.2, 6X, F6.2,   6X,F7.0)) CRK 662
 1030 FORMAT    ( 3(/),15X*LOAD DISTRIBUTION FACTOR, RATIO* 10X,F8.2     CRK 663
     1             / ,15X*LANE DISTRIBUTION FACTOR, RATIO* 10X,F8.2     CRK 664
     3             / ,15X*DESIGN PERIOD, YEARS          * 10X,F8.0)     CRK 665
 1035 FORMAT    ( 15X*TRAFFIC GROWTH RATE, RATIO     * 10X,F8.2 )        CRK 666
 1040 FORMAT    (A10, F10.0, 2F5.0, 2F10.0)                              CRK 667
 1050 FORMAT    (A10, F10.0, 2F5.0, 5F10.0 / (8F10.0))                   CRK 668
 1060 FORMAT    ( 3(/), 30X, *MATERIAL PARAMETERS* // 10X*MATERIAL*      CRK 669
     1          11X, 5( A10, 1X))                                       CRK 670
 1070 FORMAT    (10X*THICKNESS* 5X, 5F11.2)                              CRK 671
 1080 FORMAT    (10X*POISSONS RATIO*  5F11.2)                            CRK 672
 1090 FORMAT    ( 6(/), 10X *VARIATIONS OF E VALUES IN SPACE AND TIME*   CRK 673
     1          /, 10X *MATERIAL  CONF * 6A10 / 22X, 6A10/)              CRK 674
 1100 FORMAT    ( 9X, A10, F5.2, F8.0, 5F10.0/ 19X, 6F10.0 )             CRK 675
 1110 FORMAT    ( 20X, *MEAN* F8.0, 5F10.0 / 19X, 6F10.0 )               CRK 676
 1120 FORMAT    ( 9X, A10, *MEAN * F8.0, 5F10.0 / 22X, 6F10.0 )          CRK 677
 1130 FORMAT    ( / , 10X*E - MEAN VALUE* 5F11.0 )                       CRK 678
 1140 FORMAT    ( 10X *E - CONF VALUE* 5F11.0)                           CRK 679
 1150 FORMAT    ( 10X *CONFIDENCE LEVEL* 5(F9.2,2X))                     CRK 680
 1160 FORMAT    ( 10X *COF VAR,PERCENT * 5(F9.2,2X))                     CRK 681
 1170 FORMAT    ( 3(/), 20X, 3HN = EE.1,11H * (1/E) ** F5.2              CRK 682
     1          /, 30X *LOG  STANDARD DEVIATION OF* F5.2                 CRK 683
     2          /, 30X *AND CONFIDENCE LEVEL      * F5.2, 4(/))          CRK 684
 1190 FORMAT    (10X* LOAD     DEPTH - INCHES  TANGENTIAL STRAIN*/)      CRK 685
 1200 FORMAT    ( 12F5.0 )                                               CRK 686
 1210 FORMAT    ( 3(/), 23X *MONTH* 12X *TRAFFIC PERCENTAGE* /12         CRK 687
     1          ( /, 20X, A10, 15X, F10.2), // 25X *SUM* 17X,F10.2 )     CRK 688
 1220 FORMAT    ( 4(/), 50X *N TABLE - ACTUAL* // 10X *LOAD    YEAR  *   CRK 689
     1          *   N = MONTHLY* /)                                      CRK 690
 1230 FORMAT    (4(/), 50X *N TABLE - ACTUAL* / 46X *FROM TRAFFIC *      CRK 691
     1          *DATA INPUT* //  15X, 6A10/20X,6A10)                    CRK 692
 1235 FORMAT    ( 20X*LOAD* F5.0 )                                       CRK 693
 1240 FORMAT    ( /, 10X, F3.0)                                          CRK 694
 1250 FORMAT    (10X, F3.0, 5X, I3, 6X, F10.2 )                          CRK 695
```

```
1260 FORMAT   ( 18X, I2, 4X, 6F10.2 / 28X, 6F10.2)                          CRK 696
1270 FORMAT   ( A8, 12F6.0 )                                                CRK 697
1280 FORMAT   ( 10X, A8, F7.0, 5F10.0 / 20X, 6F10.0 )                       CRK 698
1290 FORMAT   ( 4(/), 50X *N TABLE - THEORETICAL* // 10X *LOAD* 5X          CRK 699
     1         *CONFIDENCE* 5X *MEAN VALUE* / 19X *LEVEL* F6.3/)            CRK 700
1300 FORMAT   (4(/), 50X *N TABLE - THEORETICAL* //15X,*LOAD*F5.0/10X       CRK 701
     1         *CONF * 4X, 6A10 / 10X *LEVEL* 7X, 6A10)                    CRK 702
1310 FORMAT   ( 10X, F5.3, 2X, 6F10.0 / 20X, 6F10.0 )                       CRK 703
1320 FORMAT   ( 10X*MEAN* 3X, 6F10.0/ 20X, 6F10.0)                          CRK 704
1330 FORMAT   ( 10X, F3.0, 3X, F10.2, 5X, F10.2)                            CRK 705
1340 FORMAT   ( 4(/), 50X *N ACTUAL / N THEORETICAL* /10X*LOAD*F5.0/        CRK 706
     1         10X *YEAR CONF* 6A10 / 22X, 6A10 )                          CRK 707
1360 FORMAT   (10X,I2,F6.3,2X,6E10.3,/24X,6E10.3/14X*MEAN*3X                CRK 708
     1         6E10.3, / 24X, 6E10.3 )                                     CRK 709
1370 FORMAT   ( 4(/), 10X *MONTH  CONF    (N/N)T   LOG(N/N)T   LOG SD*      CRK 710
     1         6X *K* 7X *A* 7X *CI* / )                                   CRK 711
1380 FORMAT   ( 10X, I3, F8.3, 3E11.3,   3E9.2      / 17X *MEAN*2E11.3)     CRK 712
1390 FORMAT   (10X,I3,F8.4,F6.0,2(10X*-*),8X,*-*2F9.0/17X*MEAN*F6.0,        CRK 713
     1         10X*-*)                                                     CRK 714
1400 FORMAT   ( 4(/), 15X *LOAD* 5X *MATERIAL* 8X *VERTICAL  STRESS*        CRK 715
     1         7X *TANGENTIAL STRESS* /  40X, 2(*TOP* 7X *BOTTOM*7X))      CRK 716
1410 FORMAT   ( 2 (3F10.0) )                                                CRK 717
1420 FORMAT   (1H1,3(/),23X, *RADIAL* 4X, 2(*......*A10*,......*2X)/        CRK 718
     1         7X,  *LOAD  MATERIAL  PRESSURE*2X, 2(*VERTICAL *            CRK 719
     2         *STRESS  RADIAL*2X)/ 23X *(INPUT)* 3X, 2(*MEAN* 5X          CRK 720
     3         *DESIGN  STRESS*2X)//F10.0,  4(/,11X, A10,                  CRK 721
     4         11X, 3F8.3, 1X, 3F8.3  ))                                   CRK 722
1421 FORMAT   (11X, A10, F8.3, 3X, 3F8.3, 1X, 3F8.3/ )                      CRK 723
1430 FORMAT   ( 4(/), 9X, 3(*......*A10*,......*2X)/, 9X, 3(*VER*           CRK 724
     1         *TICAL STRESS  RADIAL*2X)/, 9X, 3(*MEAN* 5X*DESIGN*         CRK 725
     2         *  STRESS* 2X) // 4( 8X, 3F8.3, 1X, 3F8.3, 1X, 3F8.3/))     CRK 726
1440 FORMAT   (4(/), 9X, *.....*A10*.....* / 9X *VERTICAL STRESS*           CRK 727
     1         *  RADIAL* / 9X *MEAN* 5X *DESIGN  STRESS*//                 CRK 728
     2         4(8X,3F8.3/))                                               CRK 729
1450 FORMAT   (1H1,4(/),5X, *YEAR*I3,/15X, 6(A10,1X)/, 5X*HI-LO-REPT*)      CRK 730
1460 FORMAT   ( 5X, A10,  6(E11.3))                                         CRK 731
1470 FORMAT   ( 5X*CUMULATIVE*)                                             CRK 732
1480 FORMAT   ( 5X, *STRAIN TO BEGINNING OF MONTH *)                        CRK 733
1490 FORMAT   (  5X, A10, 6E11.3 )                                          CRK 734
1500 FORMAT   ( 5X, *STRAIN THROUGH MONTH*)                                 CRK 735
1510 FORMAT   (5X, *DEPTH*, 5 ( / 5X, A10, F11.1 ))                         CRK 736
1520 FORMAT   (5X*VERT. DSP.*6E11.3/ 5X*V  STRESS *6E11.3/                  CRK 737
     1         5X*R  STRESS *6E11.3)                                       CRK 738
1530 FORMAT   ( 5X, *DEFORMATION AT MONTH N* )                              CRK 739
1540 FORMAT   (5X, *DEFORMATION DUE TO REPITIONS THROUGH MONTH (N-1)*)      CRK 740
1550 FORMAT   ( 5X, *DEFORMATION AT MONTH N - DEFORMATION AT MONTH N-1*     CRK 741
     1)                                                                     CRK 742
1560 FORMAT   ( 5X, *CUMULATIVE DEFORMATION  THROUGH MONTH N* )             CRK 743
1570 FORMAT   ( 5X, *TOTAL CUMULATIVE DEFORMATION     RUT DEPTH*/           CRK 744
     1          15X, 6E11.3)                                               CRK 745
      END                                                                   CRK 746
```

```
      SUBROUTINE LAYER (IK, IZ)                                             CRK 747
      COMMON /LAY/ EE(5, 12), V(5), NS, TMIN(5), IM, NL, A(20),             CRK 748
     1       TIRE(20), EA(5, 12), DRCB(5), DZOB(5), RO(5), EM(5),           CRK 749
     2       DRC(5)                                                         CRK 750
      COMMON /PRIN/ AN1(13, 5, 20), AN2(13, 5, 20), AN3(13, 5, 20),         CRK 751
     1       DSP(12, 3), N18, LOAD(20), MAT(5), MONTH(12)                   CRK 752
      DIMENSION ZZ(11), E(5), H(4), HH(4), AZ(400), AJ(400)                 CRK 753
      REAL LOAD                                                             CRK 754
C         LAYER DOES CALCULATIONS FOR EACH DEPTH, MEAN AND                  CRK 755
C         CONFIDENCE VALUES OF ELASTIC MODULUS, EITHER ONE                  CRK 756
C         OR TWELVE MONTHS, AND FINALLY FOR EACH LOAD GROUP                 CRK 757
                N = NS-1                                                    CRK 758
C  ** START ON A NEW R **                                                   CRK 759
                R = 0.0                                                     CRK 760
                ITN = 46                                                    CRK 761
                ITN4 = ITN*4                                                CRK 762
          DO 220 M = 1, NL                                                  CRK 763
          IF (IZ-1)  5, 1, 5                                                CRK 764
     1    IF (IK-1)  2, 2, 3                                               CRK 765
     2  PRINT 240, LOAD(M)                                                 CRK 766
          GO TO 5                                                           CRK 767
     3    PRINT 230, LOAD(M), TMIN(1), MONTH                               CRK 768
     5              MT = M                                                 CRK 769
                    AR = A(M)                                               CRK 770
                    ARF = AR*TIRE(M)                                        CRK 771
                    ZZ(1) = TMIN(1)                                         CRK 772
C  ** ADJUST LAYER DEPTHS **                                                CRK 773
                    HH(1) = TMIN(1)                                         CRK 774
                    H(1) = HH(1)                                            CRK 775
          DO 10 I = 2, N                                                    CRK 776
                    HH(I) = TMIN(I)                                         CRK 777
    10              H(I) = H(I-1)+HH(I)                                     CRK 778
          DO 20 I = 1, IZ                                                   CRK 779
    20              ZZ(I) = H(I)                                            CRK 780
          DO 220 IE = 1, 2                                                  CRK 781
          DO 210 MM = 1, IK                                                 CRK 782
                    MN = 0                                                  CRK 783
                    MMT = MM                                                CRK 784
          IF (IE-1) GO TO 40                                                CRK 785
          DO 30 I = 1, NS                                                   CRK 786
    30              E(I) = EE(I, MM)                                        CRK 787
          GO TO 70                                                          CRK 788
    40    IF (IZ-1) 50,50,220                                               CRK 789
    50    DO 60 I = 1, NS                                                   CRK 790
    60              E(I) = EA(I, MM)                                        CRK 791
    70    CONTINUE                                                          CRK 792
          DO 90 I = 1, IZ                                                   CRK 793
          DO 90 J = 1, N                                                    CRK 794
                    TZ = ABS(H(J)-ZZ(I))                                    CRK 795
          IF (TZ-.0001) 80,80,90                                            CRK 796
    80              ZZ(I) = -H(J)                                           CRK 797
    90    CONTINUE                                                          CRK 798
          IF ((MN .EQ. 0) .AND. (IZ .GT. 1)) ZZ(1) = -ZZ(1)                 CRK 799
C  ** CALCULATE THE PARTITION **                                            CRK 800
          CALL PART (NTEST, AZ, ITN, AR)                                    CRK 801
C  ** CALCULATE THE COEFFICIENTS **                                         CRK 802
          DO 100 I = 1, ITN4                                                CRK 803
                    IT = I                                                  CRK 804
```

```
            P = AZ(I)
      CALL COEE (IT, N, E, V, H, NS, P)
            PA = P*AR
      CALL BESSEL (1, PA, Y)
            AJ(I) = Y
  100       CONTINUE
            NX = 0
            IZT = 0
C  ** START ON A NEW Z **
  110       IZT = IZT+1
      IF (IZT-IZ) 120,120,200
  120       Z = ABS(ZZ(IZT))
C  ** FIND THE LAYER CONTAINING Z **
            TZZ = 0.0
      DO 130 J1 = 1, N
            J = NS-J1
      IF (Z-H(J)) 130,140,140
  130       CONTINUE
            L = 1
      GO TO 160
  140       L = J+1
      IF (ZZ(IZT)) 150,160,160
  150       L = J
            TZZ = 1.0
  160       CONTINUE
      CALL CALCIN (V, E, NTEST, ARP, ITN, AZ, Z, R, AJ, IK, IZ,
     1      IM, MPT, L, AR, TZZ, NX, MT, IZT, MN, IE)
      IF (IZ-1) 190,190,170
  170       CONTINUE
      IF (TZZ) 190,190,180
  180       ZZ(IZT) = -ZZ(IZT)
      IF (IZ .EQ. IZT) NX = 1
C     NA = 1    SUBGRADE CALCULATIONS
            IZT = IZT-1
  190       CONTINUE
      GO TO 110
  200       CONTINUE
  210       CONTINUE
  220       CONTINUE
      RETURN
  230 FORMAT  ( 4(/), 50X *TANGENTIAL STRAIN*/ 15X *LOAD*
     1        F5.0, 3X, *DEPTH* F5.0/ 10X, 6A10/ 15X, 6A10)
  240 FORMAT  ( 10X, F5.0 )
      END
```

```
      SUBROUTINE CALCIN (V, E, NTEST, ARP, ITN, AZ, Z, R, AJ, IK,
     1      IZ, IM, MN, L, AR, TZZ, NX, M, ITZ, MN, IE)
CCALCIN *****SUBROUTINE CALCIN - N-LAYER ELASTIC SYSTEM ******
      COMMON /COECAL/ A(400, 5), B(400, 5), C(400, 5), D(400, 5)
      DIMENSION E(5), V(5), AZ(400), AJ(400), TEST(11), W(4), ANS(12),
     1      XA(5)S(12,11)
      COMMON /CAL/ IW, IDX(20),
      COMMON /PRIN/ AN1(13, 5, 20), AN2(13, 5, 20), AN3(13, 5, 20),
     1      DSP(12, 3), N18, LOAD(20), MAT(5), MONTH(12)
      REAL LOAD
   10       W(1) = 0.34785485
            W(2) = 0.65214515
            W(3) = W(2)
            W(4) = W(1)
            VL = 2.0*V(L)
            EL = (1.0+V(L))/E(L)
            VL1 = 1.0-VL
            CSZ = 0.0
            CST = 0.0
            CSR = 0.0
            CTR = 0.0
            COM = 0.0
            CML = 0.0
            NTS1 = NTEST+1
            ITS = 1
        DO 80 I = 1, ITN
C     INITIALIZE THE SUB-INTEGRALS
            RSZ = 0.0
            RST = 0.0
            RSR = 0.0
            RTR = 0.0
            ROM = 0.0
            RML = 0.0
C     COMPUTE THE SUB-INTEGRALS
            K = 4*(I-1)
        DO 20 J = 1, 4
            J1 = K+J
            P = AZ(J1)
            EP = EXP(P*Z)
            T1 = B(J1, L)*EP
            T2 = D(J1, L)/EP
            T1P = T1+T2
            T1M = T1-T2
            T1 = (A(J1, L)+B(J1, L)*Z)*EP
            T2 = (C(J1, L)+D(J1, L)*Z)/EP
            T2P = P*(T1+T2)
            T2M = P*(T1-T2)
            WA = AJ(J1)*W(J)
C     SPECIAL ROUTINE FOR R = ZERO
            PP = P*P
            RSZ = RSZ+WA*PP*(VL1*T1P-T2M)
            ROM = ROM+WA*EL*P*(2.0*VL1*T1M-T2P)
            RST = RST+WA*PP*((VL*0.5)*T1P+0.5*T2M)
            RSR = RST
   20       CONTINUE
C
            SF = (AZ(K+4)-AZ(K+1))/1.7272726
            CSZ = CSZ+RSZ*SF
```

```
            CST = CST*RST*SF                                              CRK 907
            CSR = CSR*RSH*SF                                              CRK 908
            CTR = CTR*RTH*SF                                              CRK 909
            COM = COM*ROM*SF                                              CRK 910
            CML = CMU*RMU*SF                                              CRK 911
            RSZ = 2.0*RSZ*AR*SF                                           CRK 912
            TESTH = ABS(RSZ)-10.0**(-4)                                   CRK 913
        IF (ITS-NTS1) 30,40,40                                            CRK 914
30      CONTINUE                                                          CRK 915
            TEST(ITS) = TESTH                                             CRK 916
            ITS = ITS+1                                                   CRK 917
        GO TO 80                                                          CRK 918
40      CONTINUE                                                          CRK 919
            TEST(NTS1) = TESTH                                            CRK 920
        DO 70 J = 1, NTEST                                                CRK 921
        IF (TESTH-TEST(J)) 50,60,60                                       CRK 922
50      CONTINUE                                                          CRK 923
            TESTH = TEST(J)                                               CRK 924
60      CONTINUE                                                          CRK 925
            TEST(J) = TEST(J+1)                                           CRK 926
70      CONTINUE                                                          CRK 927
        IF (TESTH) 90,90,80                                               CRK 928
80      CONTINUE                                                          CRK 929
90          CSZ = CSZ*ARP                                                 CRK 930
            CST = CST*ARP                                                 CRK 931
            CTR = CTR*ARP                                                 CRK 932
            CSR = CSR*ARP                                                 CRK 933
            COM = COM*ARP                                                 CRK 934
            CML = CMU*ARP                                                 CRK 935
            BSTS = CSZ+CST+CSR                                            CRK 936
            RSTN = (CSR-V(L)*(CST+CSZ))/E(L)                              CRK 937
            TSTN = (CST-V(L)*(CSR+CSZ))/E(L)                              CRK 938
C       STRESSES  --  CSZ  VERTICAL     CST  TANGENTIAL                   CRK 939
C                     CSR  RADIAL       CTR  SHEAR    BSTS  BULK          CRK 940
C       STRAINS       RSTN RADIAL       TSTN TANGENTIAL                   CRK 941
C                     CMU  SHEAR                                          CRK 942
C                     COM  VERTICAL DISPLACEMENT                          CRK 943
        IF (IZ-1) 100,100,170                                             CRK 944
C                                                                         CRK 945
C       IZ = 1    PART ONE    CRACKING INDEX                              CRK 946
C       IZ NOT 1  PART TWO    RUT DEPTH                                   CRK 947
C                                                                         CRK 948
100         ANS(MN) = TSTN                                                CRK 949
        IF (TZZ) 120,120,110                                              CRK 950
110         Z = -Z                                                        CRK 951
120     CONTINUE                                                          CRK 952
        IF (MM-IK) 130,140,140                                            CRK 953
130 RETURN                                                                CRK 954
140         IW = IW+1                                                     CRK 955
    CALL IOBIN (6HWRITER, Z, ANS(1), IW, IDX(IW))                         CRK 956
        IF (IW-1) 150,150,155                                             CRK 957
150     IF (IE.EQ.1)  PRINT 330, Z, ANS(1)                                CRK 958
        IF (IE.NE.1)  PRINT 335, Z, ANS(1)                                CRK 959
    RETURN                                                                CRK 960
155     IF (IE-1)  160, 160, 165                                          CRK 961
160 PRINT 340, ANS                                                        CRK 962
    RETURN                                                                CRK 963
165 PRINT 345, ANS                                                        CRK 964
    RETURN                                                                CRK 965
C                                                                         CRK 966
C                   PART TWO                                              CRK 967
170     CONTINUE                                                          CRK 968
C                                                                         CRK 969
C       M         LOAD GROUP INDEX                                        CRK 970
            LTZ = TZZ                                                     CRK 971
            ITZL = ITZ - LTZ                                              CRK 972
            AN1(MM, ITZL, M) = AN1(MM, ITZL, M)*CSZ/2.0                   CRK 973
            AN3(MM, ITZL, M) = AN3(MM, ITZL, M)*CSR/2.0                   CRK 974
C       IK        EITHER 1 OR 12                                          CRK 975
C       IK = 1    NO MONTHLY VARIATIONS ON E                              CRK 976
C       IK GT 1   MONTHLY VARIATIONS MUST BE ACCUMULATED                  CRK 977
C       MM        INDEX VARYING FROM 1 TO IK                              CRK 978
C       MM = IK   CALCULATIONS COMPLETE                                   CRK 979
C       IZ        NUMBER OF LAYERS MINUS 1                                CRK 980
        IF ((NX .EQ. 1) .AND. (M .EQ. N18)) GO TO 180                     CRK 981
        GO TO 190                                                         CRK 982
180         DSP(MM, 1) = COM                                              CRK 983
            DSP(MM, 2) = CSZ                                              CRK 984
            DSP(MM, 3) = CSR                                              CRK 985
190     CONTINUE                                                          CRK 986
C       DSP(MONTH, I)   VALUE AT SUBGRADE DUE TO 18-KIP LOAD              CRK 987
C                   I = 1     VERTICAL DISPLACEMENT                       CRK 988
C                   I = 2     VERTICAL STRESS                             CRK 989
C                   I = 3     RADIAL STRESS                               CRK 990
C                                                                         CRK 991
        IF (MM-IK) 260,200,200                                            CRK 992
200     CONTINUE                                                          CRK 993
C                                                                         CRK 994
C       NO MONTHLY VARIATIONS IN ELASTIC MODULUS                          CRK 995
        IF (IK-1) 210,210,260                                             CRK 996
210         MN = MN+1                                                     CRK 997
            ANS(MN) = CSZ                                                 CRK 998
        IF (NX-1) 220,250,220                                             CRK 999
220     CONTINUE                                                          CRK1000
            ANS(MN+2) = CSR                                               CRK1001
        IF (MN-2) 230,240,240                                             CRK1002
230 RETURN                                                                CRK1003
240         MN = 0                                                        CRK1004
    PRINT 350, LOAD(M), MAT(ITZ), (ANS(I), I = 1, 4)                      CRK1005
    RETURN                                                                CRK1006
C                                                                         CRK1007
C                   ANS(1) = VERTICAL STRESS AT TOP OF LAYER              CRK1008
C                   ANS(3) =                 AT BOTTOM OF LAYER           CRK1009
C                   ANS(2) = RADIAL STRESS AT TOP OF LAYER                CRK1010
C                   ANS(4) =                 AT BOTTOM OF LAYER           CRK1011
C                                                                         CRK1012
C       SUBGRADE (NO BOTTOM OF LAYER)                                     CRK1013
250         ANS(MN+1) = CSR                                               CRK1014
            MN = 0                                                        CRK1015
    PRINT 360, LOAD(M), MAT(ITZ+1), ANS(1), ANS(2)                        CRK1016
    RETURN                                                                CRK1017
C                                                                         CRK1018
C                                                                         CRK1019
C       MONTHLY VARIATIONS IN ELASTIC MODULUS                             CRK1020
260     IF (MM-1) 270,270,280                                             CRK1021
C       FIRST MONTH INITIALIZATION                                        CRK1022
```

```
270           II = 0
280           II = II+1
              MN = MN+1
C
              XANS(II, MN) = CSZ
          IF (NX .EQ. 1) XANS(II, MN+1) = CSR
              XANS(II, MN+2) = CSR
          IF ((II .EQ. 12) .AND. (NX .EQ. 1)) GO TO 290
      RETURN
290       CONTINUE
C
C         VALUES ARE PRINTED IN BLOCKS OF SIX MONTHS
C
              J = 0
              IZ1 = IZ-1
          DO 310 I = 1, IZ1
              J = J+1
              JP = J+3
          DO 300 K = 1, 12, 6
              KK = K+5
      PRINT 370, (MONTH(KI), KI = K, KK), MAT(I+1)
      PRINT 380, ((XANS(NI, MX), NI = K, KK), MX = J, JP)
300       CONTINUE
              J = JP
310       CONTINUE
C
C         PRINT SUBGRADE VALUES
              J = J+1
              J1 = J+1
          DO 320 K = 1, 12, 6
              KK = K+5
      PRINT 370, (MONTH(KI), KI = K, KK), MAT(IZ+1)
      PRINT 390, ((XANS(NI, MX), NI = K, KK), MX = J, J1)
320       CONTINUE
      RETURN
C
330   FORMAT    ( 10X, *MEAN VALUE*, 4X, F6.2, 8X, E10.3 )
335   FORMAT    ( 10X, *CONF VALUE*, 4X, F6.2, 8X, E10.3 )
340   FORMAT    ( 15X,*MEAN VALUES*/10X,6E10.3/15X,6E10.3 )
345   FORMAT    ( 15X,*CONFIDENCE VALUES*/10X,6E10.3/15X,6E10.3 )
350   FORMAT    ( 14X, F4.0, 4X, A10, 6X, 2E10.2, 3X, 2E10.2)
360   FORMAT    ( 14X, F4.0, 4X, A10, 6X, E10.2, 13X, E10.2 )
370   FORMAT    ( 24X, 6A10  / 13X, A10  )
380   FORMAT    ( 19X *VERT* / 18X*TOP*  4X, 6E10.3 / 18X *BOTTOM *
     1          6E10.3 / 19X*RADIAL*/ 18X *TOP*  4X,6E10.3/ 18X
     2          *BOTTOM*  6E10.3 /)
390   FORMAT    ( 19X *VERT*  2X, 6E10.3  / 19X  *RAD    * 6E10.3//)
      END
```

```
CRK1023
      SUBROUTINE PART (NTEST, AZ, ITN, AR)                                  CRK1071
      DIMENSION AZ(400), BZ(400)                                            CRK1072
CPART   ******SUBROUTINE PART - 5-LAYER ELASTIC SYSTEM ******               CRK1073
C         ** COMPUTE ZEROS OF J1(X) AND J0(X), SET UP GAUSS CONSTANTS **    CRK1074
 10           BZ(1) = 0.0                                                   CRK1075
              BZ(2) = 1.0                                                   CRK1076
              BZ(3) = 2.40048                                               CRK1077
              BZ(4) = 3.8317                                                CRK1078
              BZ(5) = 5.5201                                                CRK1079
              BZ(6) = 7.01556                                               CRK1080
              K = ITN+1                                                     CRK1081
          DO 20 I = 7, K, 2                                                 CRK1082
              T = 1/2                                                       CRK1083
              TD = 4.0*T-1.0                                                CRK1084
 20           BZ(I) = 3.1415927*(T-0.25+0.050661/TD-0.053041/TD             CRK1085
     1             **3+0.262051/TD**5)                                      CRK1086
          DO 30 I = 8, ITN, 2                                               CRK1087
              T = (I-2)/2                                                   CRK1088
              TD = 4.0*T+1.0                                                CRK1089
 30           BZ(I) = 3.1415927*(T+0.25-0.151982/TD+0.0153999/TD            CRK1090
     1             **3-0.245270/TD**5)                                      CRK1091
              G1 = 0.8611363                                                CRK1092
              G2 = 0.33998104                                               CRK1093
              ZF = AR                                                       CRK1094
              NTEST = 2                                                     CRK1095
C         ** COMPUTE POINTS FOR LEGENDRE-GAUSS INTEGRATION **               CRK1096
              K = 1                                                         CRK1097
              ZF = 2.0*ZF                                                   CRK1098
              SZ2 = 0.0                                                     CRK1099
          DO 40 I = 1, ITN                                                  CRK1100
              SZ1 = SZ2                                                     CRK1101
              SZ2 = BZ(I+1)/ZF                                              CRK1102
              SF = SZ2-SZ1                                                  CRK1103
              PM = SZ2+SZ1                                                  CRK1104
              SG1 = SF*G1                                                   CRK1105
              SG2 = SF*G2                                                   CRK1106
              AZ(K) = PM-SG1                                                CRK1107
              AZ(K+1) = PM+SG2                                              CRK1108
              AZ(K+2) = PM+SG2                                              CRK1109
              AZ(K+3) = PM+SG1                                              CRK1110
              K = K+4                                                       CRK1111
 40       CONTINUE                                                          CRK1112
      RETURN                                                                CRK1113
      END                                                                   CRK1114
CRK1065
CRK1066
CRK1067
CRK1068
CRK1069
CRK1070
```

```
      FUNCTION POLY (CM, A, K, DVS)                                     CRK1115
C                                                                       CRK1116
C     NS        NUMBER OF MATERIALS                                     CRK1117
C     K         MATERIAL NUMBER UNDER CONSIDERATION                     CRK1118
C     A         DESIGN VERTICAL STRESS                                  CRK1119
C     CM        CUMULATIVE EQUIVALENT 18-KIP AXLE APPLICATIONS          CRK1120
C     DVS       DESIGN RADIAL STRESS                                    CRK1121
C                                                                       CRK1122
      GO TO (423,413,403), K                                            CRK1123
C     SUBGRADE                                                          CRK1124
403   S1 = -A$ALN = ALOG10(CM)                                          CRK1125
      E = 0.34561*S1-0.04064*S1*ALN-0.06511*S1*S1+0.00283               CRK1126
     1     *S1**3.0+0.00744*S1*S1*ALN                                   CRK1127
      POLY = AMAX1(E, 0.0)                                              CRK1128
      RETURN                                                            CRK1129
C                                                                       CRK1130
C     BASE                                                              CRK1131
413   CONTINUE                                                          CRK1132
      S1 = -A$S3 = -DVS                                                 CRK1133
      ALN = ALOG10(CM)$ALN2 = ALN**2                                    CRK1134
      E = 0.57852-0.20640*S3+0.07854*S1-0.01464*S3*ALN                  CRK1135
     1     -0.00121*S1*ALN-0.00408*S1*S3+0.03846*ALN2-0.00093           CRK1136
     2     *S1*S1-0.00062*ALN*S3*S3-0.00292*ALN*ALN2+0.00204            CRK1137
     3     *S3**3+0.0001*S1**3-0.0004*S3*S3*S1+0.00006                  CRK1138
     4     *S1*S1*S3+0.00046*S1*S3*ALN                                  CRK1139
      POLY = AMAX1(E, 0.0)                                              CRK1140
      RETURN                                                            CRK1141
423   S1 = -A$S3 = -DVS                                                 CRK1142
      ALN = ALOG10(CM)$ALN2 = ALN*ALN                                   CRK1143
      E = -0.75465+0.25605*ALN+0.17009*S1-0.14433*ALN*S3                CRK1144
     1     +0.01187*ALN*S1+0.01139*S1*S3+0.04947*S3*S3                  CRK1145
     2     -0.01132*S1*S1+0.03340*ALN*S3*S3+0.00115*ALN                 CRK1146
     3     *S1*S1-0.01885*S3**3+0.00025*S1**3+0.00367*S3                CRK1147
     4     *S3*S1-0.00072*S1*S1*S3-0.01018*S1*S3*ALN                    CRK1148
      POLY = AMAX1(E, 0.0)                                              CRK1149
      RETURN                                                            CRK1150
      END                                                               CRK1151
```

```
      FUNCTION XNORM (X, MU, SIGMA)                                     CRK1152
      REAL MU                                                           CRK1153
      Z = X+0.005                                                       CRK1154
      A = 0.0                                                           CRK1155
10    A = A+0.01*EXP(-Z*Z/2.)/(2.*3.1415926)**0.5                       CRK1156
      Z = Z+0.01                                                        CRK1157
      IF (Z-5.0) 10,10,20                                               CRK1158
20    XNORM = A                                                         CRK1159
      RETURN                                                            CRK1160
      END                                                               CRK1161
```

```
      FUNCTION ALPHA (CONF)                                             CRK1162
      A = 0.5-CONF                                                      CRK1163
      C = 0.0                                                           CRK1164
      DELT = 0.0001                                                     CRK1165
      Z = 0.00005                                                       CRK1166
   10 C = C+DELT*EXP(-Z*Z/2.)/(SQRT(2.*3.1415926))                      CRK1167
      IF (C-ABS(A)) 20,30,30                                            CRK1168
   20 Z = Z+DELT                                                        CRK1169
      GO TO 10                                                          CRK1170
   30 AA = DELT/2.0+Z                                                   CRK1171
      IF (A) 50,40,40                                                   CRK1172
   40 ALPHA = AA                                                        CRK1173
      RETURN                                                            CRK1174
   50 ALPHA = -AA                                                       CRK1175
      RETURN                                                            CRK1176
      END                                                               CRK1177
```

```
      SUBROUTINE COEE (KIN, N, E, V, H, NS, P)                          CRK1178
CCOEE   ******SUBROUTINE COEE - 5-LAYER ELASTIC SYSTEM ******           CRK1179
      COMMON /COECAL/ A(400, 5), B(400, 5), C(400, 5), D(400, 5)        CRK1180
      DIMENSION E(5), V(5), H(4), X(5,5,4), SC(4), PM(4,4,4), FM(2,2)   CRK1181
      DIMENSION SV1(4,2), CV1(2,1), SV2(4,4), CV2(2,2), SV3(4,8), CV3(2,CRK1182
     14), SV4(4,16), CV4(2,8), T(8), NT(4)                              CRK1183
            LC = KIN                                                    CRK1184
CS-MK      SET UP MATRIX X =DI*MI*KI*K*M*D                             CRK1185
C     COMPUTE THE MATRICES X(K)                                         CRK1186
      DO 10 K = 1, N                                                    CRK1187
            T1 = E(K)*(1.0+V(K+1))/(E(K+1)*(1.0+V(K)))                  CRK1188
            T1P = T1-1.0                                                CRK1189
            PM = P*H(K)                                                 CRK1190
            PM2 = PM**2.0                                               CRK1191
            VK2 = 2.0*V(K)                                              CRK1192
            VKP2 = 2.0*V(K+1)                                           CRK1193
            VK4 = 2.0*VK2                                               CRK1194
            VKP4 = 2.0*VKP2                                             CRK1195
            VKK8 = 8.0*V(K)*V(K+1)                                      CRK1196
C                                                                       CRK1197
            X(K, 1, 1) = VK4-3.0-T1                                     CRK1198
            X(K, 2, 1) = 0.0                                            CRK1199
            X(K, 3, 1) = T1M*(PM2-VK4+1.0)                              CRK1200
            X(K, 4, 1) = -2.0*T1M*P                                     CRK1201
C                                                                       CRK1202
            T3 = PM2*(VK2-1.0)                                          CRK1203
            T4 = VKK8+1.0-3.0*VKP2                                      CRK1204
            T5 = PM2*(VKP2-1.0)                                         CRK1205
            T6 = VKK8+1.0-3.0*VK2                                       CRK1206
C                                                                       CRK1207
            X(K, 1, 2) = (T3+T4-T1*(T5+T6))/P                           CRK1208
            X(K, 2, 2) = T1*(VKP4-3.0)-1.0                              CRK1209
            X(K, 4, 2) = T1M*(1.0-PM2-VKP4)                             CRK1210
C                                                                       CRK1211
            X(K, 3, 4) = (T3-T4-T1*(T5-T6))/P                           CRK1212
C                                                                       CRK1213
            T3 = PM2*PM-VKK8+1.0                                        CRK1214
            T4 = PM2*(VK2-VKP2)                                         CRK1215
C                                                                       CRK1216
            X(K, 1, 4) = (T3+T4+VKP2-T1*(T3+T4+VK2))/P                  CRK1217
            X(K, 3, 2) = (-T3+T4-VKP2+T1*(T3-T4+VK2))/P                 CRK1218
C                                                                       CRK1219
            X(K, 1, 3) = T1M*(1.0-PM2-VK4)                              CRK1220
            X(K, 2, 3) = 2.0*T1M*P                                      CRK1221
            X(K, 3, 3) = VK4-3.0-T1                                     CRK1222
            X(K, 4, 3) = 0.0                                            CRK1223
C                                                                       CRK1224
            X(K, 2, 4) = T1M*(PM2-VKP4+1.0)                             CRK1225
            X(K, 4, 4) = T1*(VKP4-3.0)-1.0                              CRK1226
            K = K                                                       CRK1227
   10 CONTINUE                                                          CRK1228
C     COMPUTE THE PRODUCT MATRICES PM                                   CRK1229
            SC(N) = 4.0*(V(N)-1.0)                                      CRK1230
      IF (N-2) 40,20,20                                                 CRK1231
   20 DO 30 K1 = 2, N                                                   CRK1232
            M = NS-K1                                                   CRK1233
            SC(M) = SC(M+1)*4.0*(V(M)-1.0)                              CRK1234
   30 CONTINUE                                                          CRK1235
```

```
 40     CONTINUE                                                          CRK1236
C                                                                        CRK1237
            K = N                                                        CRK1238
       DO 60 I = 1, 4                                                    CRK1239
       DO 50 J = 1, 2                                                    CRK1240
 50        SV1(I, J) = X(K, I, J+2)                                       CRK1241
 60    CONTINUE                                                          CRK1242
            CV1(1, 1) = -2.0*P*H(K)                                      CRK1243
            CV1(2, 1) = 0.0                                              CRK1244
            K = K-1                                                      CRK1245
       IF (K) 200,200,70                                                 CRK1246
C                                                                        CRK1247
 70    CONTINUE                                                          CRK1248
       DO 90 J = 1, 2                                                    CRK1249
            J1 = J+J                                                     CRK1250
            T(1) = SV1(1, J)                                             CRK1251
            T(2) = SV1(2, J)                                             CRK1252
            T(3) = SV1(3, J)                                             CRK1253
            T(4) = SV1(4, J)                                             CRK1254
       DO 80 I = 1, 4                                                    CRK1255
            SV2(I, J1-1) = X(K, I, 1)*T(1)+X(K, I, 2)*T(2)               CRK1256
 80         SV2(I, J1) = X(K, I, 3)*T(3)+X(K, I, 4)*T(4)                 CRK1257
 90    CONTINUE                                                          CRK1258
            T(1) = CV1(1, 1)                                             CRK1259
            T(2) = -2.0*P*H(K)                                           CRK1260
            CV2(1, 1) = T(1)                                             CRK1261
            CV2(1, 2) = T(2)                                             CRK1262
            CV2(2, 1) = T(1)*T(2)                                        CRK1263
            CV2(2, 2) = 0.0                                              CRK1264
            K = K-1                                                      CRK1265
       IF (K) 200,200,100                                                CRK1266
C                                                                        CRK1267
100    CONTINUE                                                          CRK1268
       DO 140 J = 1, 4                                                   CRK1269
            J1 = J                                                       CRK1270
       IF (J1-2) 120,120,110                                             CRK1271
110         J1 = J1+2                                                    CRK1272
120    CONTINUE                                                          CRK1273
            T(1) = SV2(1, J)                                             CRK1274
            T(2) = SV2(2, J)                                             CRK1275
            T(3) = SV2(3, J)                                             CRK1276
            T(4) = SV2(4, J)                                             CRK1277
       DO 130 I = 1, 4                                                   CRK1278
            SV3(I, J1) = X(K, I, 1)*T(1)+X(K, I, 2)*T(2)                 CRK1279
130         SV3(I, J1+2) = X(K, I, 3)*T(3)+X(K, I, 4)*T(4)               CRK1280
140    CONTINUE                                                          CRK1281
            T(1) = -2.0*P*H(K)                                           CRK1282
       DO 150 J = 1, 2                                                   CRK1283
            CV3(1, J) = CV2(1, J)                                        CRK1284
            CV3(2, J) = CV2(1, J)-T(1)                                   CRK1285
            CV3(1, J+2) = CV2(2, J)*T(1)                                 CRK1286
            CV3(2, J+2) = CV2(2, J)                                      CRK1287
150    CONTINUE                                                          CRK1288
            K = K-1                                                      CRK1289
       IF (K) 200,200,160                                                CRK1290
C                                                                        CRK1291
160    CONTINUE                                                          CRK1292
       DO 180 J = 1, 4                                                   CRK1293
            T(1) = SV3(1, J)                                             CRK1294
            T(2) = SV3(2, J)                                             CRK1295
            T(3) = SV3(3, J)                                             CRK1296
            T(4) = SV3(4, J)                                             CRK1297
            T(5) = SV3(1, J+4)                                           CRK1298
            T(6) = SV3(2, J+4)                                           CRK1299
            T(7) = SV3(3, J+4)                                           CRK1300
            T(8) = SV3(4, J+4)                                           CRK1301
       DO 170 I = 1, 4                                                   CRK1302
            SV4(I, J) = X(K, I, 1)*T(1)+X(K, I, 2)*T(2)                  CRK1303
            SV4(I, J+4) = X(K, I, 3)*T(3)+X(K, I, 4)*T(4)                CRK1304
            SV4(I, J+8) = X(K, I, 1)*T(5)+X(K, I, 2)*T(6)                CRK1305
170         SV4(I, J+12) = X(K, I, 3)*T(7)+X(K, I, 4)*T(8)               CRK1306
180    CONTINUE                                                          CRK1307
            T(1) = -2.0*P*H(K)                                           CRK1308
       DO 190 J = 1, 4                                                   CRK1309
            CV4(1, J) = CV3(1, J)                                        CRK1310
            CV4(2, J) = CV3(1, J)-T(1)                                   CRK1311
            CV4(1, J+4) = CV3(2, J)*T(1)                                 CRK1312
            CV4(2, J+4) = CV3(2, J)                                      CRK1313
190    CONTINUE                                                          CRK1314
C                                                                        CRK1315
200    CONTINUE                                                          CRK1316
            NT(1) = 1                                                    CRK1317
       DO 210 K = 2, N                                                   CRK1318
210         NT(K) = NT(K-1)+NT(K-1)                                      CRK1319
       DO 370 K = 1, N                                                   CRK1320
            K1 = NS-K                                                    CRK1321
       DO 220 I = 1, 4                                                   CRK1322
            PM(K1, I, 1) = 0.0                                           CRK1323
            PM(K1, I, 2) = 0.0                                           CRK1324
220    CONTINUE                                                          CRK1325
            I1 = NT(K)                                                   CRK1326
       DO 370 I = 1, I1                                                  CRK1327
            I2 = I+I1                                                    CRK1328
       GO TO (230,240,250,260), K                                        CRK1329
230    CONTINUE                                                          CRK1330
            T(3) = CV1(1, I)                                             CRK1331
            T(4) = CV1(2, I)                                             CRK1332
       GO TO 270                                                         CRK1333
240    CONTINUE                                                          CRK1334
            T(3) = CV2(1, I)                                             CRK1335
            T(4) = CV2(2, I)                                             CRK1336
       GO TO 270                                                         CRK1337
250    CONTINUE                                                          CRK1338
            T(3) = CV3(1, I)                                             CRK1339
            T(4) = CV3(2, I)                                             CRK1340
       GO TO 270                                                         CRK1341
260    CONTINUE                                                          CRK1342
            T(3) = CV4(1, I)                                             CRK1343
            T(4) = CV4(2, I)                                             CRK1344
270    CONTINUE                                                          CRK1345
            T(1) = 0.0                                                   CRK1346
            T(2) = 0.0                                                   CRK1347
       IF (T(3)+68.0) 290,280,280                                        CRK1348
280         T(1) = EXP(T(3))                                             CRK1349
290    IF (T(4)+68.0) 310,300,300                                        CRK1350
300         T(2) = EXP(T(4))                                             CRK1351
```

```
310       CONTINUE                                                      CRK1352
          DO 370 J = 1, 2                                               CRK1353
          GO TO (320,330,340,350), K                                    CRK1354
320       CONTINUE                                                      CRK1355
               T(3) = SV1(J, I)                                         CRK1356
               T(4) = SV1(J, I2)                                        CRK1357
               T(5) = SV1(J+2, I)                                       CRK1358
               T(6) = SV1(J+2, I2)                                      CRK1359
          GO TO 360                                                     CRK1360
330            T(3) = SV2(J, I)                                         CRK1361
               T(4) = SV2(J, I2)                                        CRK1362
               T(5) = SV2(J+2, I)                                       CRK1363
               T(6) = SV2(J+2, I2)                                      CRK1364
          GO TO 360                                                     CRK1365
340            T(3) = SV3(J, I)                                         CRK1366
               T(4) = SV3(J, I2)                                        CRK1367
               T(5) = SV3(J+2, I)                                       CRK1368
               T(6) = SV3(J+2, I2)                                      CRK1369
          GO TO 360                                                     CRK1370
350            T(3) = SV4(J, I)                                         CRK1371
               T(4) = SV4(J, I2)                                        CRK1372
               T(5) = SV4(J+2, I)                                       CRK1373
               T(6) = SV4(J+2, I2)                                      CRK1374
360       CONTINUE                                                      CRK1375
C                                                                       CRK1376
               PM(K1, J, 1) = PM(K1, J, 1)+T(1)*T(3)                    CRK1377
               PM(K1, J, 2) = PM(K1, J, 2)+T(1)*T(4)                    CRK1378
               PM(K1, J+2, 1) = PM(K1, J+2, 1)+T(2)*T(5)                CRK1379
               PM(K1, J+2, 2) = PM(K1, J+2, 2)+T(2)*T(6)                CRK1380
370       CONTINUE                                                      CRK1381
C     SOLVE FOR C(NS) AND D(NS)                                         CRK1382
          V2 = 2.0*V(I)                                                 CRK1383
          V21 = V2-1.0                                                  CRK1384
          DO 380 J = 1, 2                                               CRK1385
               FM(1, J) = P*PM(1, 1, J)+V2*PM(1, 2, J)+P*PM(1, 3,       CRK1386
     1              J)-V2*PM(1, 4, J)                                   CRK1387
380            FM(2, J) = P*PM(1, 1, J)+V21*PM(1, 2, J)-P*PM(1,         CRK1388
     1              3, J)+V21*PM(1, 4, J)                               CRK1389
               DFAC = SC(1)/((FM(1, 1)*FM(2, 2)-FM(2, 1)*FM(1, 2))      CRK1390
     1              *P*P)                                               CRK1391
               A(LC, NS) = 0.0                                          CRK1392
               B(LC, NS) = 0.0                                          CRK1393
               C(LC, NS) = -FM(1, 2)*DFAC                               CRK1394
               D(LC, NS) = FM(1, 1)*DFAC                                CRK1395
C     BACKSOLVE FOR THE OTHER A*B*C*D                                   CRK1396
          DO 390 K1 = 1, N                                              CRK1397
               A(LC, K1) = (PM(K1, 1, 1)*C(LC, NS)+PM(K1, 1, 2)         CRK1398
     1              *D(LC, NS))/SC(K1)                                  CRK1399
               B(LC, K1) = (PM(K1, 2, 1)*C(LC, NS)+PM(K1, 2, 2)         CRK1400
     1              *D(LC, NS))/SC(K1)                                  CRK1401
               C(LC, K1) = (PM(K1, 3, 1)*C(LC, NS)+PM(K1, 3, 2)         CRK1402
     1              *D(LC, NS))/SC(K1)                                  CRK1403
390            D(LC, K1) = (PM(K1, 4, 1)*C(LC, NS)+PM(K1, 4, 2)         CRK1404
     1              *D(LC, NS))/SC(K1)                                  CRK1405
          RETURN                                                        CRK1406
          END                                                           CRK1407
```

```
          SUBROUTINE BESSEL (NI, XI, Y)                                 CRK1408
CBESSEL ******SUBROUTINE BESSEL - 5-LAYER FLASTIC SYSTEM ******         CRK1409
          DIMENSION PZ(6), QZ(6), P1(6), Q1(6), D(20)                   CRK1410
C                                                                       CRK1411
C                                                                       CRK1412
 10            PZ(1) = 1.0                                              CRK1413
               PZ(2) = -1.125E-4                                        CRK1414
               PZ(3) = 2.8710938E-7                                     CRK1415
               PZ(4) = -2.3449658E-9                                    CRK1416
               PZ(5) = 3.9806841E-11                                    CRK1417
               PZ(6) = -1.1536133E-12                                   CRK1418
C                                                                       CRK1419
               QZ(1) = -5.0E-3                                          CRK1420
               QZ(2) = 4.6875E-6                                        CRK1421
               QZ(3) = -2.3255859E-8                                    CRK1422
               QZ(4) = 2.8307087E-10                                    CRK1423
               QZ(5) = -6.3912096E-12                                   CRK1424
               QZ(6) = 2.3124704E-13                                    CRK1425
C                                                                       CRK1426
C                                                                       CRK1427
               P1(1) = 1.0                                              CRK1428
               P1(2) = 1.875E-4                                         CRK1429
               P1(3) = -3.6914063E-7                                    CRK1430
               P1(4) = 2.7713232E-9                                     CRK1431
               P1(5) = -4.5114421E-11                                   CRK1432
               P1(6) = 1.2750463E-12                                    CRK1433
C                                                                       CRK1434
               Q1(1) = 1.5E-2                                           CRK1435
               Q1(2) = -6.5625E-6                                       CRK1436
               Q1(3) = 2.8423828E-8                                     CRK1437
               Q1(2) = -6.5625E-6                                       CRK1438
               Q1(3) = 2.8423828E-8                                     CRK1439
               Q1(4) = -3.2662024E-10                                   CRK1440
               Q1(5) = 7.1431166E-12                                    CRK1441
               Q1(6) = -2.5327056E-13                                   CRK1442
C                                                                       CRK1443
C                                                                       CRK1444
               PI = 3.1415927                                           CRK1445
               PI2 = 2.0*PI                                             CRK1446
C                                                                       CRK1447
C                                                                       CRK1448
               N = NI                                                   CRK1449
               X = XI                                                   CRK1450
          IF (X-7.0) 20,20,100                                          CRK1451
C                                                                       CRK1452
 20            X2 = X/2.0                                               CRK1453
               FAC = -X2*X2                                             CRK1454
          IF (N) 30,30,60                                               CRK1455
 30            C = 1.0                                                  CRK1456
               Y = C                                                    CRK1457
          DO 50 I = 1, 34                                               CRK1458
               T = I                                                    CRK1459
               C = FAC*C/(T*T)                                          CRK1460
               TEST = ABS(C)-10.0**(-8)                                 CRK1461
          IF (TEST) 90,90,40                                            CRK1462
 40            Y = Y+C                                                  CRK1463
 50       CONTINUE                                                      CRK1464
 60            C = X2                                                   CRK1465
```

```
            Y = C                                                       CRK1466
         DO 80 I = 1, 34                                                CRK1467
            T = 1                                                       CRK1468
            C = FAC*C/(T*(T+1.0))                                       CRK1469
            TEST = ABS(C)-10.0**(-8)                                    CRK1470
         IF (TEST) 90,90,70                                             CRK1471
 70         Y = Y+C                                                     CRK1472
 80      CONTINUE                                                       CRK1473
 90   RETURN                                                            CRK1474
100      IF (N) 110,110,130                                             CRK1475
C                                                                       CRK1476
C                                                                       CRK1477
110      DO 120 I = 1, 6                                                CRK1478
            D(I) = PZ(I)                                                CRK1479
            D(I+10) = QZ(I)                                             CRK1480
120      CONTINUE                                                       CRK1481
         GO TO 150                                                      CRK1482
C                                                                       CRK1483
130      DO 140 I = 1, 6                                                CRK1484
            D(I) = P1(I)                                                CRK1485
            D(I+10) = Q1(I)                                             CRK1486
140      CONTINUE                                                       CRK1487
150      CONTINUE                                                       CRK1488
            T1 = 25.0/X                                                 CRK1489
            T2 = T1*T1                                                  CRK1490
            P = U(6)*T2+U(5)                                            CRK1491
         DO 160 I = 1, 4                                                CRK1492
            J = 5-I                                                     CRK1493
            P = P*T2+U(J)                                               CRK1494
160      CONTINUE                                                       CRK1495
            Q = U(16)*T2+U(15)                                          CRK1496
         DO 170 I = 1, 4                                                CRK1497
            J = 5-I                                                     CRK1498
            Q = Q*T2+U(J+10)                                            CRK1499
170      CONTINUE                                                       CRK1500
            Q = Q*T1                                                    CRK1501
C                                                                       CRK1502
            T4 = SQRT(X*PI)                                             CRK1503
            T6 = SIN(X)                                                 CRK1504
            T7 = COS(X)                                                 CRK1505
C                                                                       CRK1506
         IF (N) 180,180,190                                             CRK1507
C                                                                       CRK1508
180         T5 = ((P-Q)*T6+(P+Q)*T7)/T4                                 CRK1509
         GO TO 200                                                      CRK1510
190         T5 = ((P+Q)*T6-(P-Q)*T7)/T4                                 CRK1511
200         Y = T5                                                      CRK1512
      RETURN                                                            CRK1513
      END                                                               CRK1514
```

APPENDIX 4.3

GUIDE FOR DATA INPUT

CRAKDX GUIDE FOR DATA INPUT

with supplementary notes

extract from

FLEXIBLE PAVEMENT SYSTEM - SECOND GENERATION,
INCORPORATING FATIGUE AND STOCHASTIC CONCEPTS

by

Surendra Prakash Jain

December 1971

CRAKDX GUIDE FOR DATA INPUT

PROGRAM DESCRIPTION (one card)

Alphanumeric 8A10
1 80

MATERIAL PARAMETERS (one card)

NL	NM	LDDF	LNDF	Y	GR	Qo	Q1	Q2	TEST
I 10	I 10	F 10.0	F 10.0	F 10.0	F 10.0	A2	A2	A2	F510
1 11	21	31	41	51	61 62	66 67	71 72	76 80	

NL Number of load groups.

NM Number of materials (maximum of five).

LDDF Load distribution factor, ratio.

LNDF Lane distribution factor, ratio.

Y Design period, years.

GR Traffic growth rate, ratio. Leave blank if actual traffic data is given.

Qo Provide NO if the actual traffic data for each month is not given.

Q1 Provide NO if the monthly traffic percentage does not vary.

Q2 Provide NO if elastic modulus values of the different materials do not vary monthly.

TEST Leave blank if calculations for both cracking index and rut depth.
Provide 1.0 for cracking index only.
Provide 2.0 for rut depth only.

WHEEL LOAD DATA (NL cards)

L1	L2	N	TIRE
F 10.0	F 10.0	F 10.0	F 10.0
1	11	21	31	40

L1 - L2 Axle load range, kips.

N Number of axle applications in wheel load group for first year. Leave blank if actual monthly traffic data for each year is given.

TIRE Tire pressure, PSI.

MATERIAL DATA (NM cards if Q2 = NO , NM x 2 cards if Q2 is not NO)

MAT	TMIN	NU	CONF	SIG	E(1)	E(2)	E(3)	E(4)
A 10	F 10.0	F5.0	F5.0	F 10.0	F 10.0	F 10.0	F 10.0	F 10.0
1	11	21	26	31	41	51	61	71	80

E(5)	E(6)	E(7)	E(8)	E(9)	E(10)	E(11)	E(12)
F 10.0	F 10.0	F 10.0	F 10.0	F 10.0	F 10.0	F 10.0	F 10.0
1	11	21	31	41	51	61	71	80

MAT Material identification

TMIN Thickness of material, inches. Leave blank for subgrade.

NU Poisson's ratio.

CONF Confidence level for elastic modulus.

E Elastic modulus mean value. If Q2 = NO , provide one constant value. If Q2 is not NO provide one value for each month.

SIG Standard deviation of elastic modulus, expressed as a percent of mean modulus, i.e., coefficient of variation, percent.

FATIGUE CURVE DATA

A	B	log SD	LN
F 10.0	F 10.0	F 10.0	F 10.0
1–10	11–20	21–30	31–40

A Constant of fatigue curve $N = A\left(\frac{1}{\epsilon}\right)^B$.

B Slope of fatigue curve.

log SD Log standard deviation of fatigue life.

LN Confidence level for N .

MONTHLY TRAFFIC PERCENTAGES (one card if QO is NO and Q1 is not NO)

TRAF (1)	TRAF (2)	TRAF (3)	TRAF (4)	TRAF (5)	TRAF (6)	TRAF (7)	TRAF (8)	TRAF (9)	TRAF (10)	TRAF (11)	TRAF (12)
F 5.0	F 5.0	F 5.0	F 5.0	F 5.0	F 5.0	F 5.0	F 5.0	F 5.0	F 5.0	F 5.0	F 5.0
1–5	6–10	11–15	16–20	21–25	26–30	31–35	36–40	41–45	46–50	51–55	56–60

TRAF(I) Traffic percentage for Month I. If Q1 = NO, a value of 0.0833 will be assumed for each month. No card is needed if actual traffic data for each month is given.

ACTUAL TRAFFIC DATA (number of cards = number of design years x number of load groups if QO is not NO)

YR	TR(1)	TR(2)	TR(3)	TR(4)	TR(5)	TR(6)	TR(7)	TR(8)	TR(9)	TR(10)	TR(11)	TR(12)
A8	I6	I6	I6	I6	I6	I6	I6	I6	I6	I6	I6	I6
1–8	9–15	16–21	22–27	28–33	34–39	40–45	46–51	52–57	58–63	64–69	69–75	76–80

YR Year identification.

TR(1) Monthly traffic from January to December.

Provide a full set of traffic data for each load group separately and arrange the sets in the same sequence as in wheel load group.

DENSITY AND PRESSURE PARAMETERS (NM/2 CARDS)

R(1)	EM(1)	DRC(1)	R(2)	EM(2)	DRC(2)
F10.0	F10.0	F10.0	F10.0	F10.0	F10.0
1 10	20	30	40	50	60

R(I) Unit weight of material I (lb/cu in)

EM(I) Parameter to calculate correct radial pressure for given curve for base and subbase. Leave blank if regression equation in N, Z1, Z3, and E is given. Leave blank for subgrade.

DRC(I) Radial pressure for which curves are given for material I.

APPENDIX 4.4

INPUT DATA SAMPLE

APPENDIX 4.4. INPUT DATA SAMPLE

IDENTIFICATION A4.4 INPUT DATA SAMPLE CODED BY JAIN DATE JULY 30,71 PAGE 1 OF 1

```
CRACKING INDEX AND RUT DEPTH INDEX EXAMPLE PROBLEM
         1         4       1.0       1.0       3.0
       6.0       6.0                 42.3
A.CONCRETE         1.0       0.3      0.25      25.0 1600000.0 1420000.0 1370000.0  900000.0
 600000.0  400000.0  350000.0  300000.0  420000.0  650000.0  830000.0 1310000.0
BASE               3.0       0.4      0.25      25.0   24000.0   24000.0   24000.0   15600.0
  18000.0   19600.0   21600.0   23200.0   24000.0   24000.0   24000.0   24000.0
SUBBASE            4.0      0.45      0.25      25.0   13200.0   13200.0   13200.0    7500.0
   8600.0    9800.0   10800.0   11660.0   12200.0   12400.0   12800.0   13200.0
SUBGRADE                    0.50      0.25      25.0    6600.0    6600.0    6600.0    3600.0
  4300.0    4900.0    5400.0    5800.0    6100.0    6200.0    6400.0    6600.0
     6.5E-07         3.18         0.25         0.05
FIRST YR                                                  400  4700 14600 16900 23200 17700
SECOND YR 21900 17100 32900 33700 39900 38600 37000 37700 37500 31500 73400 85200
THIRD YR  73500 74000 73000 67100 66600 63700 74100 54800
  0.08                        0.08
'0.08                         0.07                          -3.5
```

APPENDIX 4.5

CRACKING INDEX AND RUT DEPTH INDEX EXAMPLE PROBLEM

CRACKING INDEX AND RUT DEPTH INDEX EXAMPLE PROBLEM

AXLE LOAD RANGE,KIPS	AXLE LOAD MEAN,KIPS	TIRE PRESSURE	N INITIAL AXLE APPL
6 - 6	6.00	42.30	0

LOAD DISTRIBUTION FACTOR, RATIO	1.00
LANE DISTRIBUTION FACTOR, RATIO	1.00
DESIGN PERIOD, YEARS	3

MATERIAL PARAMETERS

MATERIAL	A,CONCRETE	BASE	SUB BASE	SUBGARDE
THICKNESS	1.00	3.00	4.00	
POISSONS RATIO	.30	.40	.45	.50
COF VAR,PERCENT	25.00	25.00	25.00	25.00

VARIATIONS OF E VALUES IN SPACE AND TIME

MATERIAL	CONF	JANUARY	FEBRUARY	MARCH	APRIL	MAY	JUNE
		JULY	AUGUST	SEPTEMBER	OCTOBER	NOVEMBER	DECEMBER
A,CONCRETE	.25	1330200	1180553	1138984	748238	498825	332550
		290981	249413	3491775	540394	690041	1089101
	MEAN	1600000	1420000	1370000	900000	600000	400000
		350000	300000	4200000	650000	830000	1310000
BASE	.25	19953	19953	19953	12969	14965	16295
		17958	19288	19953	19953	19953	19953
	MEAN	24000	24000	24000	15600	18000	19600
		21600	23200	24000	24000	24000	24000
SUB BASE	.25	10974	10974	10974	6235	7150	8147
		8979	9694	10143	10309	10642	10974
	MEAN	13200	13200	13200	7500	8600	9800
		10800	11660	12200	12400	12800	13200
SUBGARDE	.25	5487	5487	5487	2993	3575	4074
		4489	4822	5071	5155	5321	5487
	MEAN	6600	6600	6600	3600	4300	4900
		5400	5800	6100	6200	6400	6600

N = 6.5E-07 * (1/E) ** 3.18

LOG STANDARD DEVIATION OF	.25
AND CONFIDENCE LEVEL	.05

TANGENTIAL STRAIN

LOAD 6 DEPTH 1

JANUARY	FEBRUARY	MARCH	APRIL	MAY	JUNE
JULY	AUGUST	SEPTEMBER	OCTOBER	NOVEMBER	DECEMBER
MEAN VALUES					
2.027E-04	2.076E-04	2.089E-04	3.365E-04	3.073E-04	2.666E-04
2.284E-04	1.948E-04	1.514E-04	2.232E-04	2.221E-04	2.105E-04
CONFIDENCE VALUES					
2.438E-04	2.497E-04	2.513E-04	4.048E-04	3.696E-04	3.207E-04
2.748E-04	2.343E-04	1.822E-04	2.685E-04	2.671E-04	2.532E-04

N TABLE - ACTUAL
FROM TRAFFIC DATA INPUT

	JANUARY	FEBRUARY	MARCH	APRIL	MAY	JUNE
	JULY	AUGUST	SEPTEMBER	OCTOBER	NOVEMBER	DECEMBER
LOAD	6					
FIRST YR	0	0	0	0	0	0
	0	0	0	0	400	4700	14600
SECONDYR	16900	23200	17700	21900	17100	32900
	33700	39900	38600	37000	37700	37500
3RD YEAR	31500	73400	88200	73500	74000	73000
	67100	68600	63700	74100	54800	0

N TABLE - THEORETICAL

LOAD 6

CONF	JANUARY	FEBRUARY	MARCH	APRIL	MAY	JUNE
LEVEL	JULY	AUGUST	SEPTEMBER	OCTOBER	NOVEMBER	DECEMBER
.050	77798	72095	70632	15516	20709	32529
	53184	88304	196567	97224	58188	68955
MEAN	360778	334332	327547	71953	96036	150848
	246635	409496	911550	265370	269841	319767

N ACTUAL / N THEORETICAL

LOAD YEAR	CONF	JANUARY / JULY	FEBRUARY / AUGUST	MARCH / SEPTEMBER	APRIL / OCTOBER	MAY / NOVEMBER	JUNE / DECEMBER
1	.054	0.	0.	0.	0.	0.	0.
		0.	0.	0.	0.	0.	0.
	MEAN	0.	0.	0.	0.	0.	0.
		0.	0.	0.	1.507E-03	1.742E-02	4.966E-02
2	.054	2.172E-01	3.218E-01	2.506E-01	1.411E+00	8.257E-01	1.011E+00
		6.336E-01	4.518E-01	1.964E-01	6.466E-01	6.479E-01	5.438E-01
	MEAN	4.684E-02	6.939E-02	5.404E-02	3.044E-01	1.781E-01	2.181E-01
		1.366E-01	9.744E-02	4.235E-02	1.394E-01	1.397E-01	1.173E-01
3	.054	4.049E-01	1.018E+00	1.206E+00	4.737E+00	3.573E+00	2.244E+00
		1.262E+00	7.769E-01	3.241E-01	1.295E+00	9.418E-01	0.
	MEAN	8.731E-02	2.195E-01	2.601E-01	1.022E+00	7.705E-01	4.839E-01
		2.721E-01	1.675E-01	6.988E-02	2.792E-01	2.031E-01	0.

MONTH	CONF	(N/N)T	LOG(N/N)T	LOG SD	K	A	CI
1	.0539	0	-	-	-	0	0
	MEAN	0	-				
2	.0539	0	-	-	-	0	0
	MEAN	0	-				
3	.0539	0	-	-	-	0	0
	MEAN	0	-				
4	.0539	0	-	-	-	0	0
	MEAN	0	-				
5	.0539	0	-	-	-	0	0
	MEAN	0	-				
6	.0539	0	-	-	-	0	0
	MEAN	0	-				
7	.0539	0	-	-	-	0	0
	MEAN	0	-				
8	.0539	0	-	-	-	0	0
	MEAN	0	-				
9	.0539	0	-	-	-	0	0
	MEAN	0	-				
10	.0539	6.990E-03	-2.156E+00	4.143E-01	6.81E+00	3.26E-13	3.26E-10
	MEAN	1.5073E-03	-2.8218E+00				
11	.0539	8.776E-02	-1.057E+00	4.143E-01	4.16E+00	1.57E-05	1.57E-02
	MEAN	1.8925E-02	-1.7230E+00				
12	.0539	2.995E-01	-5.236E-01	4.143E-01	2.87E+00	2.04E-03	2.04E+00
	MEAN	6.4583E-02	-1.1899E+00				
13	.0539	5.167E+01	-2.867E-01	4.143E-01	2.30E+00	1.07E-02	1.07E+01
	MEAN	1.1143E-01	-9.5301E-01				
14	.0539	8.385E-01	-7.649E-02	4.143E-01	1.79E+00	3.65E-02	3.65E+01
	MEAN	1.8082E-01	-7.4276E-01				
15	.0539	1.089E+00	3.707E-02	4.143E-01	1.52E+00	6.44E-02	6.44E+01
	MEAN	2.3486E-01	-6.2920E-01				
16	.0539	2.501E+00	3.980E-01	4.143E-01	6.47E-01	2.59E-01	2.59E+02
	MEAN	5.3922E-01	-2.6823E-01				

CRACKING INDEX AND RUT DEPTH INDEX EXAMPLE PROBLEM

MONTH	CONF	(N/N)T	LOG(N/N)T	LOG SD	K	A	CI
17	.0539	3.326E+00	5.220E-01	4.143E-01	3.48E-01	3.64E-01	3.64E+02
	MEAN	7.1728E-01	-1.4431E-01				
18	.0539	4.338E+00	6.373E-01	4.143E-01	7.00E-02	4.72E-01	4.72E+02
	MEAN	9.3538E-01	-2.9012E-02				
19	.0539	4.971E+00	6.965E-01	4.143E-01	-7.29E-02	5.29E-01	5.29E+02
	MEAN	1.0720E+00	3.0203E-02				
20	.0539	5.423E+00	7.343E-01	4.143E-01	-1.64E-01	5.65E-01	5.65E+02
	MEAN	1.1695E+00	6.7984E-02				
21	.0539	5.620E+00	7.497E-01	4.143E-01	-2.01E-01	5.80E-01	5.80E+02
	MEAN	1.2118E+00	8.3432E-02				
22	.0539	6.266E+00	7.970E-01	4.143E-01	-3.16E-01	6.24E-01	6.24E+02
	MEAN	1.3512E+00	1.3073E-01				
23	.0539	6.914E+00	8.397E-01	4.143E-01	-4.19E-01	6.62E-01	6.62E+02
	MEAN	1.4909E+00	1.7346E-01				
24	.0539	7.458E+00	8.726E-01	4.143E-01	-4.98E-01	6.91E-01	6.91E+02
	MEAN	1.6082E+00	2.0634E-01				
25	.0539	7.863E+00	8.956E-01	4.143E-01	-5.53E-01	7.10E-01	7.10E+02
	MEAN	1.6955E+00	2.2930E-01				
26	.0539	8.881E+00	9.485E-01	4.143E-01	-6.81E-01	7.52E-01	7.52E+02
	MEAN	1.9151E+00	2.8218E-01				
27	.0539	1.009E+01	1.004E+00	4.143E-01	-8.15E-01	7.92E-01	7.92E+02
	MEAN	2.1792E+00	3.3750E-01				
28	.0539	1.482E+01	1.171E+00	4.143E-01	-1.22E+00	8.88E-01	8.88E+02
	MEAN	3.1967E+00	5.0470E-01				
29	.0539	1.840E+01	1.265E+00	4.143E-01	-1.44E+00	9.26E-01	9.26E+02
	MEAN	3.9672E+00	5.9849E-01				
30	.0539	2.064E+01	1.315E+00	4.143E-01	-1.57E+00	9.41E-01	9.41E+02
	MEAN	4.4512E+00	6.4847E-01				
31	.0539	2.190E+01	1.341E+00	4.143E-01	-1.63E+00	9.48E-01	9.48E+02
	MEAN	4.7232E+00	6.7424E-01				
32	.0539	2.268E+01	1.356E+00	4.143E-01	-1.66E+00	9.52E-01	9.52E+02
	MEAN	4.8907E+00	6.8938E-01				
33	.0539	2.300E+01	1.362E+00	4.143E-01	-1.68E+00	9.53E-01	9.53E+02
	MEAN	4.9606E+00	6.9554E-01				
34	.0539	2.430E+01	1.386E+00	4.143E-01	-1.74E+00	9.69E-01	9.59E+02
	MEAN	5.2399E+00	7.1932E-01				
35	.0539	2.524E+01	1.402E+00	4.143E-01	-1.78E+00	9.62E-01	9.62E+02
	MEAN	5.4429E+00	7.3583E-01				
36	.0539	2.524E+01	1.402E+00	4.143E-01	-1.78E+00	9.62E-01	9.62E+02
	MEAN	5.4429E+00	7.3583E-01				

LOAD	MATERIAL	RADIAL PRESSURE (INPUT)	JANUARY VERTICAL STRESS MEAN	JANUARY VERTICAL STRESS DESIGN	JANUARY RADIAL STRESS	FEBRUARY VERTICAL STRESS MEAN	FEBRUARY VERTICAL STRESS DESIGN	FEBRUARY RADIAL STRESS
6								
	BASE		-24.278	-24.278	-1.562	-24.996	-24.996	-1.641
	SUB BASE		-12.854	-12.854	-1.000	-13.149	-13.149	-1.000
	SUBGARDE	-3.500	-8.436	-10.303	-1.633	-8.572	-10.441	-1.632

MARCH VERTICAL STRESS MEAN	MARCH VERTICAL STRESS DESIGN	MARCH RADIAL STRESS	APRIL VERTICAL STRESS MEAN	APRIL VERTICAL STRESS DESIGN	APRIL RADIAL STRESS	MAY VERTICAL STRESS MEAN	MAY VERTICAL STRESS DESIGN	MAY RADIAL STRESS
-25.206	-25.206	-1.667	-24.304	-24.304	-1.000	-27.234	-27.234	-1.000
-13.236	-13.236	-1.000	-12.416	-12.416	-1.000	-13.711	-13.711	-1.000
-8.612	-10.481	-1.631	-8.071	-10.027	-1.544	-8.754	-10.679	-1.575

JUNE VERTICAL STRESS MEAN	JUNE VERTICAL STRESS DESIGN	JUNE RADIAL STRESS	JULY VERTICAL STRESS MEAN	JULY VERTICAL STRESS DESIGN	JULY RADIAL STRESS	AUGUST VERTICAL STRESS MEAN	AUGUST VERTICAL STRESS DESIGN	AUGUST RADIAL STRESS
-29.428	-29.428	-1.328	-30.121	-30.121	-1.726	-30.692	-30.692	-2.267
-14.848	-14.848	-1.000	-15.225	-15.225	-1.000	-15.579	-15.579	-1.000
-9.315	-11.180	-1.635	-9.504	-11.339	-1.666	-9.680	-11.476	-1.704

SEPTEMBER VERTICAL STRESS MEAN	SEPTEMBER VERTICAL STRESS DESIGN	SEPTEMBER RADIAL STRESS	OCTOBER VERTICAL STRESS MEAN	OCTOBER VERTICAL STRESS DESIGN	OCTOBER RADIAL STRESS	NOVEMBER VERTICAL STRESS MEAN	NOVEMBER VERTICAL STRESS DESIGN	NOVEMBER RADIAL STRESS
-17.572	-17.572	-1.000	-28.575	-28.575	-1.451	-27.686	-27.686	-1.658
-9.911	-9.911	-1.000	-14.517	-14.517	-1.000	-14.202	-14.202	-1.000
-6.959	-6.836	-1.623	-9.169	-11.045	-1.624	-9.038	-10.913	-1.625

DECEMBER VERTICAL STRESS MEAN	DECEMBER VERTICAL STRESS DESIGN	DECEMBER RADIAL STRESS
-25.466	-25.466	-1.700
-13.343	-13.343	-1.000
-8.662	-10.531	-1.631

YEAR 1

	JANUARY	FEBRUARY	MARCH	APRIL	MAY	JUNE
HI-LO-REPT						
BASE	0.	0.	0.	0.	0.	0.
SUB BASE	0.	0.	0.	0.	0.	0.
SUBGARDE	0.	0.	0.	0.	0.	0.
CUMMULATIVE						
BASE	0.	0.	0.	0.	0.	0.
SUB BASE	0.	0.	0.	0.	0.	0.
SUBGARDE	0.	0.	0.	0.	0.	0.
STRAIN TO BEGINNING OF MONTH						
BASE	0.	0.	0.	0.	0.	0.
SUB BASE	0.	0.	0.	0.	0.	0.
SUBGARDE	0.	0.	0.	0.	0.	0.
STRAIN THROUGH MONTH						
BASE	0.	0.	0.	0.	0.	0.
SUB BASE	0.	0.	0.	0.	0.	0.
SUBGARDE	0.	0.	0.	0.	0.	0.
DEPTH						
BASE	3.0					
SUB BASE	4.0					
SUBGARDE						
VERT. DSP.	1.625E-02	1.638E-02	1.642E-02	2.901E-02	2.534E-02	2.298E-02
V STRESS	-7.796E+00	-7.932E+00	-7.972E+00	-7.431E+00	-8.114E+00	-8.675E+00
R STRESS	-9.927E-01	-9.915E-01	-9.914E-01	-9.044E-01	-9.352E-01	-9.948E-01
DEFORMATION AT MONTH N						
BASE	0.	0.	0.	0.	0.	0.
SUB BASE	0.	0.	0.	0.	0.	0.
SUBGARDE	0.	0.	0.	0.	0.	0.
DEFORMATION DUE TO REPITIONS THROUGH MONTH (N-1)						
BASE	0.	0.	0.	0.	0.	0.
SUB BASE	0.	0.	0.	0.	0.	0.
SUBGARDE	0.	0.	0.	0.	0.	0.
DEFORMATION AT MONTH N - DEFORMATION AT MONTH N-1						
BASE	0.	0.	0.	0.	0.	0.
SUB BASE	0.	0.	0.	0.	0.	0.
SUBGARDE	0.	0.	0.	0.	0.	0.
CUMULATIVE DEFORMATION THROUGH MONTH N						
BASE	0.	0.	0.	0.	0.	0.
SUB BASE	0.	0.	0.	0.	0.	0.
SUBGARDE	0.	0.	0.	0.	0.	0.
TOTAL CUMULATIVE DEFORMATION	0.	0.	RUT DEPTH 0.	0.	0.	0.

YEAR 1

	JULY	AUGUST	SEPTEMBER	OCTOBER	NOVEMBER	DECEMBER
HI-LO-REPT						
BASE	0.	0.	0.	4.000E+02	4.700E+03	1.460E+04
SUB BASE	0.	0.	0.	4.000E+02	4.700E+03	1.460E+04
SUBGARDE	0.	0.	0.	4.000E+02	4.700E+03	1.460E+04
CUMMULATIVE						
BASE	0.	0.	0.	4.000E+02	5.100E+03	1.970E+04
SUB BASE	0.	0.	0.	4.000E+02	5.100E+03	1.970E+04
SUBGARDE	0.	0.	0.	4.000E+02	5.100E+03	1.970E+04
STRAIN TO BEGINNING OF MONTH						
BASE	0.	0.	0.	0.	2.626E+00	2.933E+00
SUB BASE	0.	0.	0.	0.	1.575E+00	1.637E+00
SUBGARDE	0.	0.	0.	0.	7.020E-01	1.061E+00
STRAIN THROUGH MONTH						
BASE	0.	0.	0.	3.000E+00	3.567E+00	3.353E+00
SUB BASE	0.	0.	0.	1.603E+00	1.717E+00	1.720E+00
SUBGARDE	0.	0.	0.	7.293E-01	1.191E+00	1.294E+00
DEPTH						
BASE	3.0					
SUB BASE	4.0					
SUBGARDE						
VERT. OSP.	2.108E-02	1.983E-02	1.598E-02	1.801E-02	1.733E-02	1.646E-02
V STRESS	-8.864E+00	-9.040E+00	-6.319E+00	-8.529E+00	-8.398E+00	-8.022E+00
R STRESS	-1.026E+00	-1.064E+00	-9.831E-01	-9.840E-01	-9.852E-01	-9.913E-01
DEFORMATION AT MONTH N						
BASE	0.	0.	0.	8.999E-02	1.070E-01	1.006E-01
SUB BASE	0.	0.	0.	6.412E-02	6.867E-02	6.881E-02
SUBGARDE	0.	0.	0.	1.079E-01	1.782E-01	2.000E-01
DEFORMATION DUE TO REPITIONS THROUGH MONTH (N-1)						
BASE	0.	0.	0.	0.	7.877E-02	8.800E-02
SUB BASE	0.	0.	0.	0.	6.298E-02	6.548E-02
SUBGARDE	0.	0.	0.	0.	1.050E-01	1.640E-01
DEFORMATION AT MONTH N - DEFORMATION AT MONTH N-1						
BASE	0.	0.	0.	8.999E-02	2.824E-02	1.258E-02
SUB BASE	0.	0.	0.	6.412E-02	5.690E-03	3.334E-03
SUBGARDE	0.	0.	0.	1.079E-01	7.318E-02	3.601E-02
CUMULATIVE DEFORMATION THROUGH MONTH N						
BASE	0.	0.	0.	8.999E-02	1.182E-01	1.308E-01
SUB BASE	0.	0.	0.	6.412E-02	6.981E-02	7.314E-02
SUBGARDE	0.	0.	0.	1.079E-01	1.811E-01	2.171E-01
TOTAL CUMULATIVE DEFORMATION RUT DEPTH						
	0.	0.	0.	2.620E-01	3.692E-01	4.211E-01

YEAR 2

	JANUARY	FEBRUARY	MARCH	APRIL	MAY	JUNE
HI-LO-REPT						
BASE	1.690E+04	2.320E+04	1.770E+04	2.190E+04	1.710E+04	3.290E+04
SUB BASE	1.690E+04	2.320E+04	1.770E+04	2.190E+04	1.710E+04	3.290E+04
SUBGARDE	1.690E+04	2.320E+04	1.770E+04	2.190E+04	1.710E+04	3.290E+04
CUMMULATIVE						
BASE	3.660E+04	5.980E+04	7.750E+04	9.940E+04	1.165E+05	1.494E+05
SUB BASE	3.660E+04	5.980E+04	7.750E+04	9.940E+04	1.165E+05	1.494E+05
SUBGARDE	3.660E+04	5.980E+04	7.750E+04	9.940E+04	1.165E+05	1.494E+05
STRAIN TO BEGINNING OF MONTH						
BASE	3.191E+00	3.481E+00	3.661E+00	4.334E+00	5.509E+00	5.950E+00
SUB BASE	1.675E+00	1.741E+00	1.779E+00	1.655E+00	1.803E+00	1.941E+00
SUBGARDE	1.206E+00	1.363E+00	1.464E+00	1.201E+00	1.572E+00	1.895E+00
STRAIN THROUGH MONTH						
BASE	3.377E+00	3.631E+00	3.741E+00	4.427E+00	5.581E+00	6.065E+00
SUB BASE	1.714E+00	1.771E+00	1.795E+00	1.671E+00	1.813E+00	1.956E+00
SUBGARDE	1.306E+00	1.446E+00	1.508E+00	1.238E+00	1.600E+00	1.946E+00
DEPTH						
BASE	3.0					
SUB BASE	4.0					
SUBGARDE						
VERT. OSP.	1.625E-02	1.638E-02	1.642E-02	2.961E-02	2.534E-02	2.298E-02
V STRESS	-7.796E+00	-7.932E+00	-7.972E+00	-7.431E+00	-8.114E+00	-8.675E+00
R STRESS	-9.927E-01	-9.915E-01	-9.914E-01	-9.044E-01	-9.352E-01	-9.948E-01
DEFORMATION AT MONTH N						
BASE	1.013E-01	1.089E-01	1.122E-01	1.328E-01	1.674E-01	1.820E-01
SUB BASE	6.856E-02	7.086E-02	7.182E-02	6.683E-02	7.251E-02	7.823E-02
SUBGARDE	2.060E-01	2.251E-01	2.340E-01	1.982E-01	2.429E-01	2.853E-01
DEFORMATION DUE TO REPITIONS THROUGH MONTH (N-1)						
BASE	9.574E-02	1.044E-01	1.098E-01	1.300E-01	1.653E-01	1.785E-01
SUB BASE	6.701E-02	6.964E-02	7.118E-02	6.622E-02	7.213E-02	7.763E-02
SUBGARDE	1.902E-01	2.123E-01	2.271E-01	1.923E-01	2.386E-01	2.778E-01
DEFORMATION AT MONTH N - DEFORMATION AT MONTH N-1						
BASE	5.585E-03	4.520E-03	2.400E-03	2.806E-03	2.159E-03	3.470E-03
SUB BASE	1.540E-03	1.220E-03	6.393E-04	6.122E-04	3.852E-04	5.954E-04
SUBGARDE	1.574E-02	1.284E-02	6.839E-03	5.890E-03	4.337E-03	7.531E-03
CUMULATIVE DEFORMATION THROUGH MONTH N						
BASE	1.304E-01	1.409E-01	1.433E-01	1.461E-01	1.483E-01	1.518E-01
SUB BASE	7.469E-02	7.591E-02	7.655E-02	7.716E-02	7.755E-02	7.814E-02
SUBGARDE	2.329E-01	2.457E-01	2.525E-01	2.584E-01	2.628E-01	2.703E-01
TOTAL CUMULATIVE DEFORMATION RUT DEPTH						
	4.440E-01	4.625E-01	4.724E-01	4.817E-01	4.886E-01	5.002E-01

YEAR 2

	JULY	AUGUST	SEPTEMBER	OCTOBER	NOVEMBER	DECEMBER
MI-LO-REPT						
BASE	3.370E+04	3.990E+04	3.860E+04	3.700E+04	3.770E+04	3.750E+04
SUB BASE	3.370E+04	3.990E+04	3.860E+04	3.700E+04	3.770E+04	3.750E+04
SUBGARDE	3.370E+04	3.990E+04	3.860E+04	3.700E+04	3.770E+04	3.750E+04
CUMMULATIVE						
BASE	1.831E+05	2.230E+05	2.616E+05	2.986E+05	3.363E+05	3.738E+05
SUB BASE	1.831E+05	2.230E+05	2.616E+05	2.986E+05	3.363E+05	3.738E+05
SUBGARDE	1.831E+05	2.230E+05	2.616E+05	2.986E+05	3.363E+05	3.738E+05
STRAIN TO BEGINNING OF MONTH						
BASE	5.702E+00	5.194E+00	2.932E+00	5.739E+00	5.072E+00	4.233E+00
SUB BASE	2.008E+00	2.067E+00	1.578E+00	1.985E+00	1.965E+00	1.893E+00
SUBGARDE	2.059E+00	2.202E+00	9.905E-01	2.021E+00	1.974E+00	1.784E+00
STRAIN THROUGH MONTH						
BASE	5.788E+00	5.266E+00	2.969E+00	5.795E+00	5.116E+00	4.266E+00
SUB BASE	2.020E+00	2.078E+00	1.588E+00	1.993E+00	1.972E+00	1.899E+00
SUBGARDE	2.103E+00	2.246E+00	1.006E+00	2.047E+00	1.996E+00	1.802E+00
DEPTH						
BASE	3.0					
SUB BASE	4.0					
SUBGARDE						
VERT. OSP.	2.108E-02	1.983E-02	1.598E-02	1.801E-02	1.733E-02	1.646E-02
V STRESS	-8.864E+00	-9.040E+00	-6.319E+00	-8.529E+00	-8.398E+00	-8.022E+00
R STRESS	-1.026E+00	-1.064E+00	-9.831E-01	-9.840E-01	-9.852E-01	-9.913E-01
DEFORMATION AT MONTH N						
BASE	1.736E-01	1.580E-01	8.907E-02	1.739E-01	1.535E-01	1.280E-01
SUB BASE	8.078E-02	8.313E-02	6.351E-02	7.970E-02	7.886E-02	7.596E-02
SUBGARDE	3.094E-01	3.239E-01	1.838E-01	3.030E-01	2.986E-01	2.765E-01
DEFORMATION DUE TO REPITIONS THROUGH MONTH (N-1)						
BASE	1.711E-01	1.558E-01	8.797E-02	1.722E-01	1.522E-01	1.270E-01
SUB BASE	8.030E-02	8.267E-02	6.313E-02	7.940E-02	7.859E-02	7.572E-02
SUBGARDE	2.991E-01	3.176E-01	1.810E-01	2.991E-01	2.952E-01	2.756E-01
DEFORMATION AT MONTH N - DEFORMATION AT MONTH N-1						
BASE	2.592E-03	2.157E-03	1.102E-03	1.677E-03	1.319E-03	9.843E-04
SUB BASE	4.811E-04	4.609E-04	3.814E-04	3.055E-04	2.729E-04	2.421E-04
SUBGARDE	6.360E-03	6.340E-03	2.810E-03	3.901E-03	3.418E-03	2.817E-03
CUMULATIVE DEFORMATION THROUGH MONTH N						
BASE	1.543E-01	1.565E-01	1.576E-01	1.593E-01	1.606E-01	1.616E-01
SUB BASE	7.862E-02	7.909E-02	7.947E-02	7.977E-02	8.004E-02	8.029E-02
SUBGARDE	2.767E-01	2.830E-01	2.858E-01	2.897E-01	2.931E-01	2.959E-01
TOTAL CUMULATIVE DEFORMATION RUT DEPTH						
	5.096E-01	5.186E-01	5.229E-01	5.288E-01	5.338E-01	5.378E-01

YEAR 3

	JANUARY	FEBRUARY	MARCH	APRIL	MAY	JUNE
MI-LO-REPT						
BASE	3.150E+04	7.340E+04	8.520E+04	7.350E+04	7.400E+04	7.300E+04
SUB BASE	3.150E+04	7.340E+04	8.520E+04	7.350E+04	7.400E+04	7.300E+04
SUBGARDE	3.150E+04	7.340E+04	8.520E+04	7.350E+04	7.400E+04	7.300E+04
CUMMULATIVE						
BASE	4.053E+05	4.787E+05	5.639E+05	6.374E+05	7.114E+05	7.844E+05
SUB BASE	4.053E+05	4.787E+05	5.639E+05	6.374E+05	7.114E+05	7.844E+05
SUBGARDE	4.053E+05	4.787E+05	5.639E+05	6.374E+05	7.114E+05	7.844E+05
STRAIN TO BEGINNING OF MONTH						
BASE	4.076E+00	4.219E+00	4.303E+00	5.080E+00	6.351E+00	6.791E+00
SUB BASE	1.854E+00	1.886E+00	1.903E+00	1.773E+00	1.911E+00	2.044E+00
SUBGARDE	1.681E+00	1.767E+00	1.817E+00	1.495E+00	1.906E+00	2.269E+00
STRAIN THROUGH MONTH						
BASE	4.100E+00	4.270E+00	4.354E+00	5.126E+00	6.401E+00	6.836E+00
SUB BASE	1.859E+00	1.895E+00	1.912E+00	1.780E+00	1.917E+00	2.050E+00
SUBGARDE	1.694E+00	1.795E+00	1.845E+00	1.513E+00	1.926E+00	2.289E+00
DEPTH						
BASE	3.0					
SUB BASE	4.0					
SUBGARDE						
VERT. OSP.	1.625E-02	1.638E-02	1.642E-02	2.901E-02	2.534E-02	2.298E-02
V STRESS	-7.796E+00	-7.932E+00	-7.972E+00	-7.431E+00	-8.114E+00	-8.675E+00
R STRESS	-9.927E-01	-9.915E-01	-9.914E-01	-9.044E-01	-9.352E-01	-9.948E-01
DEFORMATION AT MONTH N						
BASE	1.230E-01	1.281E-01	1.306E-01	1.538E-01	1.920E-01	2.051E-01
SUB BASE	7.436E-02	7.981E-02	7.649E-02	7.118E-02	7.669E-02	8.199E-02
SUBGARDE	2.671E-01	2.795E-01	2.863E-01	2.421E-01	2.923E-01	3.356E-01
DEFORMATION DUE TO REPITIONS THROUGH MONTH (N-1)						
BASE	1.223E-01	1.266E-01	1.291E-01	1.524E-01	1.905E-01	2.037E-01
SUB BASE	7.410E-02	7.943E-02	7.612E-02	7.091E-02	7.645E-02	8.178E-02
SUBGARDE	2.650E-01	2.752E-01	2.820E-01	2.392E-01	2.893E-01	3.326E-01
DEFORMATION AT MONTH N - DEFORMATION AT MONTH N-1						
BASE	7.295E-04	1.532E-03	1.516E-03	1.382E-03	1.494E-03	1.363E-03
SUB BASE	1.846E-04	3.758E-04	3.650E-04	2.712E-04	2.389E-04	2.091E-04
SUBGARDE	2.056E-03	4.354E-03	4.321E-03	2.809E-03	3.001E-03	2.958E-03
CUMULATIVE DEFORMATION THROUGH MONTH N						
BASE	1.623E-01	1.638E-01	1.654E-01	1.667E-01	1.682E-01	1.695E-01
SUB BASE	8.047E-02	8.085E-02	8.121E-02	8.148E-02	8.172E-02	8.193E-02
SUBGARDE	2.980E-01	3.024E-01	3.067E-01	3.096E-01	3.126E-01	3.155E-01
TOTAL CUMULATIVE DEFORMATION RUT DEPTH						
	5.408E-01	5.471E-01	5.533E-01	5.578E-01	5.625E-01	5.671E-01

YEAR 3

	JULY	AUGUST	SEPTEMBER	OCTOBER	NOVEMBER	DECEMBER
MI-LO-REPT						
BASE	6.710E+04	6.860E+04	6.370E+04	7.410E+04	5.480E+04	0.
SUB BASE	6.710E+04	6.860E+04	6.370E+04	7.410E+04	5.480E+04	0.
SUBGARDE	6.710E+04	6.860E+04	6.370E+04	7.410E+04	5.480E+04	0.
CUMMULATIVE						
BASE	8.515E+05	9.201E+05	9.838E+05	1.058E+06	1.113E+06	1.113E+06
SUB BASE	8.515E+05	9.201E+05	9.838E+05	1.058E+06	1.113E+06	1.113E+06
SUBGARDE	8.515E+05	9.201E+05	9.838E+05	1.058E+06	1.113E+06	1.113E+06
STRAIN TO BEGINNING OF MONTH						
BASE	6.406E+00	5.755E+00	3.259E+00	6.299E+00	5.539E+00	4.605E+00
SUB BASE	2.101E+00	2.153E+00	1.659E+00	2.058E+00	2.034E+00	1.959E+00
SUBGARDE	2.416E+00	2.545E+00	1.127E+00	2.285E+00	2.217E+00	1.990E+00
STRAIN THROUGH MONTH						
BASE	6.441E+00	5.783E+00	3.274E+00	6.330E+00	5.958E+00	4.605E+00
SUB BASE	2.106E+00	2.157E+00	1.663E+00	2.062E+00	2.037E+00	1.959E+00
SUBGARDE	2.434E+00	2.562E+00	1.133E+00	2.299E+00	2.226E+00	1.990E+00
DEPTH						
BASE	3.0					
SUB BASE	4.0					
SUBGARDE						
VERT. OSP.	2.108E-02	1.983E-02	1.598E-02	1.801E-02	1.733E-02	1.646E-02
V STRESS	-8.864E+00	-9.040E+00	-6.319E+00	-8.529E+00	-8.398E+00	-8.022E+00
R STRESS	-1.026E+00	-1.064E+00	-9.831E-01	-9.840E-01	-9.852E-01	-9.913E-01
DEFORMATION AT MONTH N						
BASE	1.932E-01	1.735E-01	9.822E-02	1.899E-01	1.667E-01	1.381E-01
SUB BASE	8.423E-02	8.627E-02	6.652E-02	8.248E-02	8.148E-02	7.834E-02
SUBGARDE	3.535E-01	3.695E-01	2.071E-01	3.403E-01	3.330E-01	3.075E-01
DEFORMATION DUE TO REPITIONS THROUGH MONTH (N-1)						
BASE	1.922E-01	1.726E-01	9.778E-02	1.890E-01	1.662E-01	1.381E-01
SUB BASE	8.406E-02	8.611E-02	6.638E-02	8.233E-02	8.137E-02	7.834E-02
SUBGARDE	3.509E-01	3.670E-01	2.060E-01	3.381E-01	3.316E-01	3.075E-01
DEFORMATION AT MONTH N - DEFORMATION AT MONTH N-1						
BASE	1.046E-03	8.479E-04	4.622E-04	9.206E-04	5.602E-04	0.
SUB BASE	1.738E-04	1.624E-04	1.443E-04	1.511E-04	1.046E-04	0.
SUBGARDE	2.567E-03	2.492E-03	1.170E-03	2.141E-03	1.452E-03	0.
CUMULATIVE DEFORMATION THROUGH MONTH N						
BASE	1.706E-01	1.715E-01	1.720E-01	1.729E-01	1.734E-01	1.734E-01
SUB BASE	8.211E-02	8.227E-02	8.241E-02	8.256E-02	8.267E-02	8.267E-02
SUBGARDE	3.181E-01	3.206E-01	3.218E-01	3.239E-01	3.254E-01	3.254E-01
TOTAL CUMULATIVE DEFORMATION RUT DEPTH						
	5.709E-01	5.744E-01	5.761E-01	5.794E-01	5.815E-01	5.815E-01

```
 5 AUG 71   UNIVERSITY OF TEXAS 6600   UT 2

VZE3872

16.02.50 CRK,,107,117000,77,CEDC0154,JAIN.
16.02.50 BLOWUP(CRKDEX)
16.02.50 RUN (S)
16.48.22   CTIME 012.100 SEC.  RUN= LEVEL 60=
16.48.22 LGO.
16.48.30  LOADER UNUSED STORAGE 024420.
16.48.30 - 72000CM    8.569CP    945MS      0MT
16.52.10  END - CRKDEX
16.52.11 MS      1231 PRU.
16.52.11 CP    58.072 SEC.
16.52.11 PP    28.178 SEC.
16.52.11 TM    62.996 SEC.      77 (OCTAL)
```

APPENDIX 4.6

REGRESSION ANALYSIS FOR CRACKING-PATCHING VERSUS ROUGHNESS INDEX

```
STEP01 - STEPWISE REGRESSION - VERSION OF OCT. 15,1968
THE UNIVERSITY OF TEXAS CENTER FOR HIGHWAY RESEARCH

REGRESSION EQUATION FOR  LSVSV1  AND LCP


  PROBLEM CODE                  LRSVLC
 NUMBER OF CASES                  95
 NUMBER OF ORIGINAL VARIABLES      7
 NUMBER OF VARIABLES ADDED         3
 TOTAL NUMBER OF VARIABLES        10
 NUMBER OF SUB-PROBLEMS            1

INPUT DATA


PROBLEM CARD
ROBLM   LRSVLC   95    7    3    3    0    1  10 YES YES YES          1

TRANSGENERATION CARDS
TRNGEN  822  1-0.000
TRNGEN  910  2 3.000
TRNGEN 1010  2 2.000

LABEL CARD
LAB       1LRSVSV   2   LCP   3    D1   4    D2   5    D3   6    WT   7   NXL
LAB       BARCTAN   9 CBLCP  10 SQLCP  -0        -0        -0        -0

VARIABLE FORMAT CARD
5F7.1,28X,2F7.1)
  0.              0.              3.00000000E+00  0.              8.00000000E+00  3.20000000E+01  2.00000000E+00
 3.00000000E-01   2.00000000E+00  3.00000000E+00  0.              8.00000000E+00  3.20000000E+01  2.00000000E+00
 8.45000000E-01   2.93000000E+00  3.00000000E+00  0.              8.00000000E+00  3.20000000E+01  2.00000000E+00
  0.              0.              4.00000000E+00  0.              1.20000000E+01  3.20000000E+01  2.00000000E+00
 6.15000000E-01   2.72000000E+00  4.00000000E+00  0.              1.20000000E+01  3.20000000E+01  2.00000000E+00
  0.              0.              3.00000000E+00  3.00000000E+00  8.00000000E+00  3.20000000E+01  2.00000000E+00
 5.90000000E-01   2.96000000E+00  3.00000000E+00  3.00000000E+00  8.00000000E+00  3.20000000E+01  2.00000000E+00
  0.              0.              4.00000000E+00  3.00000000E+00  4.00000000E+00  1.80000000E+01  1.00000000E+00
 5.90000000E-01   2.90000000E+00  4.00000000E+00  3.00000000E+00  4.00000000E+00  1.80000000E+01  1.00000000E+00
  0.              0.              3.00000000E+00  0.              8.00000000E+00  1.80000000E+01  1.00000000E+00
 3.50000000E-01   2.00000000E+00  3.00000000E+00  0.              8.00000000E+00  1.80000000E+01  1.00000000E+00
 6.00000000E-01   2.74000000E+00  3.00000000E+00  0.              8.00000000E+00  1.80000000E+01  1.00000000E+00
  0.              0.              2.00000000E+00  3.00000000E+00  8.00000000E+00  2.40000000E+01  2.00000000E+00
 6.80000000E-01   2.85000000E+00  2.00000000E+00  3.00000000E+00  8.00000000E+00  2.40000000E+01  2.00000000E+00
 5.50000000E-01   2.75000000E+00  2.00000000E+00  3.00000000E+00  8.00000000E+00  2.40000000E+01  2.00000000E+00
  0.              0.              3.00000000E+00  6.00000000E+00  4.00000000E+00  2.40000000E+01  2.00000000E+00
 3.20000000E-01   1.91000000E+00  3.00000000E+00  6.00000000E+00  4.00000000E+00  2.40000000E+01  2.00000000E+00
  0.              0.              2.00000000E+00  0.              4.00000000E+00  2.00000000E+00  1.00000000E+00
 3.60000000E-01   1.71000000E+00  2.00000000E+00  0.              4.00000000E+00  2.00000000E+00  1.00000000E+00
 5.10000000E-01   2.00000000E+00  2.00000000E+00  0.              4.00000000E+00  2.00000000E+00  1.00000000E+00
 6.80000000E-01   2.10000000E+00  2.00000000E+00  0.              4.00000000E+00  2.00000000E+00  1.00000000E+00
  0.              0.              1.00000000E+00  3.00000000E+00  0.              2.00000000E+00  1.00000000E+00
 1.75000000E-01   1.32000000E+00  1.00000000E+00  3.00000000E+00  0.              2.00000000E+00  1.00000000E+00
 4.10000000E-01   2.00000000E+00  1.00000000E+00  3.00000000E+00  0.              2.00000000E+00  1.00000000E+00
  0.              0.              1.00000000E+00  3.00000000E+00  4.00000000E+00  6.00000000E+00  1.00000000E+00
 2.50000000E-01   2.08000000E+00  1.00000000E+00  3.00000000E+00  4.00000000E+00  6.00000000E+00  1.00000000E+00
 4.10000000E-01   2.16000000E+00  1.00000000E+00  3.00000000E+00  4.00000000E+00  6.00000000E+00  1.00000000E+00
 4.40000000E-01   2.23000000E+00  1.00000000E+00  3.00000000E+00  4.00000000E+00  6.00000000E+00  1.00000000E+00
  0.              0.              4.00000000E+00  3.00000000E+00  4.00000000E+00  1.20000000E+01  1.00000000E+00
 4.60000000E-01   2.26000000E+00  4.00000000E+00  3.00000000E+00  4.00000000E+00  1.20000000E+01  1.00000000E+00
 5.90000000E-01   2.96000000E+00  4.00000000E+00  3.00000000E+00  4.00000000E+00  1.20000000E+01  1.00000000E+00
  0.              0.              1.00000000E+00  6.00000000E+00  4.00000000E+00  6.00000000E+00  1.00000000E+00
```

7.30000000E-01	2.89000000E+00	1.00000000E+00	6.00000000E+00	4.00000000E+00	6.00000000E+00	1.00000000E+00
0.	0.	1.00000000E+00	3.00000000E+00	4.00000000E+00	2.00000000E+00	1.00000000E+00
3.00000000E-01	2.26000000E+00	1.00000000E+00	3.00000000E+00	4.00000000E+00	2.00000000E+00	1.00000000E+00
4.40000000E-01	2.54000000E+00	1.00000000E+00	3.00000000E+00	4.00000000E+00	2.00000000E+00	1.00000000E+00
0.	0.	3.00000000E+00	0.	0.	1.20000000E+01	1.00000000E+00
4.20000000E-01	2.90000000E+00	3.00000000E+00	0.	0.	1.20000000E+01	1.00000000E+00
0.	0.	2.00000000E+00	3.00000000E+00	4.00000000E+00	6.00000000E+00	1.00000000E+00
1.70000000E-01	1.32000000E+00	2.00000000E+00	3.00000000E+00	4.00000000E+00	6.00000000E+00	1.00000000E+00
3.83000000E-01	1.71000000E+00	2.00000000E+00	3.00000000E+00	4.00000000E+00	6.00000000E+00	1.00000000E+00
4.60000000E-01	2.60000000E+00	2.00000000E+00	3.00000000E+00	4.00000000E+00	6.00000000E+00	1.00000000E+00
5.27000000E-01	2.78000000E+00	2.00000000E+00	3.00000000E+00	4.00000000E+00	6.00000000E+00	1.00000000E+00
6.55000000E-01	2.79000000E+00	2.00000000E+00	3.00000000E+00	4.00000000E+00	6.00000000E+00	1.00000000E+00
7.20000000E-01	2.80000000E+00	2.00000000E+00	3.00000000E+00	4.00000000E+00	6.00000000E+00	1.00000000E+00
0.	0.	2.00000000E+00	3.00000000E+00	8.00000000E+00	1.20000000E+01	1.00000000E+00
3.08000000E-01	2.04000000E+00	2.00000000E+00	3.00000000E+00	8.00000000E+00	1.20000000E+01	1.00000000E+00
6.18000000E-01	2.78000000E+00	2.00000000E+00	3.00000000E+00	8.00000000E+00	1.20000000E+01	1.00000000E+00
8.00000000E-01	2.85000000E+00	2.00000000E+00	3.00000000E+00	8.00000000E+00	1.20000000E+01	1.00000000E+00
0.	0.	4.00000000E+00	6.00000000E+00	0.	1.20000000E+01	1.00000000E+00
3.82000000E-01	1.71000000E+00	4.00000000E+00	6.00000000E+00	0.	1.20000000E+01	1.00000000E+00
5.27000000E-01	2.48000000E+00	4.00000000E+00	6.00000000E+00	0.	1.20000000E+01	1.00000000E+00
6.55000000E-01	2.92000000E+00	4.00000000E+00	6.00000000E+00	0.	1.20000000E+01	1.00000000E+00
7.20000000E-01	2.96000000E+00	4.00000000E+00	6.00000000E+00	0.	1.20000000E+01	1.00000000E+00
0.	0.	2.00000000E+00	3.00000000E+00	0.	6.00000000E+00	1.00000000E+00
4.30000000E-01	2.30000000E+00	2.00000000E+00	3.00000000E+00	0.	6.00000000E+00	1.00000000E+00
5.60000000E-01	2.34000000E+00	2.00000000E+00	3.00000000E+00	0.	6.00000000E+00	1.00000000E+00
7.40000000E-01	2.40000000E+00	2.00000000E+00	3.00000000E+00	0.	6.00000000E+00	1.00000000E+00
8.50000000E-01	2.48000000E+00	2.00000000E+00	3.00000000E+00	0.	6.00000000E+00	1.00000000E+00
9.70000000E-01	3.00000000E+00	2.00000000E+00	3.00000000E+00	0.	6.00000000E+00	1.00000000E+00
0.	0.	3.00000000E+00	0.	4.00000000E+00	1.20000000E+01	1.00000000E+00
3.59000000E-01	2.26000000E+00	3.00000000E+00	0.	4.00000000E+00	1.20000000E+01	1.00000000E+00
0.	0.	3.00000000E+00	0.	0.	6.00000000E+00	1.00000000E+00
2.77000000E-01	2.10000000E+00	3.00000000E+00	0.	0.	6.00000000E+00	1.00000000E+00
2.94000000E-01	2.20000000E+00	3.00000000E+00	0.	0.	6.00000000E+00	1.00000000E+00
0.	0.	2.00000000E+00	0.	0.	1.20000000E+01	1.00000000E+00
2.30000000E-01	1.49000000E+00	2.00000000E+00	0.	0.	1.20000000E+01	1.00000000E+00
0.	0.	3.00000000E+00	3.00000000E+00	0.	6.00000000E+00	1.00000000E+00
1.04000000E-01	1.32000000E+00	3.00000000E+00	3.00000000E+00	0.	6.00000000E+00	1.00000000E+00
2.80000000E-01	1.90000000E+00	3.00000000E+00	3.00000000E+00	0.	6.00000000E+00	1.00000000E+00
5.00000000E-01	2.30000000E+00	3.00000000E+00	3.00000000E+00	0.	6.00000000E+00	1.00000000E+00
5.90000000E-01	2.56000000E+00	3.00000000E+00	3.00000000E+00	0.	6.00000000E+00	1.00000000E+00
0.	0.	5.00000000E+00	6.00000000E+00	4.00000000E+00	1.80000000E+01	1.00000000E+00
5.40000000E-01	2.70000000E+00	5.00000000E+00	6.00000000E+00	4.00000000E+00	1.80000000E+01	1.00000000E+00
8.50000000E-01	2.95000000E+00	5.00000000E+00	6.00000000E+00	4.00000000E+00	1.80000000E+01	1.00000000E+00
0.	0.	3.00000000E+00	6.00000000E+00	8.00000000E+00	1.80000000E+01	1.00000000E+00
3.00000000E-01	1.95000000E+00	3.00000000E+00	6.00000000E+00	8.00000000E+00	1.80000000E+01	1.00000000E+00
6.90000000E-01	2.62000000E+00	3.00000000E+00	6.00000000E+00	8.00000000E+00	1.80000000E+01	1.00000000E+00
0.	0.	4.00000000E+00	6.00000000E+00	1.20000000E+01	1.80000000E+01	1.00000000E+00
5.60000000E-01	2.55000000E+00	4.00000000E+00	6.00000000E+00	1.20000000E+01	1.80000000E+01	1.00000000E+00
7.03000000E-01	2.72000000E+00	4.00000000E+00	6.00000000E+00	1.20000000E+01	1.80000000E+01	1.00000000E+00
8.94000000E-01	2.90000000E+00	4.00000000E+00	6.00000000E+00	1.20000000E+01	1.80000000E+01	1.00000000E+00
6.46000000E-01	2.96000000E+00	4.00000000E+00	6.00000000E+00	1.20000000E+01	1.80000000E+01	1.00000000E+00
7.30000000E-01	2.76000000E+00	4.00000000E+00	6.00000000E+00	1.20000000E+01	1.80000000E+01	1.00000000E+00
2.60000000E-01	2.00000000E+00	4.00000000E+00	6.00000000E+00	1.20000000E+01	1.80000000E+01	1.00000000E+00
0.	0.	4.00000000E+00	6.00000000E+00	4.00000000E+00	3.20000000E+01	2.00000000E+00
4.60000000E-01	2.18000000E+00	4.00000000E+00	6.00000000E+00	4.00000000E+00	3.20000000E+01	2.00000000E+00
5.90000000E-01	2.40000000E+00	4.00000000E+00	6.00000000E+00	4.00000000E+00	3.20000000E+01	2.00000000E+00
0.	0.	3.00000000E+00	3.00000000E+00	4.00000000E+00	3.20000000E+01	2.00000000E+00
2.72000000E-01	1.85000000E+00	3.00000000E+00	3.00000000E+00	4.00000000E+00	3.20000000E+01	2.00000000E+00
5.33000000E-01	2.74000000E+00	3.00000000E+00	3.00000000E+00	4.00000000E+00	3.20000000E+01	2.00000000E+00
0.	0.	3.00000000E+00	6.00000000E+00	1.20000000E+01	3.20000000E+01	2.00000000E+00
5.65000000E-01	2.32000000E+00	3.00000000E+00	6.00000000E+00	1.20000000E+01	3.20000000E+01	2.00000000E+00
7.70000000E-01	2.96000000E+00	3.00000000E+00	6.00000000E+00	1.20000000E+01	3.20000000E+01	2.00000000E+00

9.90000000E-01 3.00000000E+00 3.00000000E+00 6.00000000E+00 1.20000000E+01 3.60000000E+01 2.00000000E+00

VARIABLE		MEAN	STANDARD DEVIATION
LRSVSV	1	.37028	.29609
LCP	2	1.66758	1.14127
D1	3	2.76842	1.04630
D2	4	3.25263	2.17318
D3	5	4.75789	3.96988
#T	6	14.58947	10.05463
NXL	7	1.23158	.42408
ARCTAN	8	.33184	.25355
CBLCP	9	10.18614	8.66436
SQLCP	10	4.06961	3.09206

COVARIANCE MATRIX

VARIABLE NUMBER	1	2	3	4	5	6	7	8	9	10
1	.088	.313	.022	.121	.175	.177	.004	.075	2.421	.873
2		1.303	.061	.321	.415	-.065	-.020	.275	9.132	3.436
3			1.095	.729	1.028	5.542	.075	.019	.945	.281
4				4.723	1.977	4.764	.069	.099	3.253	1.070
5					15.760	23.974	.674	.138	6.154	1.796
6						101.096	3.649	.112	7.291	1.509
7							.180	.001	.049	-.013
8								.064	2.071	.756
9									75.071	26.421
10										9.561

CORRELATION MATRIX

VARIABLE NUMBER	1	2	3	4	5	6	7	8	9	10
1	1.000	.926	.072	.187	.149	.059	.028	.996	.944	.953
2		1.000	.051	.129	.092	-.006	-.042	.950	.923	.974
3			1.000	.321	.248	.527	.170	.071	.104	.087
4				1.000	.229	.218	.074	.180	.173	.159
5					1.000	.601	.400	.137	.179	.146
6						1.000	.856	.044	.084	.049
7							1.000	.011	.013	-.010
8								1.000	.943	.964
9									1.000	.986
10										1.000

SUE PROBLEM CARD
UBPRC 8 -0 -0 -0 -0 -0 YES YES YES

```
SUB-PROBLM     1
 DEPENDENT VARIABLE            8
 MAXIMUM NUMBER OF STEPS      20
 F-LEVEL FOR INCLUSION      .010000
 F-LEVEL FOR DELETION       .005000
 TOLERANCE LEVEL            .001000

CONTROL-DELETE CARDS
ONCEL1*********
```

STEP NUMBER 1
VARIABLE ENTERED 10

MULTIPLE R .9638
STD. ERROR FOR RESIDUALS .0680

ANALYSIS OF VARIANCE

	DF	SUM OF SQUARES	MEAN SQUARE	F RATIO
REGRESSION	1	5.613	5.613	1214.618
RESIDUAL	93	.430	.005	

VARIABLES IN EQUATION

VARIABLE	COEFFICIENT	STD. ERROR	F TO REMOVE
(CONSTANT	.01021)		
SQLCP 10	.07903	.00227	1214.6179

VARIABLES NOT IN EQUATION

VARIABLE		PARTIAL CORR.	TOLERANCE	F TO ENTER
LRSVSV	1	.96203	.0909	1142.9149
LCP	2	.19048	.0520	3.4638
D1	3	-.04650	.9924	.1994
D2	4	.10066	.9747	.9417
D3	5	-.01351	.9786	.0168
WT	6	-.01131	.9976	.0118
NXL	7	.07872	.9999	.5737
CRLCP	9	-.17712	.0274	2.9796

STEP NUMBER 2
VARIABLE ENTERED 2

MULTIPLE R .9651
STD. ERROR FOR RESIDUALS .0671

ANALYSIS OF VARIANCE

	DF	SUM OF SQUARES	MEAN SQUARE	F RATIO
REGRESSION	2	5.629	2.815	625.130
RESIDUAL	92	.414	.005	

VARIABLES IN EQUATION

VARIABLE	COEFFICIENT	STD. ERROR	F TO REMOVE

VARIABLES NOT IN EQUATION

VARIABLE	PARTIAL CORR.	TOLERANCE	F TO ENTER

VARIABLES IN EQUATION				VARIABLES NOT IN EQUATION			
VARIABLE	COEFFICIENT	STD. ERROR	F TO REMOVE	VARIABLE		PARTIAL CORR.	TOLERANCE	F TO ENTER
(CONSTANT | .00006)							
LCP 2	.04949	.02659	3.4638	LRSVSV	1	.98693	.0908	3412.3257
SQLCP 10	.06125	.00982	38.9363	D1	3	-.01876	.9705	.0320
				D2	4	.12551	.9620	1.4564
				D3	5	.03079	.9288	.0863
				WT	6	.03446	.9439	.1082
				NXL	7	.10878	.9798	1.0898
				CRLCP	9	.03525	.0015	.1132

STEP NUMBER 3
VARIABLE ENTERED 4

MULTIPLE R .9657
STD. ERROR FOR RESIDUALS .0669

ANALYSIS OF VARIANCE

	DF	SUM OF SQUARES	MEAN SQUARE	F RATIO
REGRESSION	3	5.636	1.879	419.306
RESIDUAL	91	.408	.004	

VARIABLES IN EQUATION				VARIABLES NOT IN EQUATION			
VARIABLE	COEFFICIENT	STD. ERROR	F TO REMOVE	VARIABLE		PARTIAL CORR.	TOLERANCE	F TO ENTER
(CONSTANT | -.01163)							
LCP 2	.05317	.02670	3.9653	LRSVSV	1	.98677	.0895	3333.9556
D2 4	.00391	.00324	1.4564	D1	3	-.05966	.8830	.3215
SQLCP 10	.05949	.00990	36.1131	D3	5	.00698	.8949	.0044
				WT	6	.01048	.9086	.0099
				NXL	7	.10203	.9761	.9467
				CRLCP	9	.04363	.0015	.1716

STEP NUMBER 4
VARIABLE ENTERED 7

MULTIPLE R .9660
STD. ERROR FOR RESIDUALS .0670

ANALYSIS OF VARIANCE

	DF	SUM OF SQUARES	MEAN SQUARE	F RATIO
REGRESSION	4	5.640	1.410	314.532
RESIDUAL	90	.403	.004	

VARIABLES IN EQUATION				VARIABLES NOT IN EQUATION			
VARIABLE	COEFFICIENT	STD. ERROR	F TO REMOVE	VARIABLE		PARTIAL CORR.	TOLERANCE	F TO ENTER
(CONSTANT | -.03165)							
LCP 2	.05669	.02695	4.4238	LRSVSV	1	.98671	.0883	3282.1747
D2 4	.00371	.00325	1.3088	D1	3	-.07531	.8651	.5077
NXL 7	.01604	.01648	.9467	D3	5	-.03504	.7630	.1094

SQLCP 10	.05827	.00998	34.0788	WT 6	-.15379	.2331	2.1559
				CRLCP 9	.04256	.0015	.1415

STEP NUMBER 5
VARIABLE ENTERED 6

MULTIPLE R .9689
STD. ERROR FOR RESIDUALS .0665

ANALYSIS OF VARIANCE

	DF	SUM OF SQUARES	MEAN SQUARE	F RATIO
REGRESSION	5	5.649	1.130	255.289
RESIDUAL	89	.394	.004	

VARIABLES IN EQUATION

VARIABLE	COEFFICIENT	STD. ERROR	F TO REMOVE
(CONSTANT	-.05548)		
LCP 2	.04881	.02731	3.1938
D2 4	.00505	.00335	2.2730
WT 6	-.00208	.00141	2.1559
NXL 7	.05697	.03233	3.1046
SQLCP 10	.06133	.01013	36.6210

VARIABLES NOT IN EQUATION

VARIABLE	PARTIAL CORR.	TOLERANCE	F TO ENTER
LRSVSV 1	.98650	.0857	3192.5650
D1 3	.05140	.4177	.2331
D3 5	.04785	.5761	.2019
CRLCP 9	.03118	.0015	.0857

STEP NUMBER 6
VARIABLE ENTERED 3

MULTIPLE R .9689
STD. ERROR FOR RESIDUALS .0668

ANALYSIS OF VARIANCE

	DF	SUM OF SQUARES	MEAN SQUARE	F RATIO
REGRESSION	6	5.650	.942	210.946
RESIDUAL	88	.393	.004	

VARIABLES IN EQUATION

VARIABLE	COEFFICIENT	STD. ERROR	F TO REMOVE
(CONSTANT	-.07307)		
LCP 2	.04801	.02748	3.0525
D1 3	.00492	.01019	.2331
D2 4	.00482	.00340	2.0048
WT 6	-.00278	.00204	1.8578
NXL 7	.06932	.04134	2.8119
SQLCP 10	.06103	.01020	36.5246

VARIABLES NOT IN EQUATION

VARIABLE	PARTIAL CORR.	TOLERANCE	F TO ENTER
LRSVSV 1	.98662	.0856	3187.0087
D3 5	.07365	.4894	.4745
CRLCP 9	.03711	.0015	.1200

STEP NUMBER 7

VARIABLE ENTERED 5

MULTIPLE R .9671
STD. ERROR FOR RESIDUALS .0670

ANALYSIS OF VARIANCE

	DF	SUM OF SQUARES	MEAN SQUARE	F RATIO
REGRESSION	7	5.653	.808	179.799
RESIDUAL	87	.391	.004	

VARIABLES IN EQUATION				VARIABLES NOT IN EQUATION			
VARIABLE	COEFFICIENT	STD. ERROR	F TO REMOVE	VARIABLE	PARTIAL CORR.	TOLERANCE	F TO ENTER
(CONSTANT	-.08955)						
LCP 2	.04922	.02762	3.1756	LRSVSV 1	.98661	.0853	3147.2078
D1 3	.00788	.01109	.5054	CRLCP 9	.03998	.0015	.1377
D2 4	.00455	.00343	1.7548				
D3 5	.00171	.00249	.4745				
WT 6	-.00382	.00254	2.2602				
NXL 7	.08282	.04586	3.2613				
SQLCP 10	.06100	.01027	35.2851				

STEP NUMBER 8
VARIABLE ENTERED 9

MULTIPLE R .9672
STD. ERROR FOR RESIDUALS .0674

ANALYSIS OF VARIANCE

	DF	SUM OF SQUARES	MEAN SQUARE	F RATIO
REGRESSION	8	5.653	.707	155.782
RESIDUAL	86	.390	.005	

VARIABLES IN EQUATION				VARIABLES NOT IN EQUATION			
VARIABLE	COEFFICIENT	STD. ERROR	F TO REMOVE	VARIABLE	PARTIAL CORR.	TOLERANCE	F TO ENTER
(CONSTANT	-.09136)						
LCP 2	.09108	.11616	.6147	LRSVSV 1	.99154	.0836	4958.9820
D1 3	.00837	.01122	.5559				
D2 4	.00458	.00345	1.7567				
D3 5	.00175	.00250	.4882				
WT 6	-.00386	.00255	2.2812				
NXL 7	.08325	.04610	3.2610				
CBLCP 9	.00778	.02096	.1377				
SQLCP 10	.02445	.09904	.0609				

F-LEVEL OR TOLERANCE INSUFFICIENT FOR FURTHER COMPUTATION

SUMMARY TABLE

STEP NUMBER	VARIABLE ENTERED	VARIABLE REMOVED	MULTIPLE R	RSQ	INCREASE IN RSQ	F VALUE TO ENTER OR REMOVE	NUMBER OF INDEPENDENT VARIABLES INCLUDED
1	SQLCP	10	.9638	.9289	.9289	1214.6179	1
2	LCP	2	.9651	.9315	.0026	3.4638	2
3	D2	4	.9657	.9325	.0011	1.4564	3
4	NXL	7	.9660	.9332	.0007	.9467	4
5	WT	6	.9669	.9348	.0016	2.1559	5
6	D1	3	.9669	.9350	.0002	.2331	6
7	D3	5	.9671	.9353	.0004	.4745	7
8	CBLCP	9	.9672	.9354	.0001	.1377	8

LIST OF Y-VALUES, Y-ESTIMATES, AND RESIDUALS

CASE	Y-VALUE	Y-ESTIMATE	RESIDUAL
1	0.	-9.22772784E-03	9.22772784E-03
2	2.91456794E-01	3.32929214E-01	-4.14724196E-02
3	7.01584135E-01	6.63127003E-01	3.84571317E-02
4	0.	6.13487292E-03	-6.13487292E-03
5	5.51375965E-01	5.91236458E-01	-3.98604930E-02
6	0.	4.49928191E-03	-4.49928191E-03
7	5.33034110E-01	5.28349612E-01	4.68449846E-03
8	0.	-2.33655304E-02	2.33655304E-02
9	5.33034110E-01	6.36033369E-01	-1.02999258E-01
10	0.	-3.84628748E-02	3.84628748E-02
11	3.36674819E-01	3.03694067E-01	3.29807522E-02
12	5.40419500E-01	5.54607675E-01	-1.41881752E-02
13	0.	2.70008722E-02	-2.70008722E-02
14	5.97176958E-01	5.84762465E-01	1.24141928E-02
15	7.55762755E-01	7.08085558E-01	5.16771973E-02
16	0.	4.20982166E-02	-4.20982166E-02
17	3.09702945E-01	3.59428288E-01	-4.97253438E-02
18	0.	7.91064046E-03	-7.91064046E-03
19	3.45555581E-01	2.7402292YE-01	7.15326512E-02
20	4.71615568E-01	3.50067582E-01	1.21547985E-01
21	5.97176958E-01	3.79005586E-01	2.18171072E-01 *
22	0.	6.27504945E-03	-6.27504945E-03
23	1.73245066E-01	1.86978397E-01	-1.37327302E-02
24	3.89097231E-01	3.48431991E-01	4.06652397E-02
25	0.	-2.16284648E-03	2.16284648E-03
26	2.44978963E-01	3.63028480E-01	-1.18049817E-01
27	3.89097231E-01	3.86996982E-01	2.10024871E-03
28	4.14506875E-01	4.08754472E-01	5.75240248E-03
29	0.	-2.14486885E-04	2.14486885E-04
30	4.31138741E-01	4.2025597UE-01	1.08827706E-02
31	5.33034110E-01	5.23635843E-01	9.39826725E-03
32	0.	1.15641633E-02	-1.15641633E-02
33	6.36577757E-01	6.6668135dE-01	-3.61036008E-02
34	0.	1.32711825E-02	-1.32711825E-02
35	2.91456794E-01	4.3374164UE-01	-1.42284845E-01 *
36	4.14506875E-01	5.29772064E-01	-1.15265190E-01
37	0.	-2.93040974E-02	2.93040974E-02
38	3.97627992E-01	5.0944752dE-01	-1.11819536E-01
39	0.	6.20362122E-03	-6.20362122E-03
40	1.68390157E-01	1.8690696dE-01	-1.85168112E-02
41	3.65765856E-01	2.7231591UE-01	9.34499461E-02
42	4.31138741E-01	5.4495524?E-01	-1.13816506E-01
43	4.85013570E-01	6.1542458IE-01	-1.30411011E-01
44	5.79882132E-01	6.19506722E-01	-3.96245898E-02
45	6.24023053E-01	6.23606772E-01	4.16280936E-04
46	0.	-9.95128920E-03	9.95128920E-03
47	2.98779988E-01	3.43607574E-01	-4.48275855E-02
48	5.53549764E-01	5.99269671E-01	-4.5719906?E-02
49	6.74740942E-01	6.2822237dE-01	4.65185602E-02
50	0.	6.51639880E-03	-6.51638980E-03
51	3.64893489E-01	3.2386462E-01	4.1047027?E-02
52	4.85013570E-01	5.01369249E-01	-1.63556761E-02
53	5.79882132E-01	5.5282060?E-01	2.70615233E-02
54	6.24023053E-01	5.68131559E-01	5.58914967E-02
55	0.	-7.92511851E-04	7.92511851E-04
56	4.06098088E-01	4.3263177YE-01	-2.65337203E-02
57	5.10498322E-01	4.4583556?E-01	6.4052754?E-02
58	6.37070329E-01	4.66116450E-01	1.70953880E-01 *
59	7.04494064E-01	4.9406034?E-01	2.10433720E-01 *
60	7.70170914E-01	7.02444345E-01	6.77265686E-02
61	0.	-2.23079643E-02	2.23079643E-02
62	3.44670029E-01	3.98162493E-01	-5.34924632E-02
63	0.	-6.15305391E-03	6.15305391E-03
64	2.70224043E-01	3.64941892E-01	-9.47172491E-02
65	2.85943158E-01	3.9534978UE-01	-1.09405628E-01
66	0.	-3.76705651E-02	3.76705651E-02
67	2.26068388E-01	1.78033258E-01	4.80351305E-02
68	0.	7.57395584E-03	-7.57395584E-03
69	1.03627460E-01	1.88277303E-01	-8.46498430E-02
70	2.73008703E-01	3.2221512UE-01	-4.92064170E-02
71	4.63647609E-01	4.40998246E-01	2.26493627E-02
72	5.33034110E-01	5.3142428UE-01	1.60982452E-03
73	0.	-1.27205293E-03	1.27205293E-03
74	4.95133263E-01	5.7593089?E-01	-8.07976315E-02
75	7.04494064E-01	6.36901612E-01	6.75924520E-02
76	0.	-1.10088553E-02	1.10088553E-02
77	2.91456794E-01	2.90393172E-01	1.06362234E-03
78	6.03982978E-01	5.3529536dE-01	6.86876142E-02
79	0.	4.35374552E-03	-4.35374552E-03
80	5.10488322E-01	5.24520957E-01	-1.40326349E-02
81	6.12736551E-01	5.8945533UE-01	2.32812205E-02
82	5.35996055E-01	5.4310537IE-01	-7.10931559E-03
83	5.7358d129E-01	5.65968912E-01	7.58921628E-03
84	6.30577757E-01	6.0546396JE-01	2.51137942E-02
85	2.5436d059E-01	3.4651068?E-01	-9.21426289E-02
86	0.	1.95966269E-02	-1.95966263E-02
87	4.31138741E-01	4.14897336E-01	1.62414044E-02
88	5.33034110E-01	4.86505588E-01	4.65285224E-02
89	0.	-2.49685116E-03	2.49685116E-03
90	2.65575001E-01	2.9890517dE-01	-3.33301750E-02
91	4.89697775E-01	5.90573699E-01	-1.00875924E-01
92	0.	2.52224247E-02	-2.52224247E-02
93	5.14286541E-01	4.65217178E-01	4.90693628E-02
94	6.56178718E-01	5.49072755E-01	1.07105963E-01
95	7.80373080E-01	7.2845928dE-01	5.19137980E-02

FINISH CARD ENCOUNTERED
PROGRAM TERMINATED

APPENDIX 4.7

COMPUTER PROGRAM AND CALCULATED VALUES OF ROUGHNESS INDEX AND PRESENT SERVICEABILITY INDEX

```
      PROGRAM PSI (INPUT, OUTPUT, TAPE5=INPUT)
      PRINT 60
   60 FORMAT  (1H1, 5X, 36HCRK   THICKNESSES   AXLE NO.  ROUGH
     *         33HROUGH  RUT   CALC  SECTION MONTH /
     *         4X, 43HINDEX AC    B     SB     WT  AXLE  IND-I IND-T
     *         11H DEPTH  PSI  // )
   20 CONTINUE
      READ (5,30)  CI, GO, DT, DTH, WT, NXL, SVX, ROI, NSECT,MONTH
   30 FORMAT  (5FE.0, I6, 2F8.0, 2A8 )
      IF (EOF,5) 99, 40
   40 CONTINUE
*
*     CI      CRACKING INDEX
*     GO      THICKNESS OF ASPHALT CONCRETE
*     DT      THICKNESS OF BASE
*     DTH     THICKNESS OF SUBBASE
*     WT      AXLE LOAD
*     NXL     NUMBER OF AXLE
*             1 =  SINGLE AXLE
*             2 =  TANDEM AXLE
*     SVX     ROUGHNESS INDEX --  LOG (1+SLOPE VARIANCE)  OF A
*             SECTION JUST AFTER CONSTRUCTION OR AT THE BEGINNING
*             OF THE ANALYSIS PERIOD  = ROUGH IND-I.
*     ROI     RUT DEPTH INDEX
*     NSECT   SECTION NUMBER OF REFERENCE TO
*     MONTH   MONTH FOR WHICH PSI IS CALCULATED
*
         SV2 = 10.0**SVX - 1.0
*     SV2     SLOPE VARIANCE OF THE SECTION AT THE BEGINNING OF THE
*             ANALYSIS PERIOD
*
         B = -0.09136 + 0.09108*ALOG10(1.0+CI) + 0.02445*
     *           ALOG10(1.0+CI)**2.0+ 0.00778*ALOG10(1.0*C1)
     *           **3.0 + 0.00837*DO + 0.00458*DT + 0.00175*
     *           DTH - 0.00386*WT + 0.08325*NXL
*
         SV = (10.0**TAN(B) -1.0 +SV2**0.5) ** 2.0
*     SV      CALCULATED VALUE OF SLOPE VARIANCE AT ANY TIME
*             AFTER BEGINNING OF ANALYSIS PERIOD
*
         SVL = ALOG10(1.0+SV)
*     SVL     CALCULATED VALUE OF ROUGHNESS INDEX-- LOG(1+SV)  AT
*             ANY TIME AFTER BEGINNING OF ANALYSIS PERIOD =ROUGH IND-T.
*
         PSIC = 5.03 - 1.91*ALOG10(1.0+SV) - 1.38*ROI**2.0
     *        - 0.01*CI**0.5
*     PSIC    CALCULATED VALUE OF PSI
*
      PRINT  50,  CI, GO, DT, DTH, WT, NXL, SVX, SVL, ROI, PSIC,
     *        NSECT, MONTH
   50 FORMAT  ( 5X, F3.0, 3F5.2, F7.1, I3, F6.2, F7.2, F6.2, F7.2,
     *        A8, 1X, A8)
      GO TO 20
   99 CONTINUE
      END
```

CRK INDEX	THICKNESSES AC	B	SB	AXLE NO. WT	AXLE	ROUGH IND-I	ROUGH IND-T	RUT DEPTH	CALC PSI	SECTION	MONTH
0	4.00	3.00	4.00	18.0	1	.30	.28	0.00	4.50	627	B
40	4.00	3.00	4.00	18.0	1	.30	.58	.12	3.84	627	FEB
70	4.00	3.00	4.00	18.0	1	.30	.67	.13	3.64	627	MAR
230	4.00	3.00	4.00	18.0	1	.30	.97	.13	3.00	627	APR
0	3.00	6.00	8.00	18.0	1	.30	.29	0.00	4.48	623	B
90	3.00	6.00	8.00	18.0	1	.30	.75	.33	3.36	623	FEB
160	3.00	6.00	8.00	18.0	1	.30	.89	.34	3.05	623	MAR
400	3.00	6.00	8.00	18.0	1	.30	1.20	.35	2.37	623	APR
600	3.00	6.00	8.00	18.0	1	.30	1.38	.36	1.97	623	MAY
0	3.00	0.00	8.00	18.0	1	.60	.57	0.00	3.95	607	B
70	3.00	0.00	8.00	18.0	1	.60	.89	.15	3.22	607	DEC
270	3.00	0.00	8.00	18.0	1	.60	1.16	.16	2.61	607	FEB
350	3.00	0.00	8.00	18.0	1	.60	1.24	.16	2.44	607	MAR
670	3.00	0.00	8.00	18.0	1	.60	1.48	.65	1.36	607	APR
0	4.00	6.00	12.00	18.0	1	.50	.50	0.00	4.07	625	B
135	4.00	6.00	12.00	18.0	1	.50	1.00	.31	2.86	625	APR-1
290	4.00	6.00	12.00	18.0	1	.50	1.21	.32	2.40	625	MAY-1
790	4.00	6.00	12.00	18.0	1	.50	1.64	.33	1.47	625	JUL
940	4.00	6.00	12.00	18.0	1	.50	1.74	.34	1.25	625	DEC
940	4.00	6.00	12.00	18.0	1	.50	1.74	.53	1.02	625	MAR-2
960	4.00	6.00	12.00	18.0	1	.50	1.75	.53	.99	625	APR-2
970	4.00	6.00	12.00	18.0	1	.50	1.76	.53	.98	625	MAY-2
980	4.00	6.00	12.00	18.0	1	.50	1.76	.54	.95	625	JUN-2
985	4.00	6.00	12.00	18.0	1	.50	1.76	.54	.94	625	JUL-2
990	4.00	6.00	12.00	18.0	1	.50	1.77	.54	.94	625	NOV-2
0	5.00	6.00	4.00	18.0	1	.50	.50	0.00	4.08	615	B
40	5.00	6.00	4.00	18.0	1	.50	.78	.17	3.44	615	APR-1
120	5.00	6.00	4.00	18.0	1	.50	.97	.16	3.04	615	MAY-1
640	5.00	6.00	4.00	18.0	1	.50	1.51	.17	1.84	615	JUL
860	5.00	6.00	4.00	18.0	1	.50	1.67	.30	1.43	615	DEC
880	5.00	6.00	4.00	18.0	1	.50	1.68	.37	1.33	615	MAR-2
900	5.00	6.00	4.00	18.0	1	.50	1.69	.38	1.30	615	APR-2
0	5.00	6.00	4.00	18.0	1	.20	.20	0.00	4.65	629	B
10	5.00	6.00	4.00	18.0	1	.20	.35	.16	4.29	629	MAR-1
140	5.00	6.00	4.00	18.0	1	.20	.80	.16	3.35	629	APR-1
860	5.00	6.00	4.00	18.0	1	.20	1.57	.35	1.56	629	DEC-2
870	5.00	6.00	4.00	18.0	1	.20	1.58	.36	1.54	629	FEB-2
880	5.00	6.00	4.00	18.0	1	.20	1.59	.36	1.52	629	MAR-2
900	5.00	6.00	4.00	18.0	1	.20	1.60	.37	1.48	629	APR-2
0	2.00	3.00	8.00	12.0	1	.90	.89	0.00	3.32	159	B
250	2.00	3.00	8.00	12.0	1	.90	1.37	.33	2.11	159	FEB
340	2.00	3.00	8.00	12.0	1	.90	1.45	.34	1.92	159	MAR
670	2.00	3.00	8.00	12.0	1	.90	1.67	.35	1.41	159	APR
830	2.00	3.00	8.00	12.0	1	.90	1.76	.35	1.20	159	MAY
0	3.00	0.00	4.00	12.0	1	.50	.48	0.00	4.11	163	B
190	3.00	0.00	4.00	12.0	1	.50	1.04	.08	2.90	163	MAR
450	3.00	0.00	4.00	12.0	1	.50	1.31	.09	2.30	163	APR
700	3.00	0.00	4.00	12.0	1	.50	1.50	.10	1.88	163	MAY
0	4.00	3.00	4.00	12.0	1	.70	.70	0.00	3.69	151	B
80	4.00	3.00	4.00	12.0	1	.70	1.03	.27	2.87	151	APR
180	4.00	3.00	4.00	12.0	1	.70	1.19	.27	2.53	151	MAY
320	4.00	3.00	4.00	12.0	1	.70	1.51	.28	1.82	151	JUN
0	4.00	6.00	0.00	12.0	1	.70	.71	0.00	3.68	161	B
50	4.00	6.00	0.00	12.0	1	.70	.97	.26	3.00	161	APR
150	4.00	6.00	0.00	12.0	1	.70	1.16	.27	2.59	161	MAY
450	4.00	6.00	0.00	12.0	1	.70	1.47	.28	1.91	161	JUN
660	4.00	6.00	0.00	12.0	1	.70	1.62	.29	1.56	161	JUL
800	4.00	6.00	0.00	12.0	1	.70	1.72	.30	1.34	161	AUG

0	4.00	6.00	0.00	12.0	1	.70	.71	0.00	3.68	149	B
10	4.00	6.00	0.00	12.0	1	.70	.82	.10	3.41	149	MAR
50	4.00	6.00	0.00	12.0	1	.70	.97	.10	3.08	149	APR
150	4.00	6.00	0.00	12.0	1	.70	1.16	.11	2.68	149	MAY
0	1.00	3.00	0.00	6.0	1	.75	.74	0.00	3.61	744	B
10	1.00	3.00	0.00	6.0	1	.75	.85	.09	3.36	744	DEC
11	1.00	3.00	0.00	6.0	1	.75	.86	.09	3.35	744	JAN
140	1.00	3.00	0.00	6.0	1	.75	1.15	.10	2.70	744	FEB
0	1.00	6.00	4.00	6.0	1	.90	.91	0.00	3.30	720	B
150	1.00	6.00	4.00	6.0	1	.90	1.30	.14	2.41	720	APR
220	1.00	6.00	4.00	6.0	1	.90	1.37	.14	2.23	720	MAY-1
330	1.00	6.00	4.00	6.0	1	.90	1.48	.14	2.00	720	JUN-1
380	1.00	6.00	4.00	6.0	1	.90	1.52	.14	1.91	720	JUL-1
580	1.00	6.00	4.00	6.0	1	.90	1.66	.15	1.58	720	DEC-2
650	1.00	6.00	4.00	6.0	1	.90	1.71	.30	1.39	720	FEB-2
700	1.00	6.00	4.00	6.0	1	.90	1.74	.30	1.32	720	MAR-2
0	2.00	3.00	4.00	6.0	1	.50	.51	0.00	4.06	742	B
210	2.00	3.00	4.00	6.0	1	.50	1.12	.12	2.73	742	MAR
840	2.00	3.00	4.00	6.0	1	.50	1.68	.14	1.51	742	DEC-2
850	2.00	3.00	4.00	6.0	1	.50	1.68	.15	1.49	742	JAN-2
860	2.00	3.00	4.00	6.0	1	.50	1.69	.15	1.48	742	FEB-2
870	2.00	3.00	4.00	6.0	1	.50	1.70	.29	1.38	742	MAR-2
0	2.00	3.00	4.00	6.0	1	.70	.70	0.00	3.58	710	B
90	2.00	3.00	4.00	6.0	1	.70	1.06	.29	2.79	710	APR-1
210	2.00	3.00	4.00	6.0	1	.70	1.24	.12	2.51	710	MAY-1
870	2.00	3.00	4.00	6.0	1	.70	1.76	.29	1.26	710	MAR-2
920	2.00	3.00	4.00	6.0	1	.70	1.79	.29	1.19	710	MAY-2
950	2.00	3.00	4.00	6.0	1	.70	1.81	.30	1.14	710	JUN-2
970	2.00	3.00	4.00	6.0	1	.70	1.82	.31	1.11	710	JUL-2
0	1.00	3.00	0.00	2.0	1	.80	.80	0.00	3.49	743	B
50	1.00	3.00	0.00	2.0	1	.80	1.05	.06	2.95	743	MAY
200	1.00	3.00	0.00	2.0	1	.80	1.28	.22	2.37	743	JAN-2
220	1.00	3.00	0.00	2.0	1	.80	1.31	.23	2.31	743	FEB-2
250	1.00	3.00	0.00	2.0	1	.80	1.34	.24	2.24	743	MAR-2
350	1.00	3.00	0.00	2.0	1	.80	1.43	.25	2.02	743	APR-2
0	1.00	3.00	4.00	2.0	1	.80	.81	0.00	3.48	717	B
170	1.00	3.00	4.00	2.0	1	.80	1.26	.05	2.49	717	SEP
300	1.00	3.00	4.00	2.0	1	.80	1.40	.19	2.14	717	MAR
370	1.00	3.00	4.00	2.0	1	.80	1.46	.19	2.00	717	APR
450	1.00	3.00	4.00	2.0	1	.80	1.53	.20	1.84	717	MAY
0	2.00	0.00	4.00	2.0	1	.60	.61	0.00	3.87	729	B
10	2.00	0.00	4.00	2.0	1	.60	.73	.10	3.58	729	JULY
60	2.00	0.00	4.00	2.0	1	.60	.93	.11	3.17	729	APR
70	2.00	0.00	4.00	2.0	1	.60	.95	.12	3.11	729	MAY
250	2.00	0.00	4.00	2.0	1	.60	1.23	.13	2.50	729	NOV
0	3.00	3.0012.00		22.4	1	.60	.57	0.00	3.94	429	B
55	3.00	3.0012.00		22.4	1	.60	.86	.38	3.12	429	DEC
110	3.00	3.0012.00		22.4	1	.60	.97	.39	2.87	429	JAN
300	3.00	3.0012.00		22.4	1	.60	1.20	.40	2.34	429	MAR
0	3.00	3.0012.00		22.4	1	.30	.27	0.00	4.52	415	B
10	3.00	3.0012.00		22.4	1	.30	.41	.35	4.05	415	NOV
50	3.00	3.0012.00		22.4	1	.30	.60	.38	3.62	415	DEC
210	3.00	3.0012.00		22.4	1	.30	.92	.40	2.91	415	FEB
300	3.00	3.0012.00		22.4	1	.30	1.03	.40	2.67	415	MAR
0	4.00	6.00	8.00	22.4	1	.50	.48	0.00	4.11	453	B
10	4.00	6.00	8.00	22.4	1	.50	.61	.25	3.74	453	DEC
45	4.00	6.00	8.00	22.4	1	.50	.77	.27	3.39	453	FEB
70	4.00	6.00	8.00	22.4	1	.50	.84	.28	3.24	453	MAR
250	4.00	6.00	8.00	22.4	1	.50	1.12	.53	2.35	453	APR
0	5.00	9.00	4.00	22.4	1	.35	.35	0.00	4.37	475	B
10	5.00	9.00	4.00	22.4	1	.35	.49	.22	3.99	475	MAR-1
90	5.00	9.00	4.00	22.4	1	.35	.80	.22	3.35	475	APR-1
660	5.00	9.00	4.00	22.4	1	.35	1.47	.23	1.90	475	OCT
870	5.00	9.00	4.00	22.4	1	.35	1.62	.23	1.57	475	NOV
900	5.00	9.00	4.00	22.4	1	.35	1.64	.48	1.28	475	MAR-2
920	5.00	9.00	4.00	22.4	1	.35	1.65	.49	1.24	475	APR-2
0	3.00	6.0012.00		22.4	1	.90	.89	0.00	3.34	487	B
135	3.00	6.0012.00		22.4	1	.90	1.23	.48	2.24	487	FEB
200	3.00	6.0012.00		22.4	1	.90	1.31	.49	2.06	487	MAR
510	3.00	6.0012.00		22.4	1	.90	1.55	.49	1.51	487	APR
680	3.00	6.0012.00		22.4	1	.90	1.65	.50	1.27	487	MAY
980	3.00	6.0012.00		22.4	1	.90	1.82	.54	.84	487	JAN-2
0	5.00	9.00	4.00	22.4	1	.40	.40	0.00	4.27	483	B
10	5.00	9.00	4.00	22.4	1	.40	.54	.22	3.90	483	MAR-1
90	5.00	9.00	4.00	22.4	1	.40	.83	.22	3.28	483	APR-1
660	5.00	9.00	4.00	22.4	1	.40	1.48	.23	1.87	483	OCT-2
870	5.00	9.00	4.00	22.4	1	.40	1.63	.23	1.54	483	NOV
880	5.00	9.00	4.00	22.4	1	.40	1.64	.24	1.52	483	DEC-2
885	5.00	9.00	4.00	22.4	1	.40	1.64	.24	1.51	483	JAN
900	5.00	9.00	4.00	22.4	1	.40	1.65	.48	1.25	483	MAR-2
0	2.75	9.0011.00		18.0	1	.43	.44	0.00	4.20	EXMP	OCT
11	2.75	9.0011.00		18.0	1	.43	.59	.37	3.69	EXMP	DEC
82	2.75	9.0011.00		18.0	1	.43	.85	.38	3.11	EXMP	FEB
369	2.75	9.0011.00		18.0	1	.43	1.27	.40	2.19	EXMP	APR
793	2.75	9.0011.00		18.0	1	.43	1.62	.42	1.41	EXMP	JUN
932	2.75	9.0011.00		18.0	1	.43	1.72	.43	1.19	EXMP	AUG
960	2.75	9.0011.00		18.0	1	.43	1.73	.44	1.14	EXMP	OCT
968	2.75	9.0011.00		18.0	1	.43	1.74	.45	1.12	EXMP	DEC
973	2.75	9.0011.00		18.0	1	.43	1.74	.45	1.11	EXMP	FEB
985	2.75	9.0011.00		18.0	1	.43	1.75	.46	1.08	EXMP	APR
995	2.75	9.0011.00		18.0	1	.43	1.76	.47	1.05	EXMP	AUG
999	2.75	9.0011.00		18.0	1	.43	1.76	.47	1.05	EXMP	OCT
0	3.00	6.00	8.00	18.0	1	.43	.42	0.00	4.23	623E	B
90	3.00	6.00	8.00	18.0	1	.43	.84	.34	3.16	623E	FEB
160	3.00	6.00	8.00	18.0	1	.43	.97	.34	2.89	623E	MAR
400	3.00	6.00	8.00	18.0	1	.43	1.26	.35	2.26	623E	APR
600	3.00	6.00	8.00	18.0	1	.43	1.43	.36	1.87	623E	MAY
840	3.00	6.00	8.00	18.0	1	.43	1.60	.36	1.50	623E	JUN
920	3.00	6.00	8.00	18.0	1	.43	1.66	.37	1.38	623E	JUL
960	3.00	6.00	8.00	18.0	1	.43	1.68	.38	1.31	623E	AUG
0	3.00	9.0010.00		18.0	1	.43	.44	0.00	4.20	EXMP	OCT
7	3.00	9.0010.00		18.0	1	.43	.55	.37	3.76	EXMP	DEC
57	3.00	9.0010.00		18.0	1	.43	.79	.39	3.24	EXMP	FEB
301	3.00	9.0010.00		18.0	1	.43	1.20	.40	2.35	EXMP	APR
756	3.00	9.0010.00		18.0	1	.43	1.60	.42	1.46	EXMP	JUN
922	3.00	9.0010.00		18.0	1	.43	1.71	.43	1.20	EXMP	AUG
954	3.00	9.0010.00		18.0	1	.43	1.73	.44	1.15	EXMP	OCT
962	3.00	9.0010.00		18.0	1	.43	1.74	.45	1.12	EXMP	DEC
967	3.00	9.0010.00		18.0	1	.43	1.74	.46	1.10	EXMP	FEB
980	3.00	9.0010.00		18.0	1	.43	1.75	.46	1.09	EXMP	APR
994	3.00	9.0010.00		18.0	1	.43	1.76	.47	1.05	EXMP	JUN
997	3.00	9.0010.00		18.0	1	.43	1.76	.47	1.05	EXMP	AUG
998	3.00	9.0010.00		18.0	1	.43	1.76	.48	1.03	EXMP	OCT
0	4.50	9.00	4.00	18.0	1	.43	.44	0.00	4.19	EXMP	OCT
0	4.50	9.00	4.00	18.0	1	.43	.44	.19	4.14	EXMP	DEC
4	4.50	9.00	4.00	18.0	1	.43	.52	.21	3.95	EXMP	FEB
53	4.50	9.00	4.00	18.0	1	.43	.78	.22	3.40	EXMP	APR
451	4.50	9.00	4.00	18.0	1	.43	1.35	.22	2.16	EXMP	JUN
786	4.50	9.00	4.00	18.0	1	.43	1.62	.23	1.57	EXMP	AUG
853	4.50	9.00	4.00	18.0	1	.43	1.67	.24	1.47	EXMP	OCT
867	4.50	9.00	4.00	18.0	1	.43	1.68	.24	1.45	EXMP	DEC
876	4.50	9.00	4.00	18.0	1	.43	1.69	.25	1.43	EXMP	FEB
905	4.50	9.00	4.00	18.0	1	.43	1.71	.25	1.38	EXMP	APR
960	4.50	9.00	4.00	18.0	1	.43	1.74	.25	1.31	EXMP	JUN

983	4.50	9.00	4.00	18.0	1	.43	1.76	.26	1.27	EXMP	AUG
989	4.50	9.00	4.00	18.0	1	.43	1.76	.26	1.26	EXMP	OCT
0	4.50	9.00	4.00	18.0	1	.43	.44	0.00	4.19	EXMP	JULY
67	4.50	9.00	4.00	18.0	1	.43	.82	.25	3.30	EXMP	SEP
170	4.50	9.00	4.00	18.0	1	.43	1.03	.26	2.85	EXMP	NOV
199	4.50	9.00	4.00	18.0	1	.43	1.07	.28	2.74	EXMP	JAN
239	4.50	9.00	4.00	18.0	1	.43	1.12	.29	2.61	EXMP	MAR
320	4.50	9.00	4.00	18.0	1	.43	1.42	.29	1.98	EXMP	MAY
803	4.50	9.00	4.00	18.0	1	.43	1.64	.30	1.50	EXMP	JULY
895	4.50	9.00	4.00	18.0	1	.43	1.70	.30	1.36	EXMP	SEP
915	4.50	9.00	4.00	18.0	1	.43	1.71	.30	1.33	EXMP	NOV
923	4.50	9.00	4.00	18.0	1	.43	1.72	.31	1.31	EXMP	JAN
929	4.50	9.00	4.00	18.0	1	.43	1.72	.31	1.30	EXMP	MAR
955	4.50	9.00	4.00	18.0	1	.43	1.74	.32	1.26	EXMP	MAY
981	4.50	9.00	4.00	18.0	1	.43	1.76	.32	1.22	EXMP	JULY
0	3.50	9.00	8.00	18.0	1	.43	.44	0.00	4.26	EXMP	OCT
3	3.50	9.00	8.00	18.0	1	.43	.50	.32	3.91	EXMP	DEC
26	3.50	9.00	8.00	18.0	1	.43	.68	.34	3.53	EXMP	FEB
185	3.50	9.00	8.00	18.0	1	.43	1.05	.36	2.72	EXMP	APR
665	3.50	9.00	8.00	18.0	1	.43	1.53	.36	1.67	EXMP	JUN
891	3.50	9.00	8.00	18.0	1	.43	1.69	.38	1.30	EXMP	AUG
932	3.50	9.00	8.00	18.0	1	.43	1.72	.39	1.23	EXMP	OCT
942	3.50	9.00	8.00	18.0	1	.43	1.73	.40	1.21	EXMP	DEC
948	3.50	9.00	8.00	18.0	1	.43	1.73	.40	1.20	EXMP	FEB
965	3.50	9.00	8.00	18.0	1	.43	1.74	.41	1.16	EXMP	APR
988	3.50	9.00	8.00	18.0	1	.43	1.76	.41	1.13	EXMP	JUN
995	3.50	9.00	8.00	18.0	1	.43	1.76	.42	1.11	EXMP	AUG
997	3.50	9.00	8.00	18.0	1	.43	1.76	.43	1.09	EXMP	OCT
0	5.00	6.0012.00		30.0	1	.30	.27	0.00	4.52	305	B
50	5.00	6.0012.00		30.0	1	.30	.60	.33	3.67	305	MAR
400	5.00	6.0012.00		30.0	1	.30	1.14	.34	2.49	305	MAY
730	5.00	6.0012.00		30.0	1	.30	1.48	.60	1.56	305	JUN
860	5.00	6.0012.00		30.0	1	.30	1.51	.63	1.31	305	JULY
960	5.00	6.0012.00		30.0	1	.30	1.57	.65	1.14	305	JAN
0	5.00	6.0012.00		30.0	1	.25	.22	0.00	4.61	307	B
50	5.00	6.0012.00		30.0	1	.25	.55	.33	3.75	307	MAR
400	5.00	6.0012.00		30.0	1	.25	1.12	.34	2.54	307	MAY
730	5.00	6.0012.00		30.0	1	.25	1.40	.60	1.60	307	JUN
860	5.00	6.0012.00		30.0	1	.25	1.49	.63	1.35	307	JULY
960	5.00	6.0012.00		30.0	1	.25	1.55	.65	1.17	307	JAN
0	4.00	6.0012.00		30.0	1	.50	.46	0.00	4.15	323	B
50	4.00	6.0012.00		30.0	1	.50	.75	.40	3.30	323	JAN
110	4.00	6.0012.00		30.0	1	.50	.88	.41	3.01	323	FEB
160	4.00	6.0012.00		30.0	1	.50	.96	.42	2.82	323	MAR
440	4.00	6.0012.00		30.0	1	.50	1.26	.43	2.16	323	APR
870	4.00	6.0012.00		30.0	1	.50	1.56	.44	1.49	323	JUN
0	6.00	9.0012.00		30.0	1	.30	.29	0.00	4.48	311	B
10	6.00	9.0012.00		30.0	1	.30	.44	.34	4.01	311	MAR
150	6.00	9.0012.00		30.0	1	.30	.87	.35	3.08	311	MAY
470	6.00	9.0012.00		30.0	1	.30	1.26	.36	2.22	311	JUN
670	6.00	9.0012.00		30.0	1	.30	1.43	.36	1.85	311	JULY
890	6.00	9.0012.00		30.0	1	.30	1.59	.37	1.50	311	JAN
920	6.00	9.0012.00		30.0	1	.30	1.61	.60	1.15	311	APR
1000	6.00	9.0012.00		30.0	1	.30	1.67	.61	1.02	311	NOV

```
10 ALG 71   UNIVERSITY OF TEXAS 6600   UT 2

.WE7917

10.45.38 JAIN,,07.70900,17.CEDC0154.SURN.
10.45.38 RUN (S)
10.45.40   CTIME 000.301 SEC.  RUN# LEVEL 60#
10.45.40 LGO.
10.45.42  LOADER UNUSED STORAGE 055523.
10.45.42 - 11700CM     0.208CP     48MS      0MT
10.45.50  END - PSI
10.45.50 MS       114 PRU.
10.45.50 CP     1.688 SEC.
10.45.50 PP     3.987 SEC.
10.45.50 TM     2.144 SEC.       3 (OCTAL)
```

APPENDIX 5

FLEXIBLE PAVEMENT PERFORMANCE RECORD

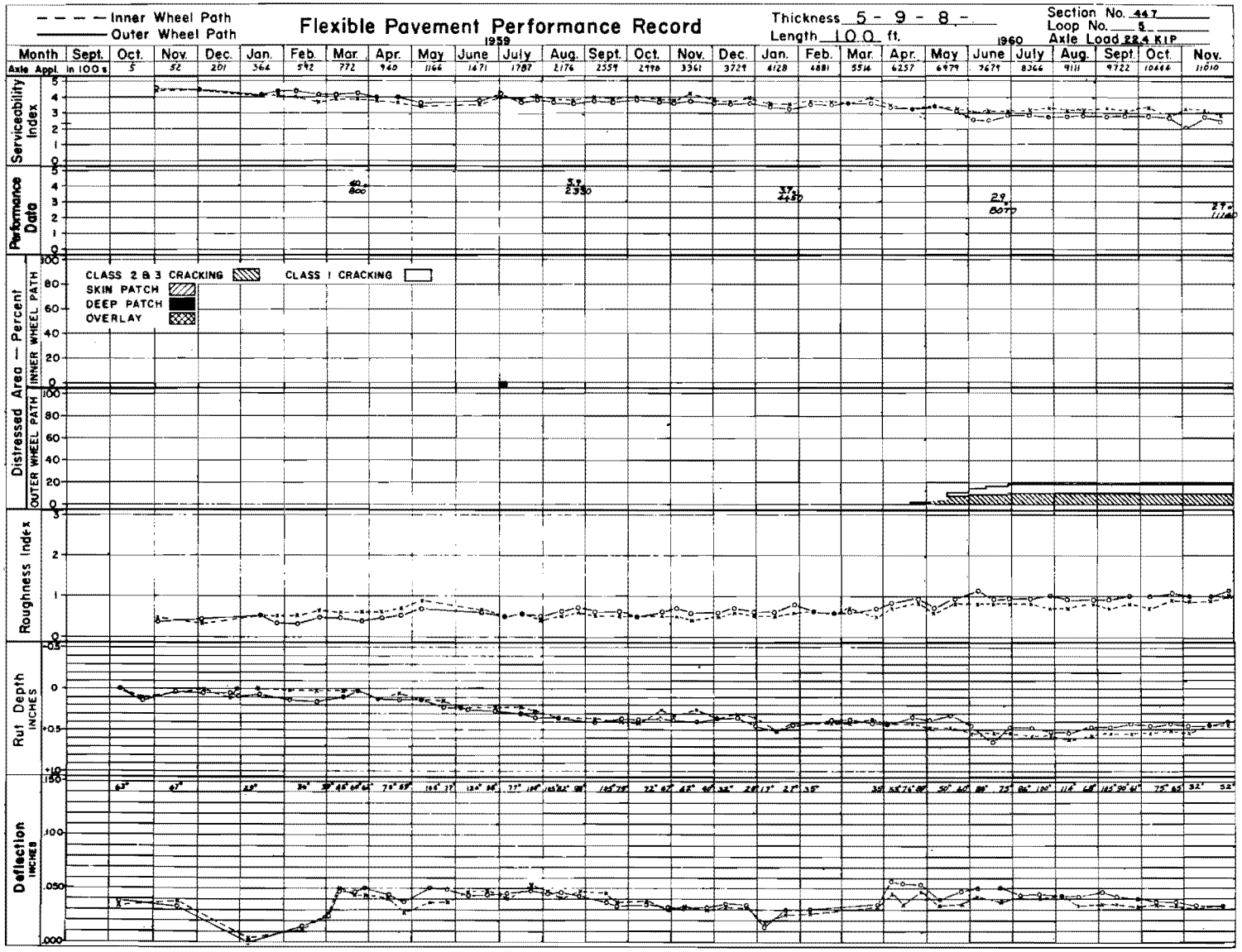

Fig A5.1. Typical AASHO Road Test section history (Ref 70)

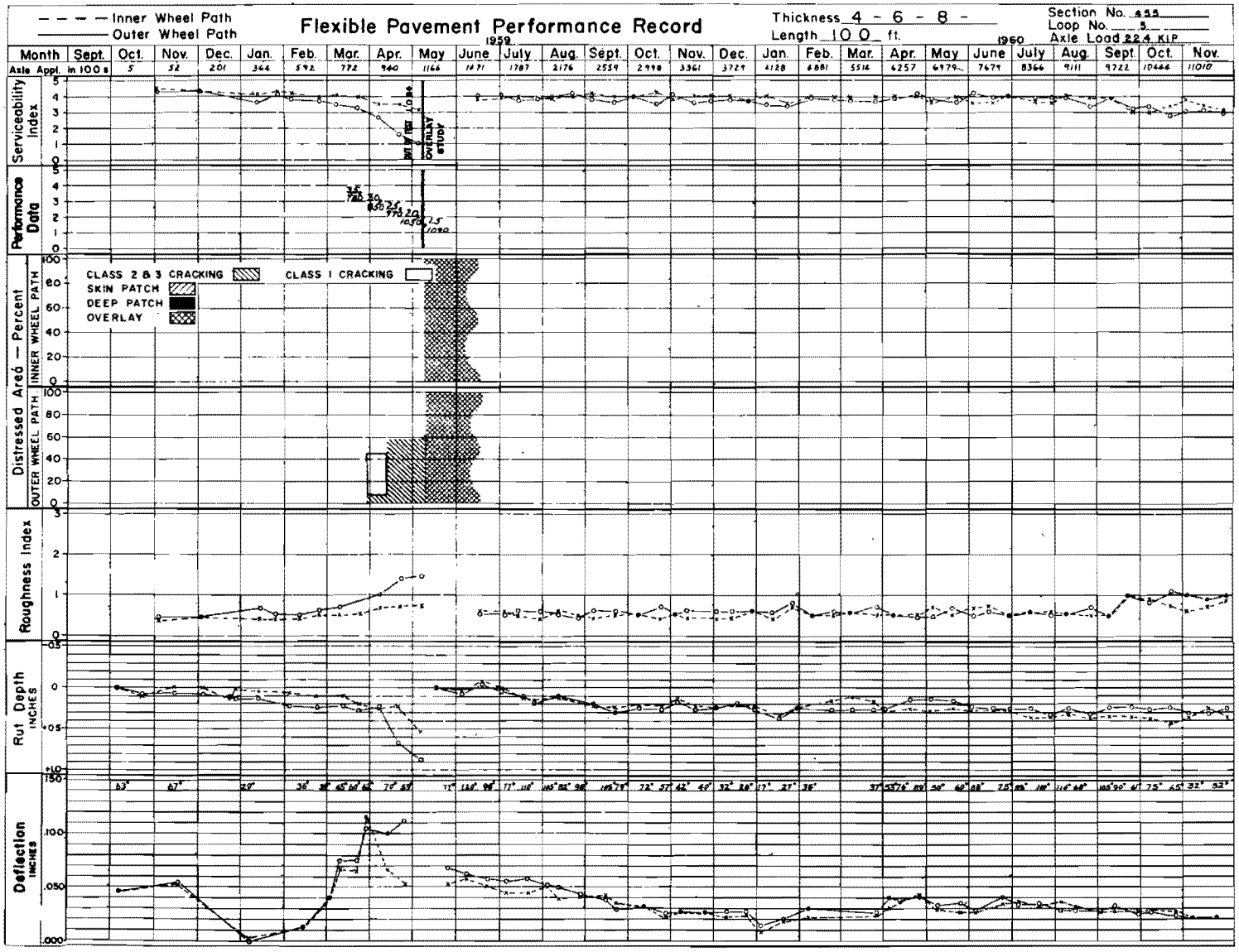

Fig A5.2. Typical AASHO Road Test section history (Ref 70).

APPENDIX 6

NOMENCLATURE

APPENDIX 6. NOMENCLATURE

This appendix gives the nomenclature for the fatigue tests used in this report (Ref 35).

Flexural Test for Asphalt Concrete

The following nomenclature applies to the flexural fatigue tests on asphalt concrete.

N_i	The number of load applications of level i to cause failure in simple loading.
n_i	The number of actual load applications of level i .
ϵ	Bending strain in flexural fatigue test.
A and B	Constants depending upon material characteristics.
E	Modulus of elasticity or stiffness.
μ	Poisson's ratio.

Repetitive Load-Deformation Tests on Base, Subbase, and Subgrade

The nomenclature used for repeated load tests on granular base and subbase and fine subgrade materials is given below. The nomenclature is also explained by Figs A6.1 and A6.2.

t	Total cumulative deformation when the maximum load is applied to the specimen.
p	Permanent cumulative deformation retained by the specimen between cyclic load applications.

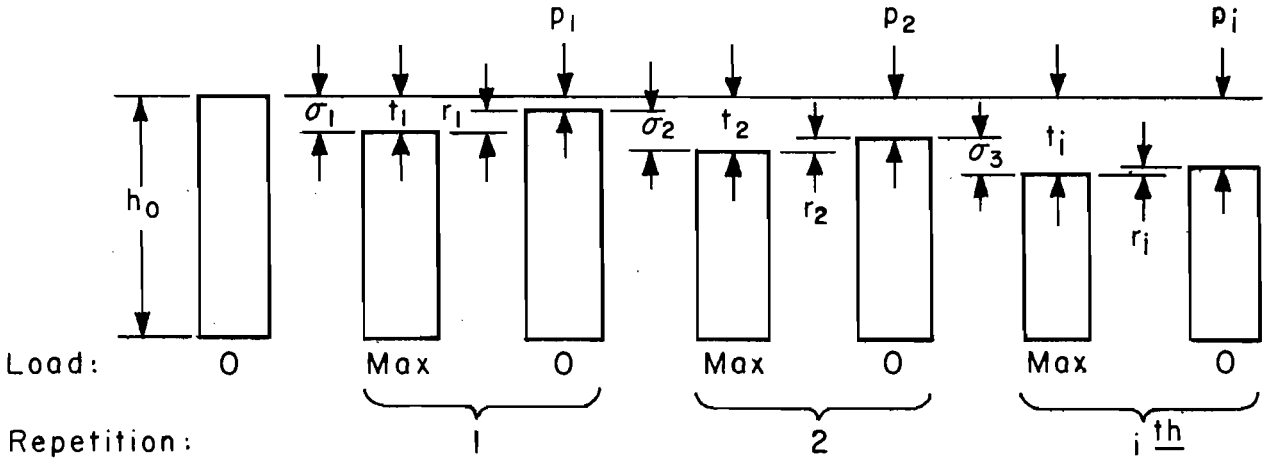

Fig A6.1. Diagrammatic representation of changes in specimen lengths during load and unload cycles (after Ref 35).

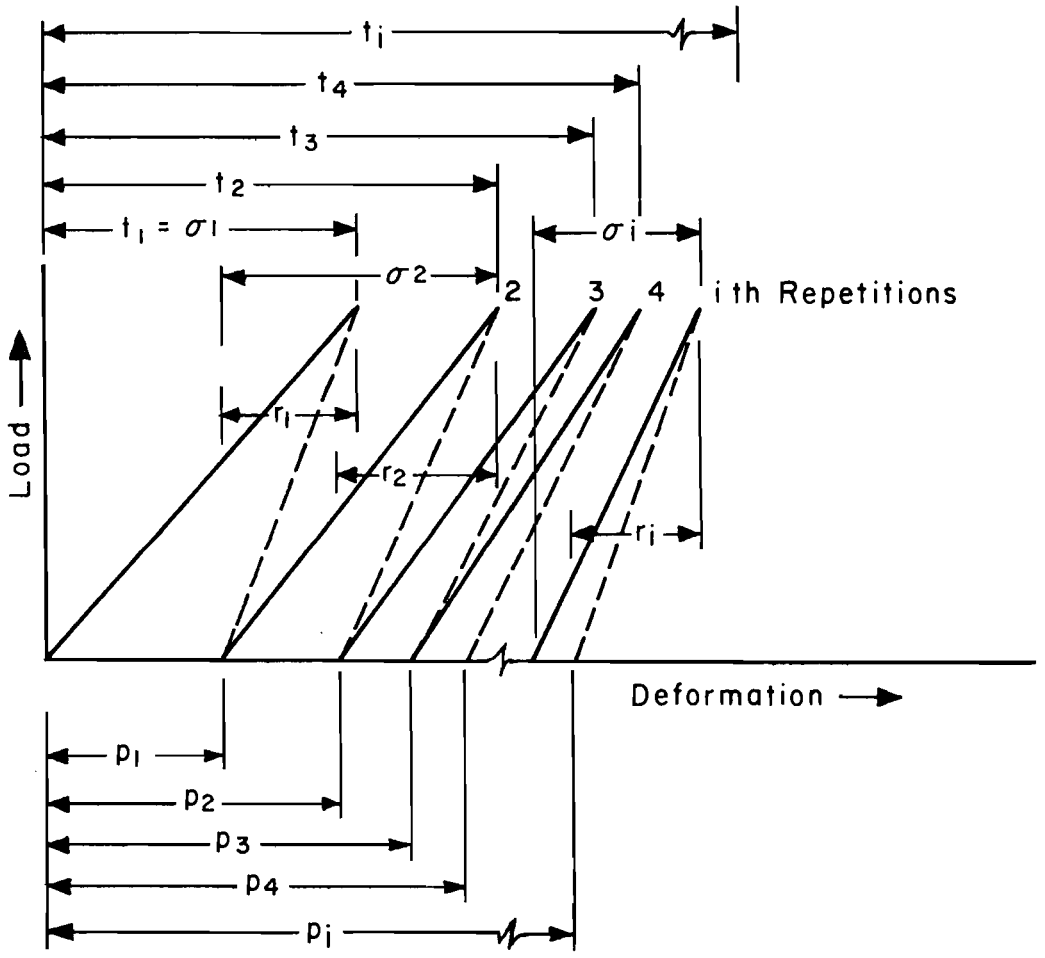

Fig A6.2. Hypothetical repetitive load-deformation relationship indicating suggested nomenclature for various types of deformations (after Ref 35).

r — Rebound non-cumulative deformation, which is equal to the difference between total and permanent deformation for any particular load application.

σ — Transient non-cumulative deformation; deformation observed from zero to maximum stress for any particular load application.

Note:

(1) Strains may be used instead of deformation.

(2) Elastic refers to a condition where rebound or transient deformation approaches constant values over several stress repetitions.

(3) Perfect resiliency is the state when continued loading produces no further total or permanent deformation, i.e., rebound equals the transient deformation.

(4) Total strains in the triaxial load are analogous to the strain observed as a point in the roadway during application of the wheel load. Permanent strains may represent the net rut depth in the pavement.

APPENDIX 7

AASHO ROAD TEST AND PRESENT SERVICEABILITY CONCEPT

APPENDIX 7. AASHO ROAD TEST AND PRESENT SERVICEABILITY CONCEPT

In this report the serviceability and performance concept using the performance data of the AASHO Road Test has been utilized to develop and verify the suitability of the suggested models. Thus, the purpose of this appendix is to discuss the AASHO Road Test and its performance conept.

Introduction

The AASHO Road Test was conceived and sponsored by the American Association of State Highway Officials as a study of the performance and capabilities of highway pavement and bridge structures of known characteristics under moving loads of known magnitude and frequency. AASHO Road Test reports (Refs 67 - 73) contain complete information about this test. The principal objective of the road test was to determine the significant relationship between pavement behavior and the major variables of design and loading. The construction of the test facility was completed in 1958. Traffic started to move over it in November 1958 and continued through November 1960. A total of 1,114,000 axle load applications was accumulated. Based on the results of the AASHO Road Test an Interim Design Guide was published in 1962.

Pavement Performance

The popular pavement service and performance concept was also developed at the AASHO Road Test in 1962. The failure of a pavement system is generally not a catastrophic occurence, as is the case in some other structures. A pavement which has been designated as "failed" in some response may still be capable of carrying traffic at a reduced service level. It is clear that cracks will occur if a pavement is overstressed, but the question is how much they are going to affect the performance of the pavement. Cracks are undesirable but the degree of undesirability is not known. Comfort and convenience may be considered inherent manifestations of pavement performance. The performance of a pavement is influenced by many factors, including applied loads, tire pressure, number of load applications, and thickness and strength

characteristics of pavement layers and subgrade. Thus, functional pavement design should correlate these factors with desired performance characteristics.

To introduce the measure of pavement performance, certain terms used in the design methods were defined as below (Ref 70):

(1) Present Serviceability Rating (PSR): The mean of the individual ratings made by the members of a specific panel of men selected for the purpose.

(2) Present Serviceability Index (PSI): A mathematical combination of values obtained from certain physical measurements of a large number of pavements so formulated as to predict the PSR for those pavements within prescribed limits. This represents the ability of the pavement to serve high-speed, high-volume, mixed traffic in its existing condition. (The definition applies to the condition existing - on the date of rating, not to the condition assumed the next day or at any future or past date.)

(3) Performance Index: A summary of PSI values over a period of time (See Fig A7.1).

Present Serviceability Index Equation

Based on regression analysis of measurement and panel ratings on 49 rigid and 74 flexible pavement test sections, the following index equations were suggested (Ref 70):

For flexible pavements,

$$PSI = 5.03 - 1.91 \log (1 + \overline{SV}) - 1.38 \overline{RD}^2 - 0.01\sqrt{C + P} \qquad (A7.1)$$

For rigid pavements,

$$PSI = 5.41 - 1.78 \log (1 + \overline{SV}) - 0.09\sqrt{C + P} \qquad (A7.2)$$

where slope variance $\overline{SV}$ is the statistical measure of the variability of the slope of the pavement. It is a direct measurement of the longitudinal roughness of the pavement. A continuous analog trace of the pavement slope is obtained from the profilometer, and a point measurement of slope S_1 at a one-foot interval is obtained. Then

$$SV = 10^6 \times \text{slope variance} = 10^6 \times \sigma_s^2$$

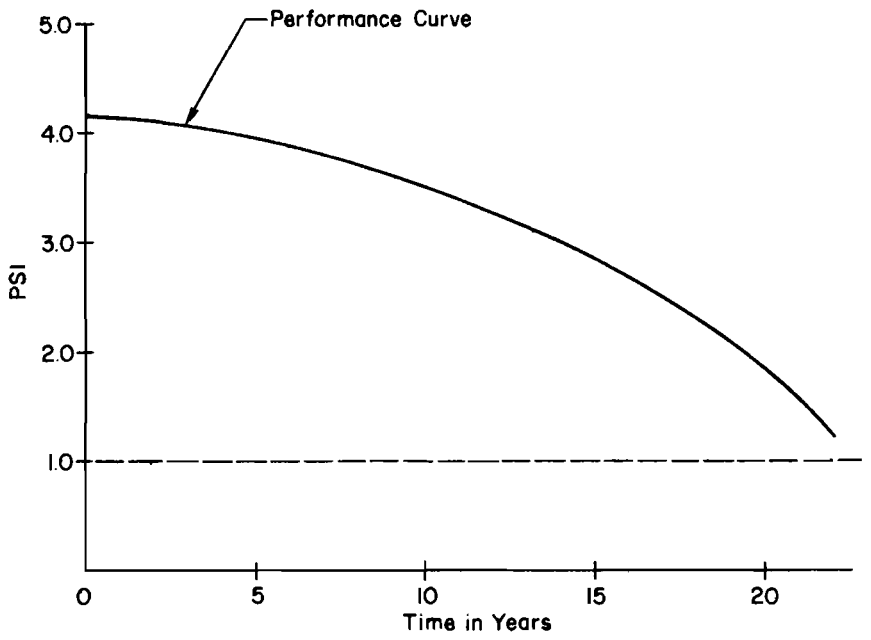

Fig A7.1. Performance curve.

$$= 10^6 \sum_{t=1}^{n} (S_1 - \bar{S})^2/(n-1) \qquad \text{(A7.3)}$$

where

n = number of measurements

$\bar{S}$ = mean slope measurement

Rut depth $\overline{RD}$ is the measurement of the amount of permanent deformation in the transverse profile of the pavement. It is measured in inches below the center of a 4-foot span placed across the wheel path. These measurements are made throughout the length of the section and then averaged.

Cracking and patching C + P is the measurement of the major cracking (classes 2 and 3) and patching in square feet per 1000-square-foot area of flexible pavement. In rigid pavement, class 2 and sealed cracks are measured in feet by 1000 square feet area of pavement.

As seen from the PSI equation, slope variance is the most important single variable influencing the PSI of the pavement. Rutting plays a secondary role while cracking and patching was found to have only a minor role in determination of the serviceability or riding quality of the pavement. However, it is emphasized that this does not mean that cracking is of minor importance as far as the design or structural behavior, pavement life, or even the serviceability is concerned, because cracking in the pavement is itself indicative of other forms of distress and is a direct indication of a structural inadequacy somehwere in the pavement. By the time enough cracks are developed in the pavement it is already rough in terms of slope variance. Therefore, it seems that the slope variance is the cause of detrimental effects of cracking.

AASHO Road Test Data

AASHO Road Test data are a good source of performance data. Performance data in the form of plots of cracking and patching, roughness index, PSI, and rut depth are available for each test section. Typical plots of this data are shown in Appendix 5. These plots were used in the development and verification of the models discussed in this report.

APPENDIX 8

COMPARISON OF DISTRESS MODELS - PLOTS

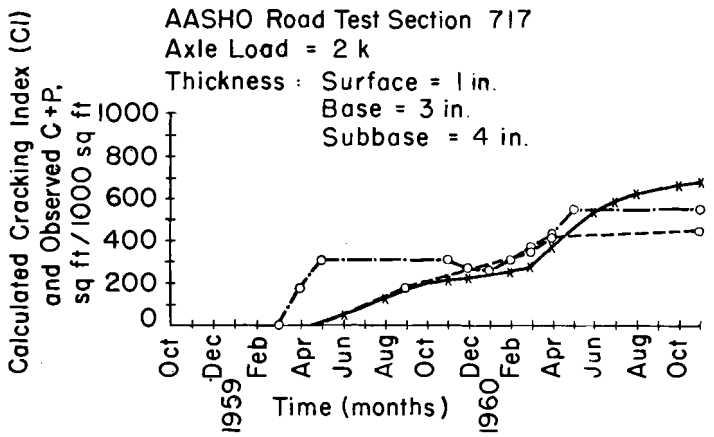

Fig A8.1. Computed cracking index (CI) versus observed cracking-patching (C + P).

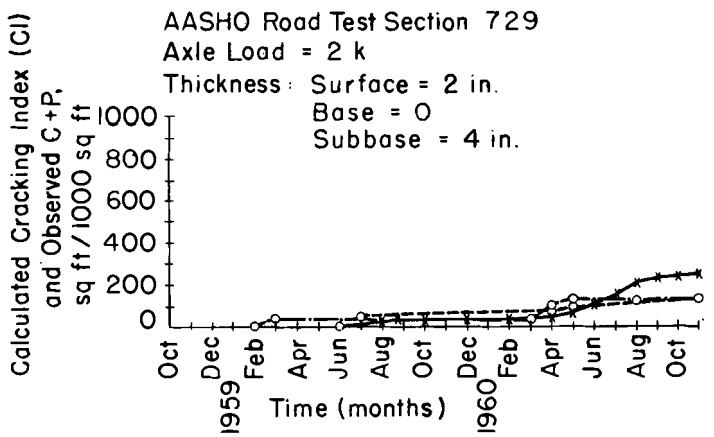

Fig A8.2. Computed cracking index (CI) versus observed cracking-patching (C + P).

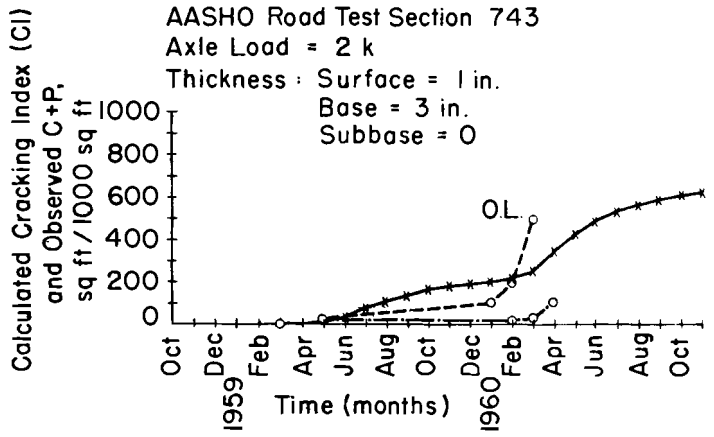

Fig A8.3. Computed cracking index (CI) versus observed cracking-patching (C + P).

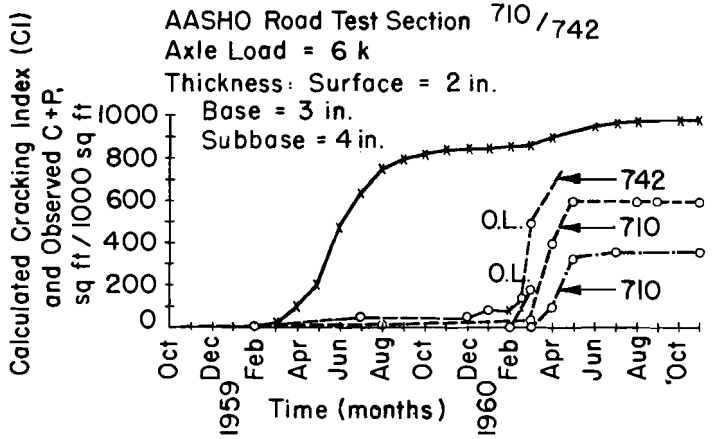

Fig A8.4. Computed cracking index (CI) versus observed cracking-patching (C + P).

Observed (inner wheel) — Calculated
Observed (outer wheel) — Section Overload at Point ○ O.L.

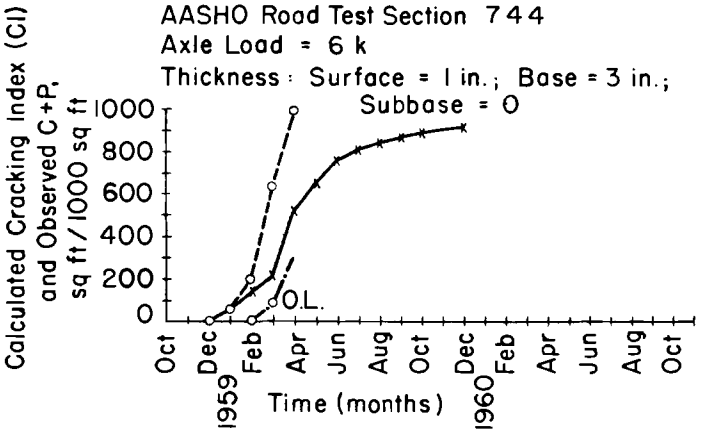

Fig A8.5. Computed cracking index (CI) versus observed cracking-patching (C + P).

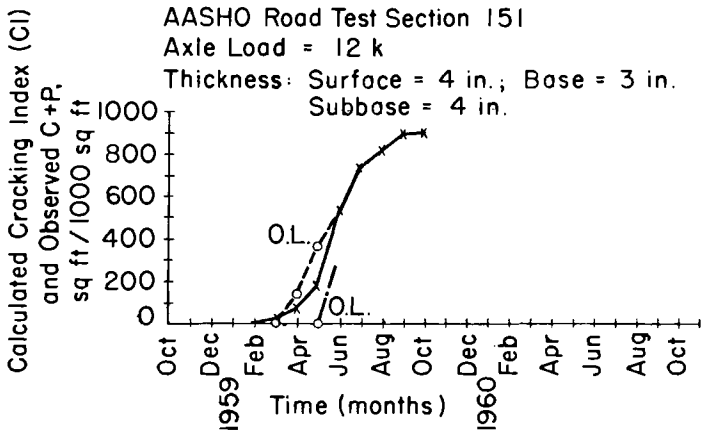

Fig A8.6. Computed cracking index (CI) versus observed cracking-patching (C + P).

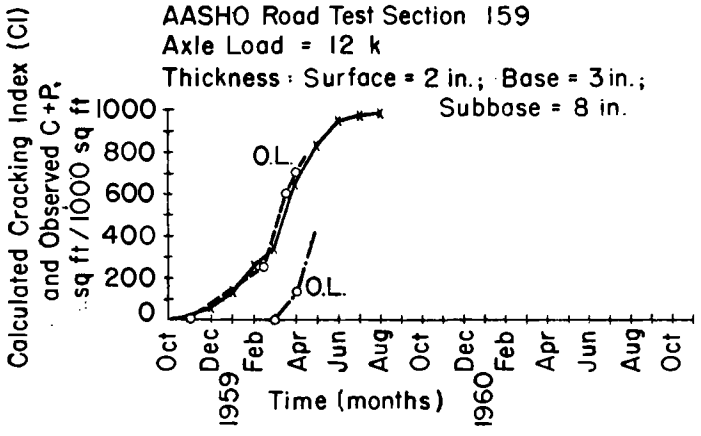

Fig A8.7. Computed cracking index (CI) versus observed cracking-patching (C + P).

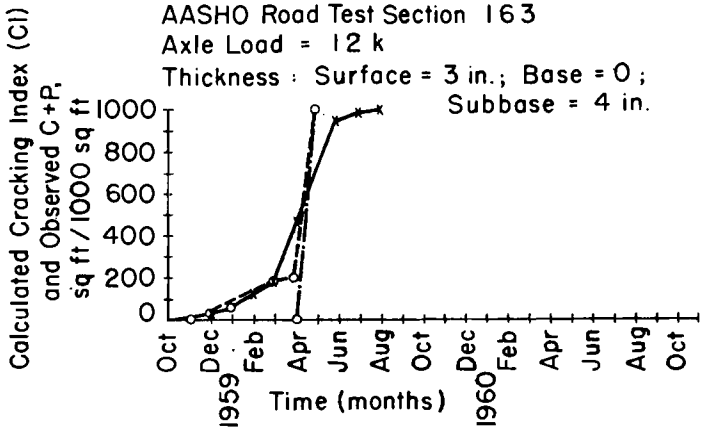

Fig A8.8. Computed cracking index (CI) versus observed cracking-patching (C + P).

Observed (inner wheel) —o— Calculated —x—
Observed (outer wheel) —o— Section Overload at Point = O.L

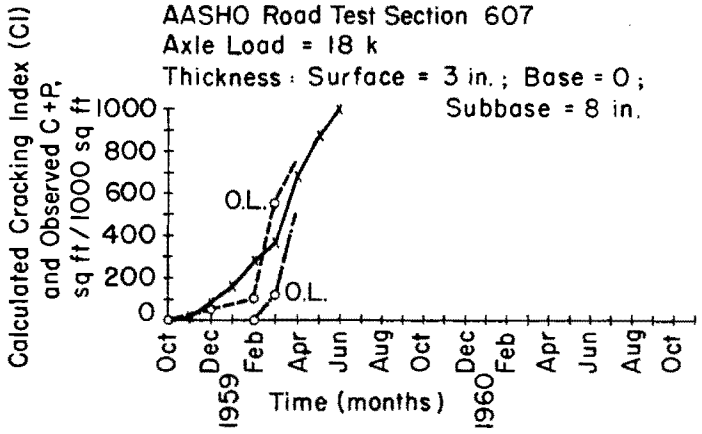

Fig A8.9. Computed cracking index (CI) versus observed cracking-patching (C + P).

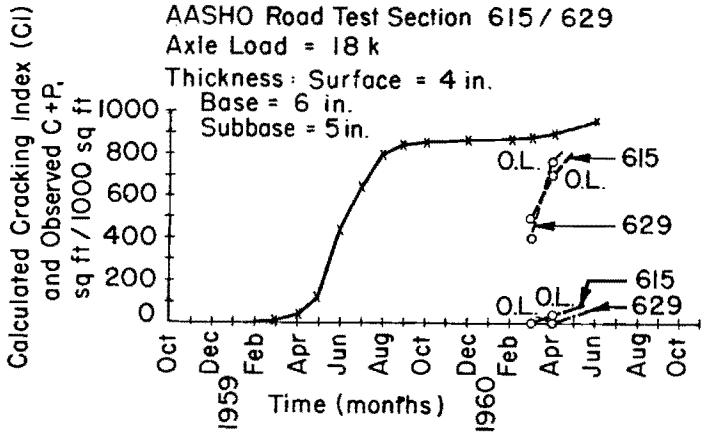

Fig A8.10. Computed cracking index (CI) versus observed cracking-patching (C + P).

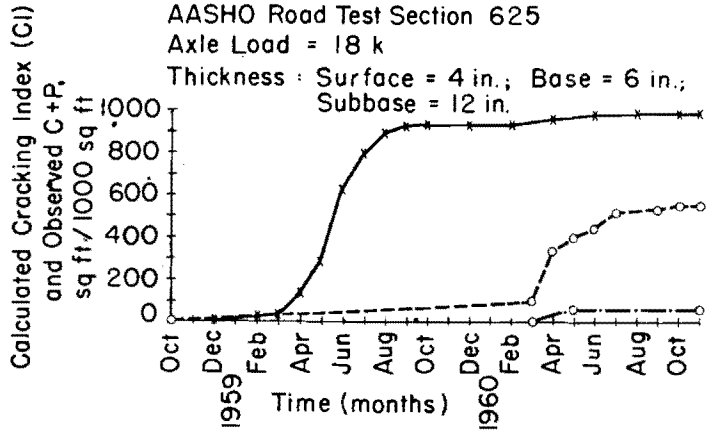

Fig A8.11. Computed cracking index (CI) versus observed cracking-patching (C + P).

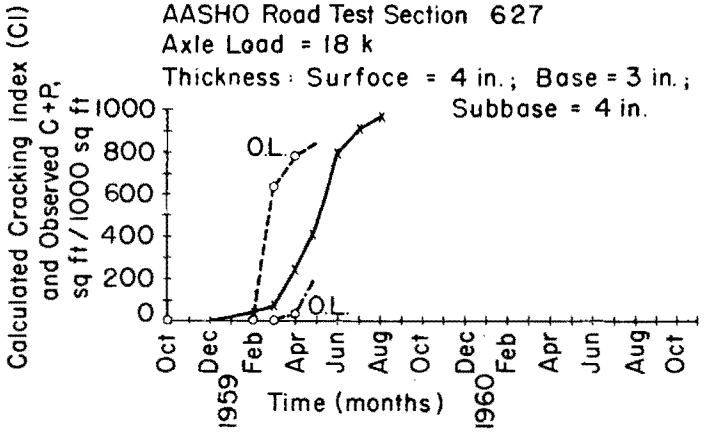

Fig A8.12. Computed cracking index (CI) versus observed cracking-patching (C + P).

Observed (inner wheel) — Calculated
Observed (outer wheel) — Section Overload at Point ○ O.L.

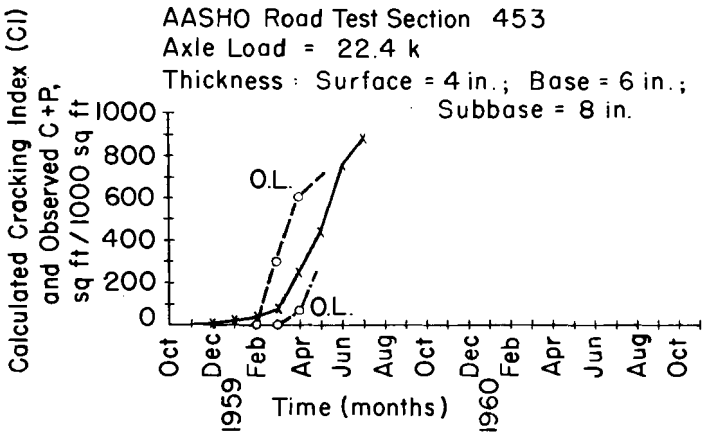

Fig A8.13. Computed cracking index (CI) versus observed cracking-patching (C + P).

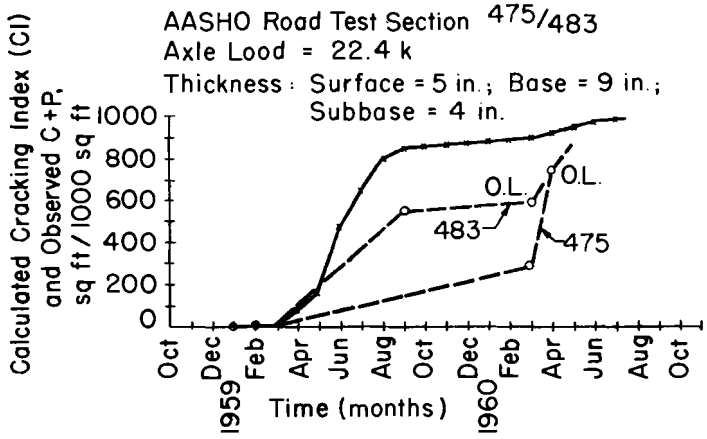

Fig A8.14. Computed cracking index (CI) versus observed cracking-patching (C + P).

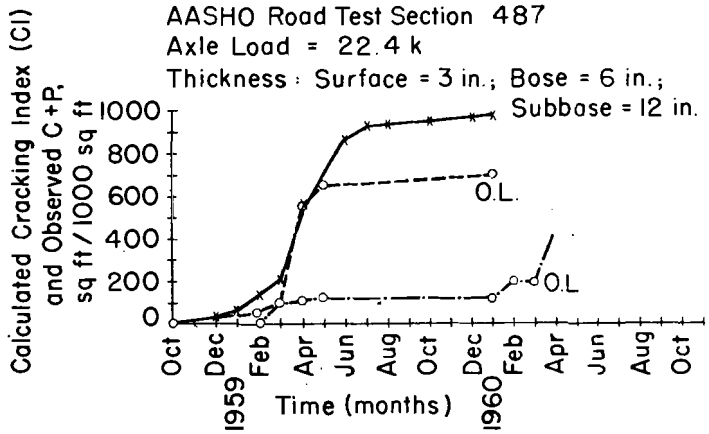

Fig A8.15. Computed cracking index (CI) versus observed cracking-patching (C + P).

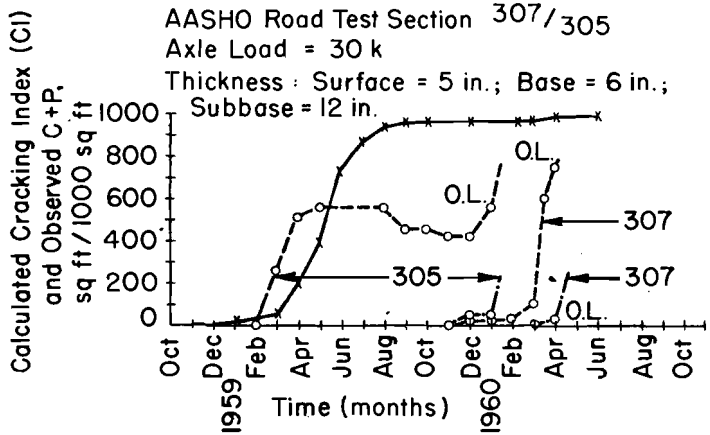

Fig A8.16. Computed cracking index (CI) versus observed cracking-patching (C + P).

Observed (inner wheel) — Calculated
Observed (outer wheel) — Section Overload at Point ○ O.L.

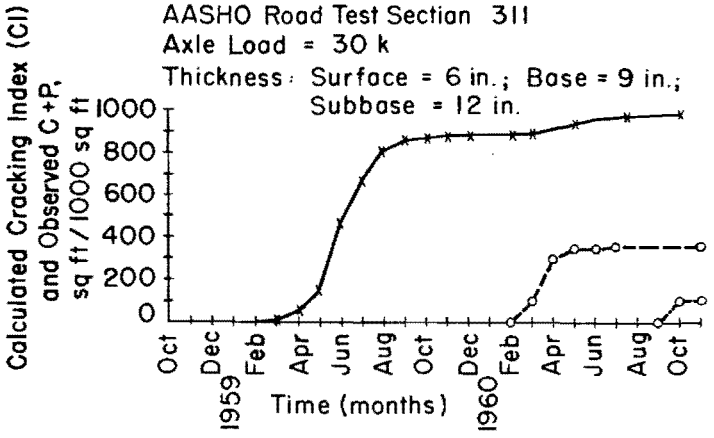

Fig A8.17. Computed cracking index (CI) versus observed cracking-patching (C + P).

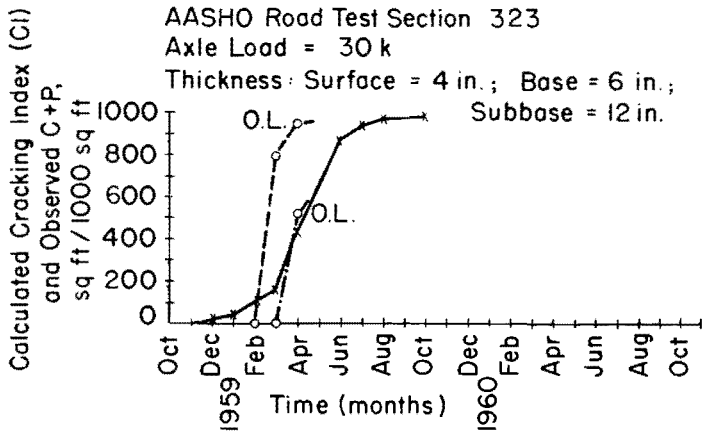

Fig A8.18. Computed cracking index (CI) versus observed cracking-patching (C + P).

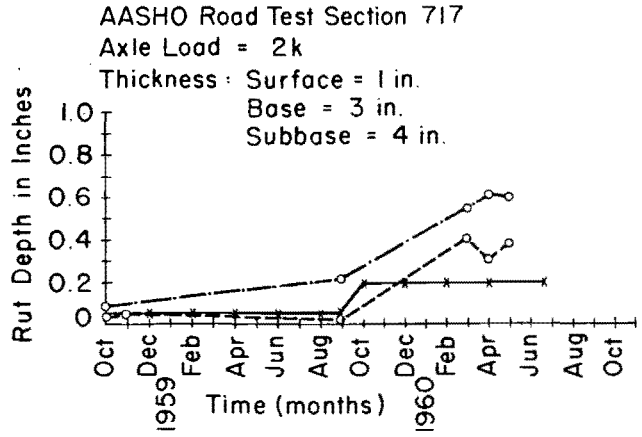

Fig A8.19. Observed versus calculated rut depth index.

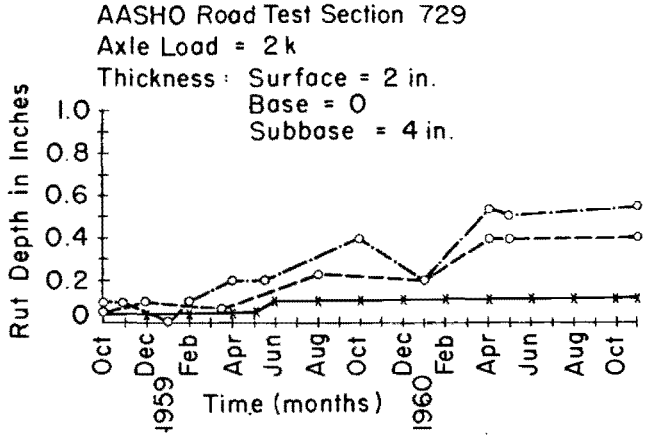

Fig A8.20. Observed versus calculated rut depth index.

Observed (inner wheel) —×— Calculated
Observed (outer wheel) —○— Section Overload at Point : O.L

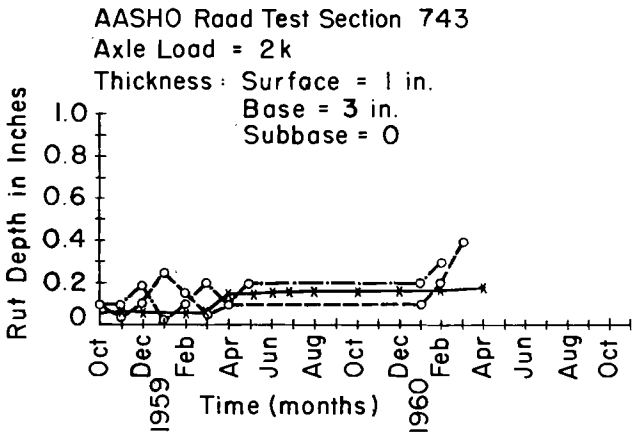

Fig A8.21. Observed versus calculated rut depth index.

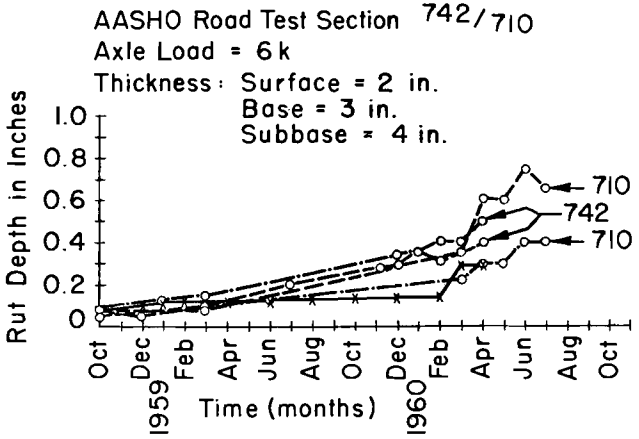

Fig A8.22. Observed versus calculated rut depth index.

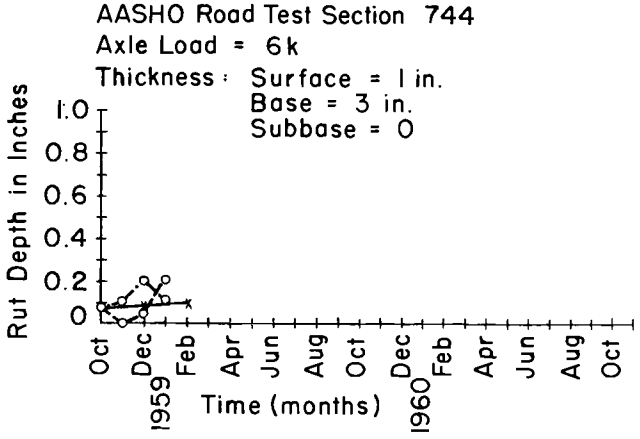

Fig A8.23. Observed versus calculated rut depth index.

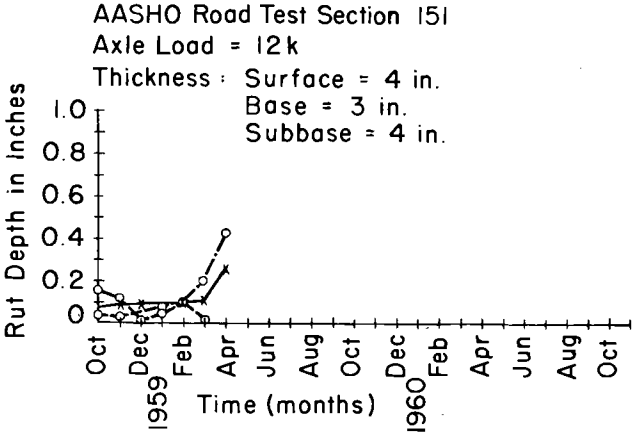

Fig A8.24. Observed versus calculated rut depth index.

Observed (inner wheel) — Calculated
Observed (outer wheel)

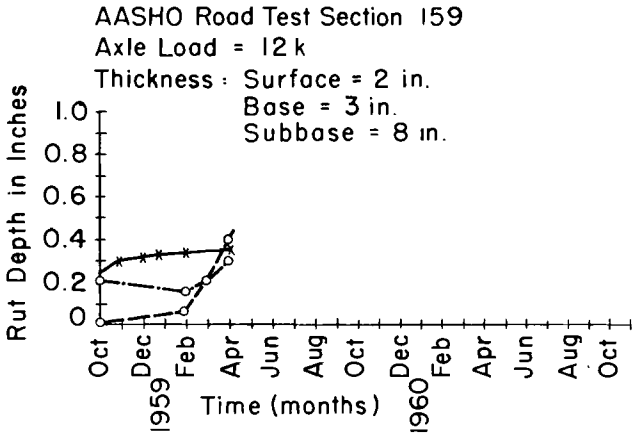

Fig A8.25. Observed versus calculated rut depth index.

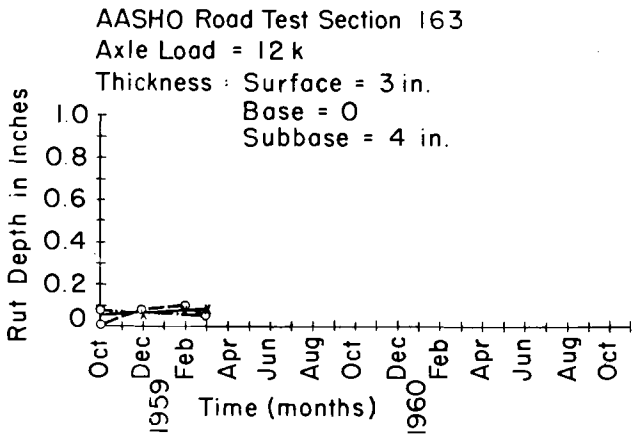

Fig A8.26. Observed versus calculated rut depth index.

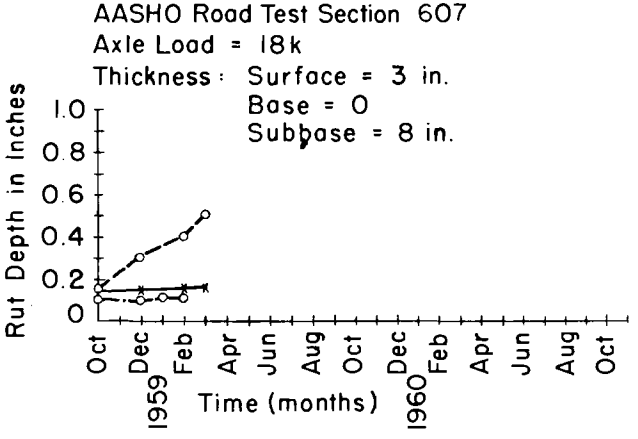

Fig A8.27. Observed versus calculated rut depth index.

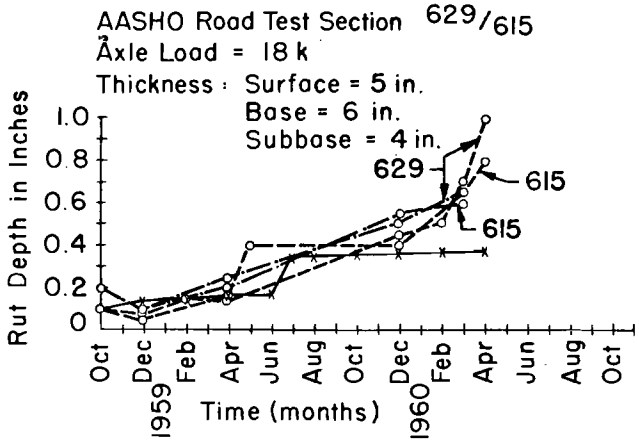

Fig A8.28. Observed versus calculated rut depth index.

Observed (inner wheel) — Calculated
Observed (outer wheel)

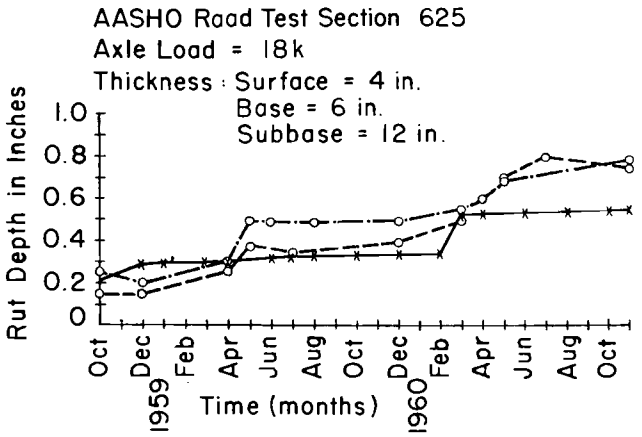

Fig A8.29. Observed versus calculated rut depth index.

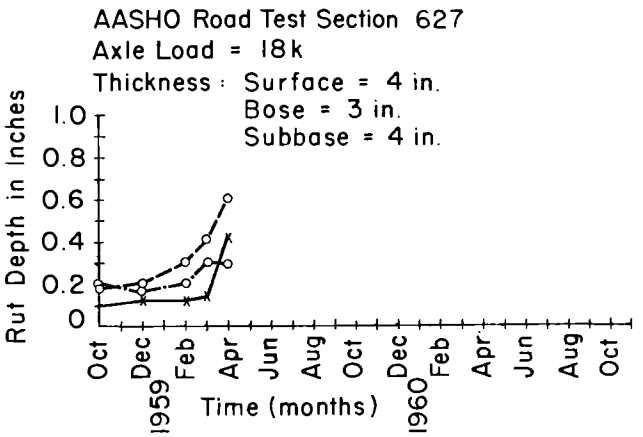

Fig A8.30. Observed versus calculated rut depth index.

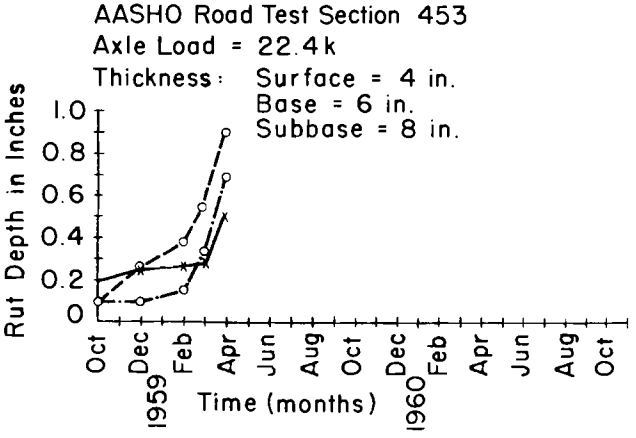

Fig A8.31. Observed versus calculated rut depth index.

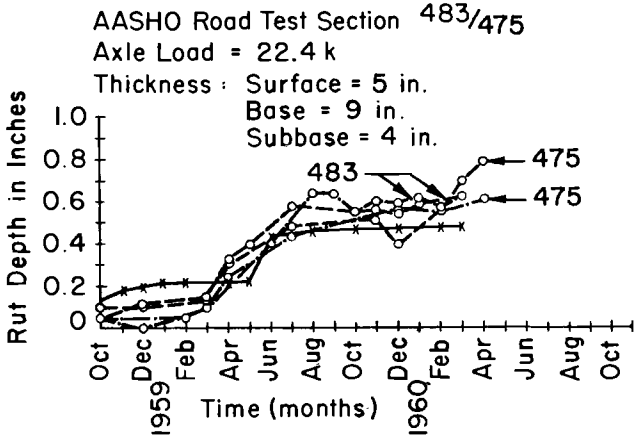

Fig A8.32. Observed versus calculated rut depth index.

Observed (inner wheel) —·—o—·— Calculated ——x——
Observed (outer wheel) —·—o—·—

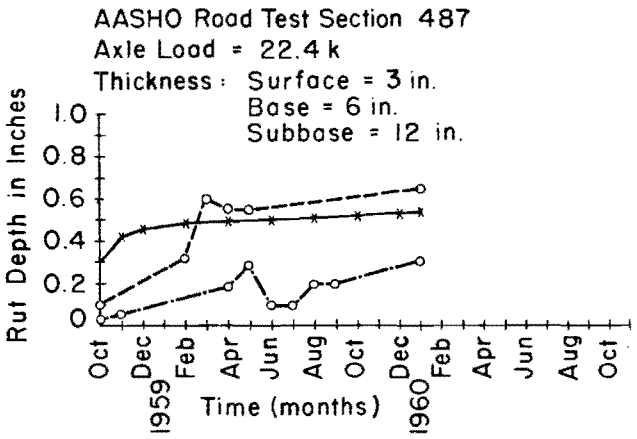

Fig A8.33. Observed versus calculated rut depth index.

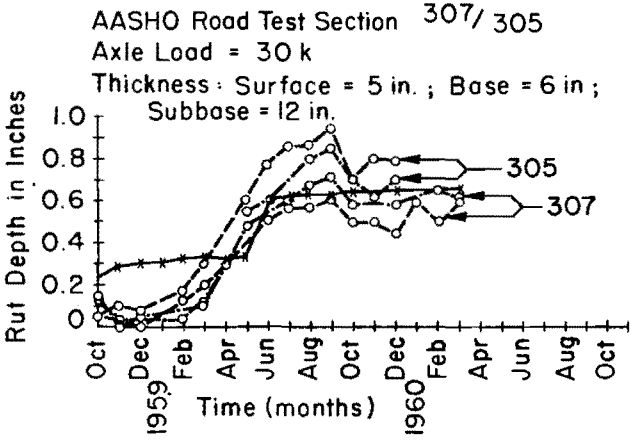

Fig A8.34. Observed versus calculated rut depth index.

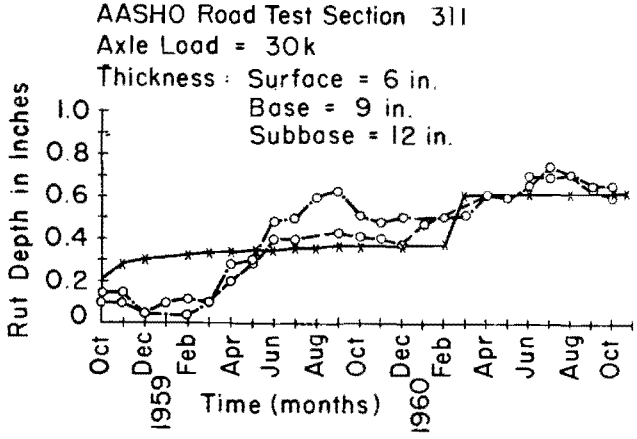

Fig A8.35. Observed versus calculated rut depth index.

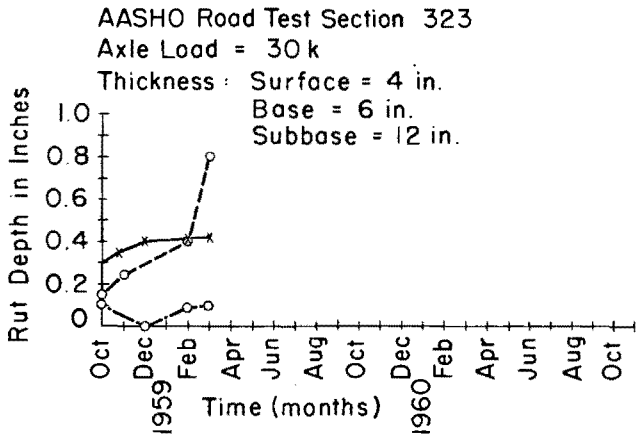

Fig A8.36. Observed versus calculated rut depth index.

Observed (inner wheel) — —o— — Calculated
Observed (outer wheel) — —o— —

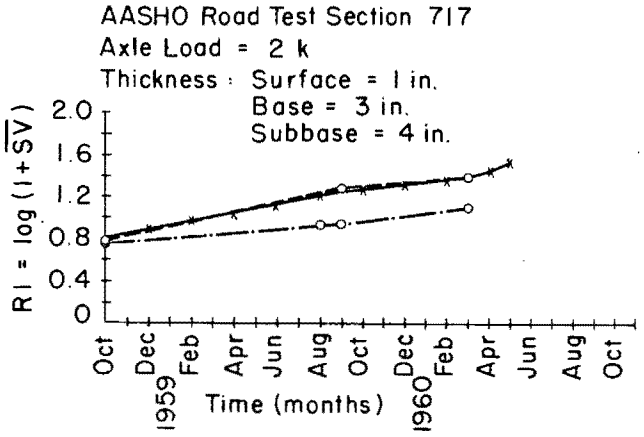

Fig A8.37. Observed versus calculated roughness index, RI.

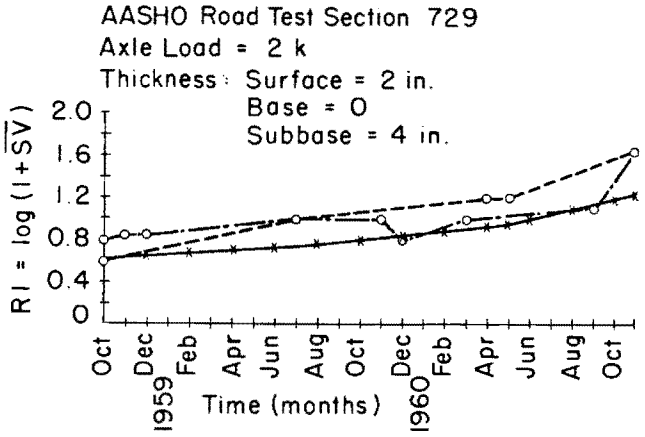

Fig A8.38. Observed versus calculated roughness index, RI.

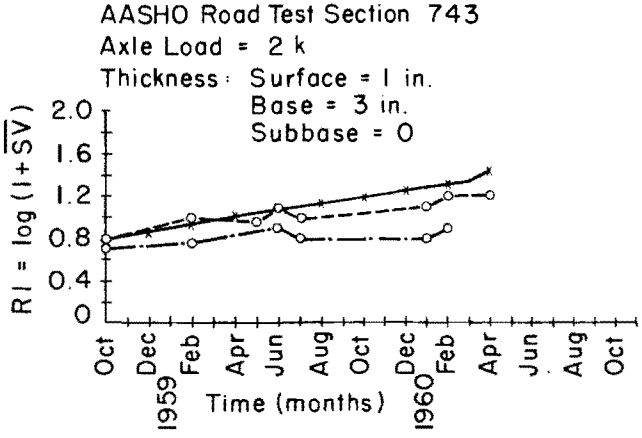

Fig A8.39. Observed versus calculated roughness index, RI.

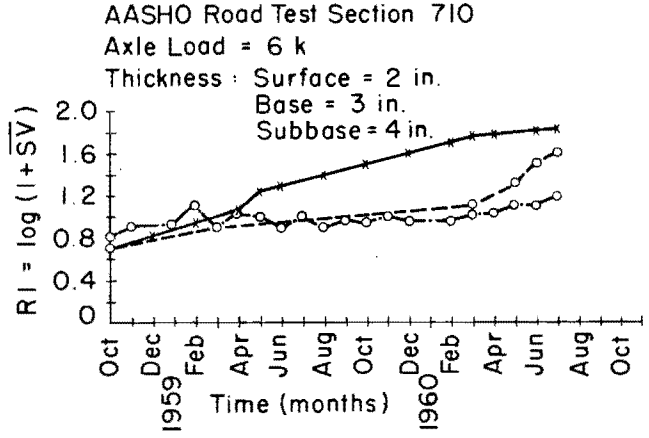

Fig A8.40. Observed versus calculated roughness index, RI.

Observed (inner wheel) — —o— — Calculated ———
Observed (outer wheel) — —c— —

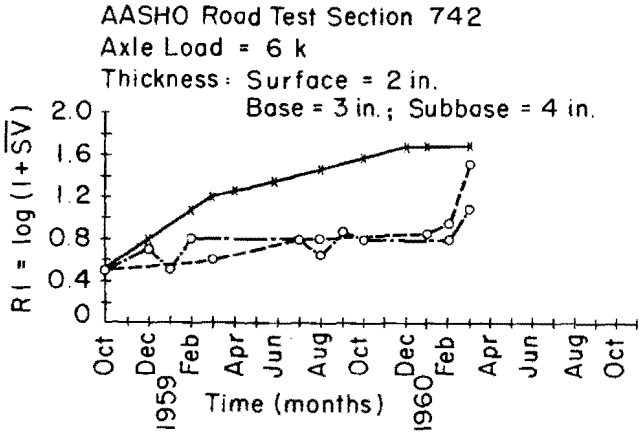

Fig A8.41. Observed versus calculated roughness index, RI.

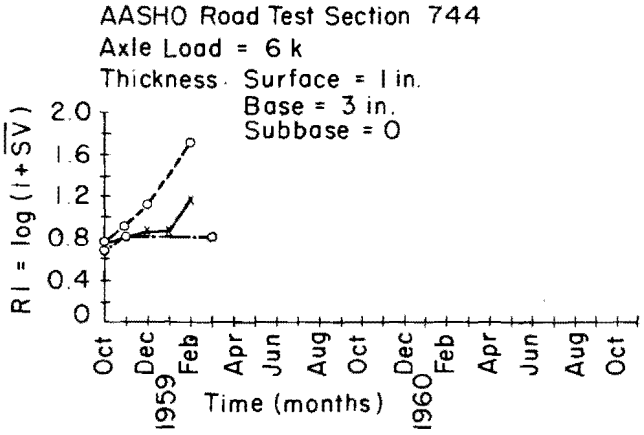

Fig A8.42. Observed versus calculated roughness index, RI.

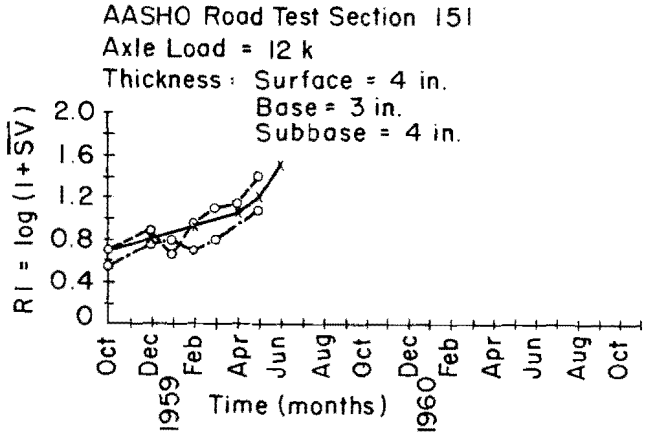

Fig A8.43. Observed versus calculated roughness index, RI.

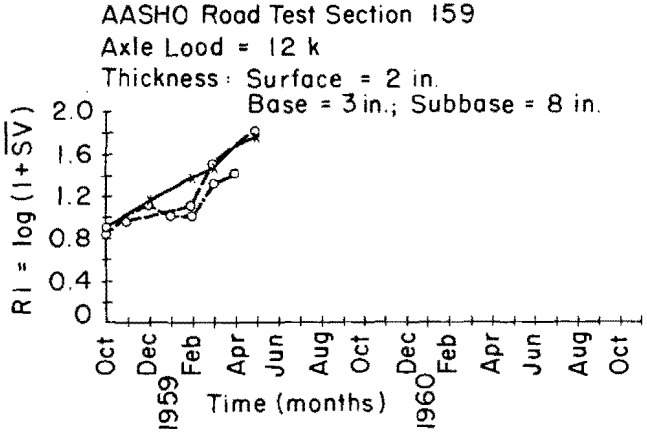

Fig A8.44. Observed versus calculated roughness index, RI.

Observed (inner wheel) — —o— — Calculated ——•——
Observed (outer wheel) — —o— —

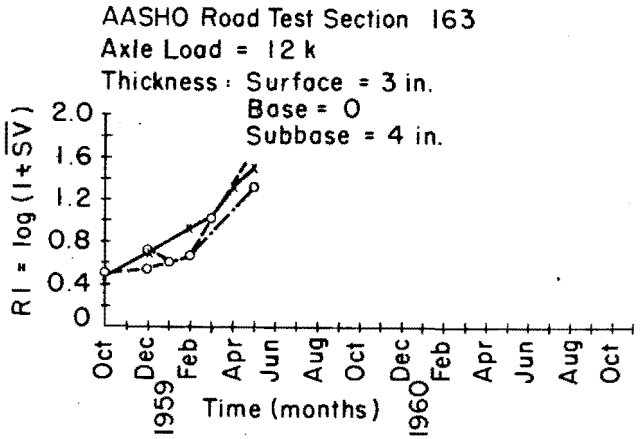

Fig A8.45. Observed versus calculated roughness index, RI.

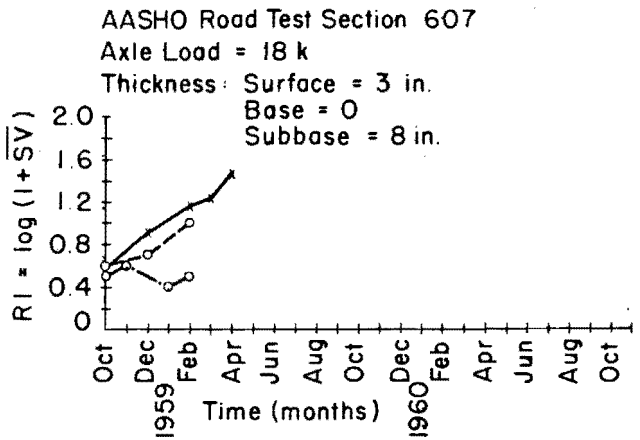

Fig A8.46. Observed versus calculated roughness index, RI.

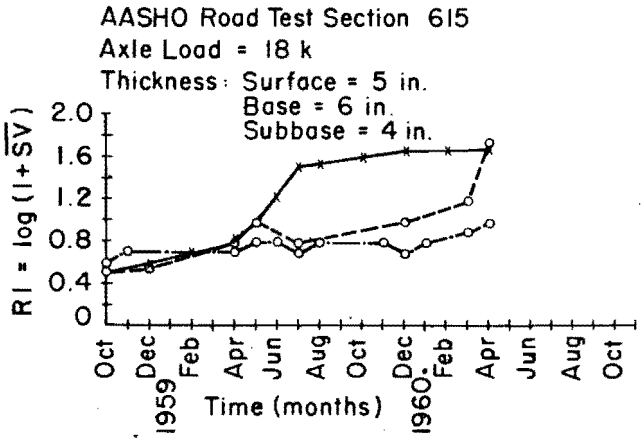

Fig A8.47. Observed versus calculated roughness index, RI.

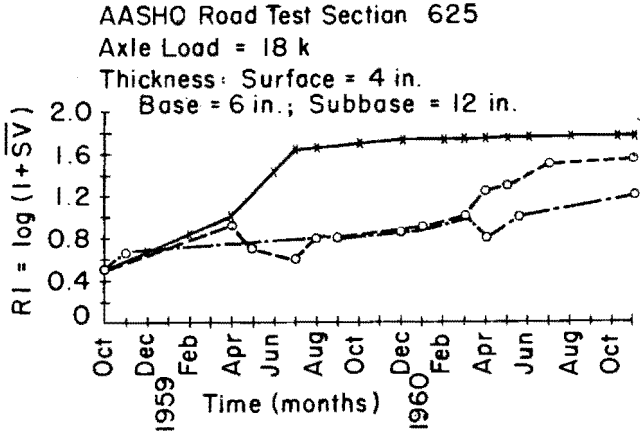

Fig A8.48. Observed versus calculated roughness index, RI.

Observed (inner wheel) —o— Calculated
Observed (outer wheel) —o—

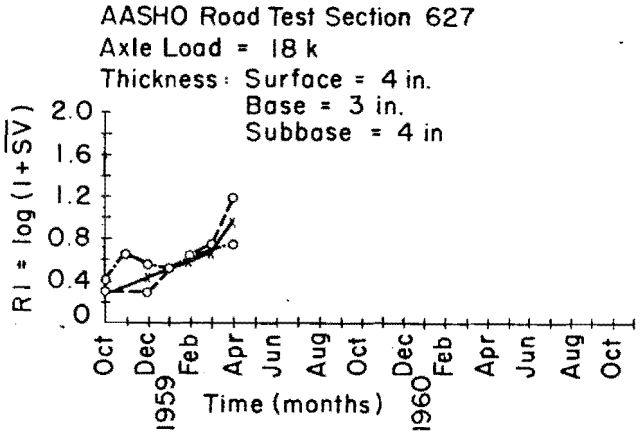

Fig A8.49. Observed versus calculated roughness index, RI.

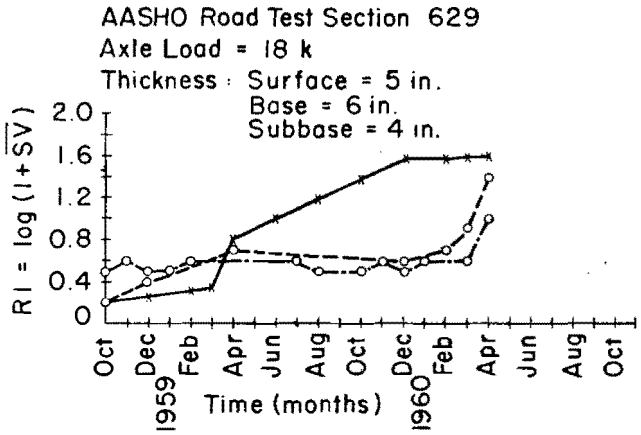

Fig A8.50. Observed versus calculated roughness index, RI.

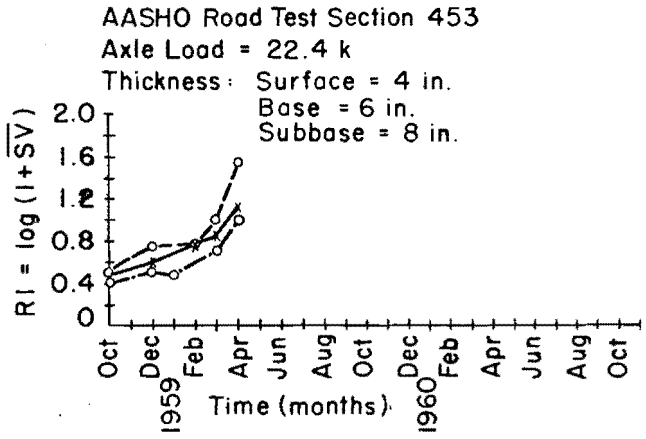

Fig A8.51. Observed versus calculated roughness index, RI.

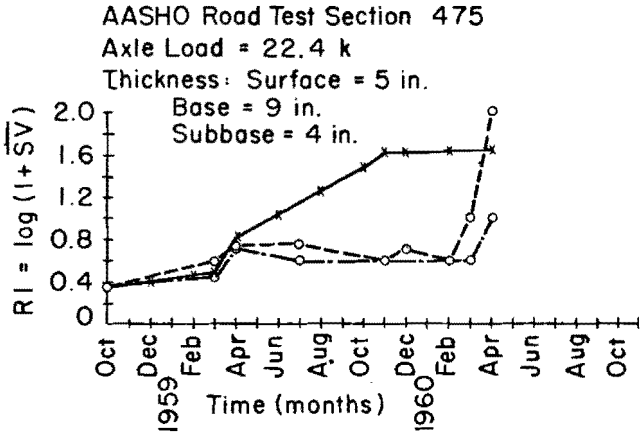

Fig A8.52. Observed versus calculated roughness index, RI.

Observed (inner wheel) — Calculated
Observed (outer wheel)

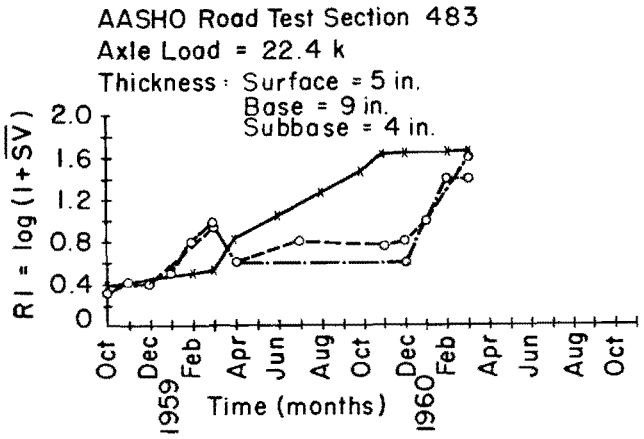

Fig A8.53. Observed versus calculated roughness index, RI.

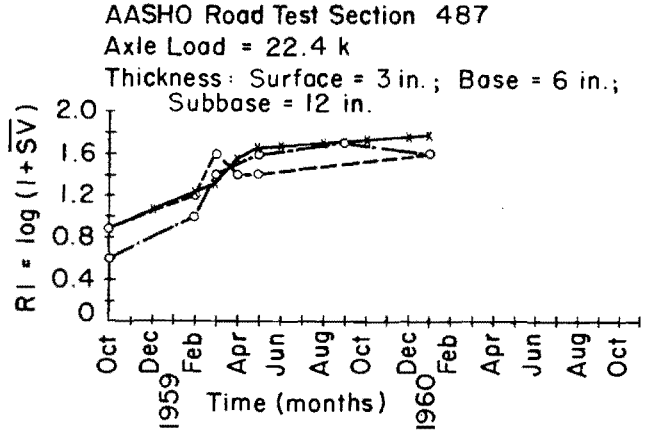

Fig A8.54. Observed versus calculated roughness index, RI.

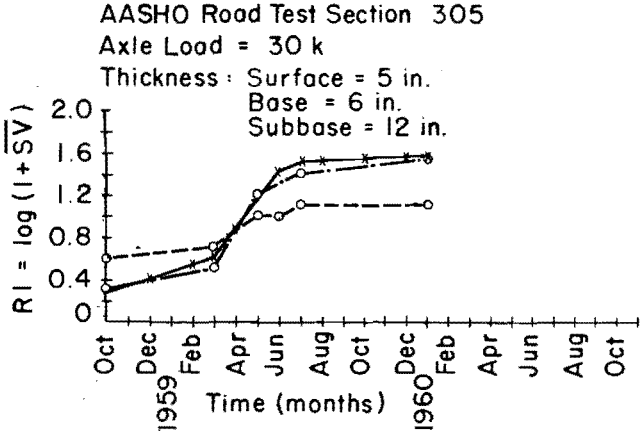

Fig A8.55. Observed versus calculated roughness index, RI.

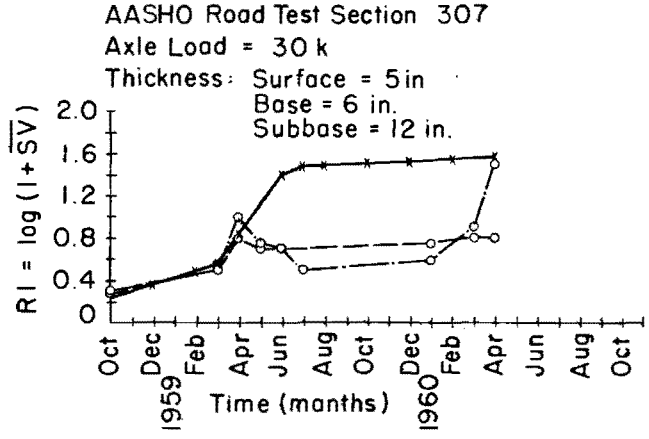

Fig A8.56. Observed versus calculated roughness index, RI.

Observed (inner wheel) —o— Calculated
Observed (outer wheel) —o—

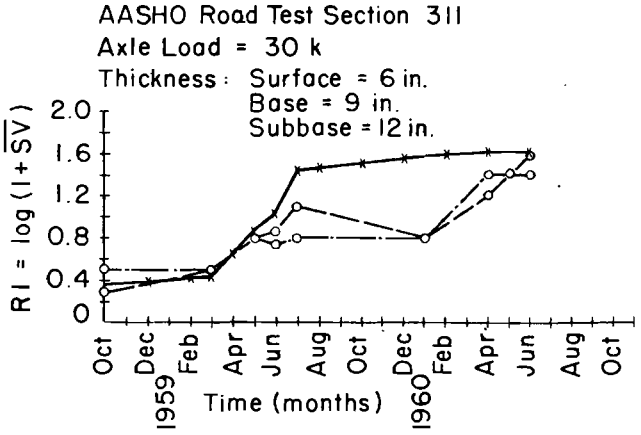

Fig A8.57. Observed versus calculated roughness index, RI.

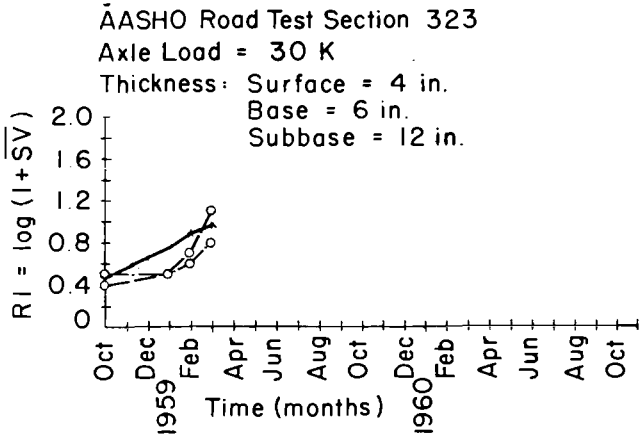

Fig A8.58. Observed versus calculated roughness index, RI.

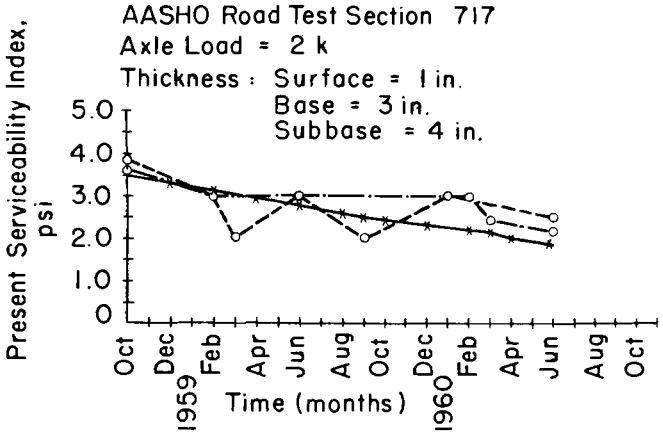

Fig A8.59. Observed versus calculated present serviceability index.

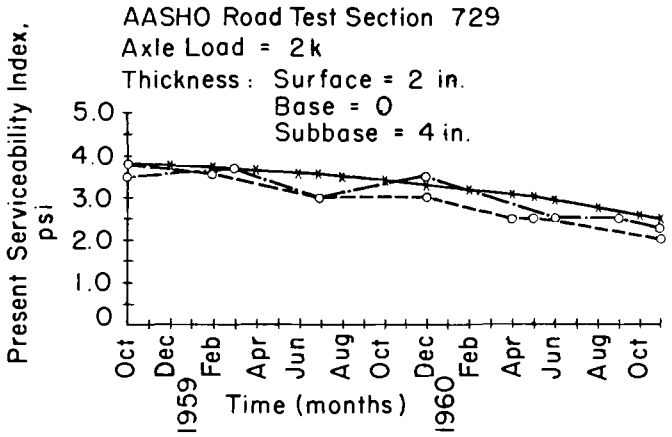

Fig A8.60. Observed versus calculated present serviceability index.

Observed (inner wheel) —o— Calculated
Observed (outer wheel) —o—

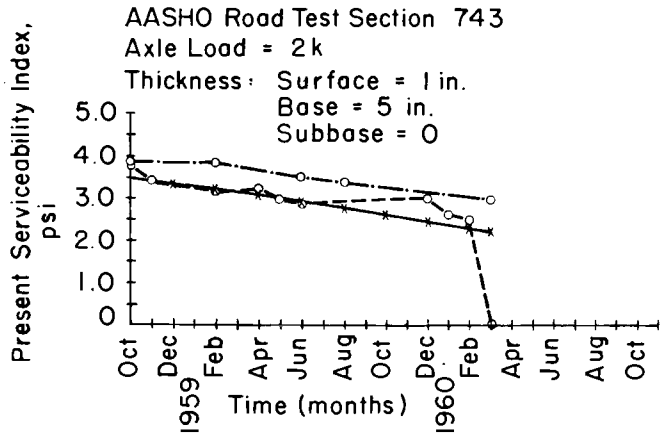

Fig A8.61. Observed versus calculated present serviceability index.

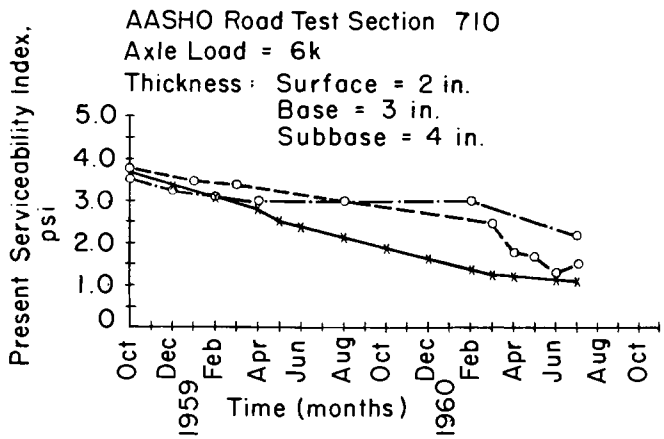

Fig A8.62. Observed versus calculated present serviceability index.

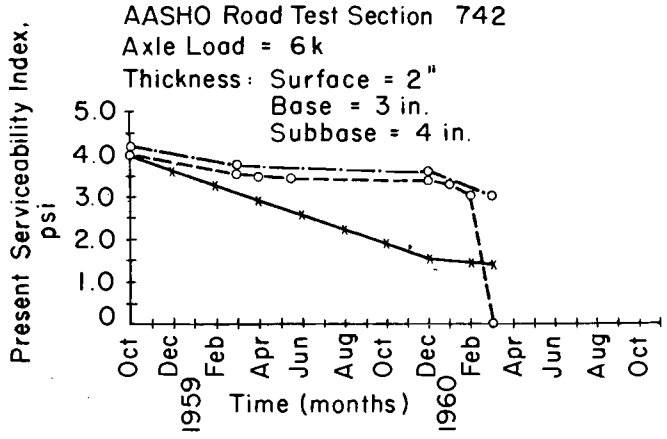

Fig A8.63. Observed versus calculated present serviceability index.

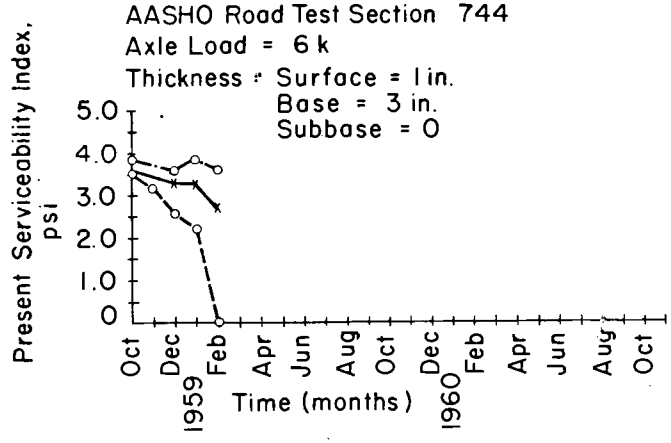

Fig A8.64. Observed versus calculated present serviceability index.

Observed (inner wheel) —o— Calculated —*—
Observed (outer wheel) —o—

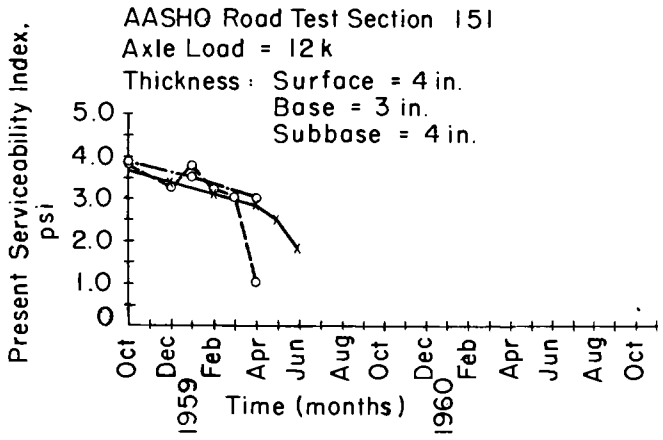

Fig A8.65. Observed versus calculated present serviceability index.

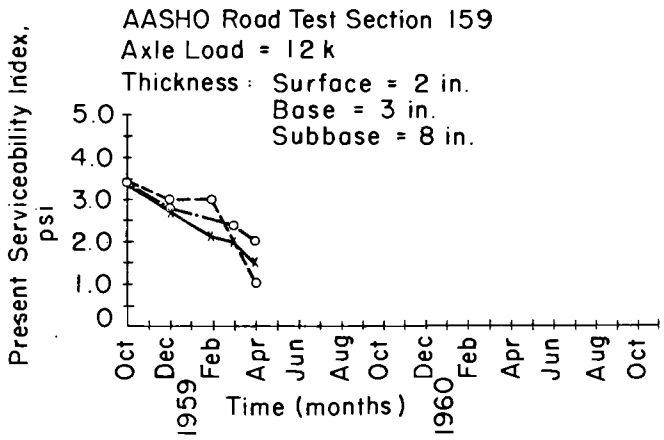

Fig A8.66. Observed versus calculated present serviceability index.

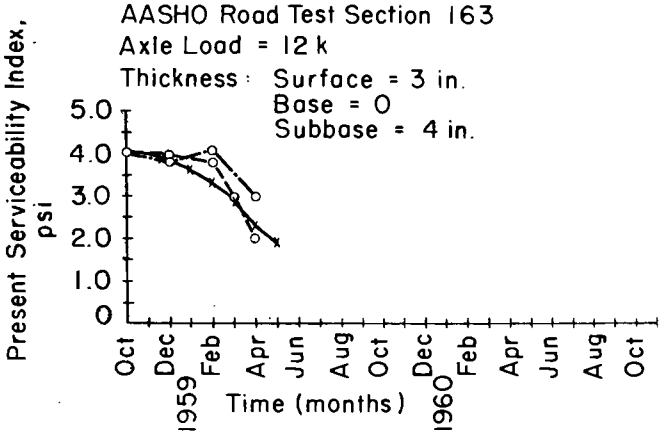

Fig A8.67. Observed versus calculated present serviceability index.

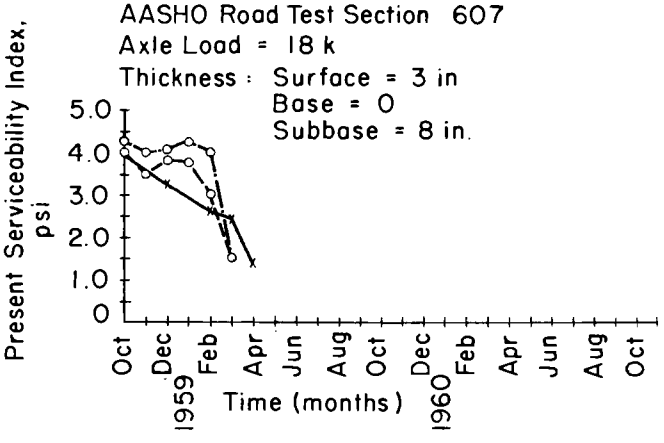

Fig A8.68. Observed versus calculated present serviceability index.

Observed (inner wheel) —o— Calculated
Observed (outer wheel) —o—

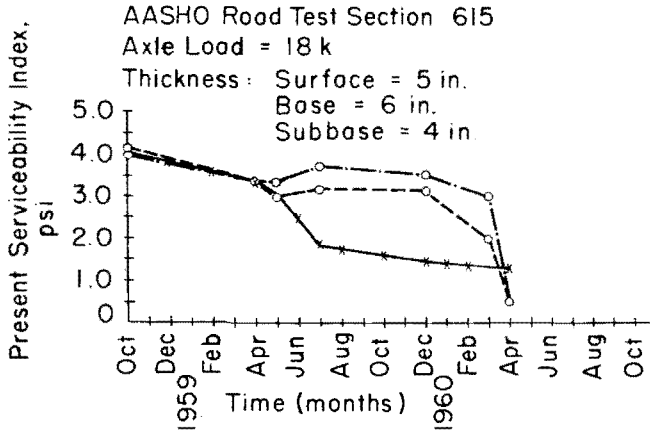

Fig A8.69. Observed versus calculated present serviceability index.

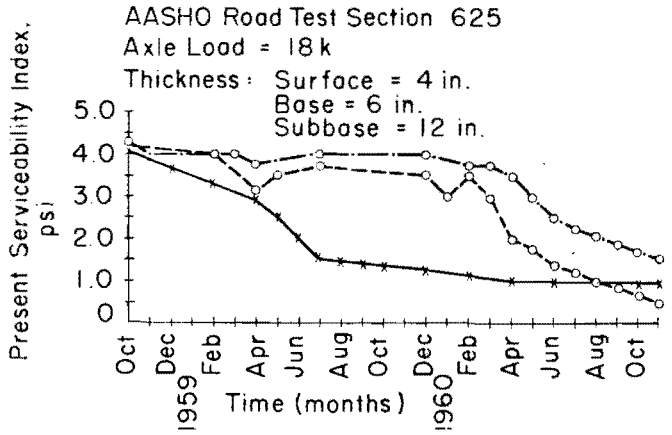

Fig A8.70. Observed versus calculated present serviceability index.

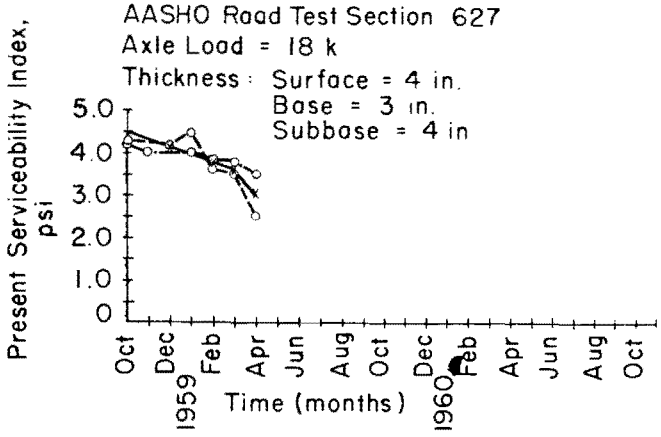

Fig A8.71. Observed versus calculated present serviceability index.

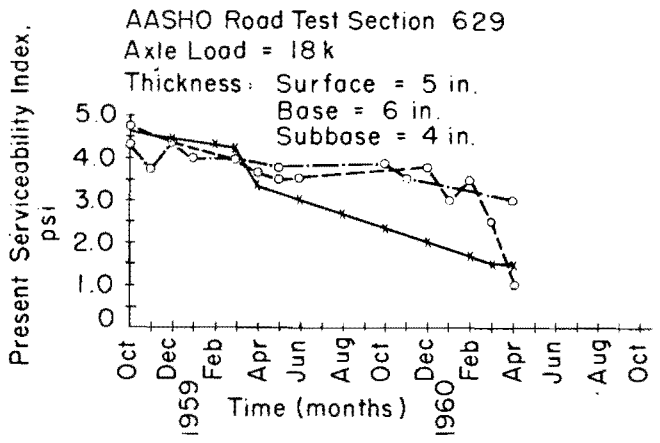

Fig A8.72. Observed versus calculated present serviceability index.

Observed (inner wheel) —o— Calculated —*—
Observed (outer wheel) —o—

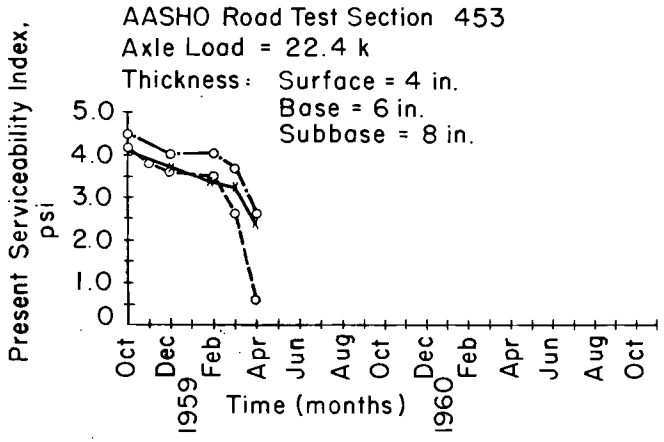

Fig A8.73. Observed versus calculated present serviceability index.

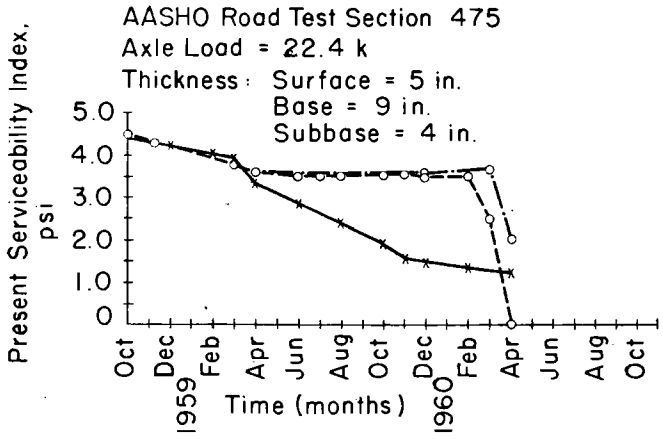

Fig A8.74. Observed versus calculated present serviceability index.

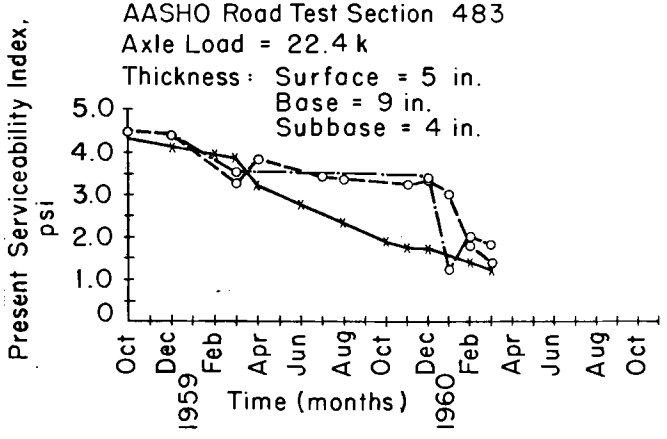

Fig A8.75. Observed versus calculated present serviceability index.

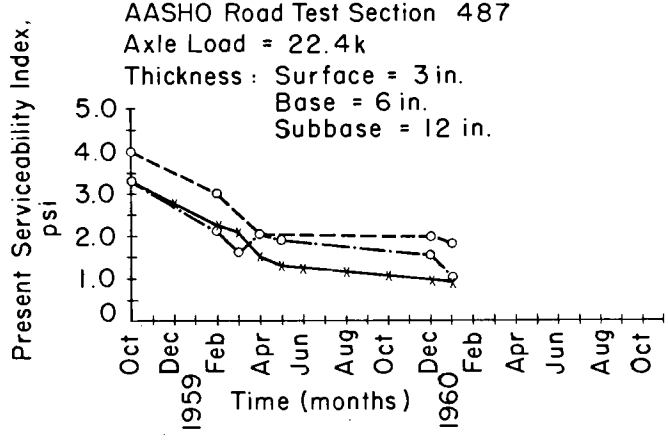

Fig A8.76. Observed versus calculated present serviceability index.

Observed (inner wheel) —o— Calculated —x—
Observed (outer wheel) —o—

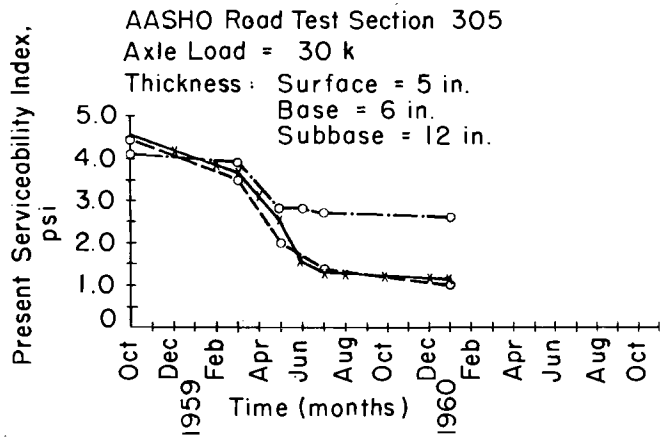

Fig A8.77. Observed versus calculated present serviceability index.

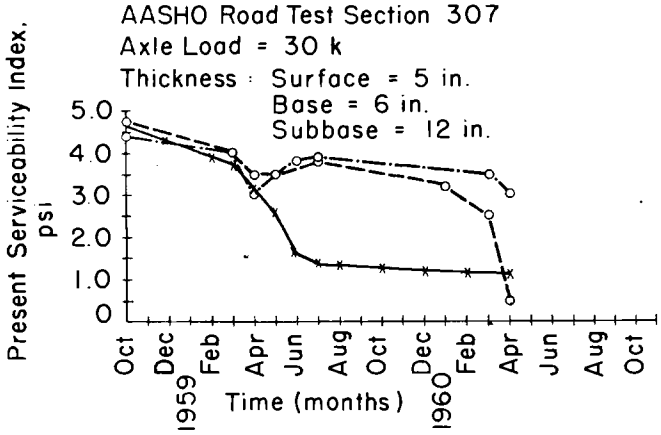

Fig A8.78. Observed versus calculated present serviceability index.

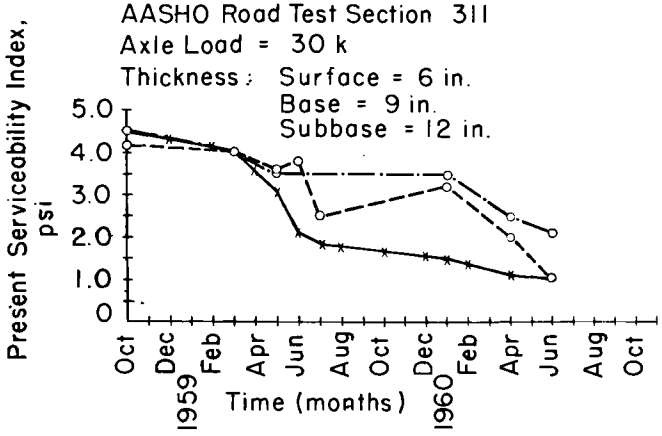

Fig A8.79. Observed versus calculated present serviceability index.

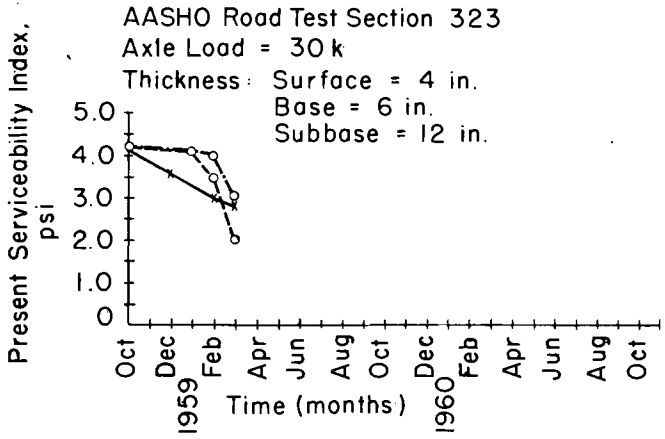

Fig A8.80. Observed versus calculated present serviceability index.

Observed (inner wheel) —o— Calculated —x—
Observed (outer wheel) —o—

APPENDIX 9

COMPUTER INPUT AND OUTPUT FOR EXAMPLE PROBLEMS

TABLE A9.1. EXAMPLE PROBLEM

THE CONSTRUCTION MATERIALS UNDER CONSIDERATION ARE

LAYER	MATERIALS CODE	NAME	COST PER CY	STR. COEFF.	MIN. DEPTH	MAX. DEPTH	SALVAGE PCT.	TRIAXIAL CLASS
1	A	ASPHALT CONCRETE	10.00	.44	3.00	3.00	50.00	.50
2	B	BASE MATERIAL	5.00	.14	6.00	6.00	50.00	1.00
3	C	SUBBASE MATERIAL	2.00	.11	8.00	8.00	50.00	3.70
		SUBBGRADE	0.00	0.00	0.00	0.00	0.00	5.60

NUMBER OF OUTPUT PAGES DESIRED(8 DESIGNS/PAGE)	3
TOTAL NUMBER OF INPUT MATERIALS,EXCLUDING SUBGRADE	3
LENGTH OF THE ANALYSIS PERIOD (YEARS)	2.2
WIDTH OF EACH LANE (FEET)	12.0
REGIONAL FACTOR	1.0
SERVICEABILITY INDEX OF THE INITIAL STRUCTURE	4.2
SERVICEABILITY INDEX P1 AFTER AN OVERLAY	4.2
MINIMUM SERVICEABILITY INDEX P2	1.5
SWELLING CLAY PARAMETERS -- P2 PRIME	4.20
B1	0.0000
ONE-DIRECTION ADT AT BEGINNING OF ANALYSIS PERIOD (VEHICLES/DAY)	1370
ONE-DIRECTION ADT AT END OF ANALYSIS PERIOD (VEHICLES/DAY)	1371
ONE-DIRECTION 2-YR ACCUMULATED NO. OF EQUIVALENT 18-KIP AXLES	1102700
PROPORTION OF ADT ARRIVING EACH HOUR OF CONSTRUCTION (PERCENT)	6.0
THE ROAD IS IN A RURAL AREA.	
MINIMUM TIME TO FIRST OVERLAY (YEARS)	.5
MINIMUM TIME BETWEEN OVERLAYS (YEARS)	.5
TIME TO FIRST SEAL COAT AFTER INITIAL OR OVERLAY CONST.(YEARS)	2.2
TIME BETWEEN SEAL COATS (YEARS)	2.2
MAX FUNDS AVAILABLE PER SQ.YD. FOR INITIAL DESIGN (DOLLARS)	15.00
MAXIMUM ALLOWED THICKNESS OF INITIAL CONSTRUCTION (INCHES)	60.0
MINIMUM OVERLAY THICKNESS (INCHES)	0.0
ACCUMULATED MAXIMUM DEPTH OF ALL OVERLAYS (INCHES)	8.0
ASPHALTIC CONCRETE PRODUCTION RATE (TONS/HOUR)	75.0
ASPHALTIC CONCRETE COMPACTED DENSITY (TONS/C.Y.)	1.80
C.L. DISTANCE OVER WHICH TRAFFIC IS SLOWED IN THE O.D. (MILES)	0.00
C.L. DISTANCE OVER WHICH TRAFFIC IS SLOWED IN THE N.O.D. (MILES)	0.00
DETOUR DISTANCE AROUND THE OVERLAY ZONE (MILES)	0.00
OVERLAY CONSTRUCTION TIME (HOURS/DAY)	0.0
NUMBER OF OPEN LANES IN RESTRICTED ZONE IN O.D.	1
NUMBER OF OPEN LANES IN RESTRICTED ZONE IN N.O.D.	2
PROPORTION OF VEHICLES STOPPED BY ROAD EQUIPMENT IN O.D. (PERCENT)	0.00
PROPORTION OF VEHICLES STOPPED BY ROAD EQUIPMENT IN N.O.D. (PERCENT)	0.00
AVERAGE TIME STOPPED BY ROAD EQUIPMENT IN O.D. (HOURS)	0.000
AVERAGE TIME STOPPED BY ROAD EQUIPMENT IN N.O.D. (HOURS)	0.000
AVERAGE APPROACH SPEED TO THE OVERLAY ZONE (MPH)	35.0
AVERAGE SPEED THROUGH OVERLAY ZONE IN O.D. (MPH)	35.0
AVERAGE SPEED THROUGH OVERLAY ZONE IN N.O.D. (MPH)	35.0
TRAFFIC MODEL USED IN THE ANALYSIS	3
FIRST YEAR COST OF ROUTINE MAINTENANCE (DOLLARS/LANE MILE)	50.00
INCREMENTAL INCREASE IN MAINT. COST PER YEAR (DOLLARS/LANE MILE)	20.00
COST OF A SEAL COAT (DOLLARS/LANE MILE)	900.00
INTEREST RATE OR TIME VALUE OF MONEY (PERCENT)	5.0

TABLE A9.2. EXAMPLE PROBLEM

```
 FOR THE 3 LAYER DESIGN WITH THE FOLLOWING MATERIALS--
          MATERIALS                  COST     STR.      MIN.      MAX.  SALVAGE TRIAXIAL
LAYER CODE       NAME              PER CY   COEFF.    DEPTH     DEPTH    PCT.    CLASS
  1     A  ASPHALT CONCRETE        10.00      .44      3.00      3.00    50.00     .50
  2     B  BASE MATERIAL            5.00      .14      6.00      6.00    50.00    1.00
  3     C  SUBBASE MATERIAL         2.00      .11      8.00      8.00    50.00    3.70
           SUBBGRADE                0.00     0.00      0.00      0.00     0.00    5.60

  3    THE OPTIMAL DESIGN FOR THE MATERIALS UNDER CONSIDERATION--
       FOR INITIAL CONSTRUCTION THE DEPTHS SHOULD BE
             ASPHALT CONCRETE       3.00 INCHES
             BASE MATERIAL          6.00 INCHES
             SUBBASE MATERIAL       8.00 INCHES
       THE LIFE OF THE INITIAL STRUCTURE =    .59 YEARS
       THE OVERLAY SCHEDULE IS
              2.50 INCH(ES) (INCLUDING 1 INCH LEVEL-UP) AFTER    .59 YEARS.
             TOTAL LIFE =       3.06YEARS/
       THERE SHOULD NOT BE ANY SEAL COATS.

       THE TOTAL COSTS PER SQ. YD. FOR THESE CONSIDERATIONS ARE
             INITIAL CONSTRUCTION COST          2.111
             TOTAL ROUTINE MAINTENANCE COST      .014
             TOTAL OVERLAY CONSTRUCTION COST     .661
             TOTAL USER COST DURING
                    OVERLAY CONSTRUCTION        0.000
             TOTAL SEAL COAT COST               0.000
             SALVAGE VALUE                     -1.135
             TOTAL OVERALL COST                 1.651


       NUMBER OF FEASIBLE DESIGNS EXAMINED FOR THIS SET --       1


         AT THE OPTIMAL SOLUTION, THE FOLLOWING
         BOUNDARY RESTRICTIONS ARE ACTIVE--
                   1. THE MINIMUM DEPTH OF LAYER  1
                   2. THE MAXIMUM DEPTH OF LAYER  1
                   3. THE MINIMUM DEPTH OF LAYER  2
                   4. THE MAXIMUM DEPTH OF LAYER  2
                   5. THE MINIMUM DEPTH OF LAYER  3
                   6. THE MAXIMUM DEPTH OF LAYER  3




  A SUMMARY OF THE BEST DESIGN FOR EACH COMBINATION
    OF MATERIALS, IN ORDER OF INCREASING TOTAL COST

        DESIGN NUMBER     TOTAL COST
              3             1.651

  THE MATERIALS ASSOCIATED WITH EACH OF THE FOLLOWING DESIGN
  NUMBERS DO NOT HAVE AT LEAST ONE FEASIBLE DESIGN.

                          1
                          2
```

TABLE A9.3. EXAMPLE PROBLEM

THE CONSTRUCTION MATERIALS UNDER CONSIDERATION ARE

LAYER	MATERIALS CODE	NAME	COST PER CY	STR. COEFF.	MIN. DEPTH	MAX. DEPTH	SALVAGE PCT.	TRIAXIAL CLASS
1	A	ASPHALT CONCRETE	4.40	.44	2.00	6.00	50.00	.50
2	B	BASE MATERIAL	1.40	.14	3.00	9.00	50.00	1.00
3	C	SUB BASE MATERIAL	1.10	.11	4.00	16.00	50.00	3.70
		SUB GRADE	0.00	0.00	0.00	0.00	0.00	5.60

NUMBER OF OUTPUT PAGES DESIRED(8 DESIGNS/PAGE)	3
TOTAL NUMBER OF INPUT MATERIALS,EXCLUDING SUBGRADE	3
LENGTH OF THE ANALYSIS PERIOD (YEARS)	2.2
WIDTH OF EACH LANE (FEET)	12.0
REGIONAL FACTOR	1.0
SERVICEABILITY INDEX OF THE INITIAL STRUCTURE	4.2
SERVICEABILITY INDEX P1 AFTER AN OVERLAY	4.2
MINIMUM SERVICEABILITY INDEX P2	1.5
SWELLING CLAY PARAMETERS -- P2 PRIME	4.20
R1	0.0000
ONE-DIRECTION ADT AT BEGINNING OF ANALYSIS PERIOD (VEHICLES/DAY)	1370
ONE-DIRECTION ADT AT END OF ANALYSIS PERIOD (VEHICLES/DAY)	1371
ONE-DIRECTION 2-YR ACCUMULATED NO. OF EQUIVALENT 18-KIP AXLES	1102700
PROPORTION OF ADT ARRIVING EACH HOUR OF CONSTRUCTION (PERCENT)	6.0
THE ROAD IS IN A RURAL AREA.	
MINIMUM TIME TO FIRST OVERLAY (YEARS)	2.2
MINIMUM TIME BETWEEN OVERLAYS (YEARS)	2.2
TIME TO FIRST SEAL COAT AFTER INITIAL OR OVERLAY CONST.(YEARS)	2.2
TIME BETWEEN SEAL COATS (YEARS)	2.2
MAX FUNDS AVAILABLE PER SQ.YD. FOR INITIAL DESIGN (DOLLARS)	15.00
MAXIMUM ALLOWED THICKNESS OF INITIAL CONSTRUCTION (INCHES)	60.0
MINIMUM OVERLAY THICKNESS (INCHES)	0.0
ACCUMULATED MAXIMUM DEPTH OF ALL OVERLAYS (INCHES)	0.0
ASPHALTIC CONCRETE PRODUCTION RATE (TONS/HOUR)	75.0
ASPHALTIC CONCRETE COMPACTED DENSITY (TONS/C.Y.)	1.80
C.L. DISTANCE OVER WHICH TRAFFIC IS SLOWED IN THE O.D. (MILES)	0.00
C.L. DISTANCE OVER WHICH TRAFFIC IS SLOWED IN THE N.O.D. (MILES)	0.00
DETOUR DISTANCE AROUND THE OVERLAY ZONE (MILES)	0.00
OVERLAY CONSTRUCTION TIME (HOURS/DAY)	0.0
NUMBER OF OPEN LANES IN RESTRICTED ZONE IN O.D.	1
NUMBER OF OPEN LANES IN RESTRICTED ZONE IN N.O.D.	2
PROPORTION OF VEHICLES STOPPED BY ROAD EQUIPMENT IN O.D. (PERCENT)	0.00
PROPORTION OF VEHICLES STOPPED BY ROAD EQUIPMENT IN N.O.D. (PERCENT)	0.00
AVERAGE TIME STOPPED BY ROAD EQUIPMENT IN O.D. (HOURS)	0.000
AVERAGE TIME STOPPED BY ROAD EQUIPMENT IN N.O.D. (HOURS)	0.000
AVERAGE APPROACH SPEED TO THE OVERLAY ZONE (MPH)	35.0
AVERAGE SPEED THROUGH OVERLAY ZONE IN O.D. (MPH)	35.0
AVERAGE SPEED THROUGH OVERLAY ZONE IN N.O.D. (MPH)	35.0
TRAFFIC MODEL USED IN THE ANALYSIS	3
FIRST YEAR COST OF ROUTINE MAINTENANCE (DOLLARS/LANE MILE)	50.00
INCREMENTAL INCREASE IN MAINT. COST PER YEAR (DOLLARS/LANE MILE)	20.00
COST OF A SEAL COAT (DOLLARS/LANE MILE)	900.00
INTEREST RATE OR TIME VALUE OF MONEY (PERCENT)	5.0

TABLE A9.4. EXAMPLE PROBLEM

SUMMARY OF THE BEST DESIGN STRATEGIES
IN ORDER OF INCREASING TOTAL COST

	1	2	3	4	5	6	7	8
MATERIAL ARRANGEMENT	ABC	ABC	ABC	ABC	ABC	AB	ABC	ABC
INIT. CONST. COST	1.022	1.022	1.022	1.022	1.022	1.022	1.022	1.022
OVERLAY CONST. COST	0.000	0.000	0.000	0.000	0.000	0.000	0.000	0.000
USER COST	0.000	0.000	0.000	0.000	0.000	0.000	0.000	0.000
SEAL COAT COST	0.000	0.000	0.000	0.000	0.000	0.000	0.000	0.000
ROUTINE MAINT. COST	.017	.017	.017	.017	.017	.017	.017	.017
SALVAGE VALUE	-.459	-.459	-.459	-.459	-.459	-.459	-.459	-.459
TOTAL COST	.580	.580	.580	.580	.580	.580	.580	.580
NUMBER OF LAYERS	3	3	3	3	3	2	3	3
LAYER DEPTH (INCHES)								
D(1)	4.50	4.25	4.00	3.00	2.75	5.50	3.75	3.50
D(2)	9.00	9.00	9.00	9.00	9.00	9.00	9.00	9.00
D(3)	4.00	5.00	6.00	10.00	11.00		7.00	8.00
NO.OF PERF.PERIODS	1	1	1	1	1	1	1	1
PERF. TIME (YEARS)								
T(1)	2.4	2.4	2.4	2.4	2.4	2.4	2.4	2.4
OVERLAY POLICY(INCH) (INCLUDING LEVEL-UP)								
NUMBER OF SEAL COATS	0	0	0	0	0	0	0	0
SEAL COAT SCHEDULE (YEARS)								

(Continued)

TABLE A9.4. (Continued)

SUMMARY OF THE BEST DESIGN STRATEGIES
IN ORDER OF INCREASING TOTAL COST

	9	10	11	12	13	14	15	16
MATERIAL ARRANGEMENT	ABC	AB	ABC	ABC	ABC	ABC	ABC	ABC
INIT. CONST. COST	1.022	1.024	1.024	1.024	1.024	1.024	1.024	1.024
OVERLAY CONST. COST	0.000	0.000	0.000	0.000	0.000	0.000	0.000	0.000
USER COST	0.000	0.000	0.000	0.000	0.000	0.000	0.000	0.000
SEAL COAT COST	0.000	0.000	0.000	0.000	0.000	0.000	0.000	0.000
ROUTINE MAINT. COST	.017	.017	.017	.017	.017	.017	.017	.017
SALVAGE VALUE	-.459	-.460	-.460	-.460	-.460	-.460	-.460	-.460
TOTAL COST	.580	.580	.580	.580	.580	.580	.580	.580
NUMBER OF LAYERS	3	2	3	3	3	3	3	3
LAYER DEPTH (INCHES)								
D(1)	3.25	5.75	4.75	4.50	4.25	3.75	3.50	3.25
D(2)	9.00	8.25	8.25	8.25	8.25	8.25	8.25	8.25
D(3)	9.00		4.00	5.00	6.00	8.00	9.00	10.00
NO.OF PERF.PERIODS	1	1	1	1	1	1	1	1
PERF. TIME (YEARS)								
T(1)	2.4	2.4	2.4	2.4	2.4	2.4	2.4	2.4
OVERLAY POLICY(INCH) (INCLUDING LEVEL-UP)								
NUMBER OF SEAL COATS	0	0	0	0	0	0	0	0
SEAL COAT SCHEDULE (YEARS)								

(Continued)

TABLE A9.4. (Continued)

SUMMARY OF THE BEST DESIGN STRATEGIES
IN ORDER OF INCREASING TOTAL COST

	17	18	19	20	21	22	23	24
MATERIAL ARRANGEMENT	ABC	ABC	ABC	AB	ABC	ABC	ABC	ABC
INIT. CONST. COST	1.024	1.024	1.024	1.025	1.025	1.025	1.025	1.025
OVERLAY CONST. COST	0.000	0.000	0.000	0.000	0.000	0.000	0.000	0.000
USER COST	0.000	0.000	0.000	0.000	0.000	0.000	0.000	0.000
SEAL COAT COST	0.000	0.000	0.000	0.000	0.000	0.000	0.000	0.000
ROUTINE MAINT. COST	.017	.017	.017	.017	.017	.017	.017	.017
SALVAGE VALUE	-.460	-.460	-.460	-.460	-.460	-.460	-.460	-.460
TOTAL COST	.580	.580	.580	.581	.581	.581	.581	.581
NUMBER OF LAYERS	3	3	3	2	3	3	3	3
LAYER DEPTH (INCHES)								
D(1)	3.00	2.75	4.00	6.00	5.00	4.75	4.50	4.25
D(2)	8.25	8.25	8.25	7.50	7.50	7.50	7.50	7.50
D(3)	11.00	12.00	7.00		4.00	5.00	6.00	7.00
NO.OF PERF.PERIODS	1	1	1	1	1	1	1	1
PERF. TIME (YEARS)								
T(1)	2.4	2.4	2.4	2.4	2.4	2.4	2.4	2.4
OVERLAY POLICY(INCH) (INCLUDING LEVEL-UP)								
NUMBER OF SEAL COATS	0	0	0	0	0	0	0	0
SEAL COAT SCHEDULE (YEARS)								

THE TOTAL NUMBER OF FEASIBLE DESIGNS CONSIDERED WAS 993

TABLE A9.5. EXAMPLE PROBLEM

THE CONSTRUCTION MATERIALS UNDER CONSIDERATION ARE

LAYER	MATERIALS CODE	NAME	COST PER CY	STR. COEFF.	MIN. DEPTH	MAX. DEPTH	SALVAGE PCT.
1	A	ASPHALT CONCRETE	10.00	.90	3.00	3.00	50.00
2	B	BASE MATERIAL	5.00	.45	6.00	6.00	50.00
3	C	SUBBASE MATERIAL	2.00	.30	8.00	8.00	50.00
		SUBBGRADE	0.00	.17	0.00	0.00	0.00

NUMBER OF OUTPUT PAGES DESIRED(8 DESIGNS/PAGE)	3
TOTAL NUMBER OF INPUT MATERIALS,EXCLUDING SUBGRADE	3
LENGTH OF THE ANALYSIS PERIOD (YEARS)	2.2
WIDTH OF EACH LANE (FEET)	12.0
DISTRICT TEMPERATURE CONSTANT	30.0
SERVICEABILITY INDEX OF THE INITIAL STRUCTURE	4.2
SERVICEABILITY INDEX P1 AFTER AN OVERLAY	4.2
MINIMUM SERVICEABILITY INDEX P2	1.5
SWELLING CLAY PARAMETERS -- P2 PRIME	4.20
B1	0.0000
ONE-DIRECTION ADT AT BEGINNING OF ANALYSIS PERIOD (VEHICLES/DAY)	1370
ONE-DIRECTION ADT AT END OF ANALYSIS PERIOD (VEHICLES/DAY)	1371
ONE-DIRECTION 2-YR ACCUMULATED NO. OF EQUIVALENT 18-KIP AXLES	1102700
PROPORTION OF ADT ARRIVING EACH HOUR OF CONSTRUCTION (PERCENT)	6.0
THE ROAD IS IN A RURAL AREA.	
MINIMUM TIME TO FIRST OVERLAY (YEARS)	.5
MINIMUM TIME BETWEEN OVERLAYS (YEARS)	.5
TIME TO FIRST SEAL COAT AFTER INITIAL OR OVERLAY CONST.(YEARS)	2.2
TIME BETWEEN SEAL COATS (YEARS)	2.2
MAX FUNDS AVAILABLE PER SQ.YD. FOR INITIAL DESIGN (DOLLARS)	15.00
MAXIMUM ALLOWED THICKNESS OF INITIAL CONSTRUCTION (INCHES)	60.0
MINIMUM OVERLAY THICKNESS (INCHES)	0.0
ACCUMULATED MAXIMUM DEPTH OF ALL OVERLAYS (INCHES)	8.0
ASPHALTIC CONCRETE PRODUCTION RATE (TONS/HOUR)	75.0
ASPHALTIC CONCRETE COMPACTED DENSITY (TONS/C.Y.)	1.80
C.L. DISTANCE OVER WHICH TRAFFIC IS SLOWED IN THE O.D. (MILES)	0.00
C.L. DISTANCE OVER WHICH TRAFFIC IS SLOWED IN THE N.O.D. (MILES)	0.00
DETOUR DISTANCE AROUND THE OVERLAY ZONE (MILES)	0.00
OVERLAY CONSTRUCTION TIME (HOURS/DAY)	0.0
NUMBER OF OPEN LANES IN RESTRICTED ZONE IN O.D.	1
NUMBER OF OPEN LANES IN RESTRICTED ZONE IN N.O.D.	2
PROPORTION OF VEHICLES STOPPED BY ROAD EQUIPMENT IN O.D. (PERCENT)	0.00
PROPORTION OF VEHICLES STOPPED BY ROAD EQUIPMENT IN N.O.D. (PERCENT)	0.00
AVERAGE TIME STOPPED BY ROAD EQUIPMENT IN O.D. (HOURS)	0.000
AVERAGE TIME STOPPED BY ROAD EQUIPMENT IN N.O.D. (HOURS)	0.000
AVERAGE APPROACH SPEED TO THE OVERLAY ZONE (MPH)	35.0
AVERAGE SPEED THROUGH OVERLAY ZONE IN O.D. (MPH)	35.0
AVERAGE SPEED THROUGH OVERLAY ZONE IN N.O.D. (MPH)	35.0
TRAFFIC MODEL USED IN THE ANALYSIS	3
FIRST YEAR COST OF ROUTINE MAINTENANCE (DOLLARS/LANE MILE)	50.00
INCREMENTAL INCREASE IN MAINT. COST PER YEAR (DOLLARS/LANE MILE)	20.00
COST OF A SEAL COAT (DOLLARS/LANE MILE)	900.00
INTEREST RATE OR TIME VALUE OF MONEY (PERCENT)	5.0

(Continued)

TABLE A9.5. (Continued)

FOR THE 3 LAYER DESIGN WITH THE FOLLOWING MATERIALS--

LAYER	MATERIALS CODE	NAME	COST PER CY	STR. COEFF.	MIN. DEPTH	MAX. DEPTH	SALVAGE PCT.
1	A	ASPHALT CONCRETE	10.00	.90	3.00	3.00	50.00
2	B	BASE MATERIAL	5.00	.45	6.00	6.00	50.00
3	C	SUBBASE MATERIAL	2.00	.30	8.00	8.00	50.00
		SUBGRADE	0.00	.17	0.00	0.00	0.00

3 THE OPTIMAL DESIGN FOR THE MATERIALS UNDER CONSIDERATION--
FOR INITIAL CONSTRUCTION THE DEPTHS SHOULD BE
ASPHALT CONCRETE 3.00 INCHES
BASE MATERIAL 6.00 INCHES
SUBBASE MATERIAL 8.00 INCHES

THE SCI OF THE INITIAL STRUCTURE = 1.469
THE LIFE OF THE INITIAL STRUCTURE = .53 YEARS
THE OVERLAY SCHEDULE IS
3.00 INCH(ES) (INCLUDING 1 INCH LEVEL-UP) AFTER .53 YEARS.
TOTAL LIFE = 2.31YEARS/
THERE SHOULD NOT BE ANY SEAL COATS.

THE TOTAL COSTS PER SQ. YD. FOR THESE CONSIDERATIONS ARE

INITIAL CONSTRUCTION COST	2.111
TOTAL ROUTINE MAINTENANCE COST	.014
TOTAL OVERLAY CONSTRUCTION COST	.794
TOTAL USER COST DURING OVERLAY CONSTRUCTION	0.000
TOTAL SEAL COAT COST	0.000
SALVAGE VALUE	-1.198
TOTAL OVERALL COST	1.721

NUMBER OF FEASIBLE DESIGNS EXAMINED FOR THIS SET -- 1

AT THE OPTIMAL SOLUTION, THE FOLLOWING
BOUNDARY RESTRICTIONS ARE ACTIVE--
1. THE MINIMUM DEPTH OF LAYER 1
2. THE MAXIMUM DEPTH OF LAYER 1
3. THE MINIMUM DEPTH OF LAYER 2
4. THE MAXIMUM DEPTH OF LAYER 2
5. THE MINIMUM DEPTH OF LAYER 3
6. THE MAXIMUM DEPTH OF LAYER 3

A SUMMARY OF THE BEST DESIGN FOR EACH COMBINATION
OF MATERIALS, IN ORDER OF INCREASING TOTAL COST

DESIGN NUMBER	TOTAL COST
3	1.721

THE MATERIALS ASSOCIATED WITH EACH OF THE FOLLOWING DESIGN
NUMBERS DO NOT HAVE AT LEAST ONE FEASIBLE DESIGN.

1
2

THE AUTHORS

Surendra Prakash Jain is a Research Engineer Assistant, working toward his Ph.D. degree, at the Center for Highway Research at The University of Texas at Austin. His engineering experience includes work with the U. P. State Irrigation Department in India, Stanford University, Brown and Root, Inc., Houston, Texas, and the Center for Highway Research at The University of Texas at Austin. His current research efforts are primarily with (1) analysis and design of pavement management systems, (2) flexible pavement design, and (3) sensitivity analyses. He is a member of the American Society of Civil Engineers and author of several other reports.

B. Frank McCullough is an Assistant Professor of Civil Engineering at The University of Texas at Austin. His engineering experience includes work with the Texas Highway Department and the Center for Highway Research at The University of Texas at Austin. His current research is concerned with (1) systematic pavement design and (2) the evaluation and revision of the Texas Highway Department rigid pavement design procedure. He is the author of numerous publications and a member of several professional societies.

W. Ronald Hudson is an Associate Professor of Civil Engineering and Associate Dean of the College of Engineering at The University of Texas at Austin. He has had a wide variety of experience as a research engineer with the Texas Highway Department and the Center for Highway Research at The University of Texas at Austin and was Assistant Chief of the Rigid Pavement Research Branch of the AASHO Road Test. He is the author of numerous publications and was the recipient of the 1967 ASCE J. James R. Croes Medal. He is presently concerned with research in the areas of (1) analysis and design of pavement management systems, (2) measurement of pavement roughness performance, (3) slab analysis and design, and (4) tensile strength of stabilized subbase materials.